

BERICHTE

aus dem Fachbereich Geowissenschaften
der Universität Bremen

No. 288

Mohtadi, M., M. Bergenthal, A. Contreras, H. Dang, R. Düßmann,
T. Freudenthal, H. Ge, M. Iliev, K. Kaszemeik, H. Keil, M. Klann,
T. Klein, X. Li, D. Liang, A. Lückge, P. Munz, L. Palamenghi, R. Rehage,
R. Reich, M. Reuter, U. Rosiak, W. Schmidt, S. Steinke, A. Weiner

**REPORT AND PRELIMINARY RESULTS OF
RV SONNE CRUISE SO 221.
INVERS.**

Hong Kong – Hong Kong, 17.05.2012 – 07.06.2012.



The "Berichte aus dem Fachbereich Geowissenschaften" are produced at irregular intervals by the Department of Geosciences, Bremen University and by MARUM.

They serve for the publication of cruise reports, PhD-theses, experimental works, and scientific contributions made by members of the department.

Reports can be ordered from:

Monika Bachur

DFG-Forschungszentrum MARUM

Universität Bremen

Postfach 330 440

D 28334 BREMEN

Phone: (49) 421 218-65516

Fax: (49) 421 218-65515

e-mail: MBachur@uni-bremen.de

Reports can also be downloaded:

<http://www.marum.de/Page8885.html>

Citation:

Mohtadi, M. and cruise participants

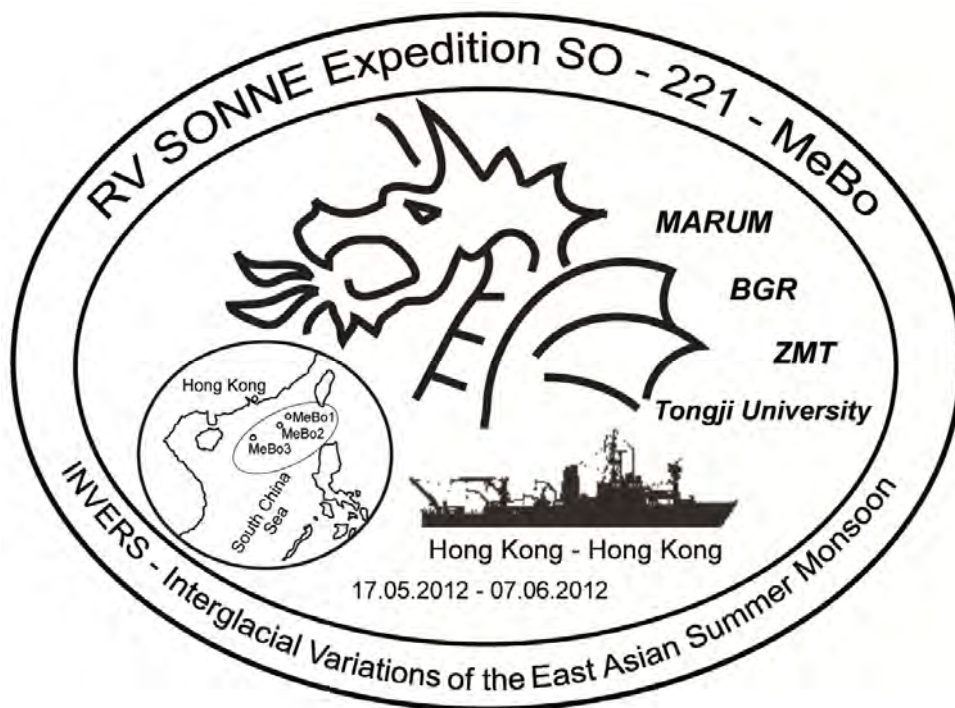
Report and preliminary results of RV SONNE Cruise SO 221. INVERS. Hong Kong – Hong Kong, 17.05.2012 – 07.06.2012.

Berichte, Fachbereich Geowissenschaften, Universität Bremen, No. 288, 168 pages. Bremen, 2012.

Cruise Report

INVERS

RV SONNE Cruise SO-221



Hong Kong (17.05.2012) - Hong Kong (07.06.2012)

Mohtadi, M., Bergenthal, M., Contreras, A., Dang, H., Düßmann, R., Freudenthal, T., Ge, H., Iliev, M., Kaszemeik, K., Keil, H., Klann, M., Klein, T., Li, X., Liang, D., Lückge, A., Munz, P., Palamenghi, L., Rehage, R., Reich, R., Reuter, M., Rosiak, U., Schmidt, W., Steinke, S. Weiner, A.

Content

1	Participants	5
2	Research Program	8
3	Narrative of the Cruise.....	11
4	CTD Profiling and Water sampling	17
4.1	Introduction.....	17
4.2	Instrumentation.....	17
5	Plankton Sampling with the Multi-net and pump	18
5.1	Introduction.....	18
5.2	Instrumentation.....	18
6	Seismic Surveying	19
6.1	Multi-channel seismic	19
6.2	Sub-bottom profiler, swath bathymetry sounder.....	22
7	Coring with the Seafloor Drill Rig MeBo	23
7.1	Introduction.....	23
7.2	Spectral Gamma Ray Borehole measurements	24
8	Sediment Sampling.....	26
8.1	Introduction.....	26
8.2	Multi-corer.....	26
8.2.1	Sub-sampling of the multi-corer.....	27
8.3	Gravity corer	27
8.3.1	Sampling of the gravity cores	27
8.3.2	Core description and color-scanning	28
9	Shipboard Results	29
9.1	Water column	29
9.2	Site Survey	31
9.3	Bore-hole logging	39
9.4	Sediments.....	41
10	Core Descriptions	49
10.1	Gravity cores.....	50
10.2	MeBo cores.....	53
11	Station List	168

Acknowledgements

The scientific party of the INVERS expedition (SO-221) gratefully acknowledges the friendly co-operation and efficient technical assistance of Captain Meyer and his crew, which all together contributed significantly to the success of this expedition. Thanks are also due to the German Research Ministry (BMBF), which funded this cruise within the project “INVERS – Interglaziale Veränderungen des ostasiatischen Sommermonsuns (SO-221)”.

1 Participants

Scientific Party SO-221

May 17 – June 7, 2012

Hong Kong – Hong Kong

Name	Discipline	Institute
Mohtadi, Mahyar	Paleoceanography	MARUM (Chief Scientist)
Bergenthal, Markus	MeBo	MARUM
Contreras Rosales, Lorena Astrid	Biogeochemistry	ZMT
Dang, Haowen	Paleoceanography	Tongji University
Düßmann, Ralf	MeBo	MARUM
Freudenthal, Tim	MeBo	MARUM
Ge, Huangmin	Geomicrobiology	Tongji University
Iliev, Milen	Seismic	GeoB
Kaszemeik, Kai	MeBo	MARUM
Keil, Hanno	Seismic	GeoB
Klann, Marco	Paleoceanography	MARUM
Klein, Thorsten	MeBo	MARUM
Li, Xiajing	Clay mineralogy	Tongji University
Liang, Dan	Micropaleontology	Tongji University
Lückge, Andreas	Organic geochemistry	BGR
Munz, Philipp Moritz	Micropaleontology	Univ. Tübingen
Palamenghi, Luisa	Seismic	GeoB
Rehage, Ralf	MeBo	MARUM
Reich, Reinhard	MeBo	Fa. Bauer
Reuter, Michael	MeBo	MARUM
Rosiak, Uwe	MeBo	MARUM
Schmidt, Werner	MeBo	MARUM
Steinke, Stephan	Paleoceanography	MARUM
Weiner, Agnes Katharina Maria	Microbiology	MARUM

Crew list SO-221

May 17 – June 07, 2012

Hong Kong – Hong Kong

Name	Rank
Meyer, Oliver	Master
Korte, Detlef	Chief Mate
Büchele, Ulrich	Officer Navigational Watch
Hoffsommer, Lars	Officer Navigational Watch
Walther, Anke	Surgeon
Guzman-Navarrete, Werner	Chief Engineer
Thomsen, Sascha	2nd. Eng.
Hermesmeyer, Dieter	2nd. Eng.
Rieper, Uwe	Electrician
Grossmann, Matthias	Ch. Electron. Eng.
Borchert, Wolfgang	System Manager
Blohm, Volker	Fitter
Krawczak, Ryszard	Motorman
Peplow, Michael	Motorman
Kallenbach, Christian	Apprentice / MPR
Schernick, Robert	Apprentice / MPR
Wieden, Wilhelm	Chief Cook
Garnitz, André	2nd Cook
Schmandke, Harald	Chief Steward
Royo, Luis	2nd Steward
Mucke, Peter	Boatswain
Bierstedt, Torsten	Multi-purpose Rating / A.B.
Dolief, Joachim	Multi-purpose Rating / A.B.
Eidam, Oliver	Multi-purpose Rating / A.B.
Ross, Reno	Multi-purpose Rating / A.B.
Stängl, Günter	Multi-purpose Rating / A.B.
Grawe, Manuel	Apprentice / MPR
Schröder, Andreas	Apprentice / MPR

Institutions

MARUM

Zentrum für Marine Umweltwissenschaften
Universität Bremen
Leobener Straße
28359 Bremen
Germany

GeoB

Fachbereich Geowissenschaften
Universität Bremen
Klagenfurter Straße
28359 Bremen
Germany

BGR

Bundesanstalt für Geowissenschaften und
Rohstoffe
Stilleweg 2
30655 Hannover
Germany

TONGJI

State Key Laboratory of Marine Geology
Tongji University
1239, Siping Road
Shanghai, 200092
P.R. China

ZMT

Leibniz-Zentrum für Marine
Tropenökologie GmbH
Fahrenheitstraße 6
28359 Bremen
Germany

Tübingen

Institut für Geowissenschaften
Eberhard-Karl Universität
Sigwartstraße 10
72076 Tübingen
Germany



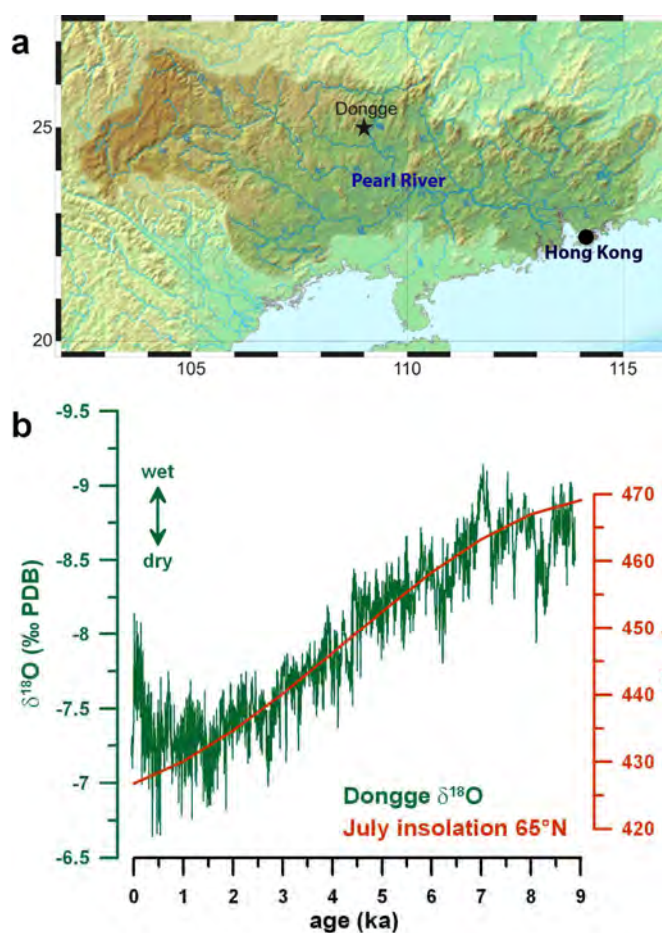
Fig. 1.1: Scientific party of expedition SO-221.

2 Research Program

High-resolution speleothem records from China have provided insights into the decadal-to millennial-scale variations of the East Asian Summer Monsoon (EASM) over the Holocene (e.g. Dykoski et al., 2005; Wang et al., 2005). The basic presumption is that shifts in the oxygen isotope ($\delta^{18}\text{O}$) composition of stalagmite calcite record changes in the amount of precipitation and thus, the EASM intensity (Wang et al., 2001; Yuan et al., 2004). These studies generally agree that the EASM reached maximum intensities during the Early Holocene around 8,000 years ago followed by a gradual decrease in summer monsoon precipitation until 2,000 years ago (Fig. 2.1). The decline in the EASM intensity has been attributed to a continuously decreasing insolation as the main driver of large-scale monsoon changes over the Holocene (Wang et al., 2005).

Figure 2.1.

a) Catchment area of the Pearl River (shaded) and the position of the Dongge Cave (star). b) Oxygen isotope record of Dongge Cave deposits during the Holocene (green; Dykoski et al., 2005). Superimposed is July insolation at 65°N (red). Note the mismatch during the past 2,000 years.



Superimposed on this general trend are abrupt, stepwise changes in the EASM rainfall on timescales of a century and shorter (Wang et al., 2005; Overpeck and Cole, 2007). Most pronounced is a shift to lighter $\delta^{18}\text{O}$ values in Dongge Cave stalagmites during the past 500 years that would suggest an increase in monsoonal rainfall despite a continuously decreasing Northern Hemisphere summer insolation (Fig. 2.1).

Moreover, the Late Holocene EASM evolution reconstructed from Dongge Cave contrasts paleo-monsoon reconstructions derived from marine sedimentary archives in the northern South China Sea (SCS) that show an increase in sea-surface salinity off the Pearl River mouth (Fig. 2.2, Wang et al., 1999a; 1999b). Present-day observations show a distinct monsoonal behavior of the Pearl River discharge that strongly influences the hydrographic characteristics of the northern SCS (Su, 2004), with a distinct freshwater plume forming during the summer monsoon, when the discharge of the Pearl River is highest (Dong et al., 2004).

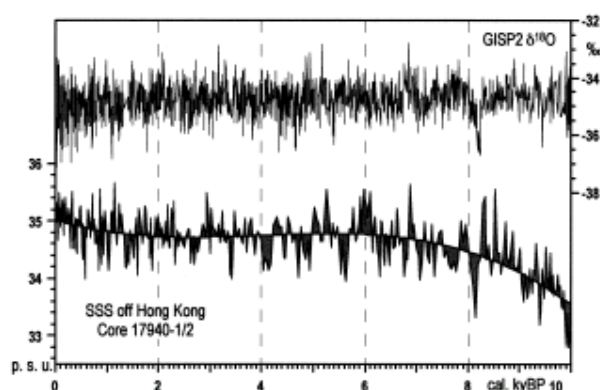


Figure 2.2. Holocene salinity reconstruction off Hong Kong (Wang et al., 1999a) showing increased salinity, indicating decreased riverine discharge during the past 2,000 years, contrasting the Dongge Cave $\delta^{18}\text{O}$ record that suggests increased rainfall during this period.

Therefore, increasing sea-surface salinity in the northern SCS implies decreasing EASM rainfall during the Late Holocene, and contradicts the $\delta^{18}\text{O}$ trend in Dongge Cave. Possible explanation for this mismatch is interfering seasonality and/or habitat effects taking place by using proxy data from different faunal groups to calculate paleo-sea-surface salinity, or other processes than EASM precipitation controlling the $\delta^{18}\text{O}$ composition of drip water in the Chinese caves (e.g. Maher, 2008). An alternative hypothesis has been put forward by Wang et al. (2008). Accordingly, the $\delta^{18}\text{O}$ of cave deposits may be influenced by changes in the Dole effect.

In addition to natural variations, human activities might have an effect on rainfall in the monsoon realm. In particular, human-induced land-cover changes result in significant alteration of surface dynamic parameters, such as albedo, surface roughness, leaf area index, and vegetation coverage. Some studies argue that human-induced forcing even superseded natural forcing as the major driver of EASM changes (Fu, 2003; Zhang et al., 2008). Evidence from archaeological sites indicate human-induced land-use change in China since more than 9,000 years ago, with a ten-fold increase of archaeological sites in rice-growing regions of China between 6,000 and 4,000 years ago (Ruddiman et al., 2008 and references therein). Numerical experiments suggest that the gradual replacement of natural ecosystems by farmland and rice paddies significantly weakened the EASM during the past 3,000 years (Fu, 2003). Anthropogenic greenhouse gases and aerosols have been identified as the main driver of temperature and precipitation variability over China since the second half of the 20th century (Zhang et al., 2008). To what extent EASM affects, or is modified by, such changes is a central question yet to be addressed in this densely populated region in order to prognosticate the variability of precipitation in Central Asia, which is of enormous importance for the development of regional national economies.

During the SO-221 INVERS cruise, it was intended to sample highly resolved marine climate archives using the Bremen Sea Floor Drill Rig (MeBo) in the northern South China Sea. Novel proxies applied to these archives combined with climate modeling will allow reconstructing the natural variability of the East Asian summer monsoon during the last interglacial (Eemian). A focus will be on changes in the vegetation and the hydrological cycle in the 400,000 km² large watershed of the Pearl River during this climate period. A model-based comparison of the natural development during the Eemian with the already anthropogenic affected Holocene development aims at assessing the relative weighting of natural and anthropogenic forcing factors. Thus, INVERS will broaden the knowledge base

on climate change in Central Asia and will improve scenarios outlining the future dynamic of the monsoon system.

References

- Dong L, Su J, Ah Wong L, Cao Z, Chen J-C (2004). Seasonal variation and dynamics of the Pearl River plume. *Cont Shelf Res* 24, 1761-1777.
- Dykoski CA, Edwards RL, Cheng H, Yuan D, Cai Y, Zhang M, Lin Y, Qing J, An Z, Revenaugh J (2005). A high-resolution, absolute-dated Holocene and deglacial Asian monsoon record from Dongge Cave, China. *Earth Planet Sci Lett* 233, 71-86.
- Fu C (2003). Potential impacts of human-induced land cover change on East Asia monsoon. *Glob Planet Change* 37, 219-229.
- Maher BA (2008). Holocene variability of the East Asian summer monsoon from Chinese cave records: a reassessment. *Holocene* 18, 861-866.
- Overpeck JT, Cole JE (2007). Climate change: Lessons from a distant monsoon. *Nature* 445, 270-271.
- Ruddiman WF, Guo Z, Zhou X, Wu H, Yu Y (2008). Early rice farming and anomalous methane trends. *Quart Sci Rev* 27, 1291-1295.
- Su J (2004) Overview of the South China Sea circulation and its influence on the coastal physical oceanography outside the Pearl River Estuary. *Cont Shelf Res* 24, 1745-1760.
- Wang L, Sarnthein M, Erlenkeuser H, Grimalt JO, Grootes P, Heilig S, Ivanova E, Kienast M, Pelejero C, Pflaumann U (1999a). East Asian monsoon climate during the Late Pleistocene: high-resolution sediment records from the South China Sea. *Mar Geol* 156, 245-284.
- Wang L, Sarnthein M, Erlenkeuser H, Grootes PM, Grimalt JO, Pelejero C, Linck G (1999b). Holocene variations in Asian Monsoon Moisture: a bidecadal sediment record from the South China Sea. *Geophys Res Lett* 26, 2889-2892.
- Wang Y, Cheng H, Edwards RL, He Y, Kong X, An Z, Wu J, Kelly MJ, Dykoski CA, Li X (2005). The Holocene Asian Monsoon: Links to Solar Changes and North Atlantic Climate. *Science* 308, 854-857.
- Wang YJ, Cheng H, Edwards RL, An ZS, Wu JY, Shen CC, Dorale JA (2001). A high-resolution absolute-dated Late Pleistocene monsoon record from Hulu Cave, China. *Science* 294, 2345-2348.
- Wang Y, Cheng H, Edwards RL, Kong X, Shao X, Chen S, Wu J, Jiang X, Wang X, An Z (2008). Millennial- and orbital-scale changes in the East Asian monsoon over the past 224,000 years. *Nature* 2008, 1090-1093.
- Yuan D, Cheng H, Edwards RL, Dykoski CA, Kelly MJ, Zhang M, Qing J, Lin Y, Wang Y, Wu J, Dorale JA, An Z, Cai Y (2004). Timing, Duration, and Transitions of the Last Interglacial Asian Monsoon. *Science* 304, 575-578.
- Zhang P, Cheng H, Edwards RL, Chen F, Wang Y, Yang X, Liu J, Tan M, Wang X, Liu J, An C, Dai Z, Zhou J, Zhang D, Jia J, Jin L, Johnson KR (2008). A Test of Climate, Sun, and Culture Relationships from an 1810-Year Chinese Cave Record. *Science* 322, 940-942.

3 Narrative of the Cruise

17.05.2012, Thursday

In the morning the first group of the scientific crew for the cruise SO-221 boarded the RV SONNE at the port of Hong Kong, P.R. China. The main target of this and the following three days was to install the 8 t Bremen Deep-Sea Drill Rig “MeBo” on RV SONNE. Supported by the well-organized and efficient Chinese dockers the discharge of the seven containers loaded with scientific equipment started immediately. Simultaneously, Chinese fitters and welders started to construct a basal frame for the MeBo Launch and Recovery System (LARS) beneath the ship's A-frame. Late in the evening the advanced preparation for the LARS setup was already ahead of the schedule, while the lab equipments were also fitted up in parts.



Fig. 3.1: RV SONNE preparing for expedition SO-221 in Hong Kong, China.

18.-20.05.2012, Friday-Sunday

Heavy rainfall over the course of Friday resulted in recurring interruption of the welding process and retardation of the LARS setup. All the labs except for the seismic could be prepared. On Saturday, the welding and the LARS setup could be finished in the morning. In the afternoon, despite the frequent rainfall with episodic shower all the MeBo containers could be placed on deck, the winch and the sheave block were installed, and the multi-corer was assembled. On Sunday, final preparations of the MeBo were finished, though occasionally interrupted by heavy rainfall, and the seismic equipment was set up. At 5 pm, RV SONNE left the dock to lie in the roads for bunkering.

21.05.2012, Monday

This day was used to check the sheave and the MeBo winch, plus the first under water test of Mebo. All the checks were successful and we left the roads at 3 pm heading towards the first station of the cruise in the South China Sea. After leaving the coastal area, the see forced some of the participants to stay in their cabins and skip the dinner. Late in the evening

we finally received the work permit from the National Ocean Bureau of China and planned the seismic profile around the first MeBo site.

22.05.2012, Tuesday

After arriving at the first way point, we started the first seismic profile with 5 kn cruise speed along an E-W Transect about 170 nm SE off Hong Kong, just north of the ODP Site 1146 and in the vicinity of the core GIK 17931 and 17932 collected during the SO-95 cruise. The aim of the survey was to find relatively shallow sites around 1000m water depth on the upper continental margin, where we expected most of the terrigenous material that have been most likely supplied by the Pearl River.

23.05.-24.05.2012, Wednesday-Thursday

In the morning of 23rd the GI gun and the streamer were collected and the first MeBo deployment started at about 20° 8' N and 116° 14' E, at about 1010m water depth. This site was selected based on the seismic and Parasound data showing more than 100m of undisturbed, well-layered sediments that could be tracked down to 1500m along almost the entire profiles on the upper continental slope.



Fig. 3.2:. Basal frame for the MeBo Launch and Recovery System beneath the ship's A-frame.



Fig. 3.3:. MeBo harbor test in Hong Kong



Fig. 3.4:. first MeBo deployment at Site GeoB16601-1.

At a calm sea and under almost perfect weather conditions the MeBo could be lowered to the seafloor and started to drill early in the afternoon at the station GeoB 16601-1. Without any interferences or malfunctions the drilling reached already 50m below surface at around 11 AM on Thursday and was expected to be on deck around midnight.

25.05.2012, Friday

At 1 AM in the morning the MeBo was finally on deck after drilling 66.15 meters below seafloor (mbsf). The entire morning was spent to handle the Me-Bo core barrels, cut and label the liners and core-catchers, while a bathymetric and Parasound survey was carried out to fill the gaps between the previous profiles. At 8 AM we started the other gears at the same station and deployed successfully the CTD-rosette water sampler, Multi-net, Multi-corer and gravity corer. Sampling and measuring of the collected material started immediately until very late in the evening. Meanwhile the MeBo was re-loaded and prepared and was lowered in the afternoon to drill a second hole at the same site. Finally at about midnight a busy day ended and the participants could get some well-deserved rest.

26.05.2012, Saturday

The entire day was spent for cutting, describing and color scanning and wrapping up the MeBo cores in the lab. On the other hand, the MeBo team was also drilling the entire day and reached the 60 mbsf late in the evening.



Fig. 3.5: Chinese cruise participants at the Geo-lab handling the MeBo cores.

27.05.2012, Sunday

In the morning the MeBo was recovered and brought on deck after drilling 73.8 mbsf. This was the longest core ever collected by the MeBo. The work on deck and in the Geo-lab began immediately and was finished late in the afternoon. After a second deployment of the Multi-net in the upper 100m of water column, RV SONNE left the first station and headed towards the second station at around 18°40' N 113°40' E. Around midnight the seismic survey began at about 1000m water depth with several profiles down- and upslope.

28.05.2012, Monday

The entire day was spent for seismic survey, while in the Geo-lab the remaining cores from the first MeBo station were opened, described and color-scanned. In general, only little lithological changes could be observed probably due to high sedimentation rates at this site suggesting a high temporal resolution of this record. In the afternoon the second MeBo core was opened and described until late in the evening. Logging data showed an almost perfect correlation between the two holes, and that the variability in gamma-ray was mainly caused by K concentration indicative of changes in the amount of clay minerals in both sedimentary records. Among others, the bore hole logging data suggest that the same sediment packages were drilled in the two MeBo deployments, a finding that was additionally confirmed by the visual description of the retrieved sediments.

29.05.2012, Tuesday

Results from the seismic and Parasound surveys revealed undisturbed sediment sequences of up to 400m thickness in the westernmost part of the study area making the selection of an appropriate site for MeBo-coring not necessarily easier, as the decision should consider the delicate balance between a high-resolution climate archive on one hand and a sufficient temporal coverage reaching back to MIS 5 on the other. At last, two sites were selected with one regarded as the “high-resolution” site at about 18° 57' N, 113° 42' E, and the other as the “lower-resolution” site at about 18° 55' N, 113° 43' E. Station GeoB 16602, the “high-res.-site”, started early in the morning of Tuesday with CTD-Rosette water sampler followed by Multi-net, Multi-corer, and gravity corer with 12m rope length. All gears were successful and the retrieved material was sampled, labelled and packed immediately after the retrieval except for the gravity core. After a short transit to the “lower-sed.-site” GeoB 16603, another 12m gravity corer was deployed with a recovery of nearly 10m, similar to GeoB 16602-4. From late evening to early morning the seismic, bathymetric and sediment surveys were conducted to fill the data gaps in the westernmost study area.

30.05.2012, Wednesday

Early in the morning the deployment of MeBo at station GeoB 16602 started under perfect weather conditions and continued the entire day. In the Geo-lab, the two gravity cores collected the day before were opened, described, color-scanned, and sampled in two series and 4 cm spacing.

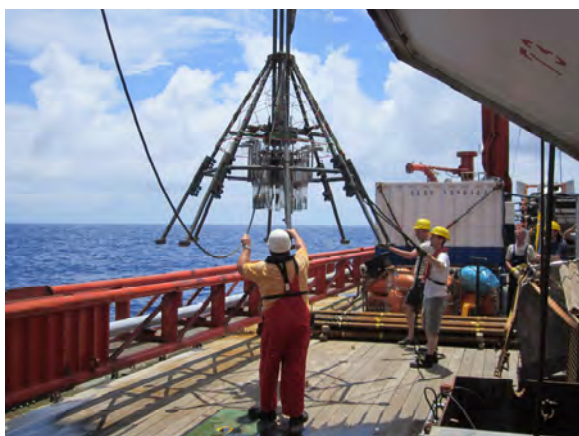


Fig. 3.6: Deploying the Multi-corer during SO-221.



Fig. 3.7: Cutting the MeBo cores at the Geo-lab.

31.05.2012, Thursday

In the afternoon the MeBo was recovered and brought sediments from down to 73.2 mbsf on deck. The core recovery was overwhelming, 106% total and 99% without the core catchers. In the mean time, another Multi-net through the upper 100 m of water column was deployed. In the evening we streamed to the site GeoB 16604, where seismic and bathymetric surveys revealed several chimney- or reef-like structures with almost no sediment cover. The deployment of a gravity corer brought no sediments but a handful of gravels and pebbles on deck consisting of carbonate rocks with manganese crusts. During the night the seismic survey was continued and ended early in the morning of the next day.

01.06.2012, Friday

Early in the morning the second MeBo deployment at GeoB 16602 started and continued the entire day, while in the Geo-lab the MeBo cores from the first deployment were cut, described and color-scanned. Late in the evening the work at Geo-lab was finished, while the MeBo-team reached the drilling depth of 40 mbsf.

02.06.2012, Saturday

The entire day was spent drilling the last barrels of the second MeBo deployment at station GeoB 16602-7. Early in the afternoon the MeBo reached 80.85 mbsf and the team started to collect the drill pipes and heave the MeBo on deck in the evening. Around 7 PM the MeBo was on deck and the same procedure of opening the core barrels and extracting the liners started, though interrupted twice by heavy rain shower. Borehole logging with natural gamma ray revealed that the penetration was in fact about 7 m deeper than the previous hole, fulfilling the expectations of the scientific party. During the night the final seismic survey of the study area started and lasted until early in the morning filling the remaining gaps in the seismic and bathymetric data.



Fig. 3.7: Cutting (left) and color scanning (right) of the MeBo cores in the Geo-lab.

03.06.2012, Sunday

Early in the morning the MeBo was already prepared for its next mission. After finishing the seismic profiling, deployment of the MeBo at the same site began (GeoB 16602-8). It was planned to drill triple cores to have a consistent recovery and avoid possible gaps between the core barrels on one hand, and on the other hand to collect more sediments, since the MeBo liners have a smaller diameter (6 cm) than the gravity core liners (12 cm). In the Geo-lab the opening, describing, scanning and storing of the core GeoB 16602-7 began and continued the entire day, while the seismic team continued processing the previous night's seismic and bathymetric data.

04.06.2012, Monday

The entire day was spent to finish the final drilling hole of the MeBo. At 7 PM the MeBo was on deck with sediments from up to 80.25 mbsf. After opening the barrels and carrying the liners in the Geo-lab, the liners were cut, sealed and labelled. Due to time restriction the last core was not opened and described in the lab but stored in the reefer. These tasks will be carried out later at MARUM, Bremen. Late in the evening and the entire night the bathymetric and Parasound surveys were completed, while the remaining scientific party started to pack and store the thus far collected material in the boxes and the reefer.

05.06.2012, Tuesday

Early in the morning we steamed to Hong Kong in order to arrive there during the high tide early in the morning of the next day. Meanwhile, all the labs were cleared and cleaned and the final preparations for disembarking were made.

06.06.-07.06.2012, Wednesday, Thursday

The final days of the cruise were spent for loading the reefer and the container. After collecting more than 370 m of sediment and 700 nm of seismic images the cruise participants disembarked on Thursday morning and the SO-221 cruise was brought to an end.

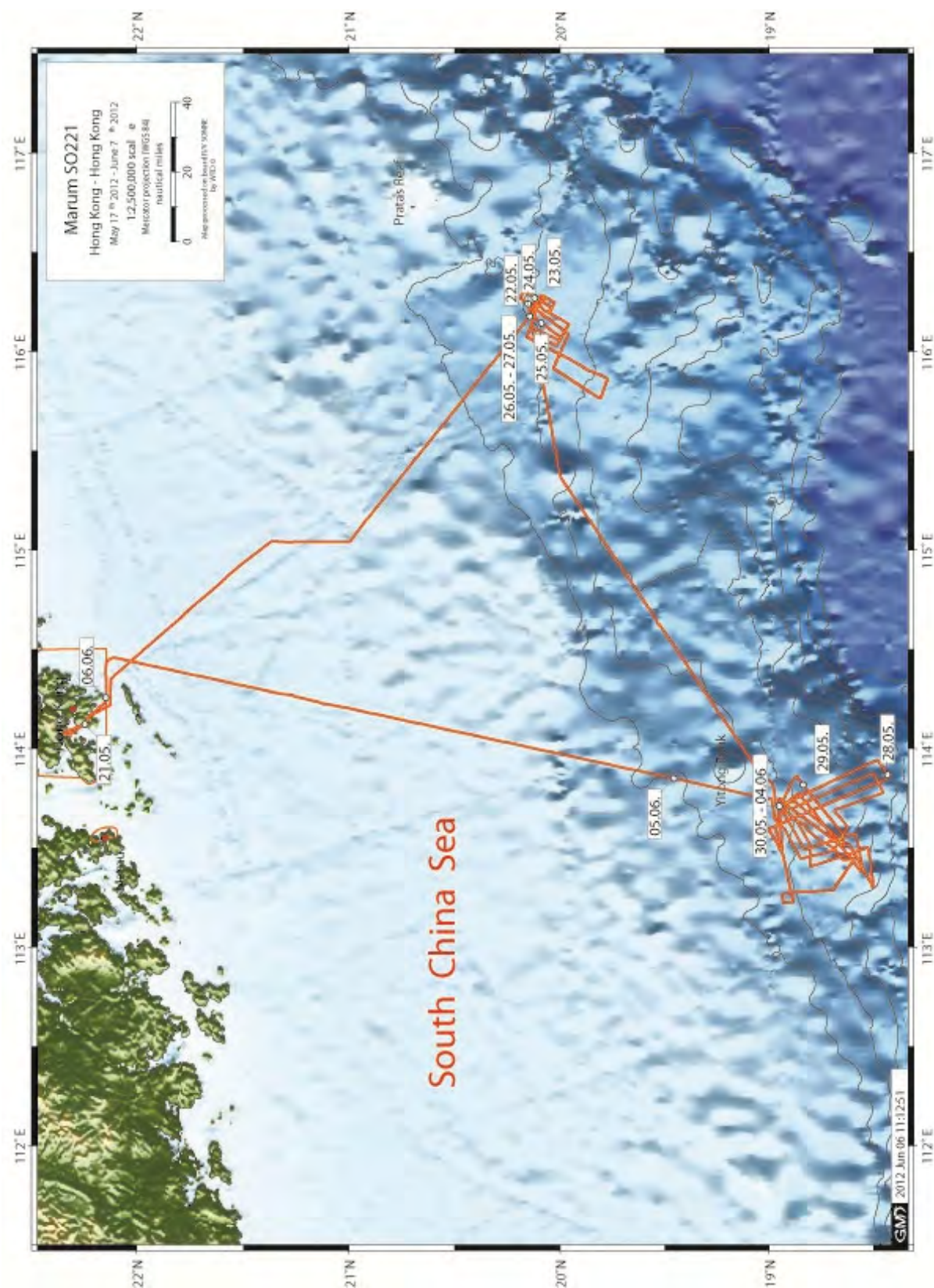


Fig. 3.11: Cruise plot of SO-221.

4 CTD Profiling and Water Sampling

(Dang, Liang, Munz, Weiner)

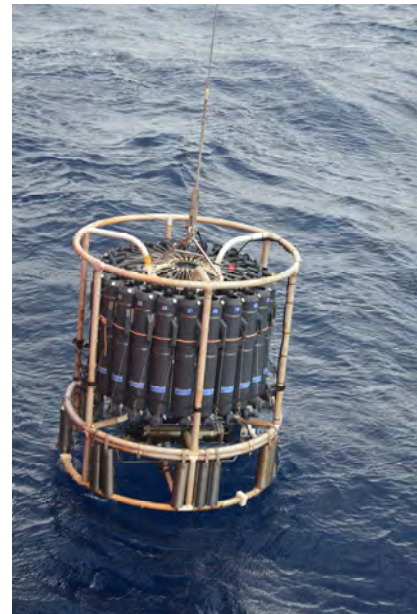
4.1 Introduction

The physicochemical properties of the water column have been measured with a CTD in order to define the water mass structure. This information was then used to define the sampling depths for rosette water sampling, which aimed at investigating the stable isotope composition of seawater. For this purpose, only small volume samples have been taken at depths including the euphotic zone, the thermocline, and the subsurface down to 800m water depth. The water samples were collected for stable carbon isotope ($\delta^{13}\text{C}$, 2 bottles) and stable oxygen isotope ($\delta^{18}\text{O}$, 1 bottle) studies at MARUM. Samples for $\delta^{13}\text{C}$ analysis were poisoned using mercury chloride (HgCl_2) and all bottles were sealed with wax. The premise of the sampling besides gaining useful information on water column characteristics and water masses at different sites is to compare water column with the planktic foraminiferal isotopic composition at different depths, the latter being collected with a Muti-net.

4.2 Instrumentation

A Seabird SBE911 CTD was used to obtain data on the physicochemical properties of the water column. Besides conductivity, temperature and pressure, the SBE911 measured dissolved oxygen (self-regenerative Clark-sensor with Teflon membrane). Water sampling was performed with a rosette water sample equipped with 24 Niskin bottles (10-liter volume each). During expedition SO-221, CTD measurements and water sampling were conducted at 2 stations (Tab. 4.1). Each cast was deployed in order to assess on one hand the water column characteristics and on the other hand to conduct a high resolution sampling of the upper 800 m of the water column.

Fig. 4.1: Deploying CTD-Rosette water sampler during the SO-221 cruise.



Tab. 4.1: CTD/Water sampler stations during cruise SO-221.

GeoB No.	Latitude [S]	Longitude [W]	Water Depth [m]	Instrument Depth [m]	Depth sampled [m]	Samples
16601-2	20°09,03′	116°14,39′	1014	800	800-700-600-500-400-375-300-200-174-150-134-110-73-48-23-8	MARUM
16602-1	18°57,07′	113°42,59′	950	800	800-700-677-600-500-400-300-268-252-222-166-146-110-85-59-45-28-18-8	MARUM

5 Plankton Sampling with the Multi-net

(Klann, Munz, Weiner)

5.1 Introduction

In order to investigate the plankton distribution and especially the assemblage of planktic foraminifera in the surface waters of the investigated area a multiple closing net (Multi-net) has been used on 2 stations during R/V Sonne cruise SO-221. Together with the CTD measurements and with the water sample analysis the Multi-net samples allow a more comprehensive characterization of the upper part of the water column.

5.2 Instrumentation

The Multi-net used during this cruise was the equipment assembled by Hydro-Bios, Kiel, Germany, made up of five individual 63µm nets, that can be remotely controlled opened consecutively, thus, allowing the sampling of five different levels within the water column. The Multi-net that has an opening of 0.25 m² was lowered to 700 m (first cast) and 100 m (second cast) water depth with 0.5 m s⁻¹ and heaved with 0.2 m s⁻¹. At pre-selected levels the nets were opened for collecting planktic foraminifera for genetic and morphological studies. Planktic foraminifera were picked immediately after the retrieval.

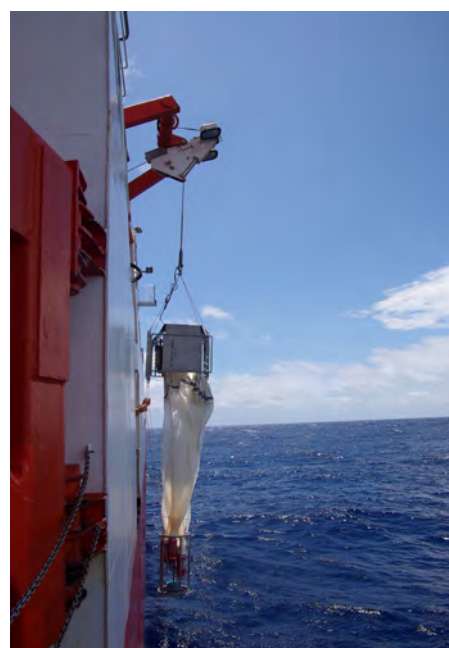


Fig. 5.1: Launch (top) and recovery (right) of the Multi-net during SO-221.

A brief overview of all stations sampled with the Multi-net can be found in Tab. 5.1. Remarkable was the very high amount of planktic foraminifera in all of the nets. The picked samples will be sent to MARUM for further analyses.

Tab. 5.1: Samples collected with the Multi-net during cruise SO-221.

GeoB No.	Latitude [°S]	Longitude [°W]	Water Depth [m]	Levels of the water column sampled [m]					Samples
				Net #1	Net #2	Net #3	Net #4	Net #5	
16601-3	20°09,05'	116°14,34'	1013	700-500	500-300	300-200	200-100	100-0	MARUM
16601-8	20°09,04'	116°14,40'	1014	100-80	80-60	60-40	40-20	20-0	MARUM
16602-2	18°57,11'	113°42,67'	950	700-500	500-300	300-200	200-100	100-0	MARUM
16602-6	18°57,18'	113°42,63'	949	100-80	80-60	60-40	40-20	20-0	MARUM

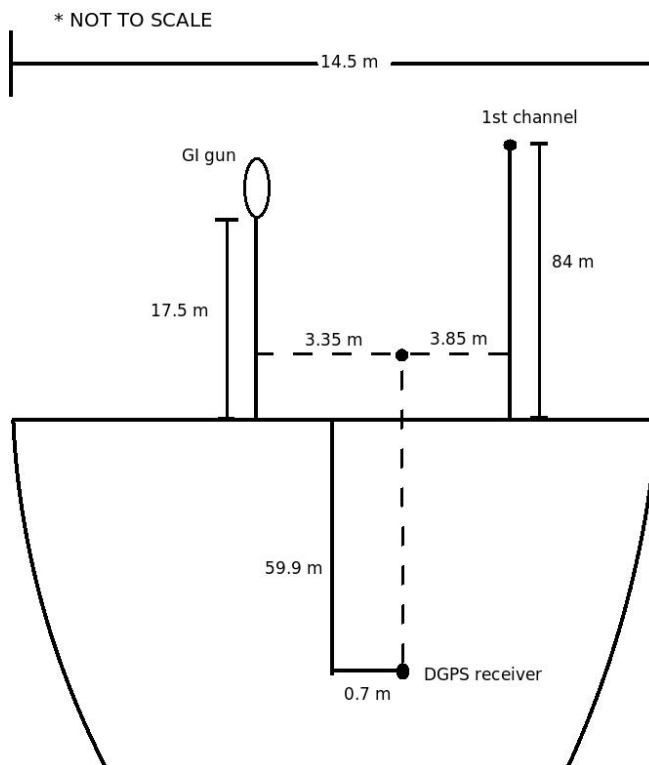
6 Seismic Surveying

(Iliev, Keil, Palamenghi)

6.1 Multi-channel Seismics

The GeoB multichannel seismic equipment was adjusted on cruise SO221 to provide high resolution seismic data on the one side and to consume as less deck space as possible due to the limitations given by the MeBo drill rig on the other. Hence only one seismic source was used at the starboard stern of the ship and a short streamer was deployed on the port side. In the following, all components are described in detail.

The seismic source used was a Soderia GI-Gun with 0.4 L generator volume and 0.4 L injector volume (frequency range app. 30-600 Hz) operated in harmonic mode. It was towed on the starboard side using the standard hanger assembly app. 17.5 m behind the stern. The gun depth was controlled by a buoy above the hanger to a total towing depth of ca. 1m. Towing geometries are shown in Figure 6.1. The gun was fired at an interval of 5000 ms.



On the port side of the ship's stern a conventional analogue streamer (Teledyne) was towed. It contains 16 groups of hydrophones with a spacing of 6.25, thus providing a total length of the active section of 100 m. Separation of the active section from the ship was maintained by an elastic stretch section of 21 m length and a lead-in of 60 m length. 20m behind the streamer a small tail buoy was connected to allow a visual position control. The streamer buoyancy was adjusted with lead attachments and towing depth was kept to approximately 1 – 1.5m by the length of the lead-in cable and the speed of the ship. No active depth levellers were available on this cruise; the quality control took place online in the recorded data by checking the shape of the sea floor reflection.

Fig. 6.1: Deck layout of the towing geometry.

However, due to mostly good to very good weather conditions the data quality did not suffer notably from the absence of direct depth control.

For data recording of the 16 channel analog streamer, the custom-designed and PC-based 16-channel seismic acquisition unit (SAU3) was used. The system consists of a 16 channel USB-AD-converter (NI USB 6259) with an additional analog amplifierboard and channel based antialias filters, limiting the maximum frequency to 500 Hz. The SAU3 was connected to a standard Lenovo Notebook equipped with the custom reliable MaMuCS (Marine MultiChannel Seismics) software for data recording, storage and online visualisation. It provides online data display of shot gathers as well as a brute stack section of the range of channels of the user's choice, and stores data in SEG-Y format on the internal hard disk drive. First back-up copies were created during intervals of no seismic activity on an external disk. The total recording length was set to 3000 ms at a sample rate of 125 μ s, a recording

delay between 500 and 2000 ms was applied to the data depending on the actual water depth. The measurement range of the AD-Converter was adjusted to 1 V.

The trigger unit controls the timing of the seismic source and the recording unit. Two different trigger units were used during this cruise. On Profiles GeoB-081 – 088 the custom made 6 channel trigger generator (SCHWABOX), which is built into the SAU3 system was used in conjunction with a two channel trigger amplifier driving the solenoid valves of the GI-gun. The SCHWABOX is connected via USB to the recording notebook and programmed with a small custom software tool. Due to minor technical problems at the beginning of profile GeoB12-089 we switched to the proven, but much more space consuming Bremen 16 channel trigger system. It is set up on an IBM compatible PC with a Windows XP operating system and includes a real-time controller interface card (SORCUS) with 16 I/O channels, synchronized by an internal clock. The unit is connected to an amplifier unit and a gun amplifier unit. The PC runs custom software.

Both systems allow defining arbitrary combinations of trigger signals. Trigger times can be changed at any time during the survey. Through this feature, the recording delay can be adjusted to any water depth without interruption of data acquisition. As only one gun was used, trigger times depend only on the water depth. Table 6.1 shows the applied trigger times.

Table 6.1: Trigger Scheme List

Profiles	Sources, shooting rate	Recording
GeoB12-081 – GeoB12-088 (Survey area 1)	Gi 0.4l, 5000ms	16 channel analogue, Recording delay 1000 ms
GeoB12-089 – GeoB12-108 (Survey area 2)	Gi 0.4l, 5000ms	16 channel analogue, Recording delay 500 – 2000 ms

Time synchronization of all systems was done based on GPS time, using the shipboard system GPS signal distributed via Ethernet UDP broadcast in the ship's network. Raw navigation data was recorded for the whole cruise on a separate navigation PC which also provided a map view of the study areas.

In total 28 multichannel seismic lines were shot during cruise SO221, approximately 700 km of seismic data were recorded in 2 different survey areas. The seismic source for all these lines worked absolutely reliably over the whole time and fired in total 54000 shots (see table 6.2 for complete profile list).

Although only a short 16 channel streamer could be used due to space restrictions on deck the data quality is generally very good. However, in the first survey area we faced very rough weather conditions which degraded the data quality to a certain extent.

Onboard processing of seismic data was carried out using the commercial software package VISTA for Windows (GEDCO). Geometry setup for this purpose was carried out using the custom seismic geometry software Wingeoapp. Brute stacks of the recorded data were created already online by the custom recording software MaMuCS.

After the preliminary processing the stacked data was loaded into our commercial seismic interpretation system Kingdom Suite (Seismic Micro Inc.). This step provided a very fast means to visualize the recorded data nearly immediately after recording in a geo-referenced system and allowed a highly flexible survey planning based on the observed sedimentary structures. Unfortunately, the USB dongle of this software failed right at the beginning of the cruise. This problem was fixed using the available permanent internet connection of the ship to set up a VPN connection to the Bremen university license server. Although this connection was frequently interrupted, Kingdom Suite could be run and used during most of the cruise time.

Table 6.2: Seismic profile list of SO-221.

Profile Nr	Start Date	Time	End Date	Time	Start Lat [N]	Lon [E]	End Lat [N]	Lon [E]	Start FFID	End FFID	Nr of shots	Profile Length [km]	Area	Comment
GeoB12-081	22.05.2012	04:10	22.05.2012	06:08	20°06.27	116°14.88	20°09.39	116°04.60	304	1736	1432	21.5	South China Sea	Survey area 1
GeoB12-082	22.05.2012	06:14	22.05.2012	11:23	20°09.02	116°04.09	19°46.61	115°51.85	1826	5548	3722	47.0	South China Sea	Survey area 1
GeoB12-083	22.05.2012	11:30	22.05.2012	12:34	19°46.50	115°51.31	19°48.30	115°46.02	5574	6299	725	9.9	South China Sea	Survey area 1
GeoB12-084	22.05.2012	12:34	22.05.2012	16:34	19°48.34	115°45.98	20°01.58	115°54.78	1	2820	2819	28.1	South China Sea	Survey area 1
GeoB12-085	22.05.2012	16:41	22.05.2012	18:54	20°01.73	115°55.20	19°57.63	116°05.10	2910	4493	1583	18.8	South China Sea	Survey area 1
GeoB12-086	22.05.2012	18:59	22.05.2012	22:49	19°57.80	116°05.50	20°11.16	116°16.59	4553	474	2648	30.7	South China Sea	Survey area 1
GeoB12-087	22.05.2012	22:50	22.05.2012	23:11	20°11.13	116°16.65	20°10.46	116°17.95	476	725	249	3.2	South China Sea	Survey area 1
GeoB12-088	22.05.2012	23:17	23.05.2012	01:04	20°10.06	116°17.98	20°02.90	116°13.60	779	2086	1307	16.8	South China Sea	Survey area 1
GeoB12-089	27.05.2012	20:03	28.05.2012	01:58	18°55.87	113°43.18	18°29.98	113°56.50	65	2926	4162	57.8	South China Sea	Survey area 2
GeoB12-090	28.05.2012	02:05	28.05.2012	03:08	18°28.51	113°56.08	18°25.66	113°51.45	2978	3734	756	10.3	South China Sea	Survey area 2
GeoB12-091	28.05.2012	03:15	28.05.2012	10:41	18°25.80	113°51.04	18°59.92	113°35.87	3810	416	5012	68.6	South China Sea	Survey area 2
GeoB12-092	28.05.2012	10:44	28.05.2012	12:11	19°00.08	113°35.67	18°56.52	113°28.80	458	767	918	13.3	South China Sea	Survey area 2
GeoB12-093	28.05.2012	12:22	28.05.2012	15:25	18°56.16	113°29.20	18°57.27	113°44.61	894	3110	2216	27.2	South China Sea	Survey area 2
GeoB12-094	28.05.2012	15:33	28.05.2012	19:34	18°56.74	113°44.63	18°40.75	113°31.74	3191	6092	2901	37.0	South China Sea	Survey area 2
GeoB12-095	28.05.2012	19:47	28.05.2012	20:10	18°40.06	113°32.19	18°38.80	113°33.58	6250	6523	273	4.3	South China Sea	Survey area 2
GeoB12-096	28.05.2012	20:14	29.05.2012	00:28	18°38.72	113°33.97	18°51.74	113°51.04	6567	2644	2995	40.0	South China Sea	Survey area 2
GeoB12-097	29.05.2012	11:50	29.05.2012	17:01	18°51.03	113°45.97	18°33.57	113°22.85	2661	2670	3660	52.4	South China Sea	Survey area 2
GeoB12-098	29.05.2012	17:08	29.05.2012	19:06	18°33.05	113°23.17	18°34.92	113°34.15	2710	4110	1400	19.7	South China Sea	Survey area 2
GeoB12-099	29.05.2012	19:11	29.05.2012	21:57	18°35.17	113°34.25	18°49.50	113°29.56	4165	108	1900	26.9	South China Sea	Survey area 2
GeoB12-100	31.05.2012	13:26	31.05.2012	13:46	18°38.81	113°30.74	18°37.27	113°30.89	25	266	241	2.6	South China Sea	Survey area 2
GeoB12-101	31.05.2012	13:52	31.05.2012	16:31	18°36.86	113°30.62	18°30.46	113°18.30	353	2231	1878	24.7	South China Sea	Survey area 2
GeoB12-102	31.05.2012	16:41	31.05.2012	18:52	18°29.98	113°18.32	18°31.53	113°29.81	2345	3916	1571	20.6	South China Sea	Survey area 2
GeoB12-103	31.05.2012	18:57	31.05.2012	22:19	18°31.83	113°30.00	18°47.61	113°24.51	3987	132	2937	31.2	South China Sea	Survey area 2
GeoB12-104	02.05.2012	12:21	02.05.2012	16:18	18°57.75	113°34.18	18°53.12	113°14.03	20	1473	2751	37.5	South China Sea	Survey area 2
GeoB12-105	02.05.2012	16:25	02.05.2012	16:55	18°53.34	113°13.62	18°55.80	113°13.31	1554	1900	346	4.7	South China Sea	Survey area 2
GeoB12-106	02.05.2012	17:02	02.05.2012	17:25	18°56.10	113°13.70	18°56.25	113°15.66	1983	2261	278	3.7	South China Sea	Survey area 2
GeoB12-107	02.05.2012	17:30	02.05.2012	20:18	18°56.00	113°15.99	18°41.92	113°17.21	2327	4378	2051	26.0	South China Sea	Survey area 2
GeoB12-108	02.05.2012	20:27	02.05.2012	22:32	18°41.41	113°17.66	18°35.55	113°26.76	4407	5953	1546	19.1	South China Sea	Survey area 2
Total:											54277	704		

6.2 Sub-bottom profiler, swath bathymetry sounder

During the cruise two different echosounders were operated by the scientific participants on a 24 hour schedule to provide high resolution information on the uppermost 50-100m of sediment and to gain detailed insight in the local bathymetry.

The hull mounted parametric sub-bottom profiler Parasound DS3 (Atlas Hydrographic) works as a narrow beam sediment echosounder, providing primary frequencies of 18 (PHF) and adjustable 18.5 – 24 kHz, thus generating parametric secondary frequencies in the range of 0.5 – 6 kHz (SLF) and 36.5 – 42 kHz (SHF) respectively. The secondary frequencies develop through nonlinear acoustic interaction of the primary waves at high signal amplitudes emitted by a transducer array of 128 transducers on a rectangular plate of approximately 1 m² in size. The wave interaction takes place only in the emission cone of the high frequency primary signals which is limited to an aperture angle of only 4° for the Parasound DS3. Therefore the footprint size is only 7% of the water depth and vertical and lateral resolution is significantly improved compared to conventional 3.5 kHz echosounder systems. The Parasound DS3 is an improvement of the former Parasound DS2 (Atlas Elektronik) and is installed on RV SONNE since 2008. The fully digital system provides important features like recording of the 18 kHz primary signal and both secondary frequencies, continuous recording of the whole water column, beam steering, different types of source signals (continuous wave, chirp, barker coded) and signal shaping. However, many of the new features are still in an experimental state. Data is digitized at a sample frequency of 96 kHz to evade aliasing effects for the high secondary frequency. A downmixing algorithm in the frequency domain is used to reduce the amount of data and allow data distribution over Ethernet.

For the standard operation a parametric frequency of 4 kHz and a sinusoidal source wavelet of 1 period were chosen to provide a good relation between signal penetration and vertical resolution. The 18 kHz primary signal and the 40 kHz parametric signal were also recorded permanently. On most lines the system was operated in the quasi-equidistant mode. This mode provides an optimal lateral coverage of the sea floor, since the echosounder calculates an intertwined trigger sequence using the 'unused' travel time of the signal in the water to emit additional pulses in a matter, which generates an equally spaced transmit/receive sequence with at least twice the rate of a standard send-receive-send-sequence. In this mode, usually a depth window of 600m was recorded in all signal frequencies. On selected profiles, for instance in vicinity of coring sites and water sampling sites the system was operated in the single pulse mode, which allow recording of the full water column and therefore provides insight in the particle concentration in the water column, especially for the higher signal frequencies.

The system worked with exceptional stability for the whole cruise period. This stability in conjunction with the automated watch keeping mode allowed a significant reduction of watch keeping times. The data quality is very high.

As the seismic data the Parasound data was loaded into the commercial seismic interpretation system Kingdom Suite (Seismic Micro) and therefore provided a very fast and valuable means to quickly get a first impression of the uppermost 50 – 80m of sediments.

Swath bathymetry was carried out along all profiles with the hull mounted Simrad EM120 (Kongsberg). The EM120 operates at a frequency of 12 kHz and provides 191 beams and a maximum swath angle of 128. To calibrate the depth determination algorithms in each survey area a deep CTD station was performed to provide a regional water sound velocity profile. The EM120 worked absolutely reliably throughout the cruise and provided a very high data quality.

7 Coring with the Seafloor Drill Rig MeBo

(Bergenthal, Düßmann, Freudenthal, Kaszemeik, Klein, Rehage, Reich, Reuter, Rosiak, Schmidt)

7.1. Introduction

During RV SONNE cruise SO221, the seafloor drilling rig MeBo (Fig. 7.1) was used for collecting long sediment cores. This device is a robotic drill that is deployed on the sea bed and remotely controlled from the vessel (Fig. 7.2). The complete MeBo-system, including drill, winch, launch and recovery system, control unit, as well as workshop and spare drill tools is shipped within six 20' containers. A steel armoured umbilical with a diameter of 32 mm is used to lower the 10-tons heavy device to the sea bed where four legs are being armed out in order to increase the stability of the rig. Copper wires and fibre optic cables within the umbilical are used for energy supply from the vessel and for communication between the MeBo and the control unit on the deck of the vessel. The maximum deployment depth in the current configuration is 2000 m.



Fig. 7.1: Launching the seafloor drill rig MeBo at station GeoB16602.

The mast with the feeding system forms the central part of the drill rig (Fig. 7.2). The drill head provides the required torque and rotary speed for rock drilling and is mounted on a guide carriage that moves up and down the mast with a maximum push force of 4 tons. A water pump provides sea water for flushing the drill string for cooling of the drill bit and for removing the drill cuttings. Core barrels and rods are stored on two magazines on the drill rig. We used wire-line core barrels (HQ) and hard metal drill bit with 55 mm core diameter (push coring). The stroke length was 2.35 m each. With complete loading of the magazines a maximum coring depth of more than 70 m can be reached. Station time can reach more than 24 hrs per deployment.

The MeBo was deployed 5 times at 2 stations to sample long cores in the South China Sea. In total, the MeBo was deployed for almost 172 hours, in which 374 m were drilled. During 4

of the 5 deployments the drill string was flushed through the upper meters in order to reach deeper coring depths. 341 m were cored in total with an average recovery rate of 94%. Detailed information on deployment of MeBo and recovery of sediments is summarized in the station list (Table 7.1).

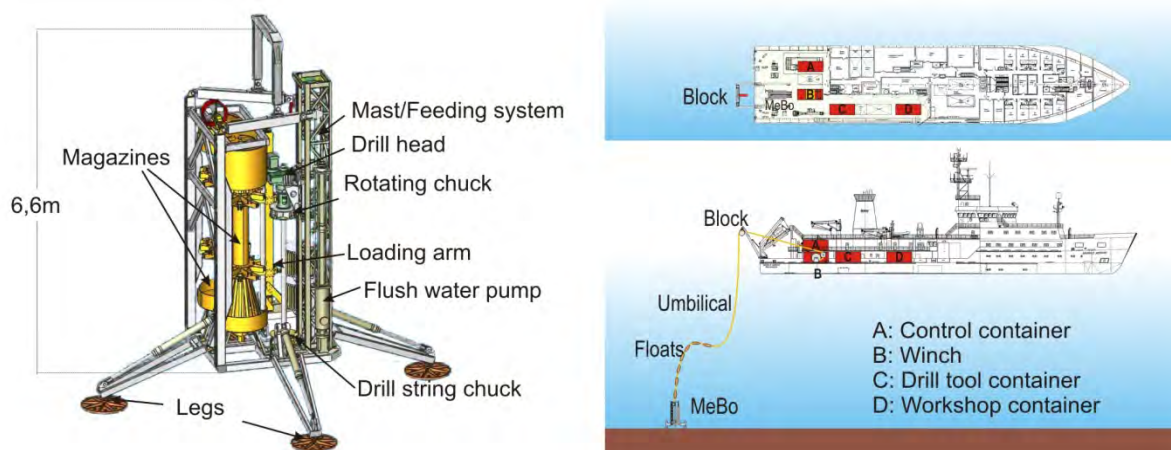


Fig. 7.2: Schematic overview of the MeBo drill rig (left) and its deployment from a research vessel (right).

Table 7.1: Station list for MeBo deployments.

Station GeoB No.	Deployment duration [hrs:min]	Latitude [N]	Longitude [E]	Water depth [m]	Drill depth [cm]	Coring interval [cm]	Recovery	Remarks
16601-1	37:58	20° 9,00'	116° 14,41'	1024	6615	0-6615	5587 cm 84%	
16601-7	34:28	20° 9,02'	116° 14,41'	1016	7380	565 - 7380	5801 cm 85%	
16602-5	32:22	18° 57,15'	113° 42,65'	963	7320	505 - 7320	7215 cm 106%	Recovery rate higher 100% due to expansion of gas-rich cores
16602-7	34:10	18° 57,1'	113° 42,6'	954	8085	1270-8085	6292 cm 92%	
16602-8	32:44	18°57,08'	113°42,57'	953	8025	975-8025	7176 cm 102%	Recovery rate higher 100% due to expansion of gas-rich cores
Total	171:42				37425	34110	32071 cm 94%	

7.2 Spectral Gamma Ray Borehole measurements

A Spectrum Gamma Ray Memory Probe (SGR-Memory) consisting of a Spectral Gamma Ray Probe (Antares 1460) combined with a Memory Data Logger (Antares 3101) was used for bore hole logging at the MeBo drilling sites. The Spectrum Gamma Ray probe is equipped with a 30 cm long scintillation crystal combined with a photo-multiplier. Light impulses that are generated by gamma ray collisions with the scintillation crystal are counted and analysed concerning the energy spectrum. The three naturally occurring gamma ray emitter - potassium, uranium and thorium - generate different energy spectra. A GeoBase software package is used to calculate a best fit for the spectra. By combining the results of the Spectrum fit with the gamma ray counts the concentrations of K, U, and Th are calculated.

The SGR-Memory is an autonomous tool that is used with the MeBo drilling system. When the maximum coring depth is reached the inner core barrel is replaced by the probe. The gravity point of the sensor is located about 125 cm above the drill bit and measures through the drill pipe. The probe is hooked up the bore hole together with the drill pipe during recovery of the drill string (logging while tripping). Tripping speed was about 1m per minute. In one case (GeoB16601-7) tripping had to be stopped due to a malfunction of the MeBo rotary head. The measurement was finished by hooking up the tool inside the drill string with the MeBo wireline winch. The SGR Memory was deployed at both MeBo drilling sites twice (Tab. 7.2).

Table 7.2: Station list for the SGR-Memory deployments.

Station GeoB No.	Latitude [S]	Longitude [W]	Water depth [m]	Logged interval [m]	Remarks
16601-1	20° 9,00'	116° 14,41'	1124	64,5 - 0	
16601-7	20° 9,02'	116° 14,41'	1016	72,1 - 0	72,1m -27,7m while tripping 30-0m lifted by wire
16602-5	18° 57,15'	113° 42,65'	963	71,6 - 0	
16602-7	18° 57,1'	113° 42,6'	954	79,2 - 0	

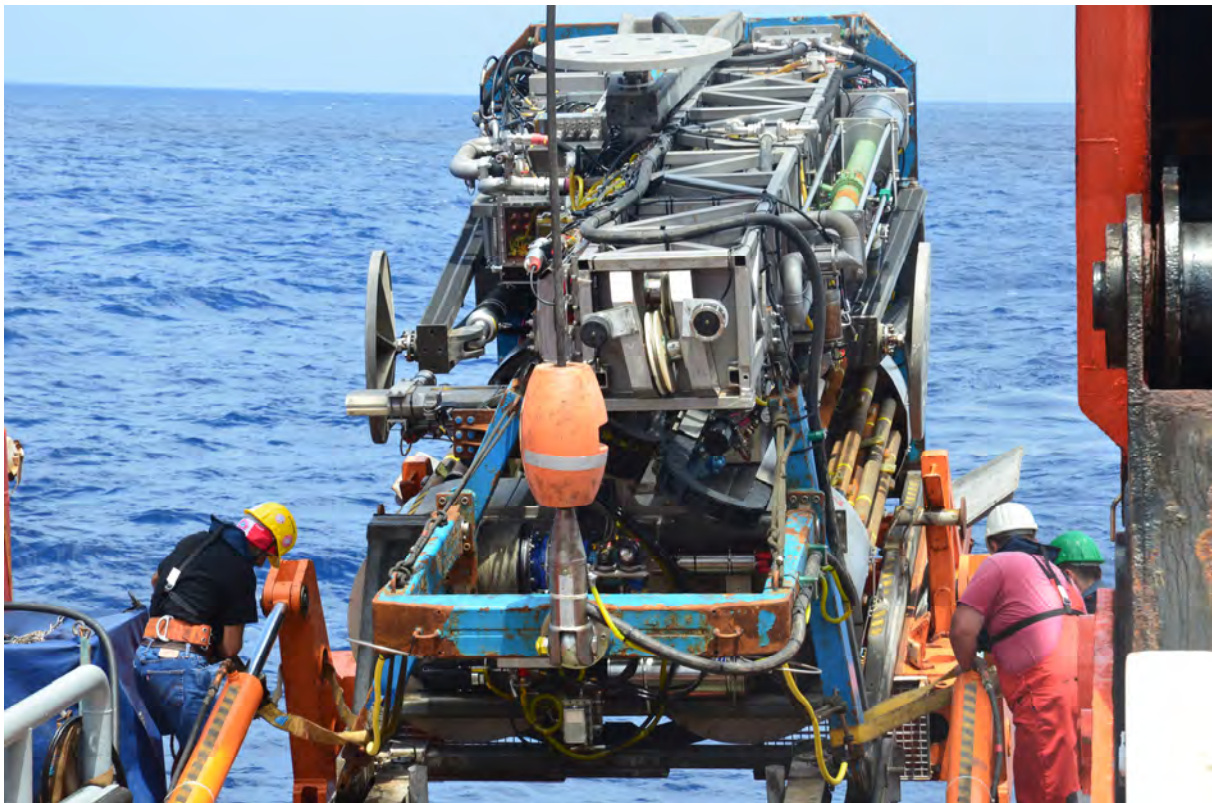


Fig. 7.3: Recovery of the seafloor drill rig MeBo at station GeoB 16602.

8 Sediment Sampling

(Contreras, Dang, Ge, Klann, Li, Liang, Lückge, Mohtadi, Munz, Steinke, Weiner)

8.1 Introduction

Aside from the MeBo drillings, sediments from the northern South China Sea were sampled at two stations GeoB 16601 and 16602. The purpose of these samplings was to characterized possible MeBo-drilling sites detected during the seismic site surveys. For these studies, a multi-corer (MUC) and a gravity corer (GC) with a tube of 12 m have been used for retrieving surface sediments and longer sediment cores, respectively.

8.2 Multi-corer

The main tool for the sampling of undisturbed surface sediments was the multi-corer (MUC) equipped with six large (diameter of 10 cm) and four smaller (diameter of 6 cm) plastic tubes of 60 cm length. During the SO-221 cruise, 4 multi-corers have been deployed (Tab. 8.1). Two of them were successful and recovered between 30 and 40 cm of undisturbed surface sediment.

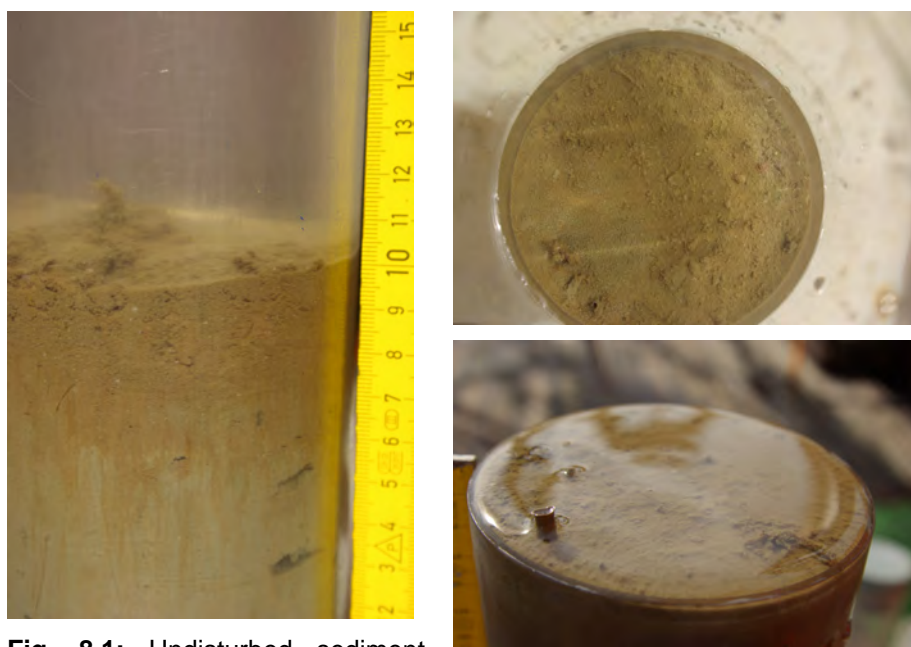


Fig. 8.1: Undisturbed sediment surface in multi-corer tubes

Table 8.1: Multi-corer sampling and sub-sampling during R/V SONNE Cruise SO-221

GeoB No.	Latitude [S]	Longitude [W]	Water Depth [m]	Large tubes (10 cm diameter)						Small tubes (6 cm)				Core length [cm]
				#1	#2	#3	#4	#5	#6	#1	#2	#3	#4	
16601-4	20°09,05′	116°14,38′	1013	-/-	-/-	-/-	-/-	-/-	-/-	-/-	-/-	-/-	-/-	empty
16601-5	20°09,04′	116°14,41′	1013	PF	PF	PF	BM	BM	Se	Co	Co	BM	AR	36
16602-3	18°57,10′	113°42,64′	951	PF	PF	PF	BM	BM	Se	Co	Co	BM	AR	34
16603-2	18°55,54′	113°43,29′	979	-/-	-/-	-/-	-/-	-/-	-/-	-/-	-/-	-/-	-/-	empty

PF	Planktic forams	MARUM/Tongji
Se	Sedimentology	Tongji
Co	Organic geochemistry	BGR/ZMT
BM	Biomarker	ZMT/Tongji
AR	Archive	MARUM

8.2.1 Sub-sampling of the multi-corer

Depending on the availability of filled tubes, the “standard” sampling scheme for the multi-corer was sampled as follows:

- 2 large tubes cut into 1 cm thick slices for planktic foraminiferal investigations (MARUM)
- 1 large tube cut into 1 cm thick slices for planktic foraminiferal investigations (Tongji)
- 1 large tube with small openings for pore water analysis (Tongji)
- 1 large tube cut into 1 cm thick slices for clay mineralogy studies (Tongji)
- 1 large tube cut into 1 cm thick slices for biomarker studies (ZMT)
- 1 small tube cut into 1 cm thick slices for biomarker studies (Tongji)
- 2 small tubes cut into 1 cm thick slices for biomarker studies (ZMT)
- 1 small tube cut into 1 cm thick slices for the archive (MARUM)

8.3 Gravity Corer

To further assess the possible MeBo drilling sites, longer sediment sequences were obtained by a gravity corer with a pipe length of 12m and a weight of 1.5 tons. Before using the coring tools, the liners had been marked lengthwise with a straight line in order to retain the orientation of the core for later paleomagnetic analyses. Once on board, the sediment core was cut into 1 m sections, closed with caps on both ends and labelled. In total, 4 cores were retrieved with recoveries between 0 cm and 1036 cm (Table 8.2). From the 4 gravity corers taken during SO-221 only one brought no sediments on deck that was due to the site selection (GeoB 16604-1). This site was selected to test whether the dome-like structures on the seafloor observed during the seismic survey were of volcanic origin, chimneys, or cold water coral reef structures.



Fig. 8.2: Sampling the gravity cores in the Geo-lab.

Altogether ~30 m of sediment cores were recovered with the gravity corer during R/V SONNE Cruise 221.

Table 8.2: List of gravity cores retrieved during R/V SONNE Cruise SO-211

GeoB No.	Gear	Latitude [°S]	Longitude [°W]	Water Depth [m]	Recovery [cm]
16601-6	12 m tube	20°09,07′	116°14,38′	1012	1037
16602-4	12 m tube	18°57,12′	113°42,64′	951	970
16603-1	12 m tube	18°55,55′	113°43,33′	980	930
16604-1	6 m tube	18°39,47′	113°30,65′	913	0

8.3.1. Sampling of the gravity corers

All of the gravity cores recovered in the northern South China Sea were cut into an archive and work half. The archive half was used for core description and color scanning. The work half was sampled with two series of syringes (10 ml) for geochemical and faunal studies, both at 4 cm intervals.

8.3.2 Core description and color scanning

The core descriptions (chapter 10) summarize the most important results of the analysis of each sediment core following procedures applied during ODP/IODP cruises. All cores were opened, described, and color-scanned.

In the core descriptions (Fig. 10.1 to 10.119) the first column displays the lithological data that are based on visual analysis of the core and are supplemented by information from binocular and smear slide analyses. The sediment classification largely follows ODP/IODP convention. Lithological names consist of a principal name based on composition, degree of lithification, and/or texture as determined from visual description and microscopic observations.

In the structure column the intensity of bioturbation together with individual or special features (turbidites, volcanic ash layers, plant debris, shell fragments, etc.) is shown. The hue and chroma attributes of color were determined by comparison with the Munsell soil color charts and are given in the color column in the Munsell notation.

A GretagMacbethTM *Spectrolino* spectrophotometer was used to measure percent reflectance values of sediment color at 36 wavelength channels over the visible light range (380-730 nm) on all of the cores. The digital reflectance data of the spectrophotometer readings were routinely obtained from the surface (measured in 1 cm steps for gravity cores and 2 cm steps for MeBo cores) of the split cores (archive half). The *Spectrolino* is equipped with a measuring aperture with folding mechanism allowing an exact positioning on the split core and is connected to a portable computer. The data are directly displayed within the software package Excel and can be controlled simultaneously.



Fig. 8.3: Preparation of the gravity corer.



Fig. 8.4: Preparation of the Multi-corer.

From all the color measurements, for each core the red/blue ratio (700 nm/450 nm) and the lightness are shown together with the visual core description. The reflectance of individual wavelengths is often significantly affected by the presence of minor amounts of oxyhydroxides or sulphides. To eliminate these effects, we used the red/blue ratio (Figs. 10.1 to 10.119).

9 Shipboard Results

9.1 Water column

Temperature and conductivity profiles at both stations show a relatively shallow mixed-layer between 20 and 40 m with temperatures around 28°C (Figs. 9.1 and 9.2). Temperature and conductivity decrease sharply until about 100 m water depth and moderately further deep until ~500 m. Below 500 m temperature and conductivity decrease only slightly until 800 m. Likewise, the oxygen content of the two stations shows a similar profile except for water depths between 100 and 200 m: while the oxygen content at station GeoB 16601-2 decreases to 3.5 mg L⁻¹ with a minimum around 150 m depth, it remains between 4 and 4.5 mg L⁻¹ at station GeoB 16602-1 (Figs. 9.1 and 9.2).

Between 500 and 800 m, the decrease in oxygen content is only about 0.5 mg L⁻¹.

The CTD data suggest that the thermocline between 100 and 200 m in the study area is filled with the North Pacific Tropical Water (NPTW) with similar oxygen contents described in the literature (e.g. Qu et al., 2000). The second decrease in the oxygen content between 400 and 500 m (300 and 400 m) at GeoB 16601-2 (GeoB 16602-1) probably represents the upper North Pacific Intermediate Water (NPIW), while the relatively stable conditions below 500 m characterize the depths occupied by the core of the NPIW.

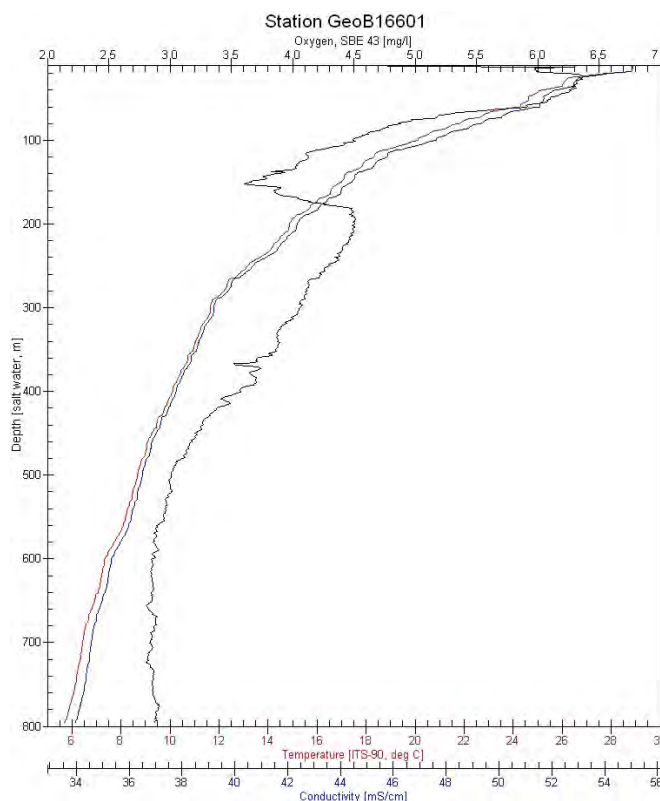


Fig. 9.1: CTD-data from station GeoB 16601-2.

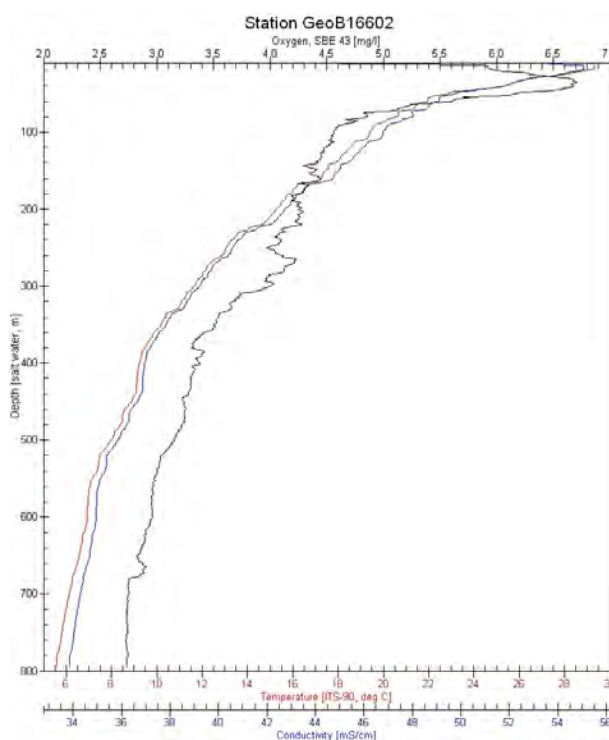


Fig. 9.2: CTD-data from station GeoB 16602-1.

Qu, T., Mitsudera, H., Yamagata, T. (2000). Intrusion of the North Pacific waters into the South China Sea. *J Geophys Res* 105, 6415-6424.

Table 9.1: Planktic foraminifera observed in the multi-net and pump samples of SO-221.

GeoB16601-3	Depth range	Identified species
25.05.12	700-500m	<i>G. ruber</i> , <i>G. siphonifera</i>
	500-300m	<i>G. siphonifera</i> , <i>G. ruber</i> , <i>H. pelagica</i> , <i>G. sacculifer</i> , <i>B. digitata</i>
	300-200m	<i>G. sacculifer</i> , <i>G. siphonifera</i> , <i>G. ruber</i> , <i>N. dutertrei</i> , <i>P. obliquiloculata</i>
	200-100 m	<i>H. pelagica</i> , <i>G. siphonifera</i> , <i>G. sacculifer</i> , <i>G. ruber</i> , <i>G. menardii</i> , <i>G. falconensis</i>
	100-0m	
GeoB16601	Pump 1	<i>G. ruber</i> , <i>G. siphonifera</i> , <i>G. sacculifer</i>
26.05.12	Time: 8h	
GeoB16601-8		
27.05.12	100-80m	<i>N. dutertrei</i> , <i>G. siphonifera</i> , <i>G. sacculifer</i> , <i>G. ruber</i>
	80-60m	<i>N. dutertrei</i> , <i>G. falconensis</i>
	60-40m	<i>G. bulloides</i> , <i>N. dutertrei</i> , <i>H. pelagica</i> , <i>G. ruber</i> , <i>G. siphonifera</i> , <i>O. universa</i> , <i>T. quinqueloba</i>
	40-20m	<i>G. siphonifera</i> , <i>G. sacculifer</i> , <i>G. ruber</i> , <i>N. dutertrei</i> , <i>P. obliquiloculata</i>
	20-0m	<i>G. siphonifera</i> , <i>G. ruber</i> , <i>O. universa</i> , <i>G. sacculifer</i>
Transit	Pump 2	<i>G. ruber</i> , <i>G. siphonifera</i> , <i>G. sacculifer</i>
27.-28.05.12	Time: 24h	
GeoB16602-2		
29.05.12	700-500m	<i>O. universa</i> , <i>G. siphonifera</i> , <i>G. ruber</i> , <i>G. sacculifer</i> , <i>N. dutertrei</i>
	500-300m	<i>G. ruber</i> , <i>G. sacculifer</i> , <i>B. digitata</i> , <i>G. siphonifera</i> , <i>T. quinqueloba</i> , <i>G. glutinata</i>
	300-200m	<i>G. ruber</i> , <i>G. sacculifer</i> , <i>G. siphonifera</i> , <i>G. falconensis</i> , <i>N. dutertrei</i> , <i>G. glutinata</i>
	200-100 m	<i>G. ruber</i> , <i>G. siphonifera</i> , <i>H. pelagica</i> , <i>N. dutertrei</i>
	100-0m	<i>G. ruber</i> , <i>G. sacculifer</i> , <i>G. glutinata</i> , <i>N. dutertrei</i> , <i>O. universa</i> , <i>G. siphonifera</i>
GeoB16602	Pump 3	<i>G. ruber</i> , <i>G. siphonifera</i> , <i>G. sacculifer</i> , benthic looking foram, menardii?
30.-31.05.12	Time: 14.5h	
GeoB16602-6		
31.05.12	100-80m	<i>G. sacculifer</i> , <i>G. siphonifera</i> , <i>H. pelagica</i> , <i>G. ruber</i>
	80-60m	<i>G. ruber</i> , <i>G. sacculifer</i> , <i>H. pelagica</i> , <i>G. siphonifera</i>
	60-40m	<i>G. ruber</i> , <i>G. sacculifer</i>
	40-20m	<i>G. ruber</i> , <i>G. sacculifer</i>
	20-0m	<i>G. ruber</i> , <i>G. sacculifer</i>
GeoB16602	Pump 4	<i>G. ruber</i> , <i>G. siphonifera</i> , <i>G. sacculifer</i> , benthic looking foram
01.-02.06.12	Time: 25.5h	
GeoB16602	Pump 5	<i>G. ruber</i> , <i>G. siphonifera</i> , <i>G. sacculifer</i>
02.06.12	Time: 25.5h	

9.2 Site Survey

Figure 9.4 shows a brute stack of seismic line GeoB12-086, reaching from 19°57.80'N / 116°05.50'E in the south-west to 20°11.16'N / 116°16.59'E in the north-east (see figure 9.3), thereby covering a depth range of approx. 1350 to 1000 m. The line crosses the MeBo site GeoB16601 towards the north-eastern end, indicated by the red line. The total signal penetration is variable, but reaches a maximum of 1000 ms two way travel time (TWT).

The profile shows, that the continental slope in the study area can be divided roughly in two different sedimentation regimes. While the upper part from offset 15000 to 27000 is characterized by a approximately 400 ms TWT thick package of well stratified sediments and a smooth seafloor surface, the lower part shows a more undulating morphology of the sea surface and also of the underlying reflectors with increasing sediment thickness towards depth. These upper sediment packages are furthermore divided in a 150 ms TWT package of reflectors showing comparatively high reflection amplitudes underlain by a 250 ms TWT thick layer of significantly weaker reflectors. The stratified upper sediments are then separated by a high amplitude reflector from the underlying acoustic basement.

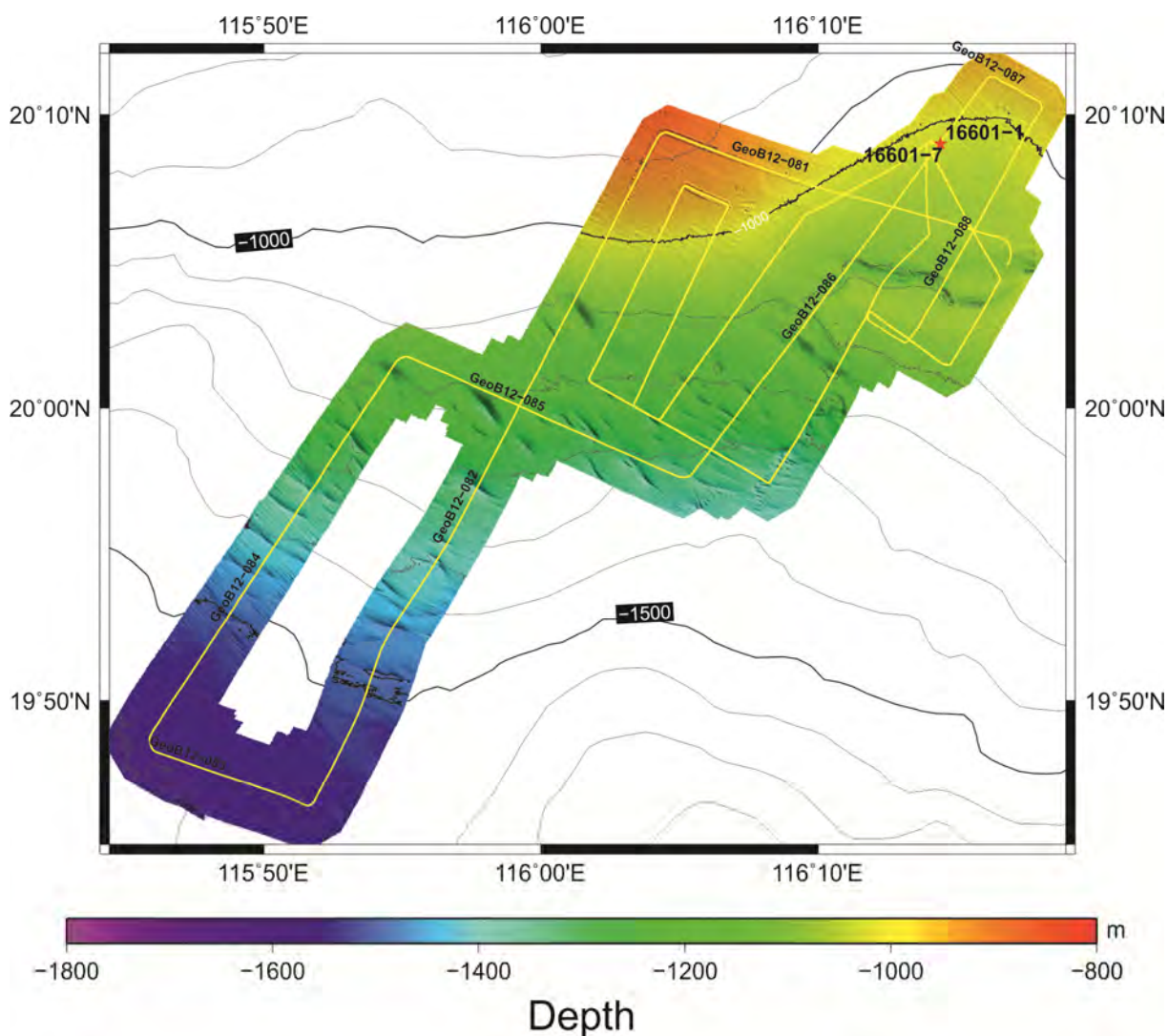


Fig. 9.3: Bathymetry of the first working area at and around GeoB 16601.

To access undisturbed sediments at the highest sedimentation rate, size 16601 was chosen as indicated in the upper well stratified sedimentation environment, especially as the influence of bottom current activity, related with the undulating sediment deposition further

down the slope could not be excluded. The close-up in figure 9.4 shows in detail the penetration of the MeBo drill cores in the sediment.

Figure 9.5 shows the parallel Parasound profile at the same lateral scaling. The signal penetration for the 4 kHz signal here reaches 100 m (based on a sound velocity of 1500 m/s). The high resolution generally shows the same separation of upper and lower part of the surveyed slope section with well stratified layers in the upper part and an undulating sedimentation pattern in the lower. Especially between offset 10000 and 16000 significant variations in layer thickness can be noted, including lateral variations in depot-centers and sections of non-deposition or erosion.

The Xisha Trough situates near 18°N in the northwest of the SCS, south of the Pearl River Mouth Basin. It is considered as a Cenozoic rift (He et al., 1980), whose evolution is closely related with the NW sub-basin, most likely had been mainly developed before 30 Ma and became a failed rift with the cease of the NW sub-basin (Shi et al., 2002). Though, its neighboring area has developed igneous activities later and some faults may be active now (He et al., 2009).

The composite GeoB12-094, -097, -101 profiles section shown in figure 9.7 was collected on the Northern flank of the Xisha Through and runs from north-east to south-west parallel to the margin (Fig. 9.6). The profile is characterized by an asymmetrical distribution of the sediment packages with respect to an outcrop of high amplitude, reflection free seafloor. The outcrop consists of a ridge elevated from a mean depth of 1500-1700 ms TWT up to a minimum depth of ca. 650 ms TWT. It has an irregular rough surface with pinnacles of variable height from few to tens of meters. No recent sedimentation seems to occur on the ridge, whereas a wedge shaped sediment package, ca. 600 ms TWT thick, downlaps the acoustic basement on the NE side of the outcrop. The sediment wedge partly climbs up the ridge root describing a broad U-shaped valley ca. 100 m deep.

The GeoB16602 coring site is located approx. 30 miles northwest of the flank of the outcropping ridge (Fig. 9.7). In the composite GeoB12-089, -093 line (Fig. 9.7) a succession of finely laminated sediments onlap the acoustic basement that makes two small sags before it deeps toward the south. The amplitude of the sedimentary sequence decreases with depth, whereas packages of re-enhanced high amplitude occur at the interface between the overlying sedimentary sequence and the acoustic basement. The acoustic record of the near surface sediments (Fig. 9.8) shows the same trend and in Site Survey Area 1 (Fig. 9.4) where, due probably to the impact of bottom current activity, the horizontal lamination is replaced by an undulating wavy deposition toward the south.

He, L.S., Wang, G.Y., Shi, X.C., 1980. Xisha Trough—a Cenozoic rift. *Geol. Rev.*, 26, 486–489.

He, L., Wang, J., Xu, X., Liang, J., Wang, H., Zhang, G., 2009. Disparity between measured and BSR heat flow in the Xisha Trough of the South China Sea and its implications for the methane hydrate. *Journal of Asian Earth Sciences*, 34, 771–780.

Shi, X., Zhou, D., Qiu, X., Zhang, Y., 2002. Thermal and rheological structures of the Xisha Trough, South China Sea. *Tectonophysics*, 351, 285–300.

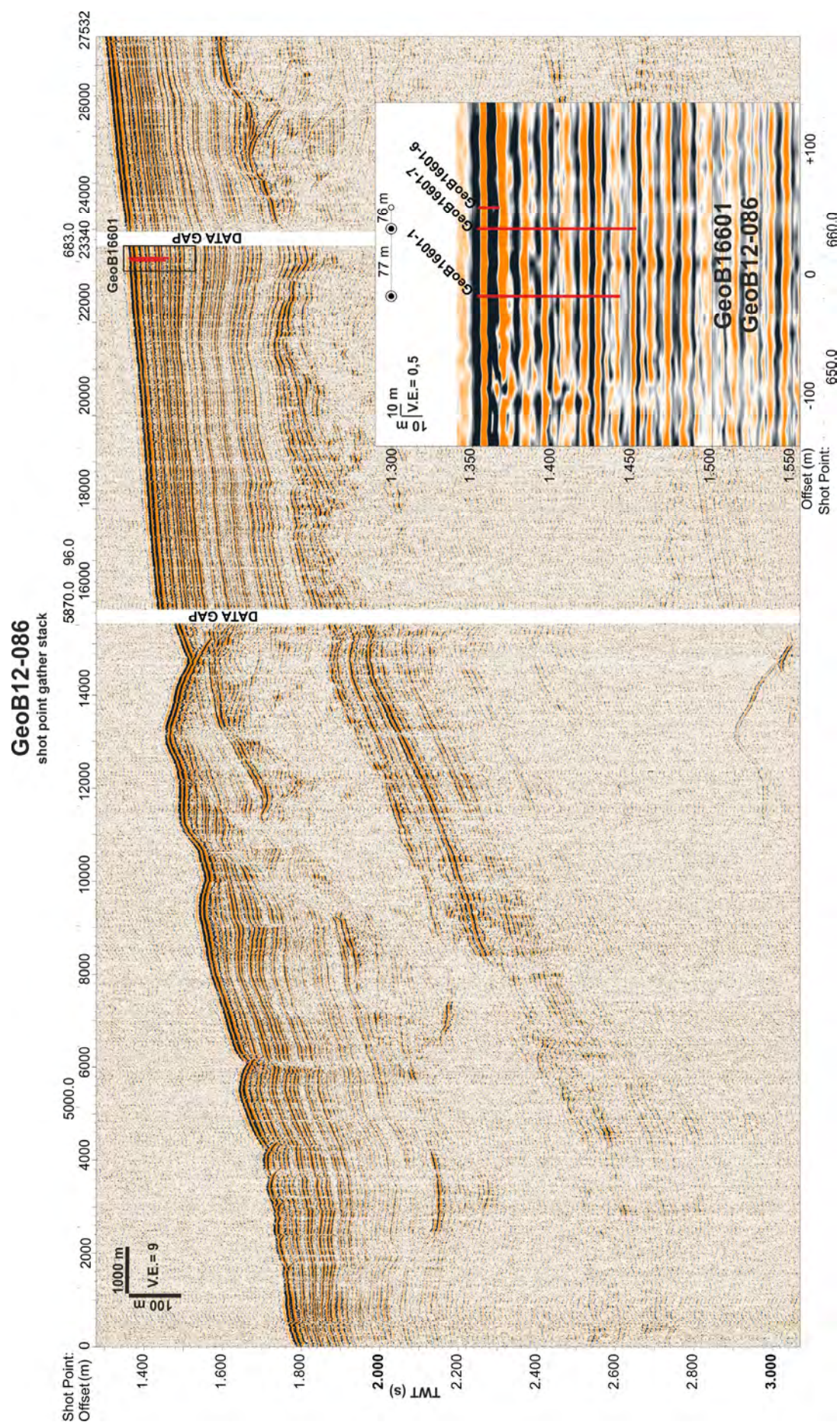


Fig. 9.4: Seismic images of the first working area at and around GeoB 16601.

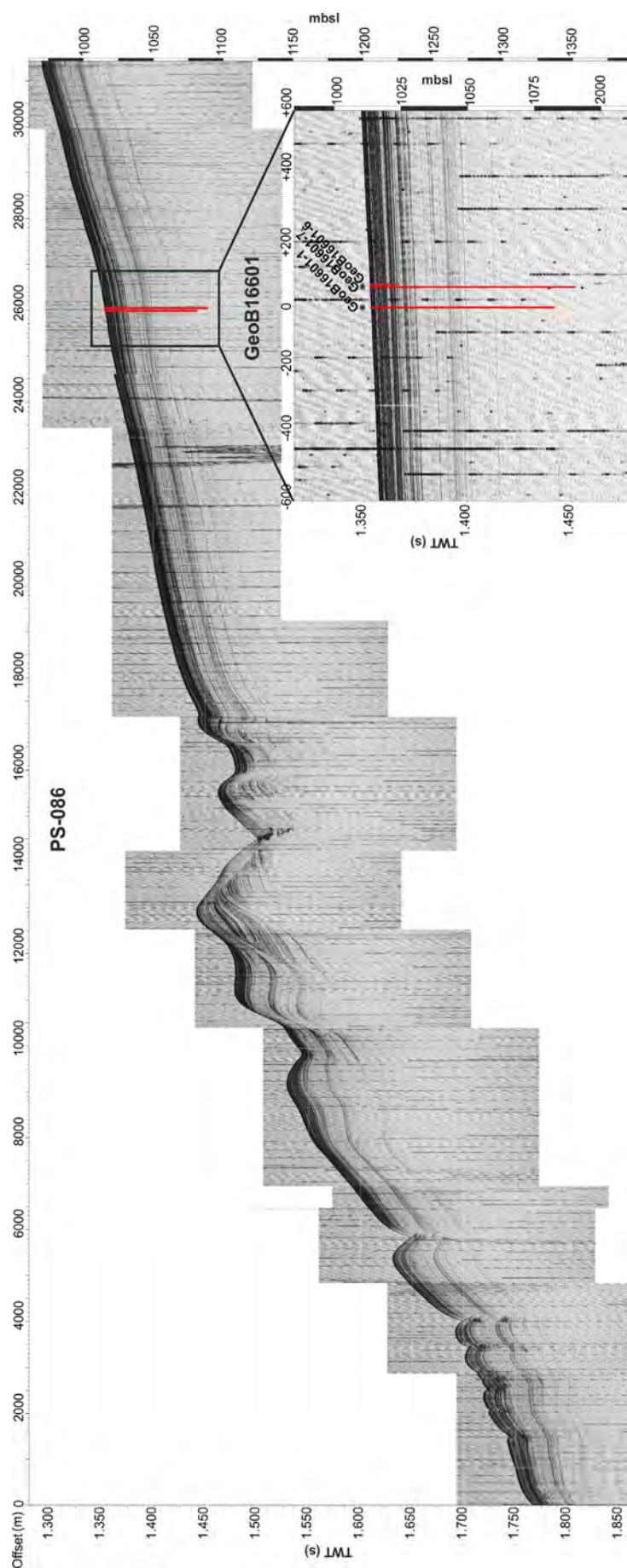


Fig. 9.5: Parasound images of the first working area at and around GeoB 16601.

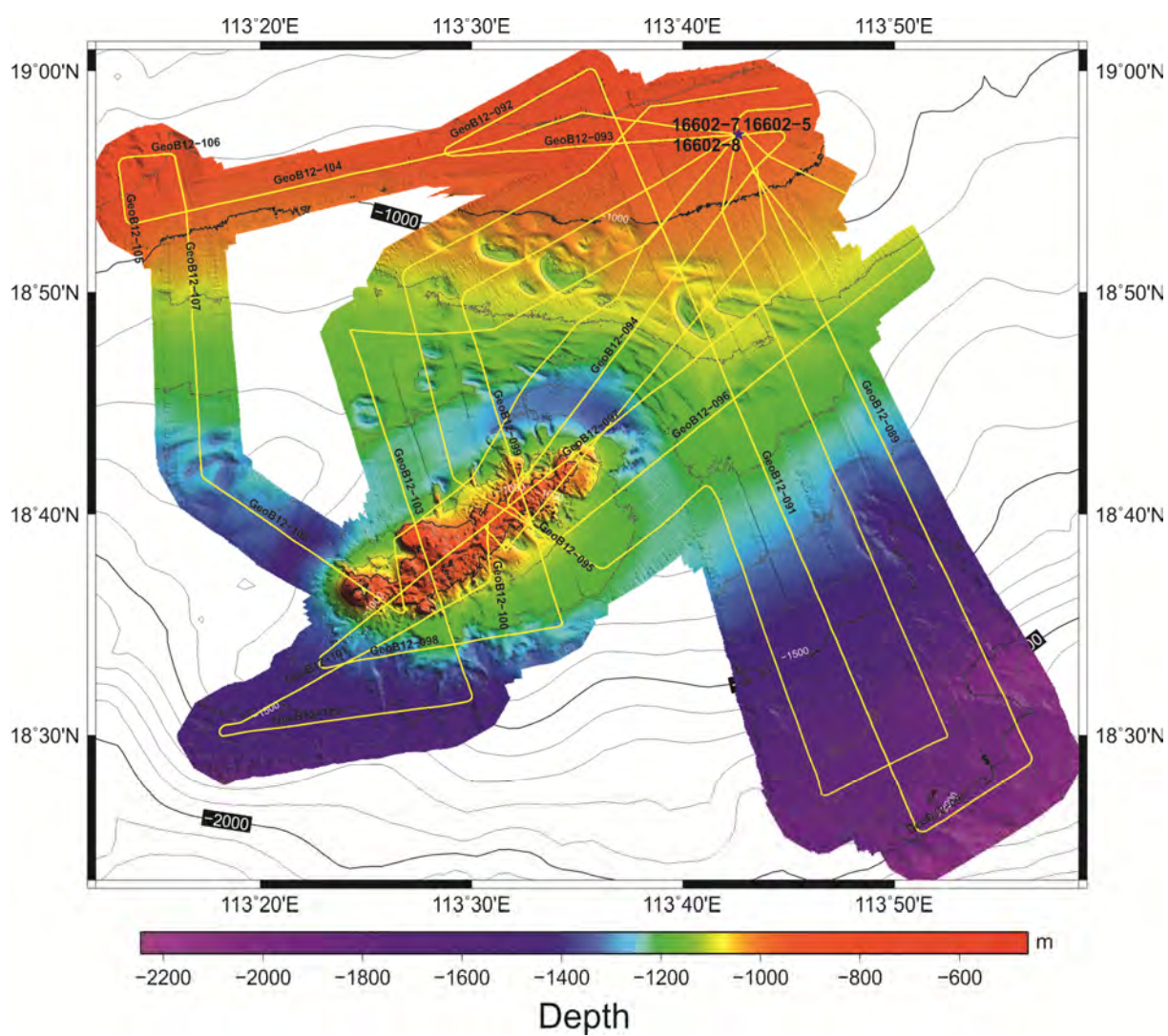


Fig. 9.6: Bathymetry of the second working area at and around GeoB 16602.



Fig. 9.7: Seismic images of the second working area at and around GeoB 16602.

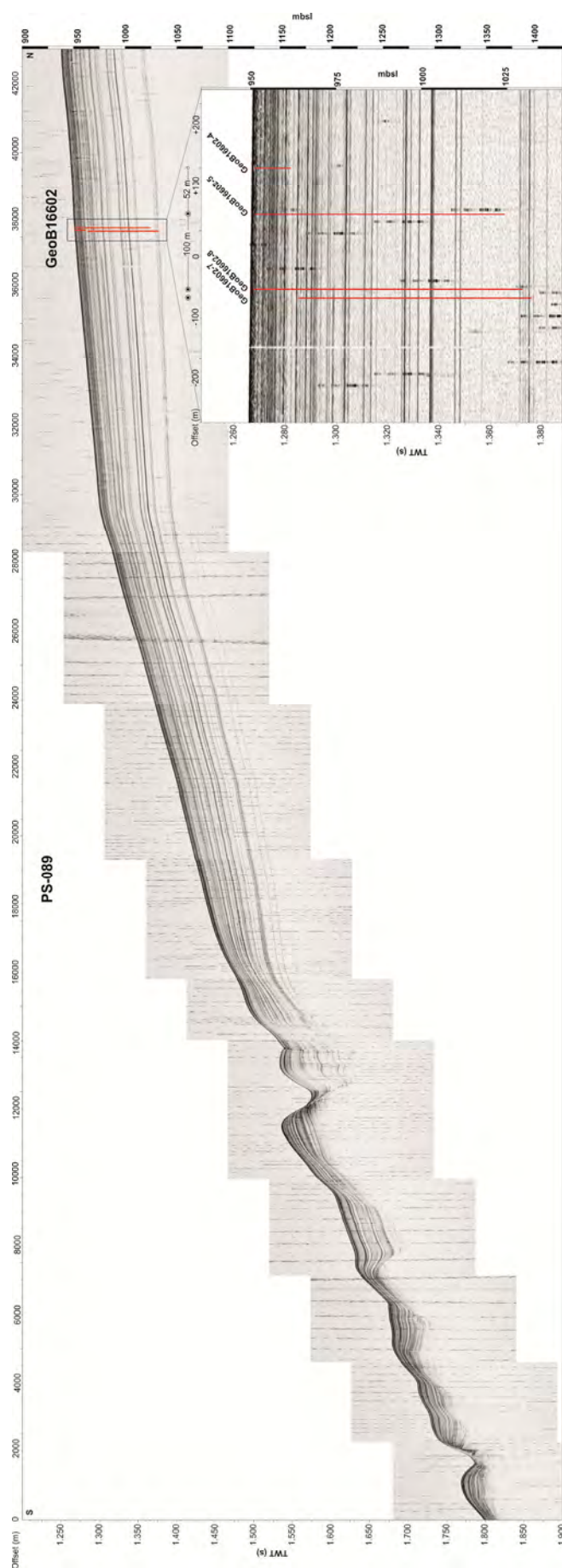


Fig. 9.8: Parasound images of the second working area at and around GeoB 16602.

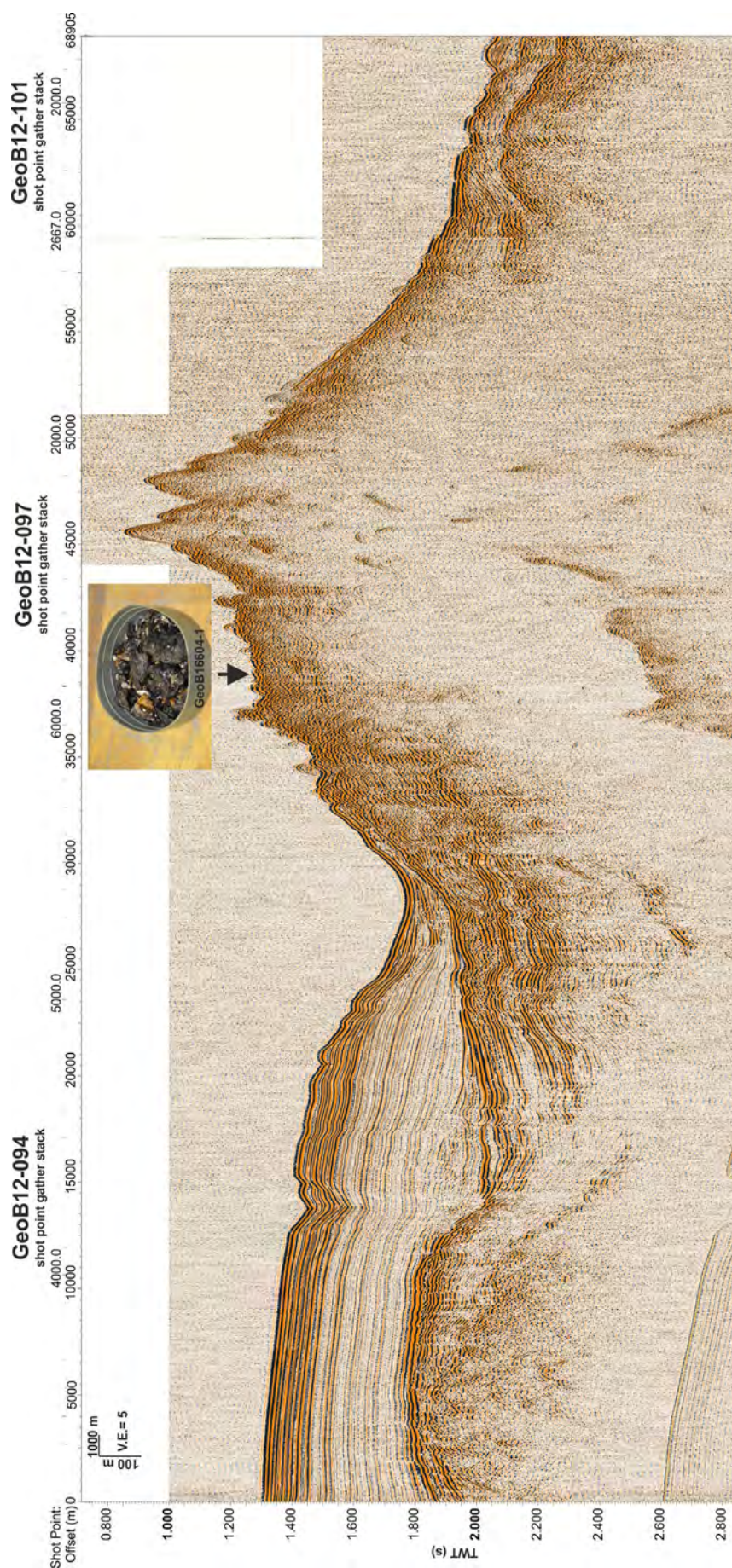


Fig. 9.9: Seismic images of the second working area at and around GeoB 16604.

9.3 Borehole logging

An overview on the results of the borehole loggings at site GeoB16601 and GeoB16602 is shown in Figures 9.10 and 9.11, respectively. At both sites two profiles were measured during separate deployments of the MeBo. A close correlation of the profiles can be observed at both sites. Natural Gamma ray intensity varies between 38 and 73 gAPI at site GeoB16601. The variations in natural gamma ray intensity are mainly attributed to changes in concentrations of Potassium (0,5 – 1,5 %) and Thorium (3,6 - 9,6 ppm), while the concentrations of Uranium are fairly low (1,2 - 2,8 ppm).

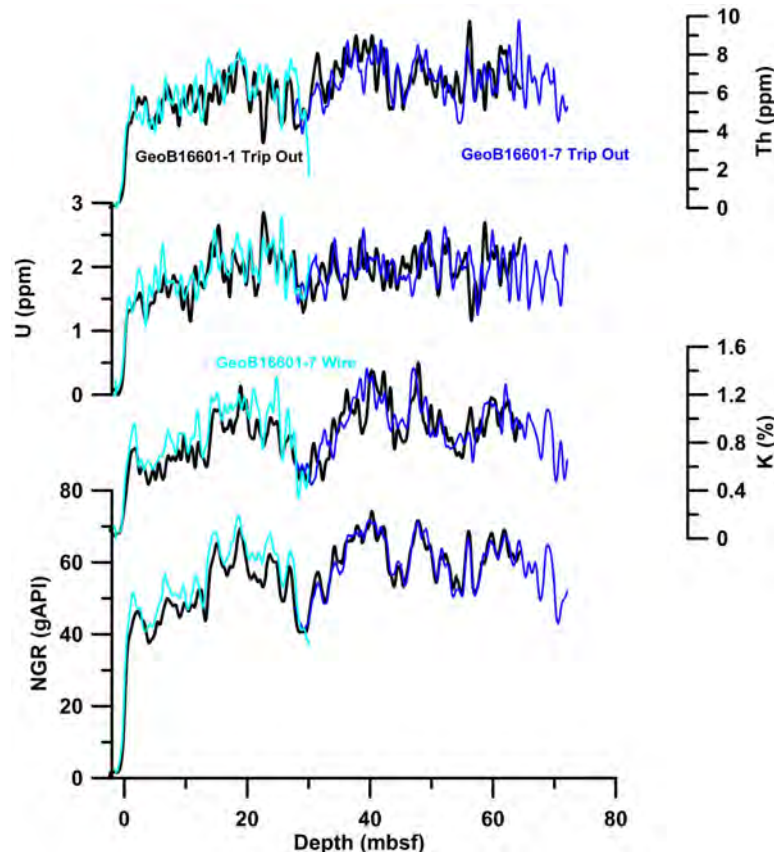


Fig. 9.10: Results of Spectral gamma ray bore hole logging at site GeoB16601.

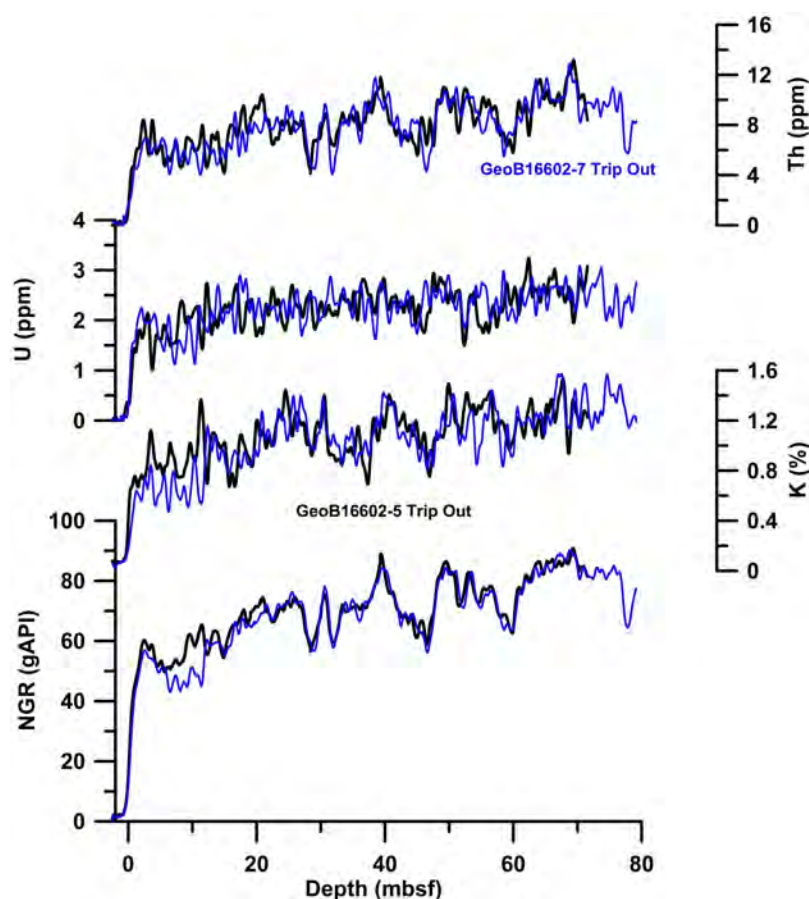
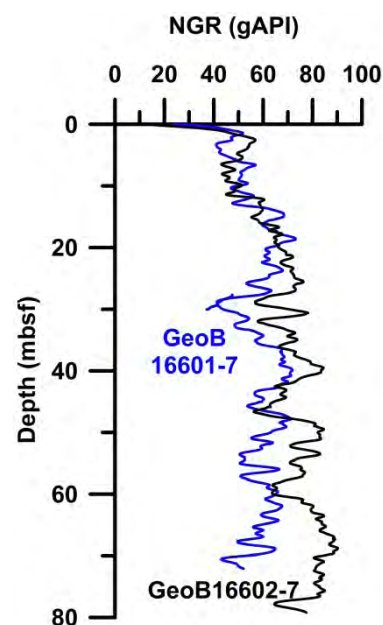


Fig. 9.11: Results of Spectral gamma ray bore hole logging at site GeoB16602.

Clay minerals are the main sources for Thorium and Potassium in marine sediments. The variability in natural gamma ray intensity can be interpreted as indicator of changes in terrestrial sediment input into the South China Sea at both sites and may thus be used for stratigraphic correlation.

Similar Patterns of variability in natural gamma ray intensity with depth were observed at both sites GeoB16601 and GeoB16602 (Figs. 9.10 and 9.11). Especially in the upper 40 m of both sites a close correlation is observed. This is an indication of similar sedimentation rates at both sites. Below 40 m the sedimentation rate seems to be higher at site GeoB16602 compared to GeoB16601

Fig. 9.12: Comparison of Natural Gamma Ray Intensity variations with depth at sites GeoB16601 and GeoB16602.



9.4 Sediments

Station GeoB 16601

At station GeoB 16601, two multi-corers (GeoB 16601-4 and GeoB 16601-5), one gravity corer (GeoB 16601-6) and two MeBo cores (GeoB 16601-1 and GeoB 16601-7) were collected. The multi-corer 16601-5 consisted of ~0.36 m olive gray nannofossil mud that was covered with 4 cm thick olive brown nannofossil mud. Planktonic foraminifera were abundant. Multi-corer GeoB 16601-4 was empty. The sediment of the gravity corer (GeoB 16601-6) taken at this station is an olive gray nannofossil mud with abundant planktonic foraminifera in the upper ~3.0 m. The sediment below ~3.0 m is a dark gray nannofossil mud with abundant foraminifera and diatoms. The dark gray nannofossil is coarser grained (silt-sized grain size) than the olive gray nannofossil mud. The two MeBo cores mainly consist of two types of sediments. A dark gray nannofossil mud with rare planktonic foraminifera and a dark gray nannofossil mud with abundant foraminifera and diatoms. A dark gray nannofossil bearing mud is partly intercalated. In addition, an olive gray nannofossil mud with abundant planktonic foraminifera is found only in the topmost part (upper ~0.08 m) of MeBo core GeoB 16601-1. The same type of sediment has been also observed in the gravity corer GeoB 16601-6 (see above). Nannofossil ooze is exclusively found below 60 m of MeBo core GeoB 16601-7. A detailed core description is given in chapter 10.

Station GeoB 16602

The multi-corer (GeoB 16602-3) deployed at this station consisted of ~0.34 m olive gray nannofossil mud covered by a 4 cm thick olive brown nannofossil mud. Planktonic foraminifera were abundant. The sediment of gravity core (GeoB 16602-4) is a gray nannofossil-bearing mud in the upper ~1.4 m and a dark gray nannofossil mud below ~1.4 m. The recovered sediment of the two MeBo cores GeoB 16602-5 and GeoB 16602-7 represents an alternate succession (interbedding) of dark gray nannofossil mud and gray nannofossil mud. Planktonic foraminifera are rather rare. Nannofossil ooze occurs partly below 59 m of MeBo core GeoB 16602-7. A detailed core description is given in chapter 10. MeBo core GeoB 16602-8 has not been opened onboard.

Station GeoB 16603

At station GeoB 16603, a gravity corer (GeoB16603-1) and multi-corer (GeoB16603-2) were deployed. The sediment of the gravity core GeoB 16603-1 is a dark gray nannofossil mud. Planktonic foraminifera are abundant in the upper 1.0 m. A detailed core description is given in chapter 10. Multi-corer GeoB16603-2 was empty.

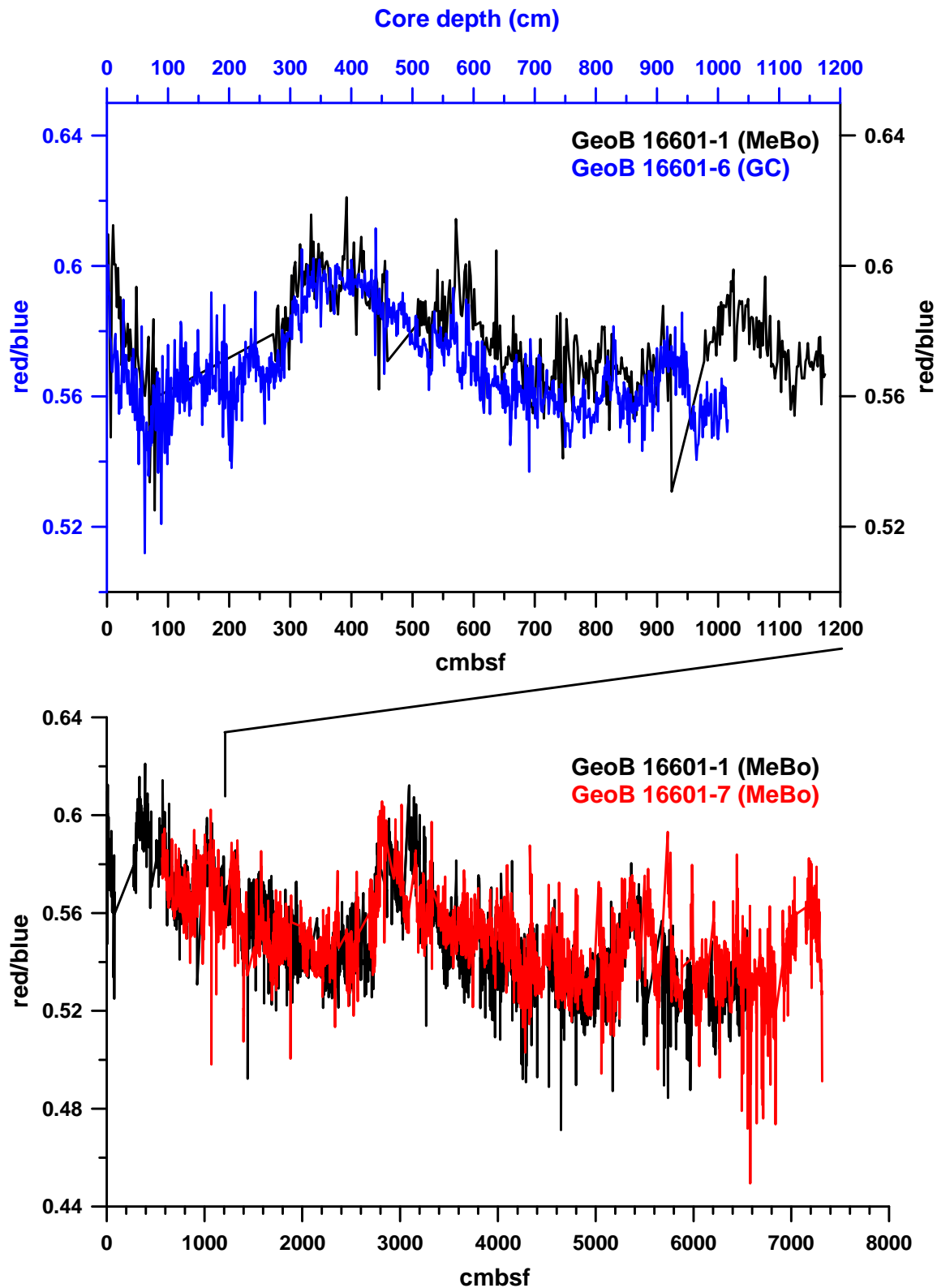


Fig. 9.13: Top panel shows the preliminary correlation between the gravity core GeoB 16601-6 (blue) and the upper sections of the MeBo core GeoB 16601-1 (black). Notable is a possible compaction of the gravity core by about 1 m between 700 and 1030 cm core depth. Bottom panel: correlation between the two MeBo cores deployed at the same site (GeoB 16601).

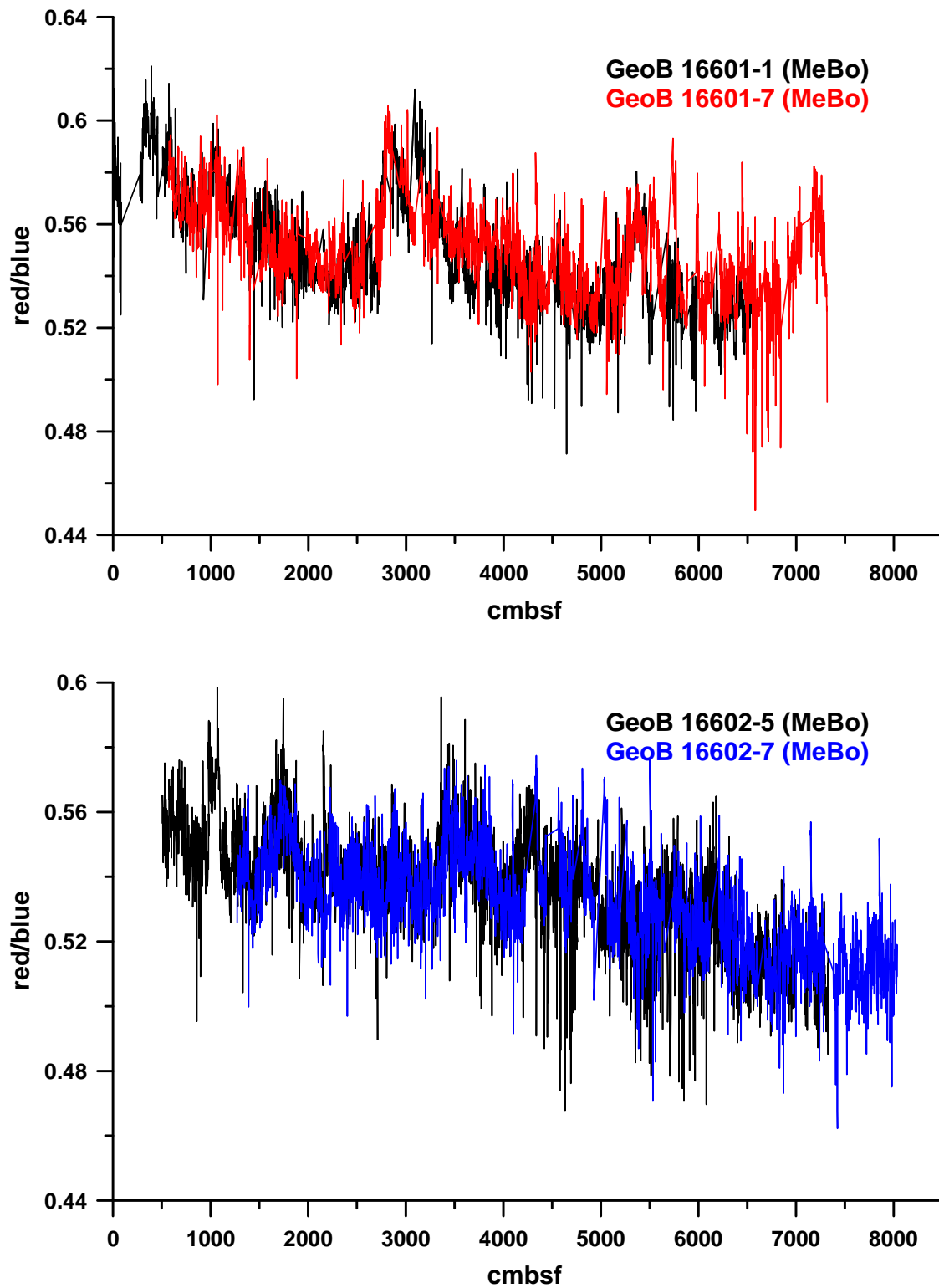


Fig. 9.14: Correlation between the two MeBo cores from the GeoB 16601 (top panel) and the two MeBo cores retrieved at site GeoB 16602 (bottom panel).

Tab. 9.2: Recovery table for MeBo-Core GeoB 16601-1.

Core No.	start of drilling (cm bsf)	end of drilling (cm bsf)	length of Sect. #1 (cm)	length of Sect. #2 (cm)	length of core catcher (cm)	recovery (%)
1 P	0	270	66	0	17	35
2 P	270	505	120	53	17	81
3 P	505	740	120	99	17	100
4 P	740	975	44	125	17	79
5 P	975	1210	120	112	17	106
6 P	1210	1445	120	96	17	99
7 P	1445	1680	120	110	17	105
8 P	1680	1915	120	126	18	112
9 P	1915	2150	120	52	17	80
10 P	2150	2385	120	101	17	101
11 P	2385	2620	120	84	17	94
12 P	2620	2855	131	0	17	63
13 P	2855	3090	120	41	17	76
14 P	3090	3325	120	52	17	80
15 P	3325	3560	120	80	17	92
16 P	3560	3795	120	59	17	83
17 P	3795	4030	120	126	17	112
18 P	4030	4265	120	117	17	108
19 P	4265	4500	125	0	17	60
20 P	4500	4735	120	50	17	80
21 P	4735	4970	120	105	17	103
22 P	4970	5205	120	111	13	104
23 P	5205	5440	120	92	17	97
24 P	5440	5675	78	0	17	40
25 P	5675	5910	120	25	17	69
26 P	5910	6145	62	0	17	34
27 P	6145	6380	120	118	14	107
28 P	6380	6615	120	37	17	74
sum :			3146	1971	470	
total recovery:					5587	84%

Tab. 9.3: Recovery table for MeBo-Core GeoB 16601-7.

Core No.	start of drilling (cm bsf)	end of drilling (cm bsf)	length of Section #1 (cm)	length of Section #2 (cm)	length of core catcher (cm)	recovery (%)
1 P	565	800	120	98	17	100
2 P	800	1035	120	77	17	91
3 P	1035	1270	120	48	17	79
4 P	1270	1505	120	30	17	71
5 P	1505	1740	120	106	17	103
6 P	1740	1975	120	14	17	64
7 P	1975	2210	120	106	17	103
8 P	2210	2445	120	27	17	70
9 P	2445	2680	116	0	15	56
10 P	2680	2915	120	44	16	77
11 P	2915	3150	120	38	17	74
12 P	3150	3385	120	47	16	78
13 P	3385	3620	120	126	17	112
14 P	3620	3855	120	126	17	112
15 P	3855	4090	120	105	11	100
16 P	4090	4325	120	126	12	110
17 P	4325	4560	120	72	17	89
18 P	4560	4795	120	98	17	100
19 P	4795	5030	120	48	17	79
20 P	5030	5265	120	126	17	112
21 P	5265	5500	120	46	17	78
22 P	5500	5735	120	24	17	69
23 P	5735	5970	135	0	14	63
24 P	5970	6205	120	33	17	72
25 P	6205	6440	120	125	12	109
26 P	6440	6675	120	76	17	91
27 P	6675	6910	120	32	17	72
28 P	6910	7145	130	0	16	62
29 P	7145	7380	120	34	16	72
sum:			3501	1832	468	
total recovery:					5801	85%

Tab. 9.4: Recovery table for MeBo-Core GeoB 16602-5.

Core No.	start of drilling (cm bsf)	end of drilling (cm bsf)	length of Section #1 (cm)	length of Section #2 (cm)	length of core catcher (cm)	recovery (%)
1 P	505	740	120	99	17	100
2 P	740	975	120	108	17	104
3 P	975	1210	120	101	17	101
4 P	1210	1445	120	114	17	107
5 P	1445	1680	120	114	17	107
6 P	1680	1915	120	114	17	107
7 P	1915	2150	120	116	17	108
8 P	2150	2385	120	125	17	111
9 P	2385	2620	120	126	11	109
10 P	2620	2855	120	126	17	112
11 P	2855	3090	120	110	17	105
12 P	3090	3325	120	105	17	103
13 P	3325	3560	120	114	17	107
14 P	3560	3795	120	107	17	104
15 P	3795	4030	120	115	17	107
16 P	4030	4265	120	122	12	108
17 P	4265	4500	120	122	17	110
18 P	4500	4735	120	123	17	111
19 P	4735	4970	120	126	12	110
20 P	4970	5205	120	126	17	112
21 P	5205	5440	120	107	14	103
22 P	5440	5675	120	112	17	106
23 P	5675	5910	120	108	17	104
24 P	5910	6145	120	126	17	112
25 P	6145	6380	120	126	17	112
26 P	6380	6615	120	126	12	110
27 P	6615	6850	120	126	17	112
28 P	6850	7085	131	0	17	63
29 P	7085	7320	120	111	17	106
sum:			3491	3255	469	
total recovery:					7215	106%
without core catcher:					6746	99%

Tab. 9.5: Recovery table for MeBo-Core GeoB 16602-7.

Core No.	start of drilling (cm bsf)	end of drilling (cm bsf)	length of Section #1 (cm)	length of Section #2 (cm)	length of core catcher (cm)	recovery (%)
1 P	1270	1505	120	101	17	101
2 P	1505	1740	120	114	17	107
3 P	1740	1975	120	126	17	112
4 P	1975	2210	120	126	17	112
5 P	2210	2445	120	120	14	108
6 P	2445	2680	120	108	17	104
7 P	2680	2915	120	105	17	103
8 P	2915	3150	120	116	17	108
9 P	3150	3385	120	126	14	111
10 P	3385	3620	120	108	17	104
11 P	3620	3855	120	126	12	110
12 P	3855	4090	120	127	12	110
13 P	4090	4325	119	0	17	58
14 P	4325	4560	105	0	8	48
15 P	4560	4795	120	20	17	67
16 P	4795	5030	122	0	11	57
17 P	5030	5265	120	35	13	71
18 P	5265	5500	120	122	10	107
19 P	5500	5735	134	0	17	64
20 P	5735	5970	120	112	13	104
21 P	5970	6205	130	0	17	63
22 P	6205	6440	120	108	17	104
23 P	6440	6675	120	38	11	72
24 P	6675	6910	120	105	17	103
25 P	6910	7145	120	122	13	109
26 P	7145	7380	135	0	9	61
27 P	7380	7615	120	124	17	111
28 P	7615	7850	120	123	14	109
29 P	7850	8085	120	49	17	79
sum:			3505	2361	426	
total recovery:					6292	92%

Tab. 9.6: Recovery table for MeBo-Core GeoB 16602-8.

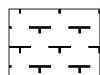
Core No.	start of drilling (cm bsf)	end of drilling (cm bsf)	length of Section #1 (cm)	length of Section #2 (cm)	length of core catcher (cm)	recovery (%)
1 P	975	1210	120	112	17	106
2 P	1210	1445	120	111	17	106
3 P	1445	1680	120	105	17	103
4 P	1975	1915	120	102	17	102
5 P	2210	2150	120	99	13	99
6 P	2445	2385	120	106	17	103
7 P	2680	2620	120	61	17	84
8 P	2915	2855	120	103	17	102
9 P	2855	3090	120	102	17	102
10 P	3090	3325	120	97	17	100
11 P	3325	3560	109	0	11	51
12 P	3560	3795	120	104	13	101
13 P	3795	4030	98	0	13	47
14 P	4030	4265	120	123	13	109
15 P	4265	4500	120	106	17	103
16 P	4500	4735	120	126	17	112
17 P	4735	4970	120	126	17	112
18 P	4970	5205	120	126	17	112
19 P	5205	5440	120	125	13	110
20 P	5440	5675	120	119	14	108
21 P	5675	5910	120	110	17	105
22 P	5910	6145	120	115	12	105
23 P	6145	6380	120	118	17	109
24 P	6380	6615	120	125	17	111
25 P	6615	6850	120	127	12	110
26 P	6850	7085	120	126	12	110
27 P	7085	7320	120	105	17	103
28 P	7320	7555	120	123	17	111
29 P	7555	7790	120	114	17	107
30 P	7790	8025	120	127	17	112
sum:			3567	3143	466	
total recovery:					7176	102%
Without core catcher:						95%

10 Core Descriptions

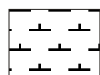
Lithology

one major component

calcareous

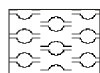


foraminiferal ooze



nannofossil ooze

siliceous



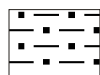
siliceous ooze

diatom ooze

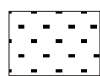
terrigenous



clay



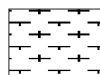
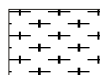
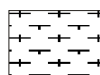
silt



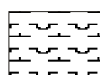
sand

mixtures

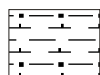
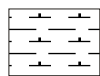
calcareous

nannofossil-bearing
foram oozeforam-nannofossil
ooze or nannofossil-
foram oozeforam-bearing
nannofossil ooze

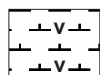
siliceous

diatomaceous nanno-
fossil ooze or diatom-
bearing nannofossil ooze

terrigenous/volcanic

clayey nannofossil ooze
or clay-bearing nanno-
fossil oozesilty nanno-
fossil ooze or
nannofossil silt

nannofossil clay

volcanic ash-bearing
nannofossil ooze

Structures



weakly bedded



bedded/laminated

mm
cm
dm
dimension of
bedding

scoured bedding



bioturbated (<30% of sediment)



bioturbated (<30-60% of sediment)



bioturbated (>60% of sediment)



turbidite



possible turbidite



erosive contact



wavy bedding



graded bedding

Fossils



shells



shell fragments



plant/wood fragments

Others



volcanic ash layer



pumice fragment

Colour

Munsell value



>6



3



5



2.5



4

Fig. 10.1: Legend for the core descriptions.

10.1 Gravity cores

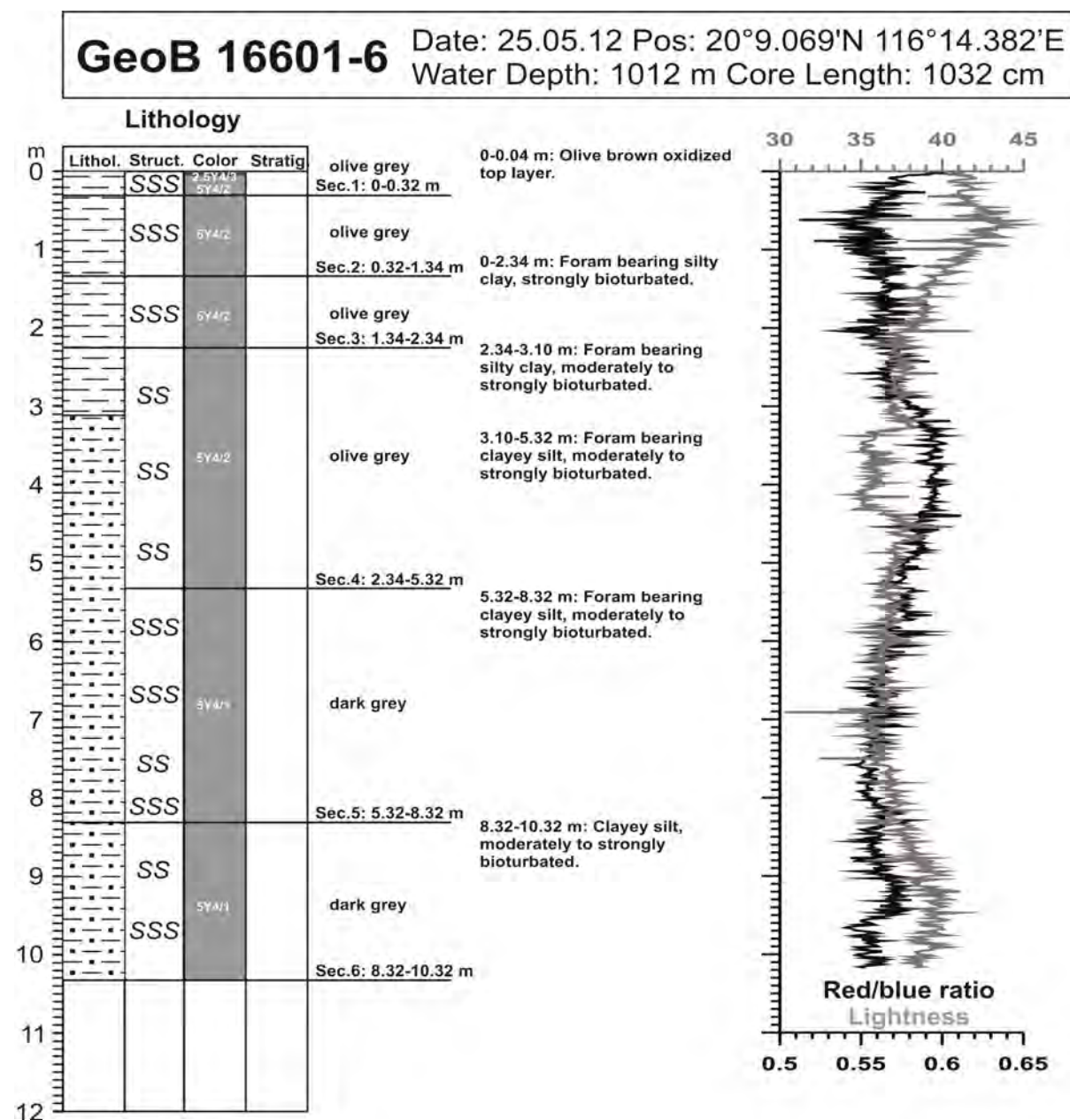


Fig. 10.2: Core description of core GeoB 16601-6.

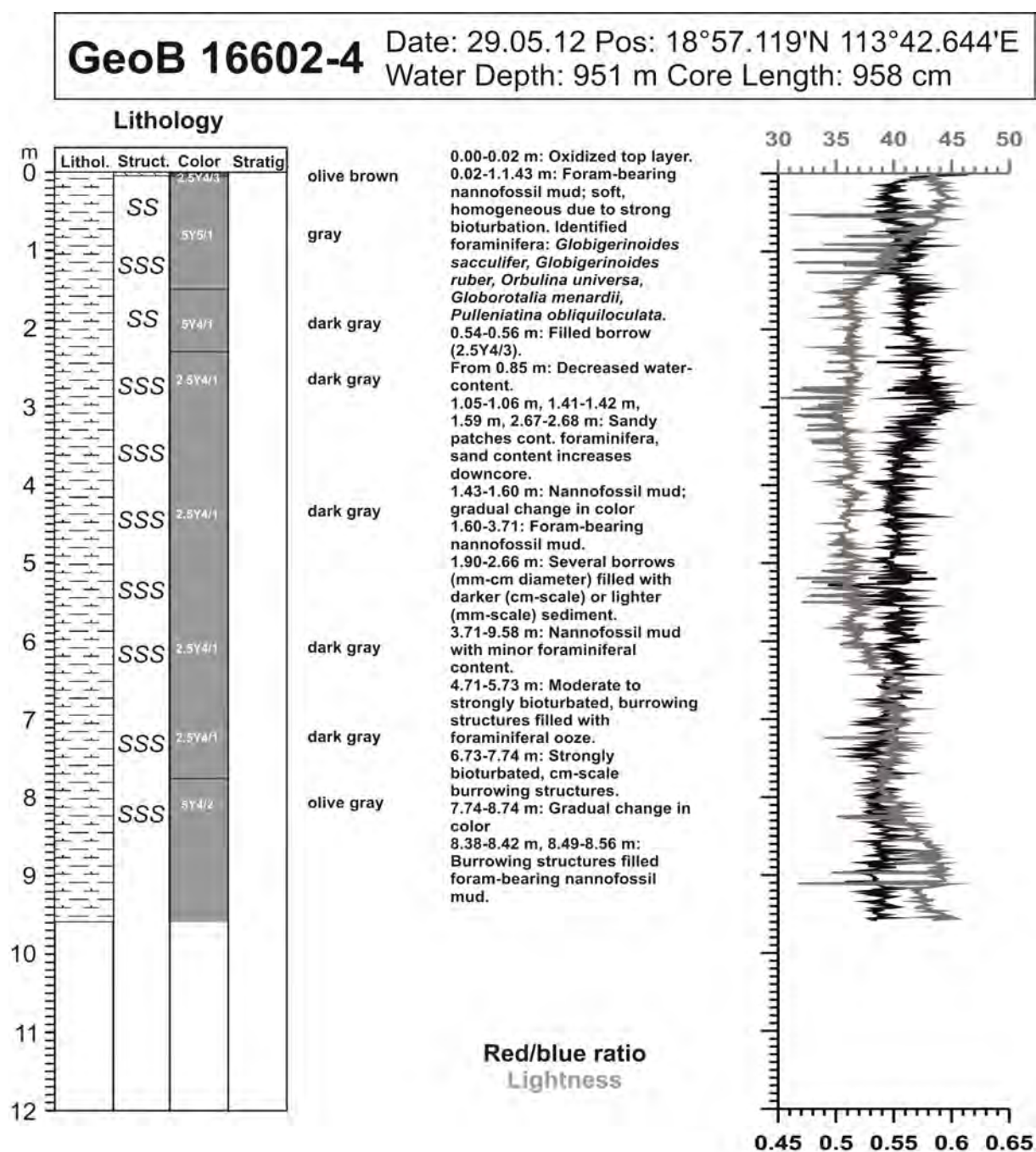


Fig. 10.3: Core description of core GeoB 16602-4.

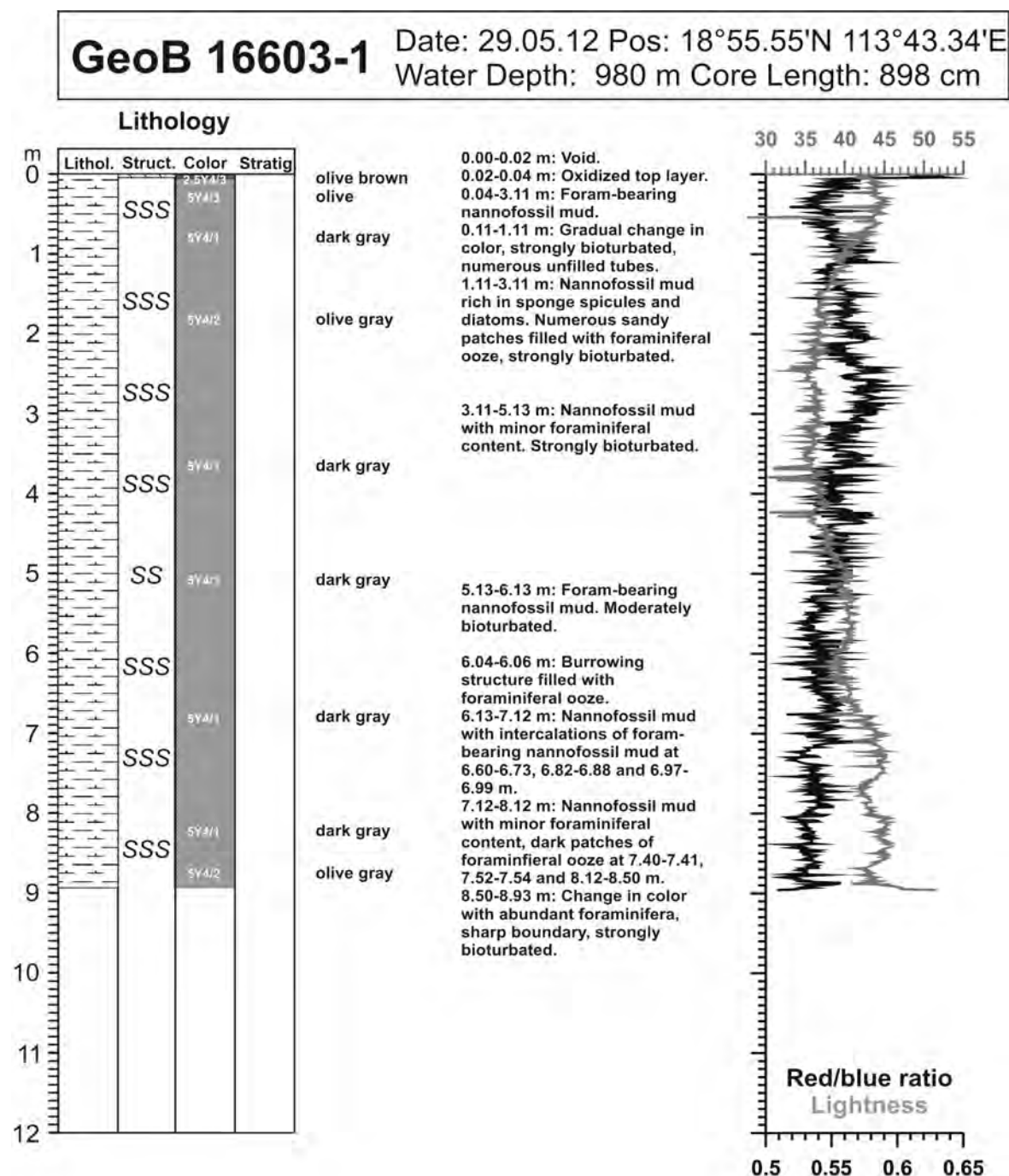


Fig. 10.4: Core description of core GeoB 16603-1.

10.2 MeBo cores

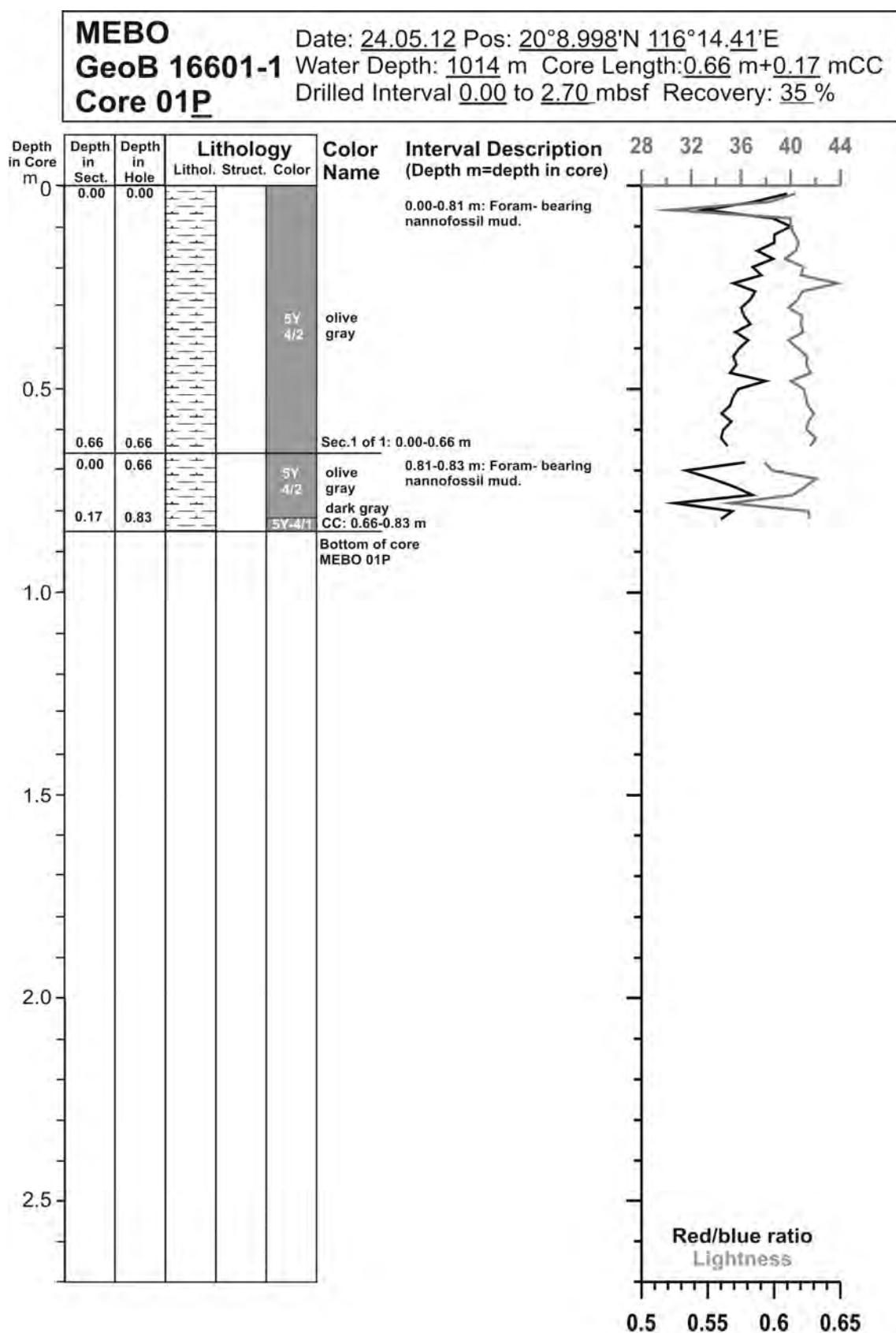


Fig. 10.5: Core description of MeBo core GeoB 16601-1 (1/28).

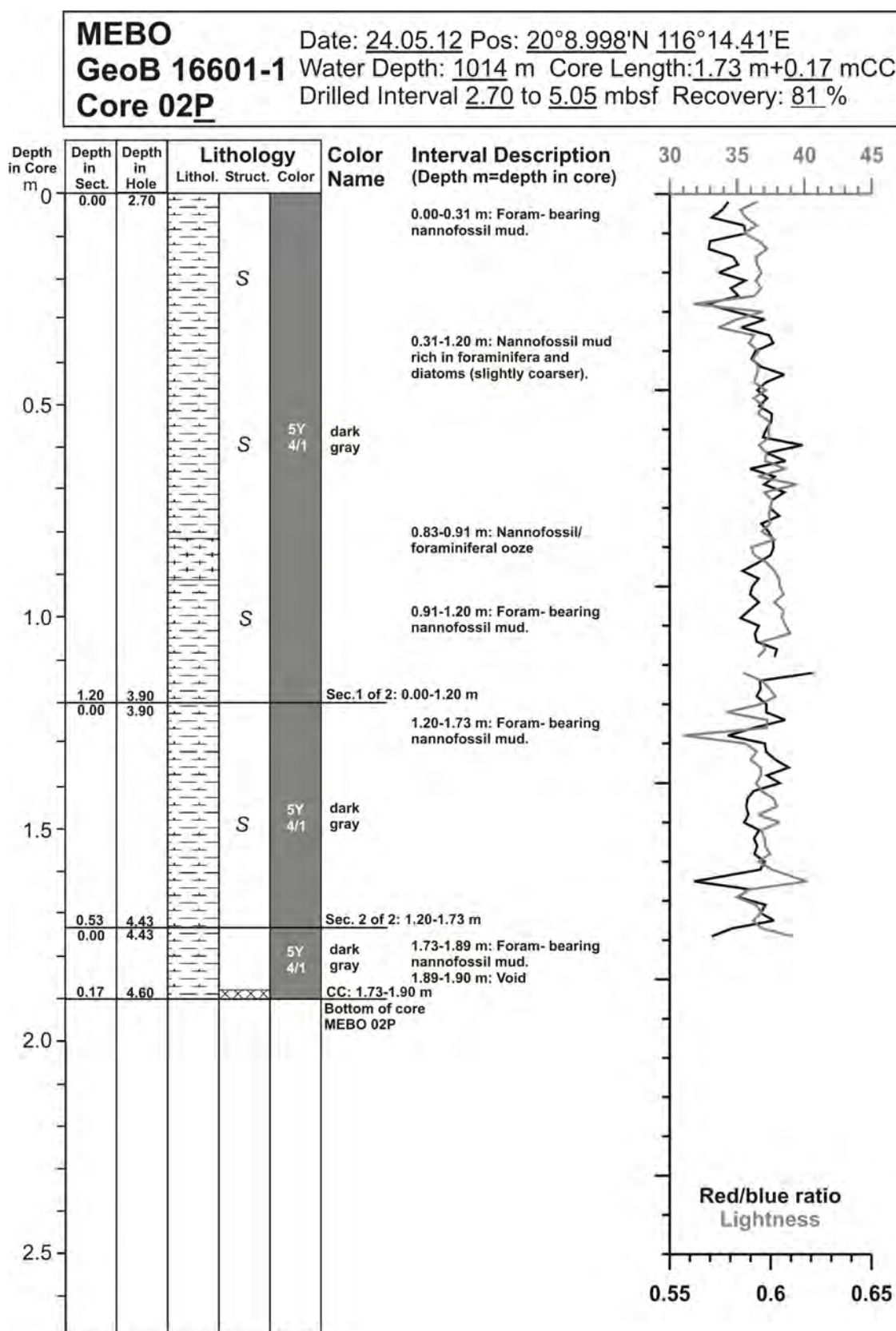


Fig. 10.6: Core description of MeBo core GeoB 16601-1 (2/28).

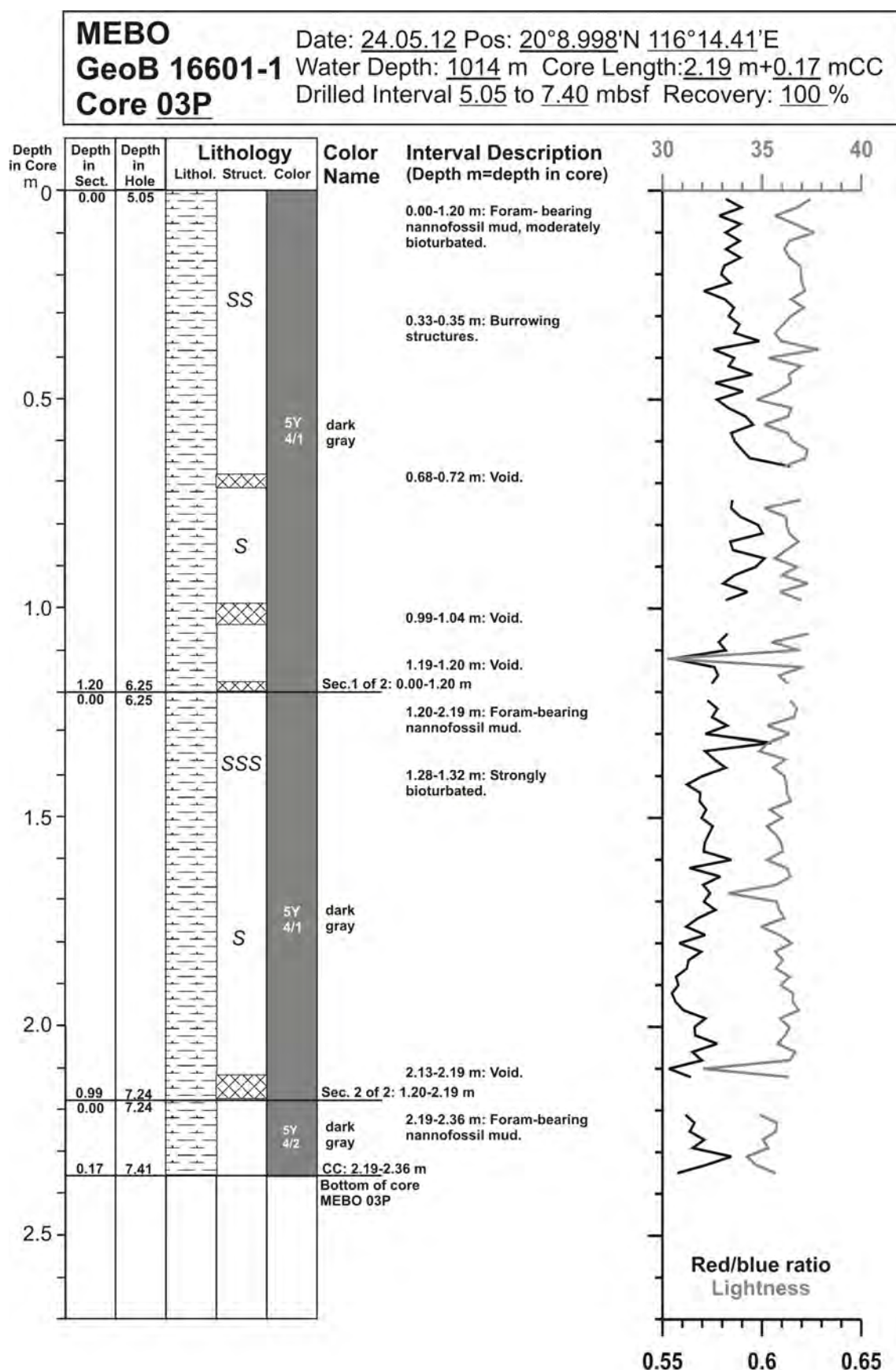


Fig. 10.7: Core description of MeBo core GeoB 16601-1 (3/28).

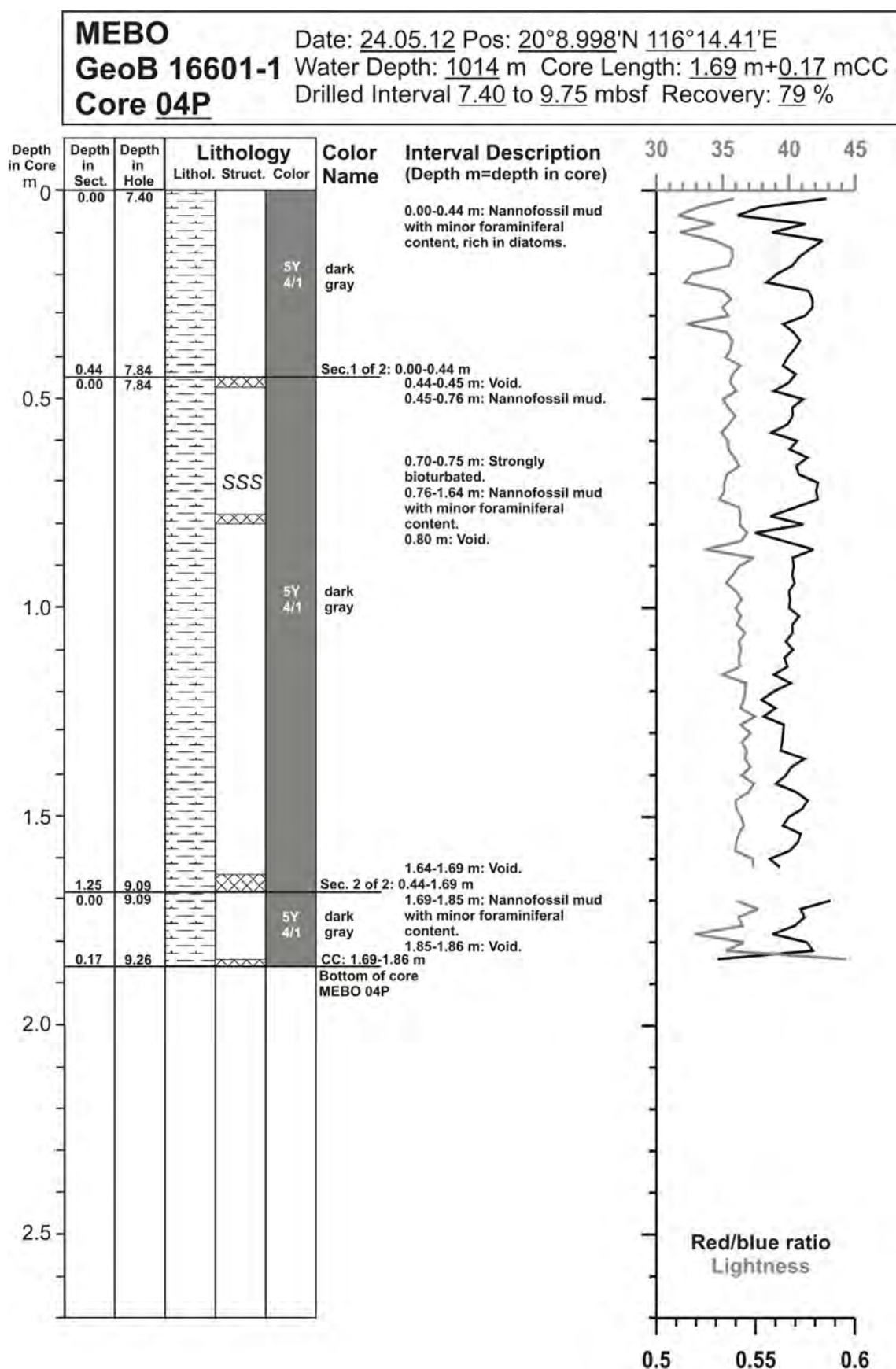


Fig. 10.8: Core description of MeBo core GeoB 16601-1 (4/28).

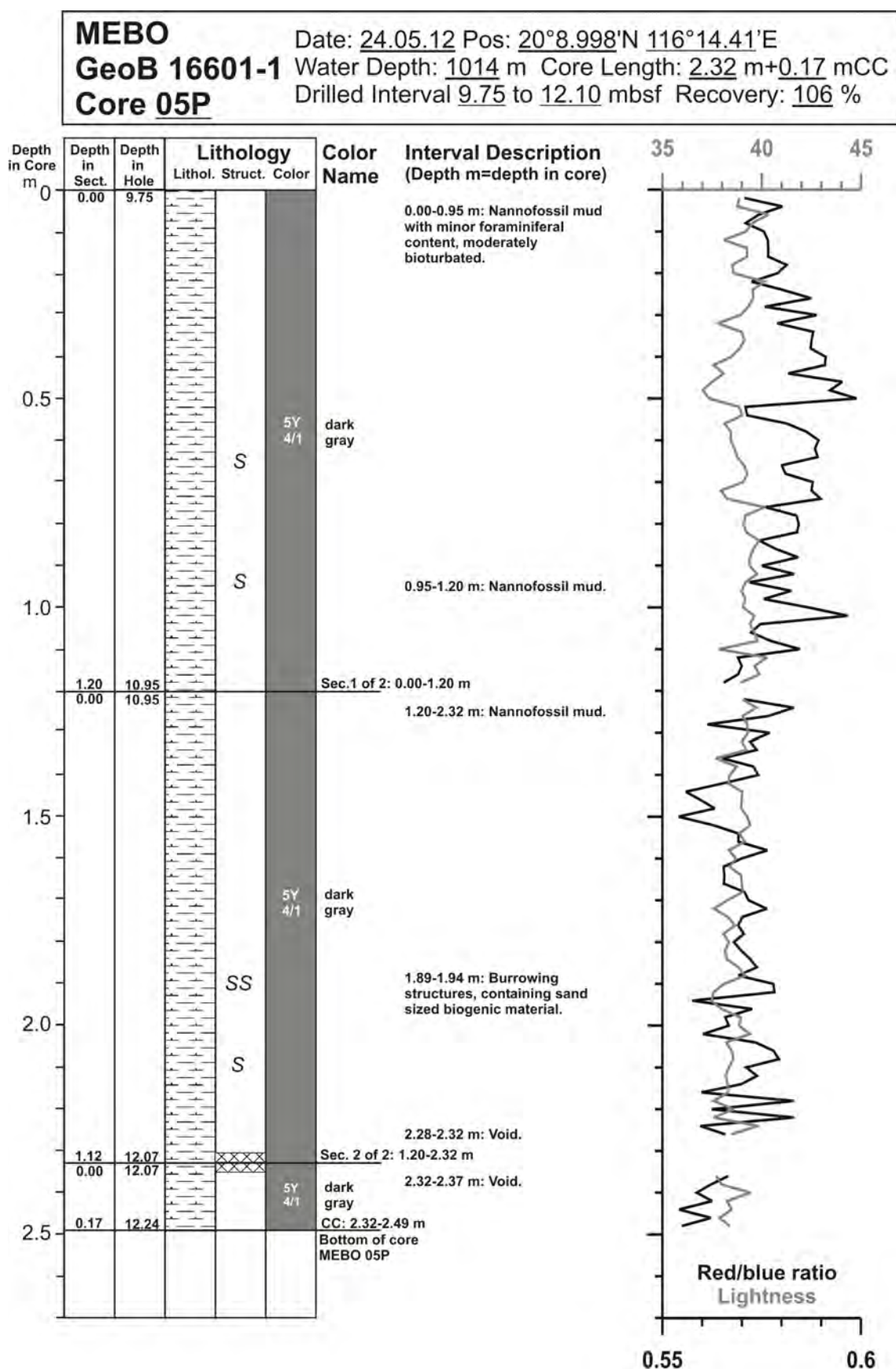


Fig. 10.9: Core description of MeBo core GeoB 16601-1 (5/28).

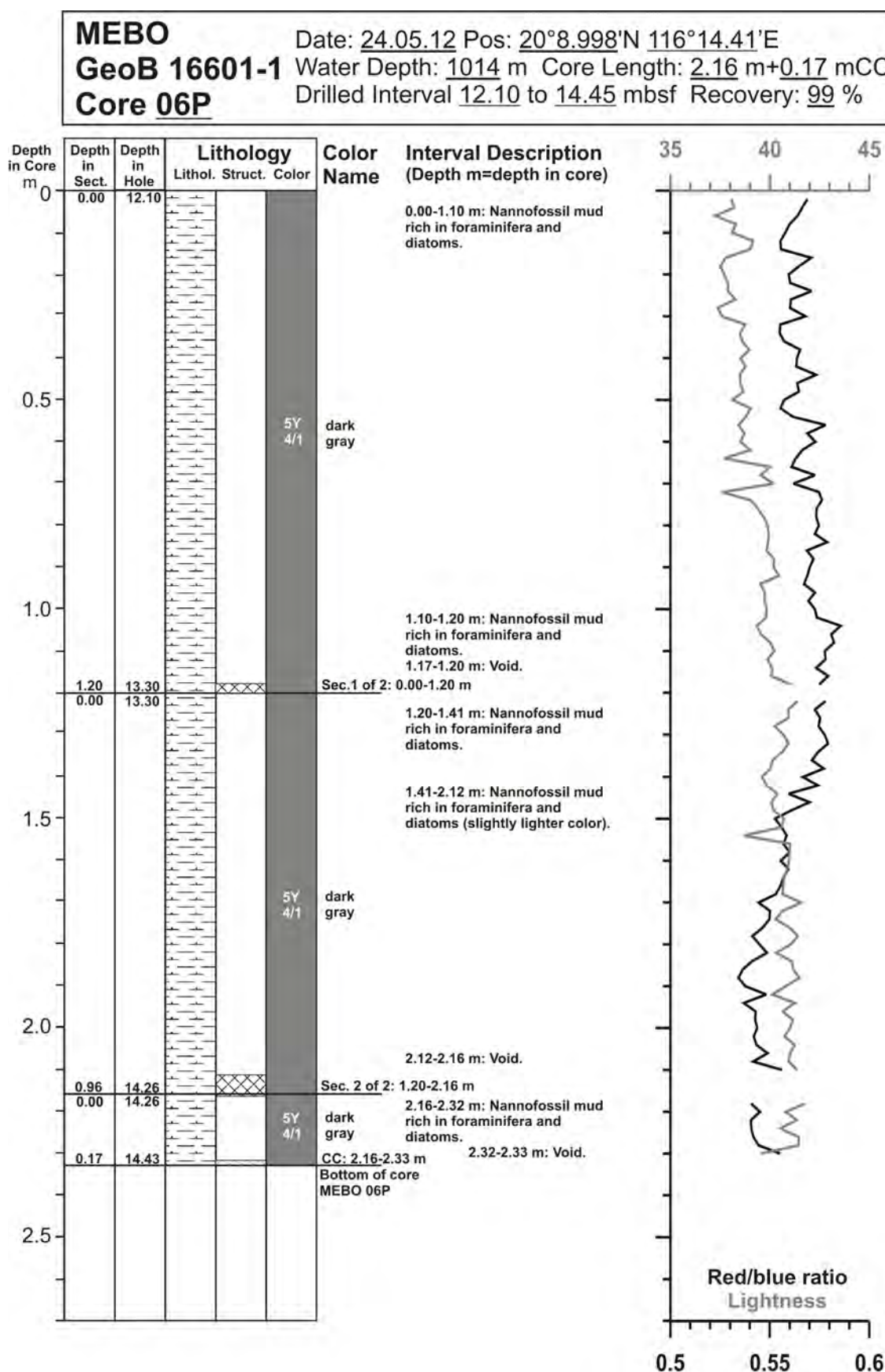


Fig. 10.10: Core description of MeBo core GeoB 16601-1 (6/28).

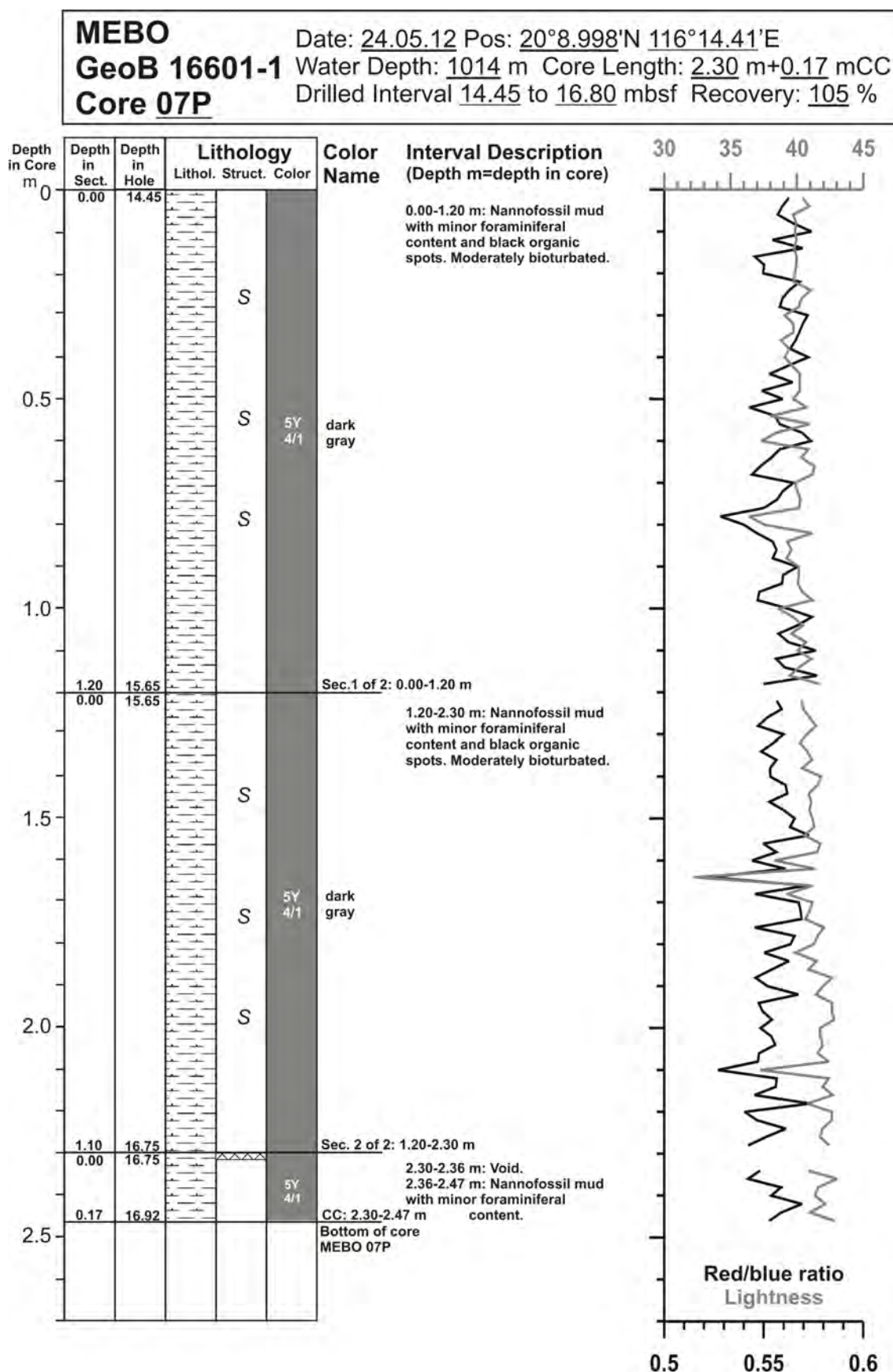


Fig. 10.11: Core description of MeBo core GeoB 16601-1 (7/28).

Fig.

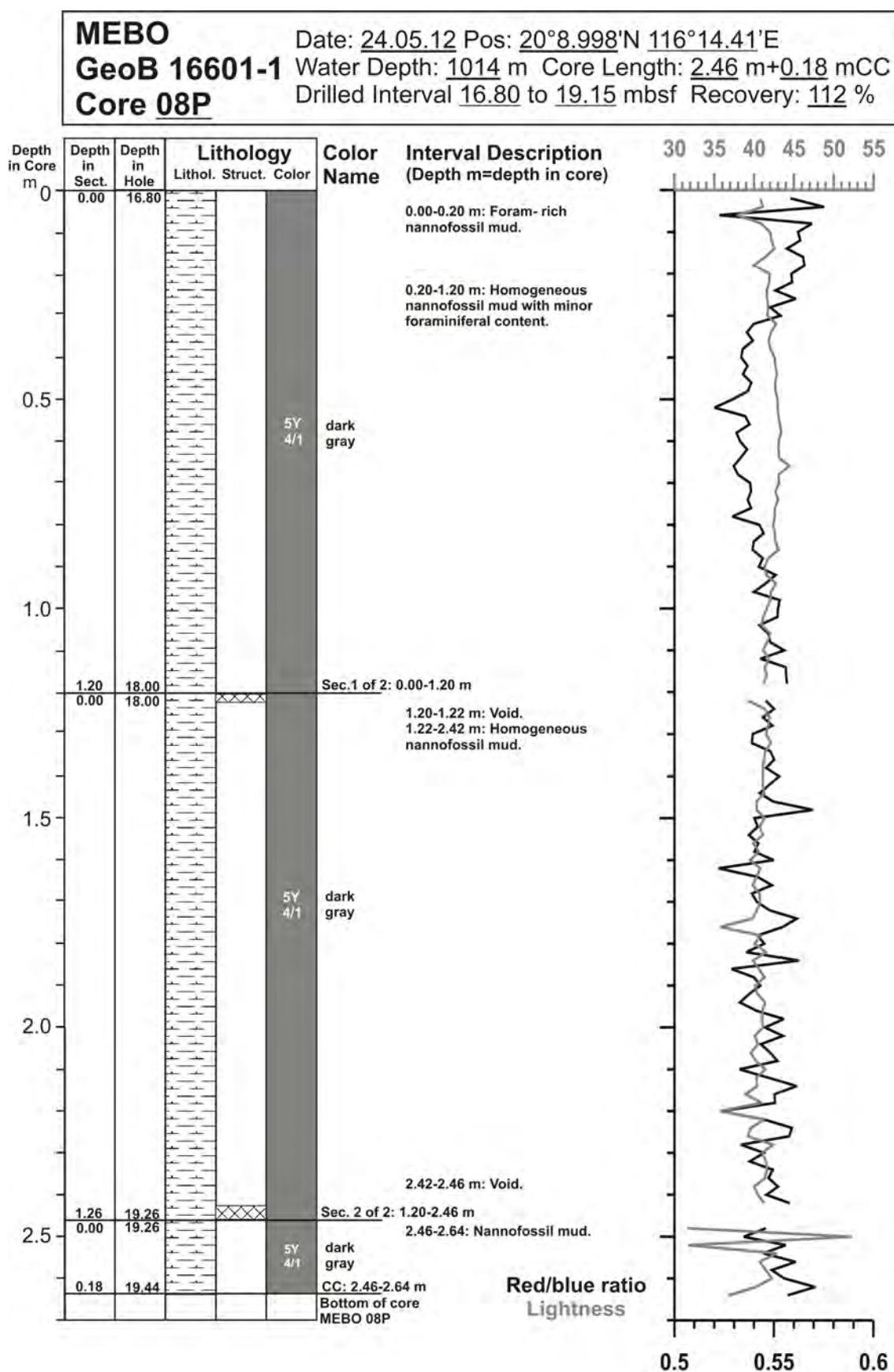


Fig. 10.12: Core description of MeBo core GeoB 16601-1 (8/28).

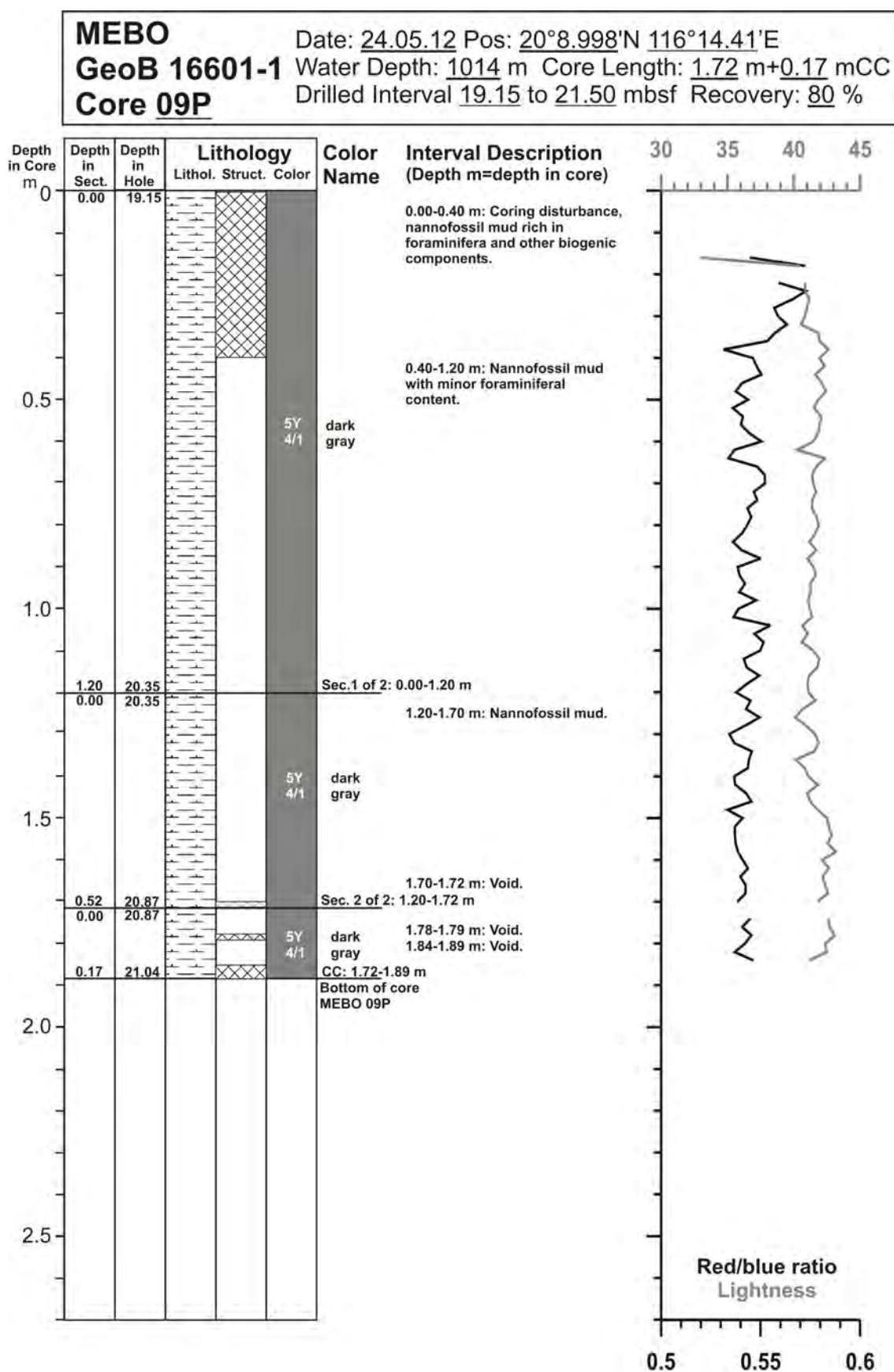


Fig. 10.13: Core description of MeBo core GeoB 16601-1 (9/28).

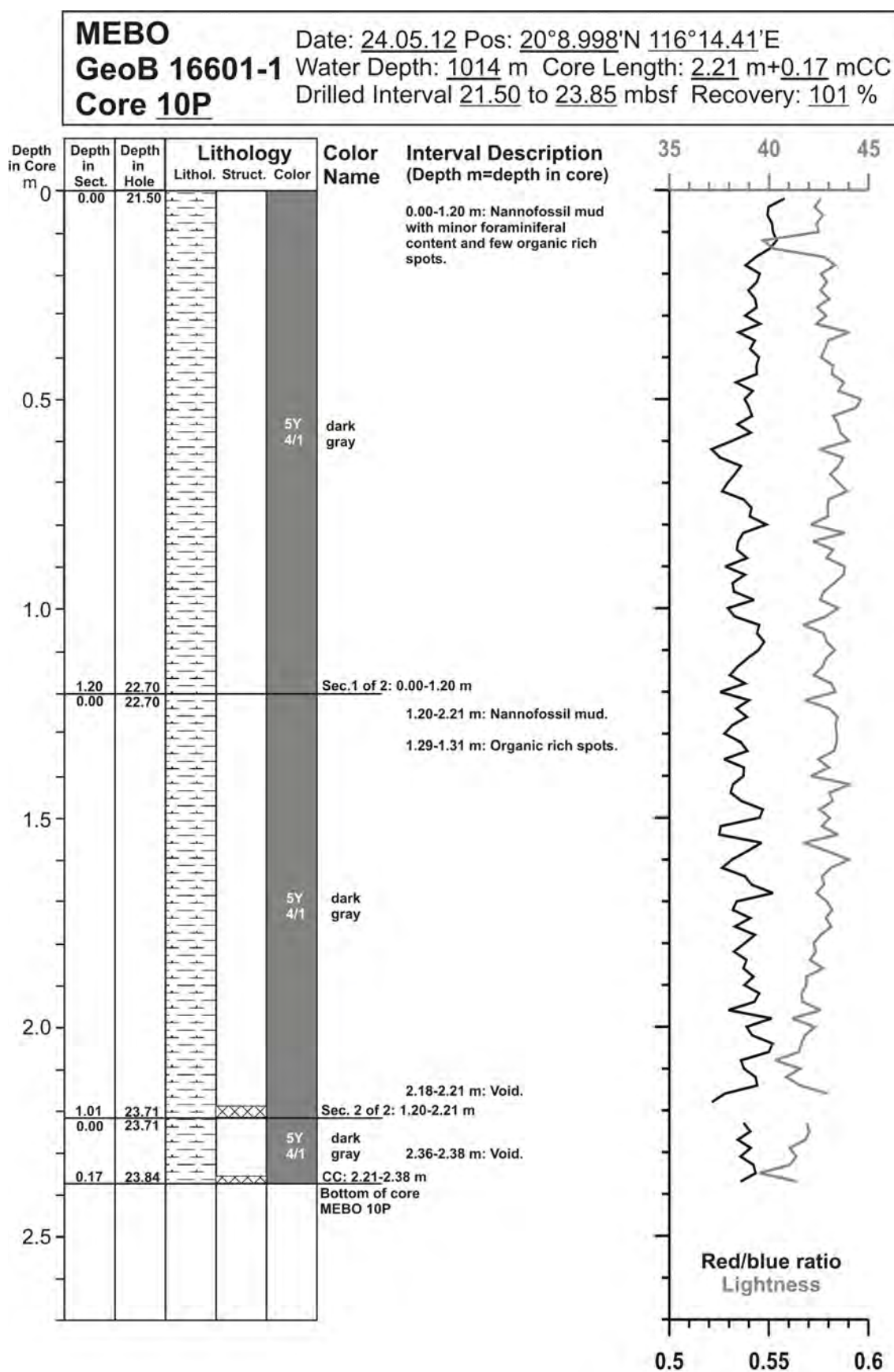


Fig. 10.14: Core description of MeBo core GeoB 16601-1 (10/28).

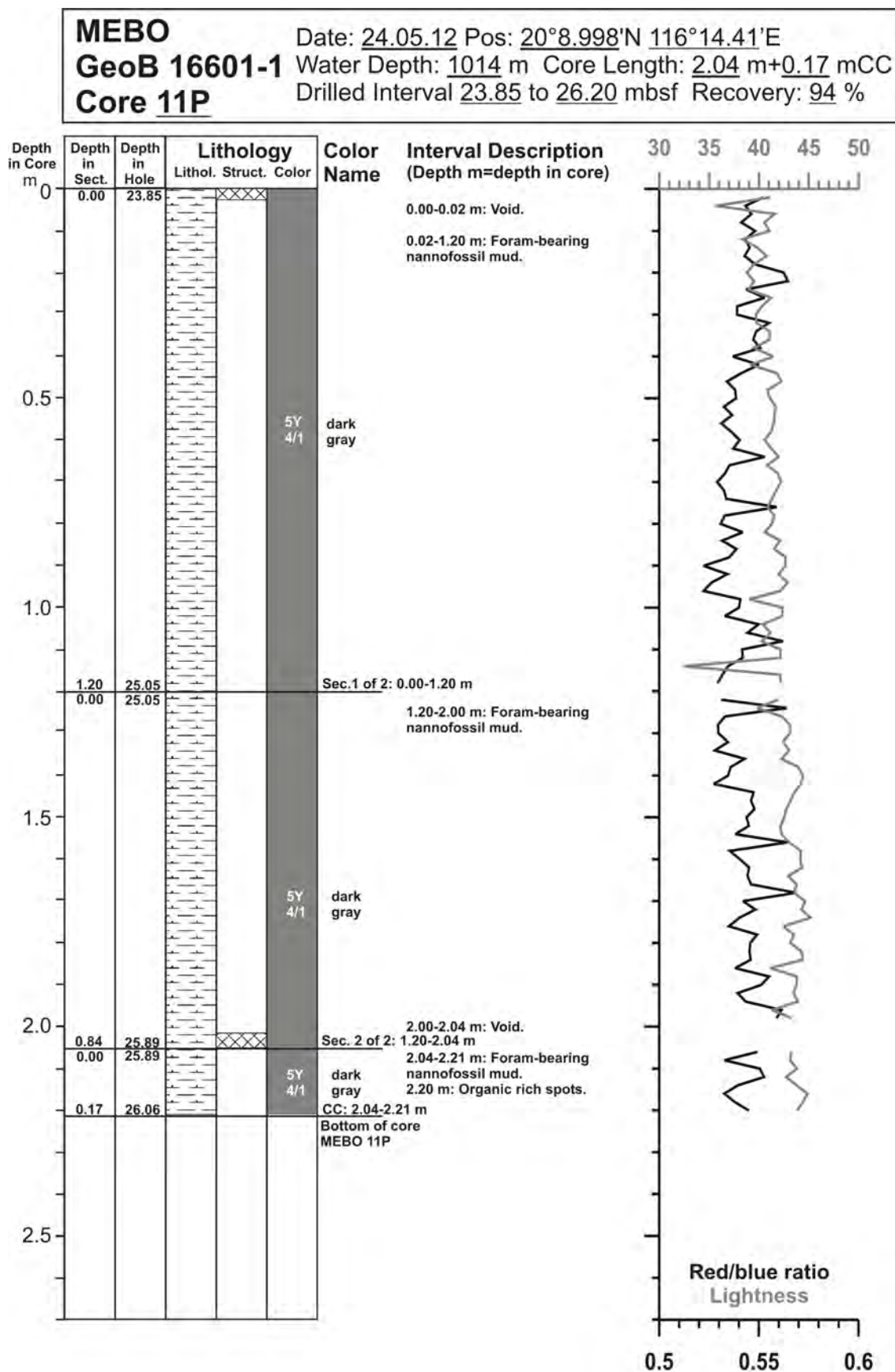


Fig. 10.15: Core description of MeBo core GeoB 16601-1 (11/28).

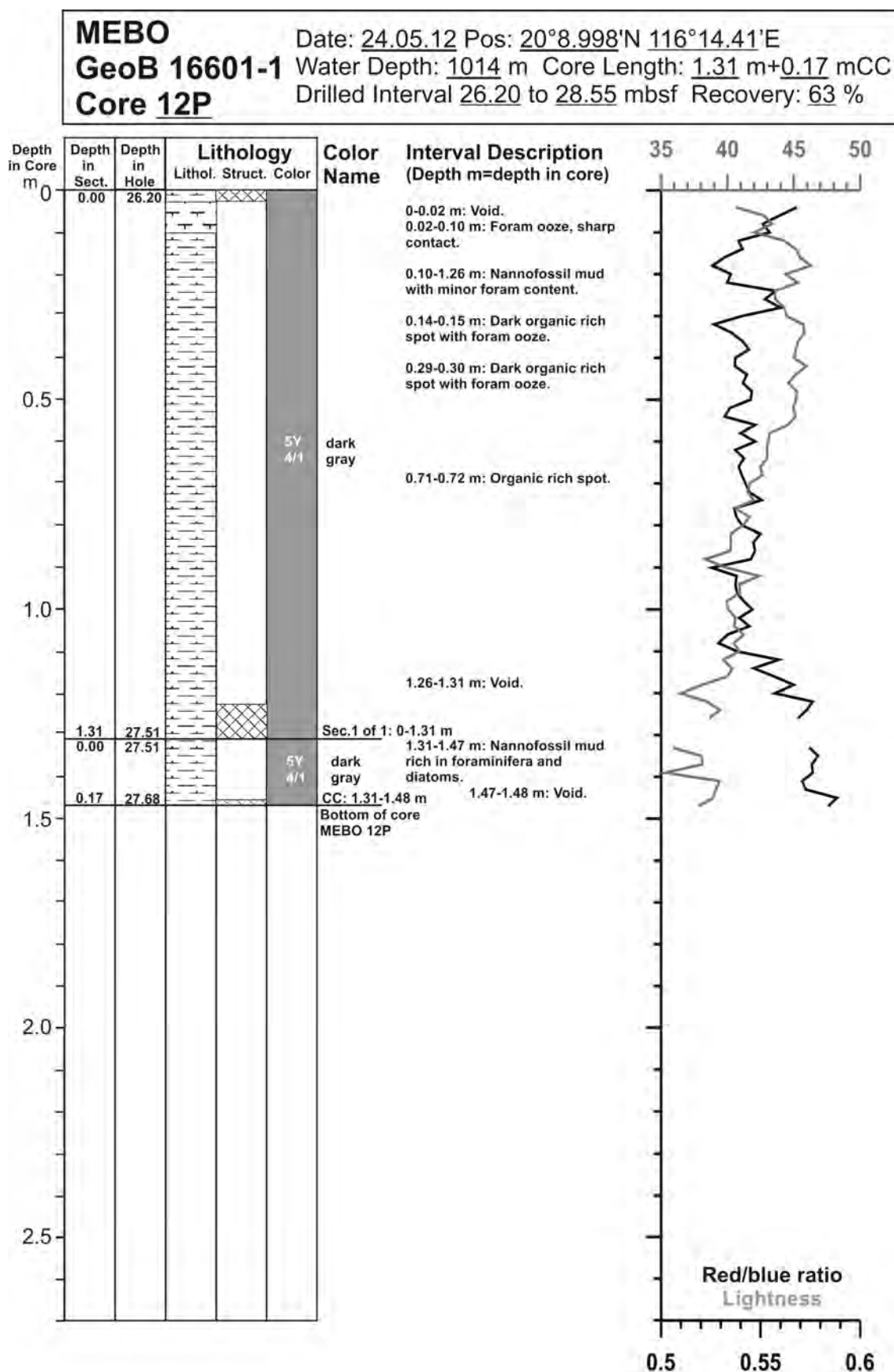


Fig. 10.16: Core description of MeBo core GeoB 16601-1 (12/28).

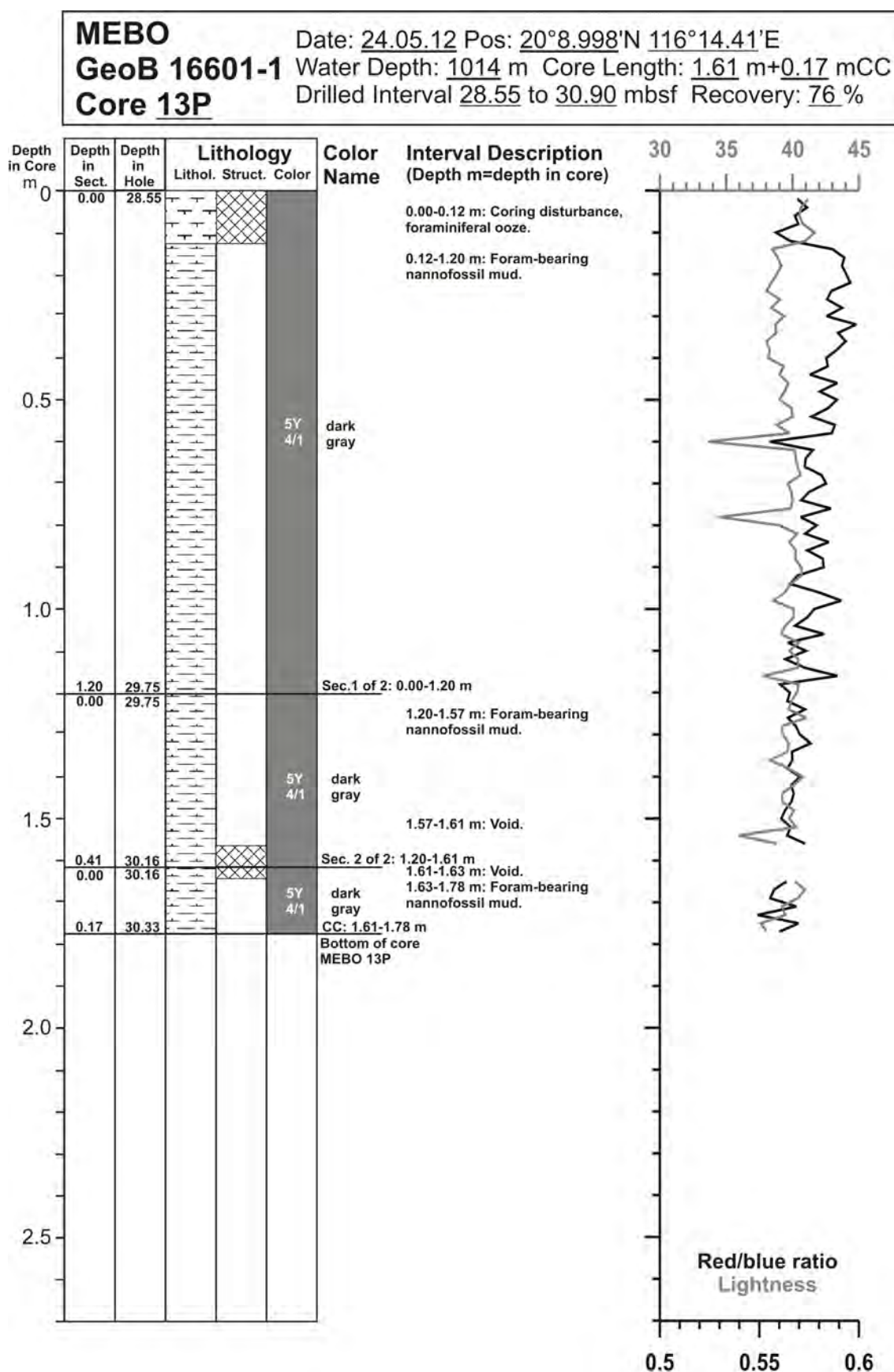


Fig. 10.17: Core description of MeBo core GeoB 16601-1 (13/28).

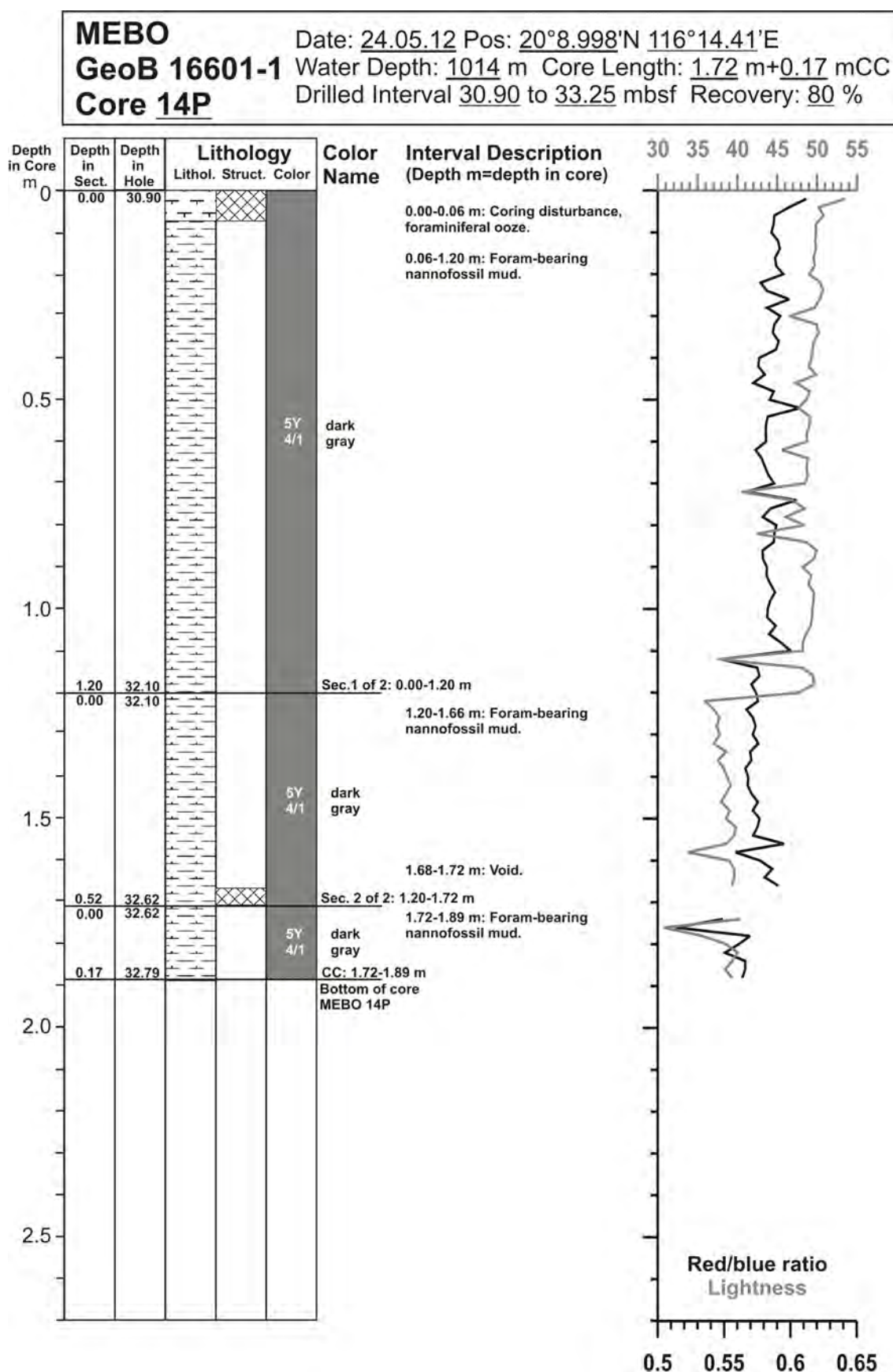


Fig. 10.18: Core description of MeBo core GeoB 16601-1 (14/28).

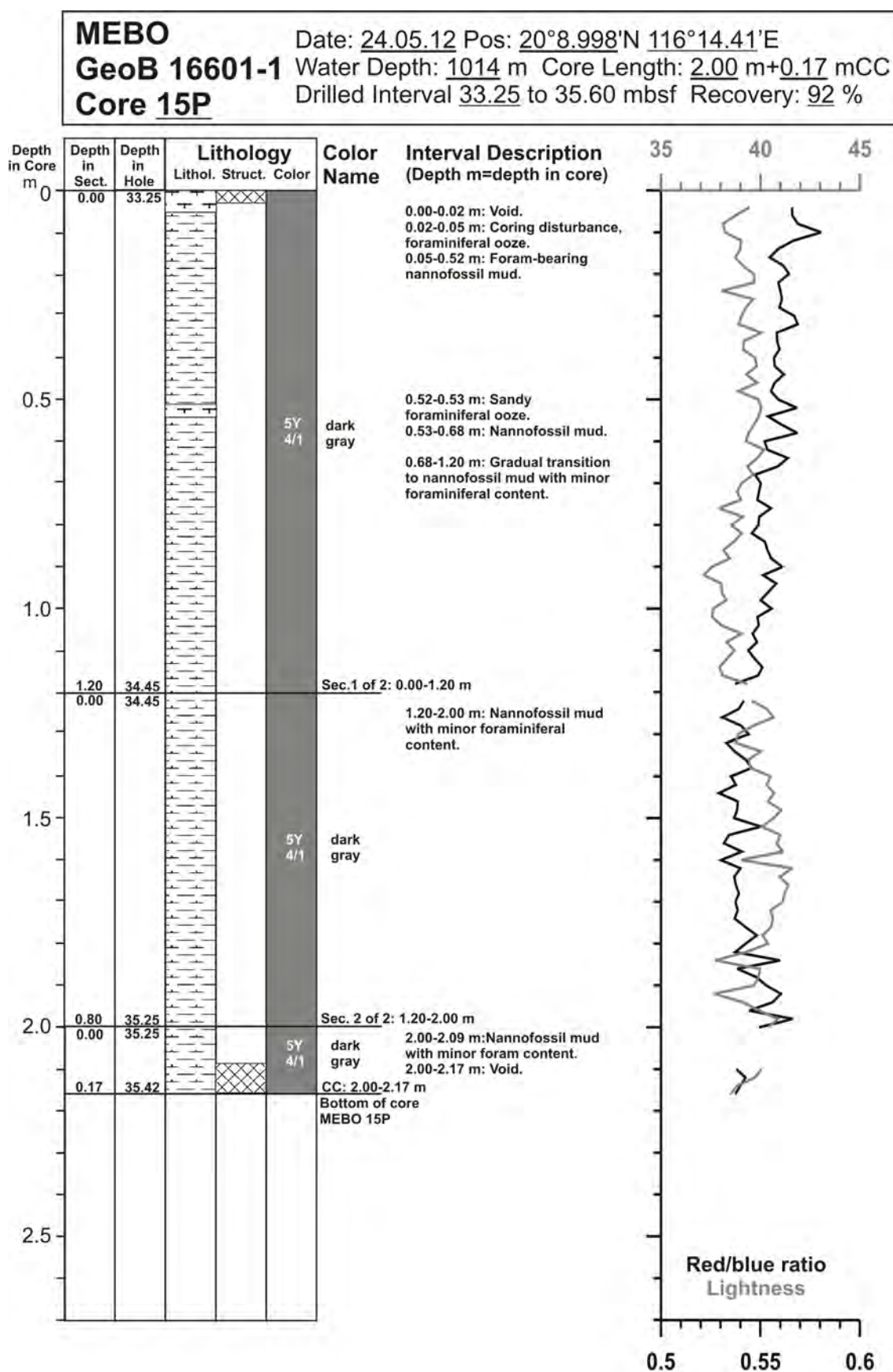


Fig. 10.19: Core description of MeBo core GeoB 16601-1 (15/28).

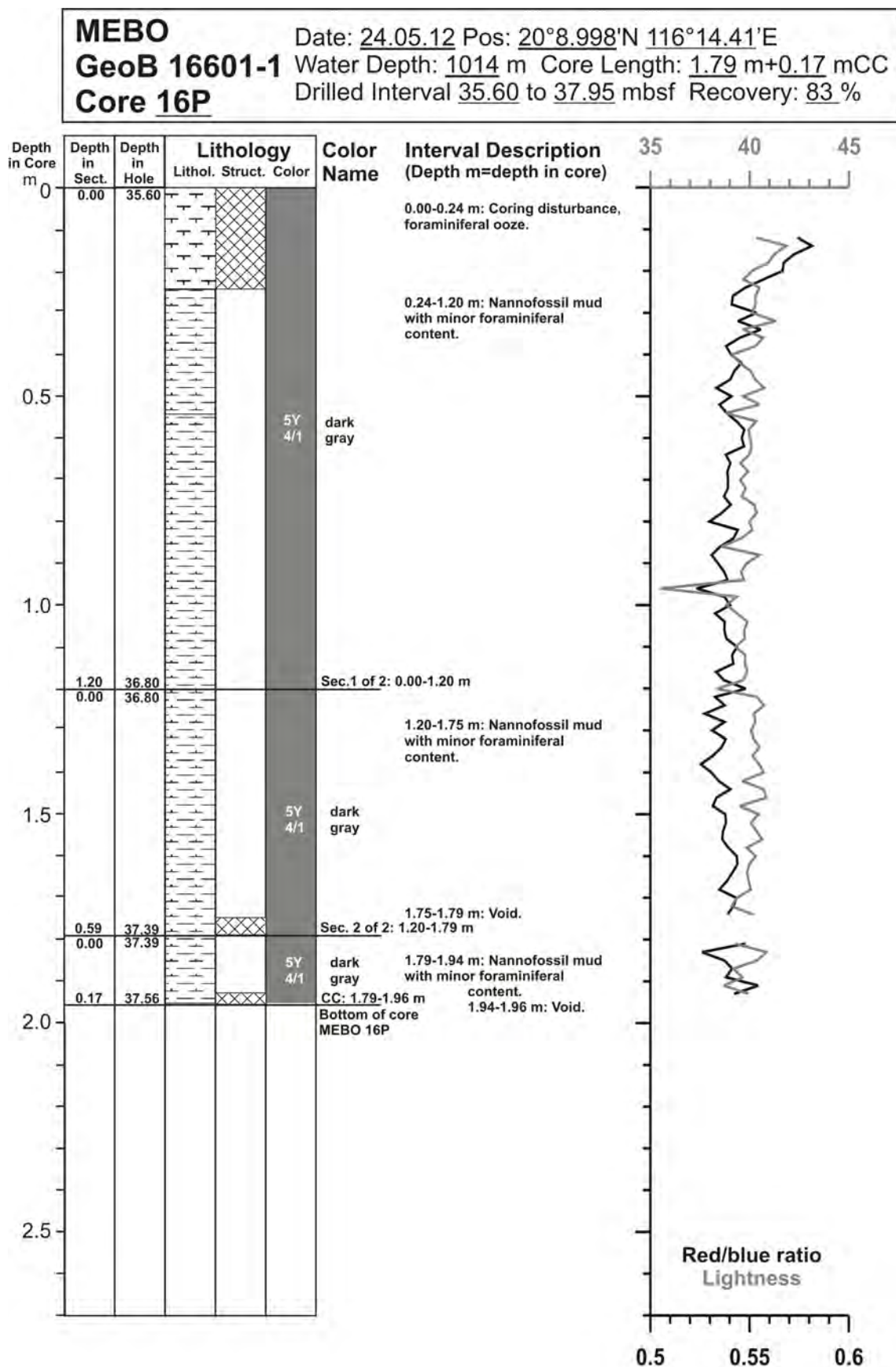


Fig. 10.20: Core description of MeBo core GeoB 16601-1 (16/28).

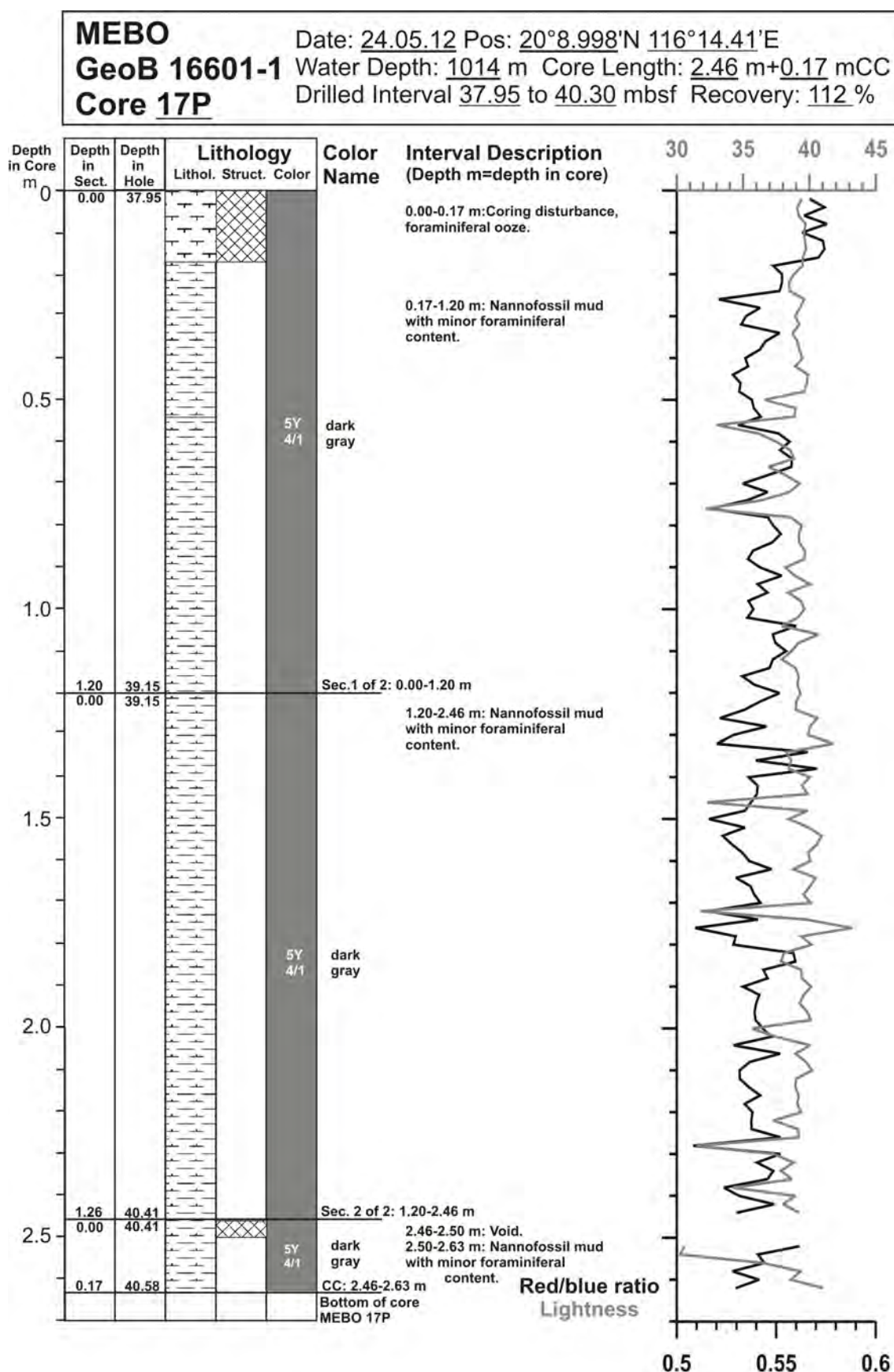


Fig. 10.21: Core description of MeBo core GeoB 16601-1 (17/28).

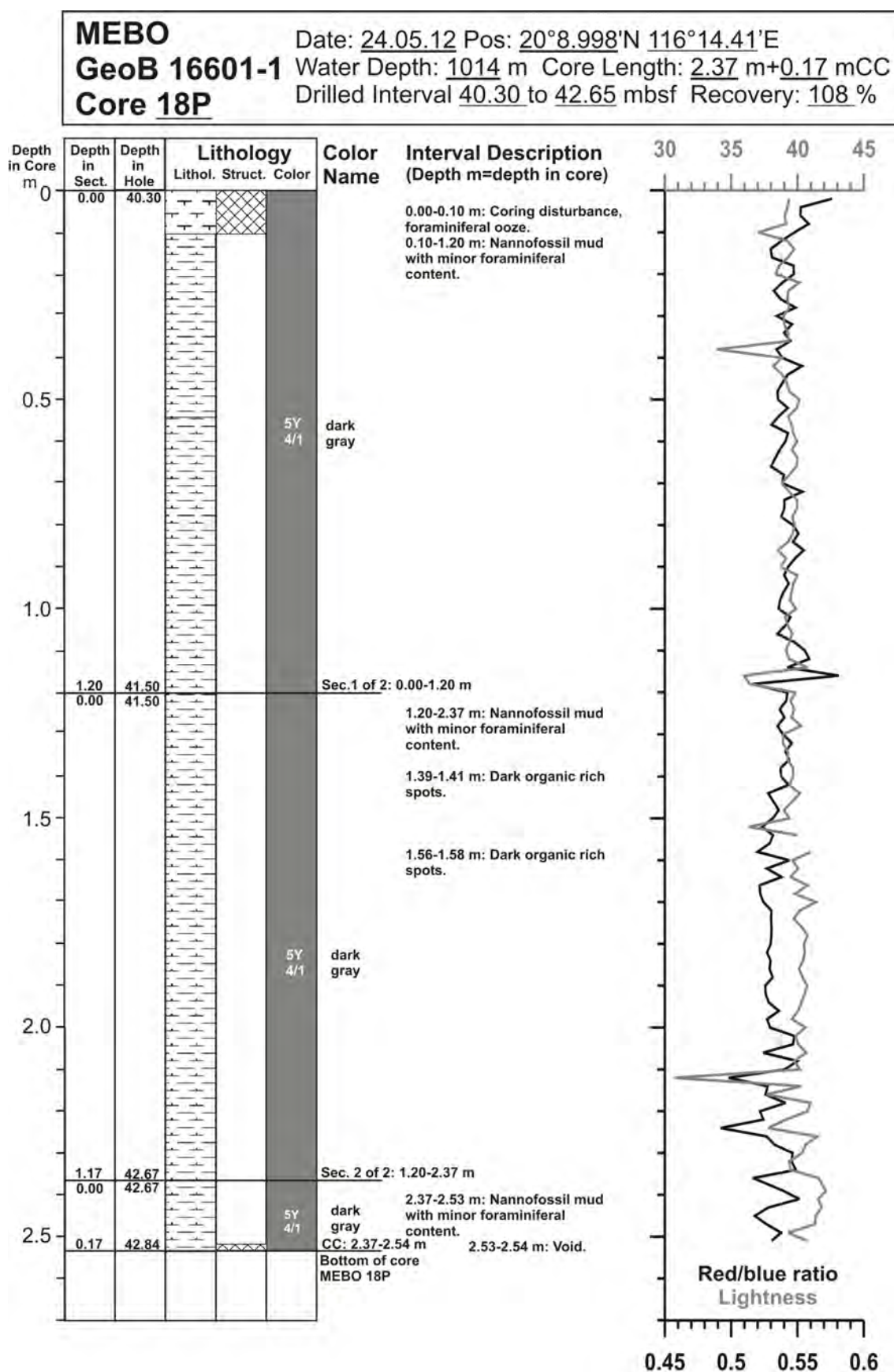


Fig. 10.22: Core description of MeBo core GeoB 16601-1 (18/28).

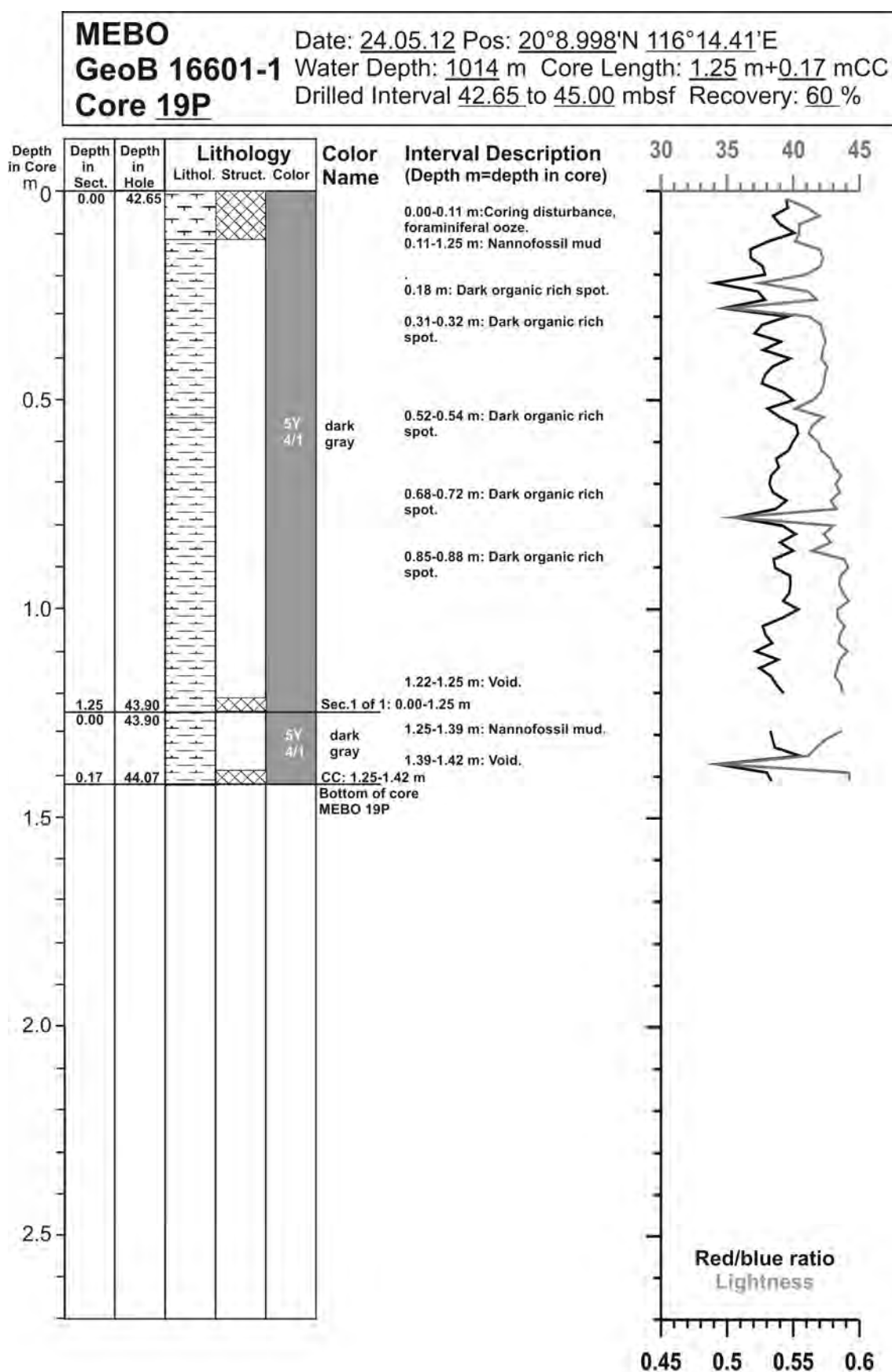


Fig. 10.23: Core description of MeBo core GeoB 16601-1 (19/28).

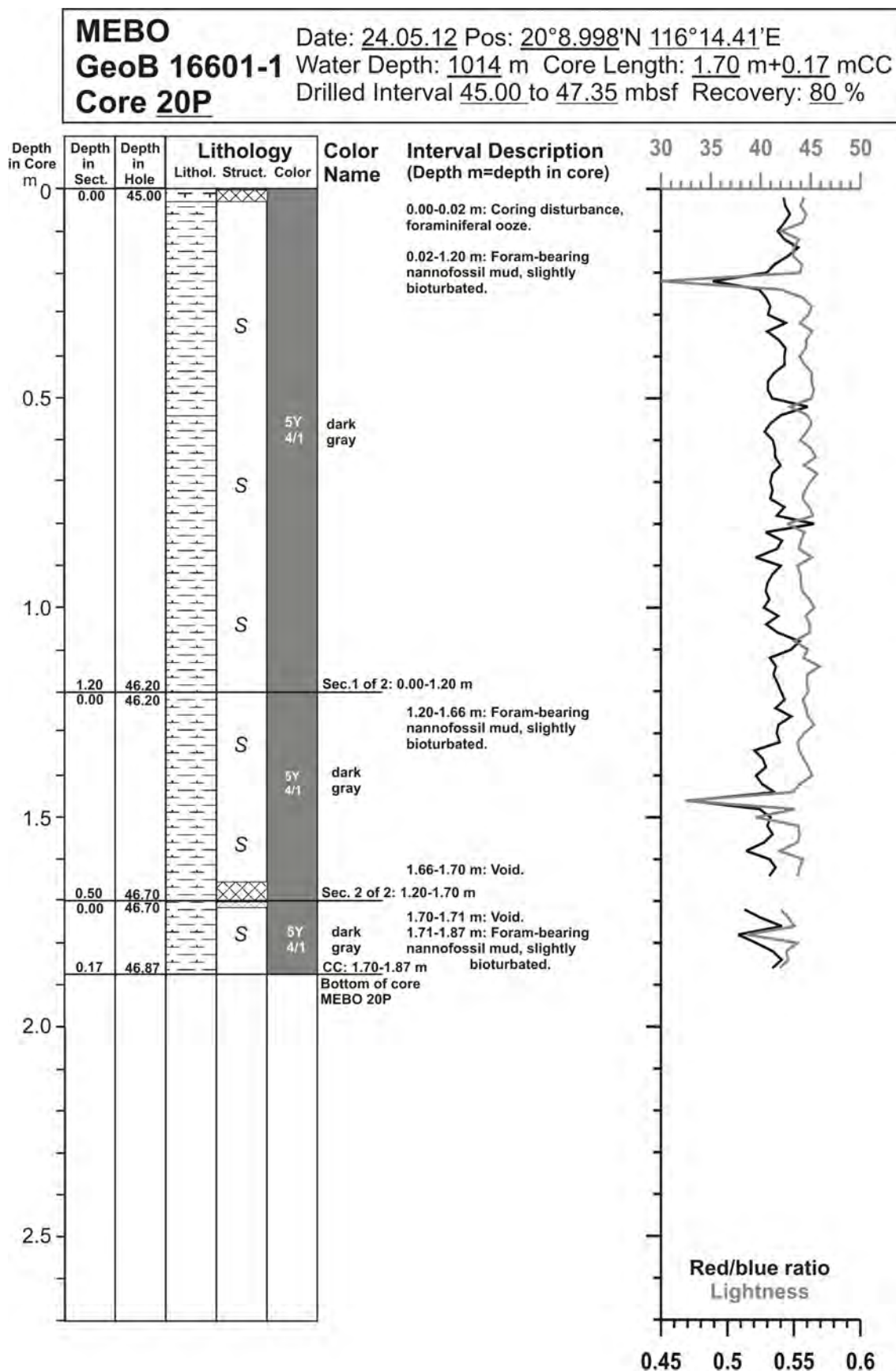


Fig. 10.24: Core description of MeBo core GeoB 16601-1 (20/28).

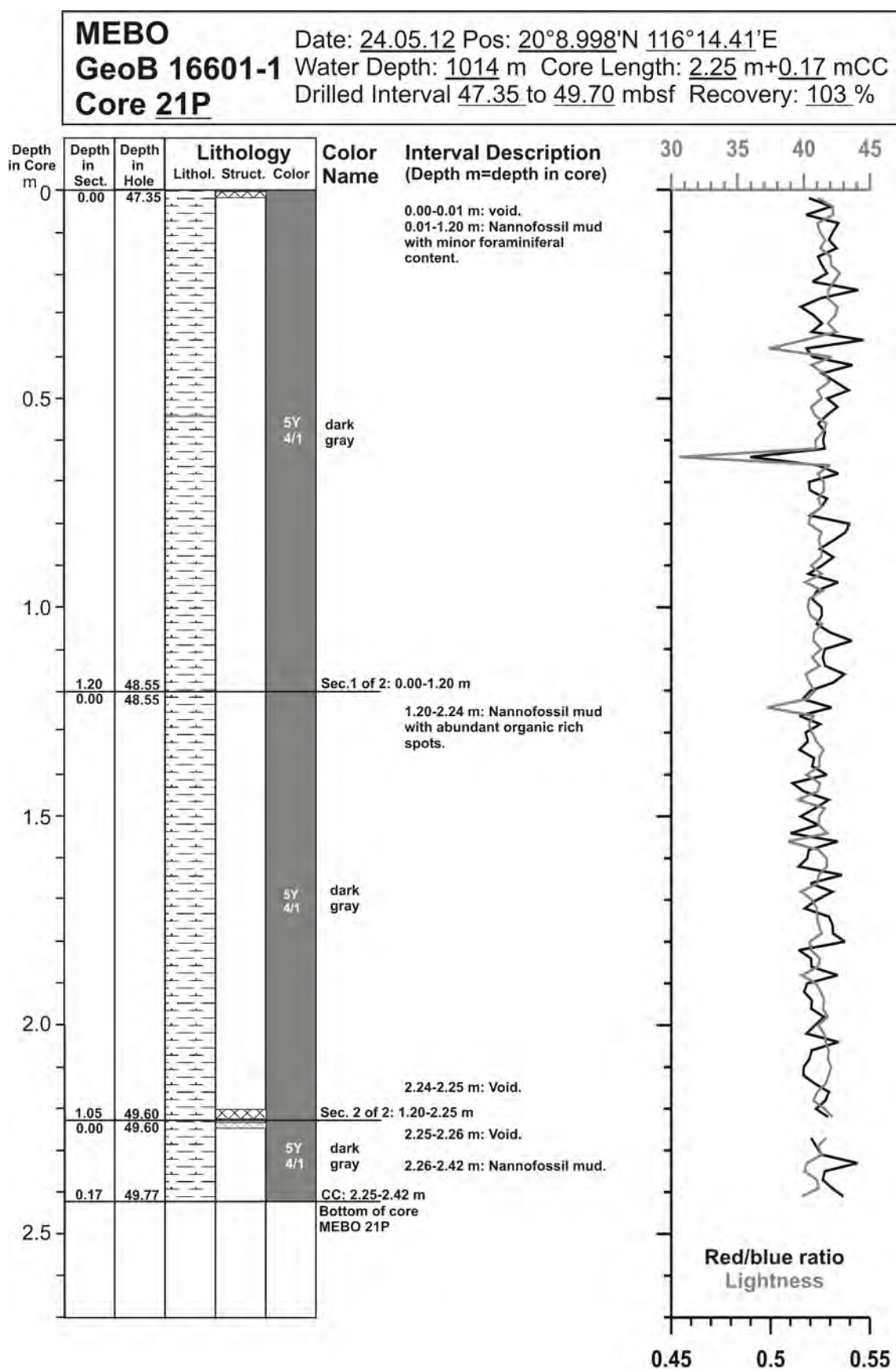


Fig. 10.25: Core description of MeBo core GeoB 16601-1 (21/28).

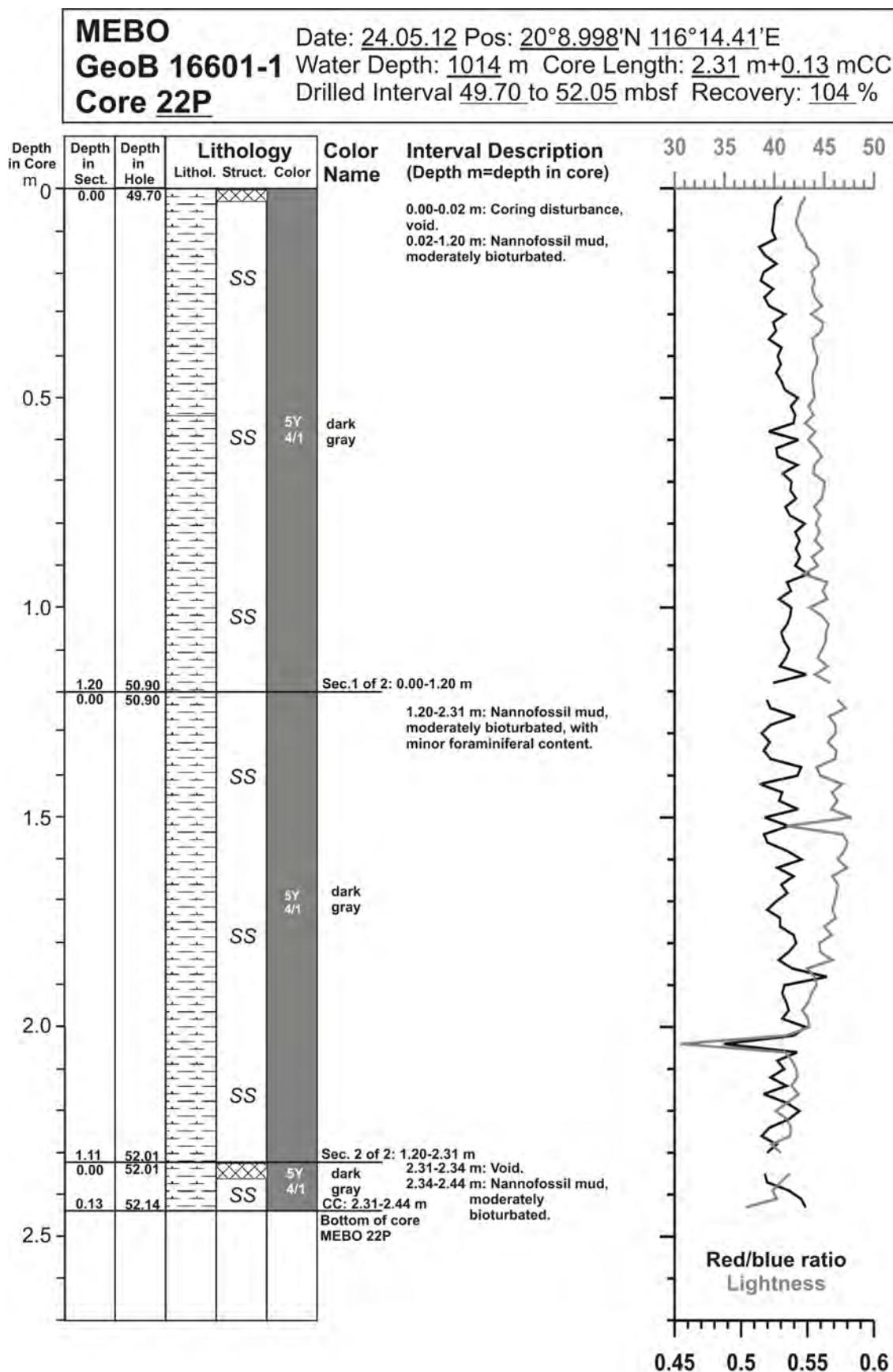


Fig. 10.26: Core description of MeBo core GeoB 16601-1 (22/28).

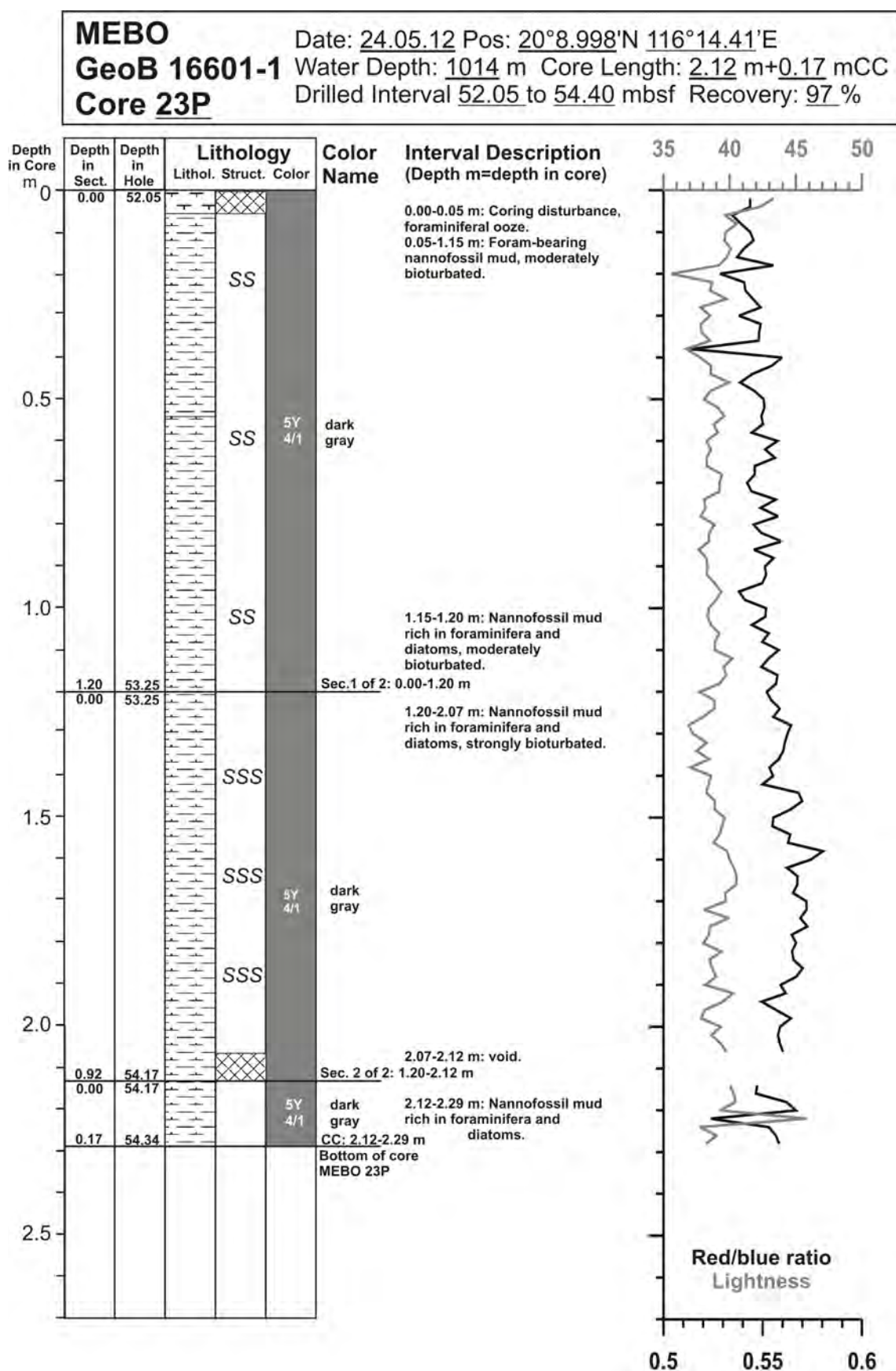


Fig. 10.27: Core description of MeBo core GeoB 16601-1 (23/28).

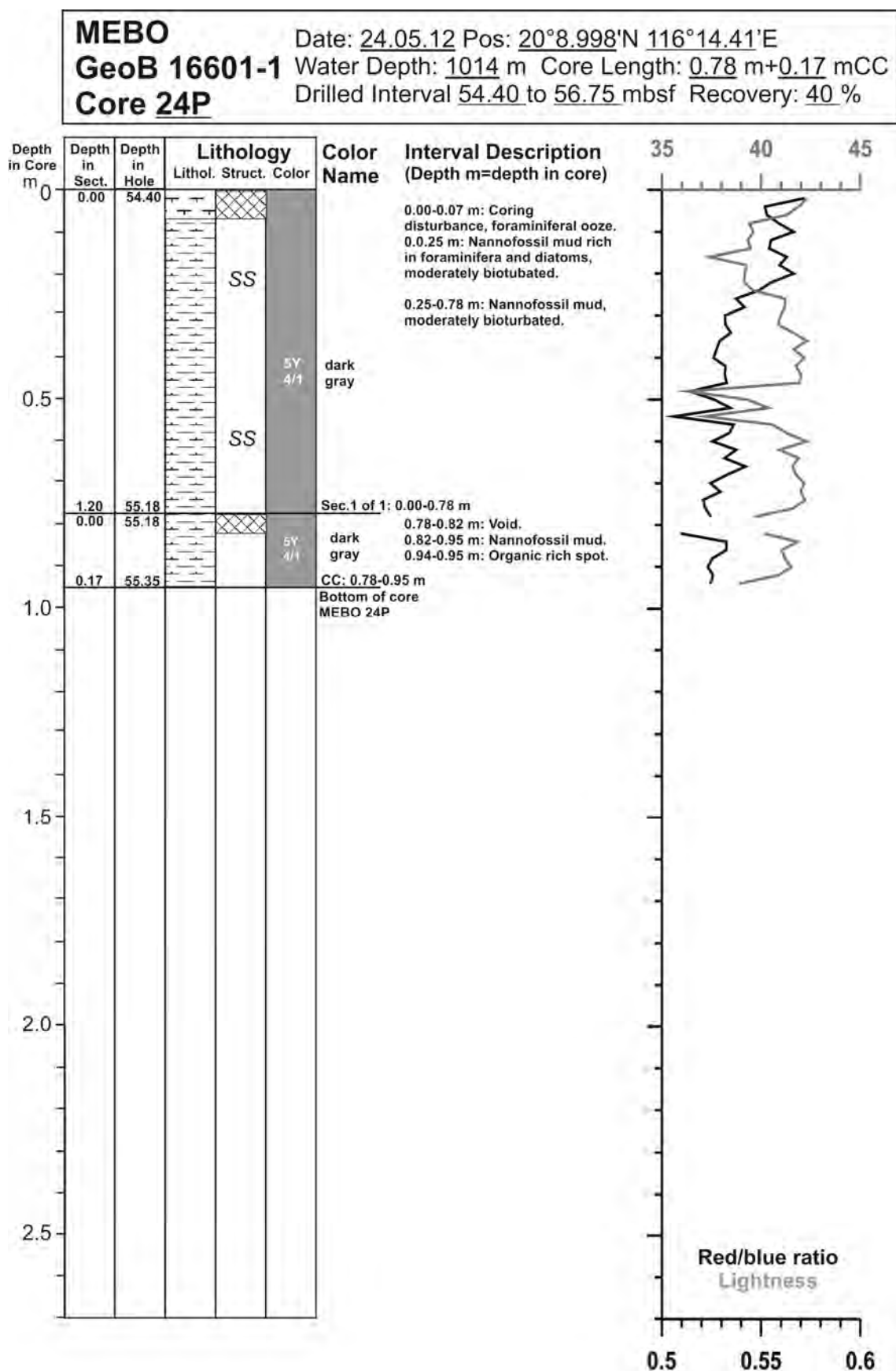


Fig. 10.28: Core description of MeBo core GeoB 16601-1 (24/28).

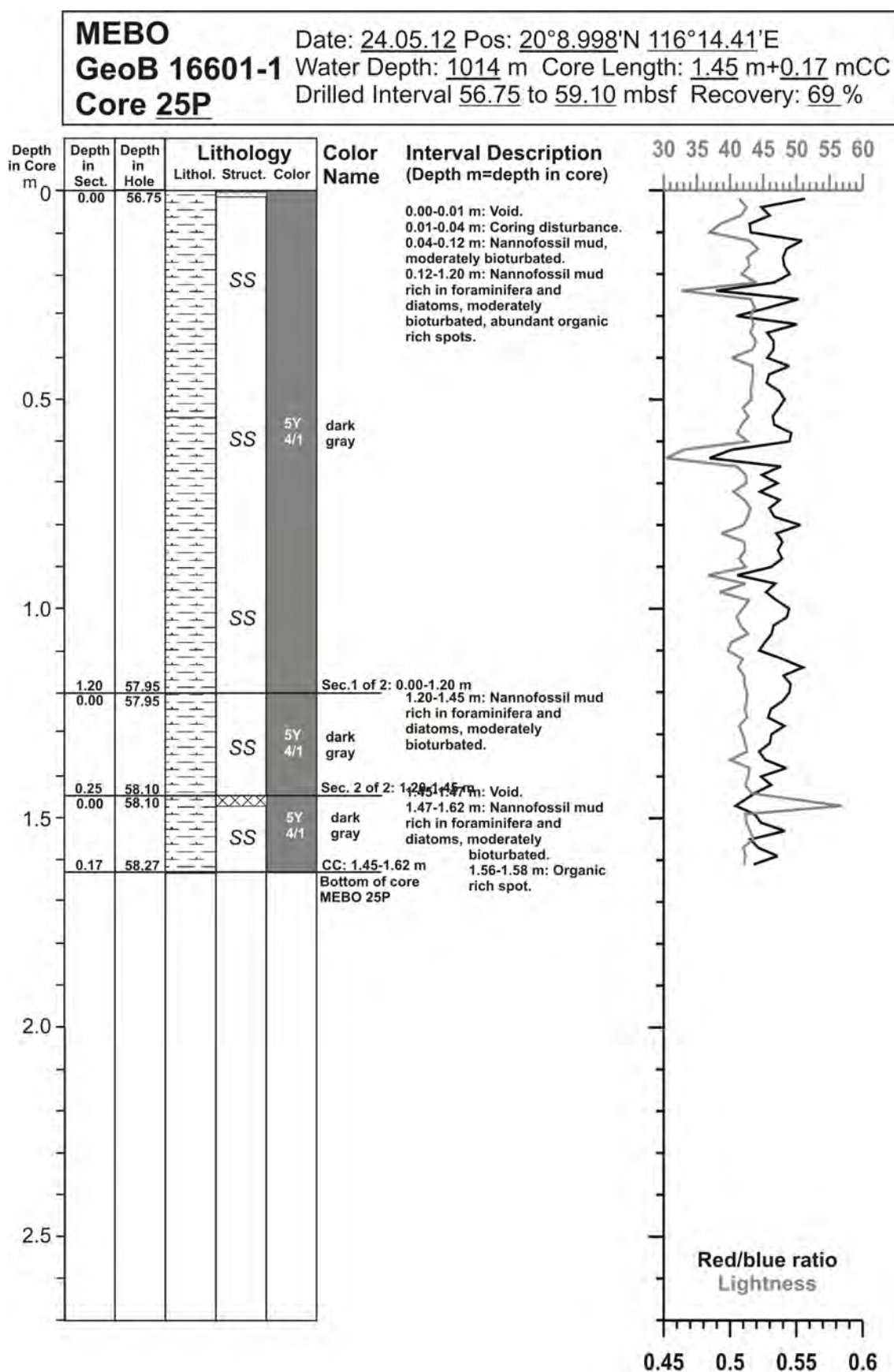


Fig. 10.29: Core description of MeBo core GeoB 16601-1 (25/28).

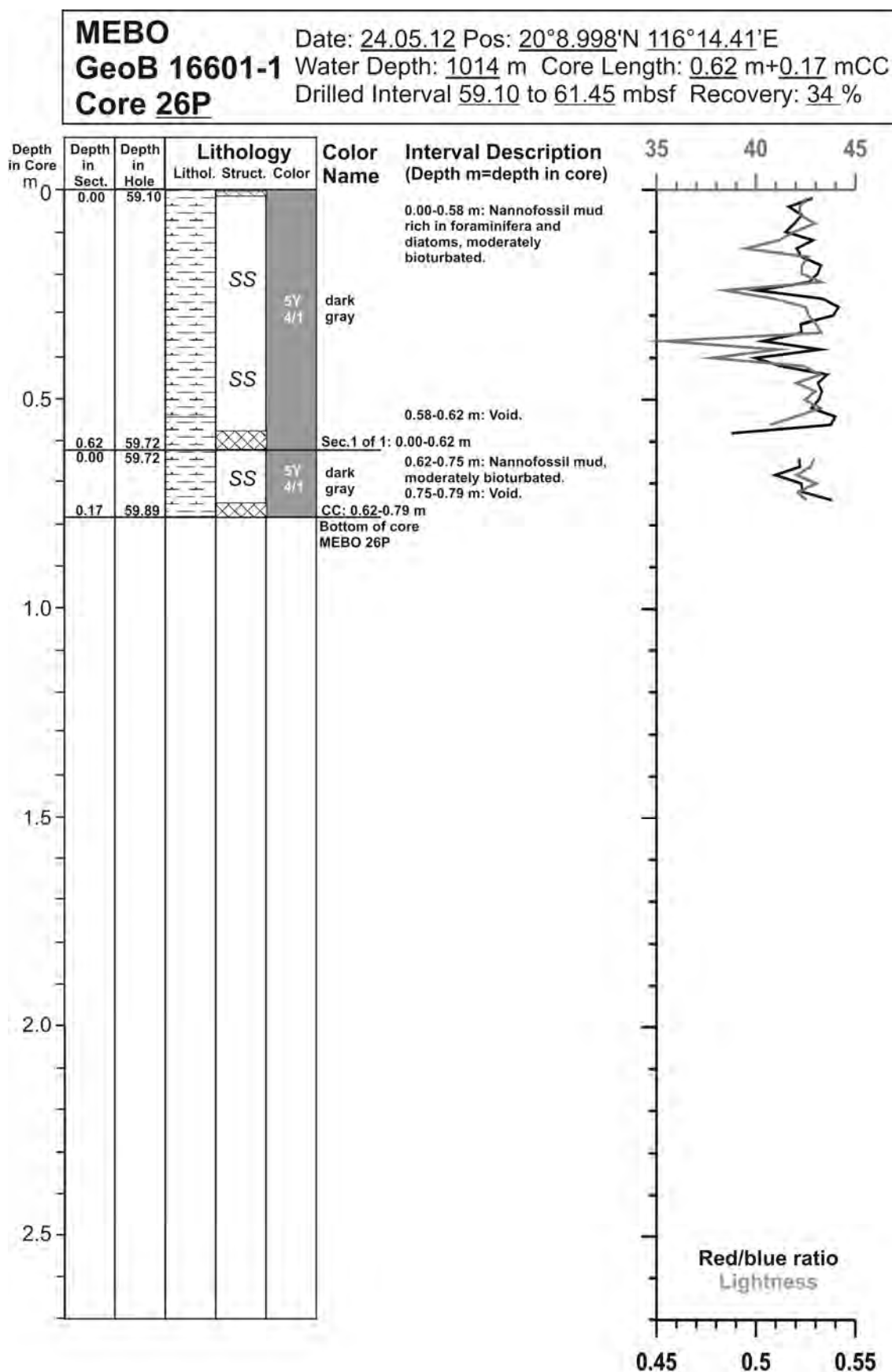


Fig. 10.30: Core description of MeBo core GeoB 16601-1 (26/28).

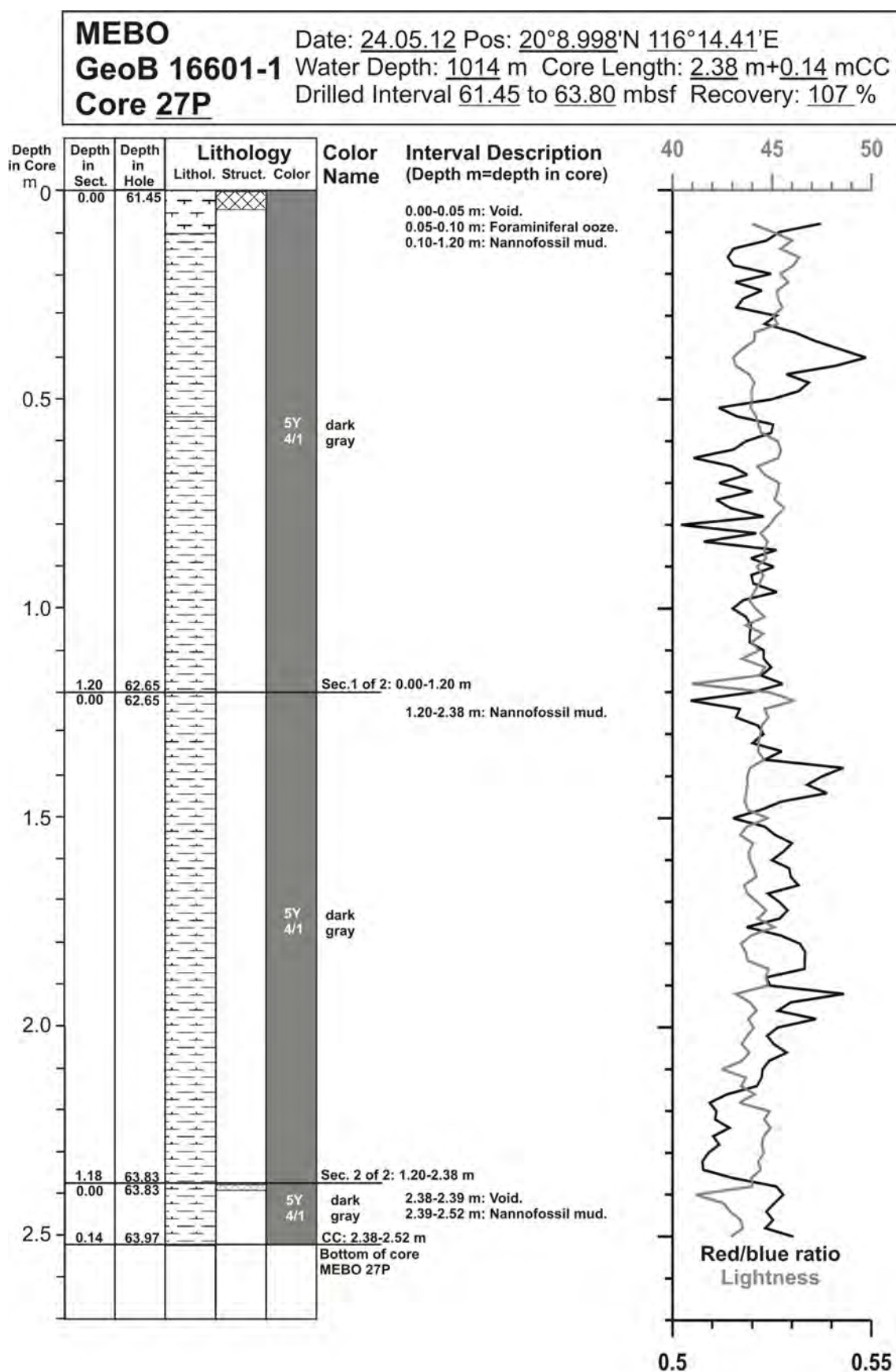


Fig. 10.31: Core description of MeBo core GeoB 16601-1 (27/28).

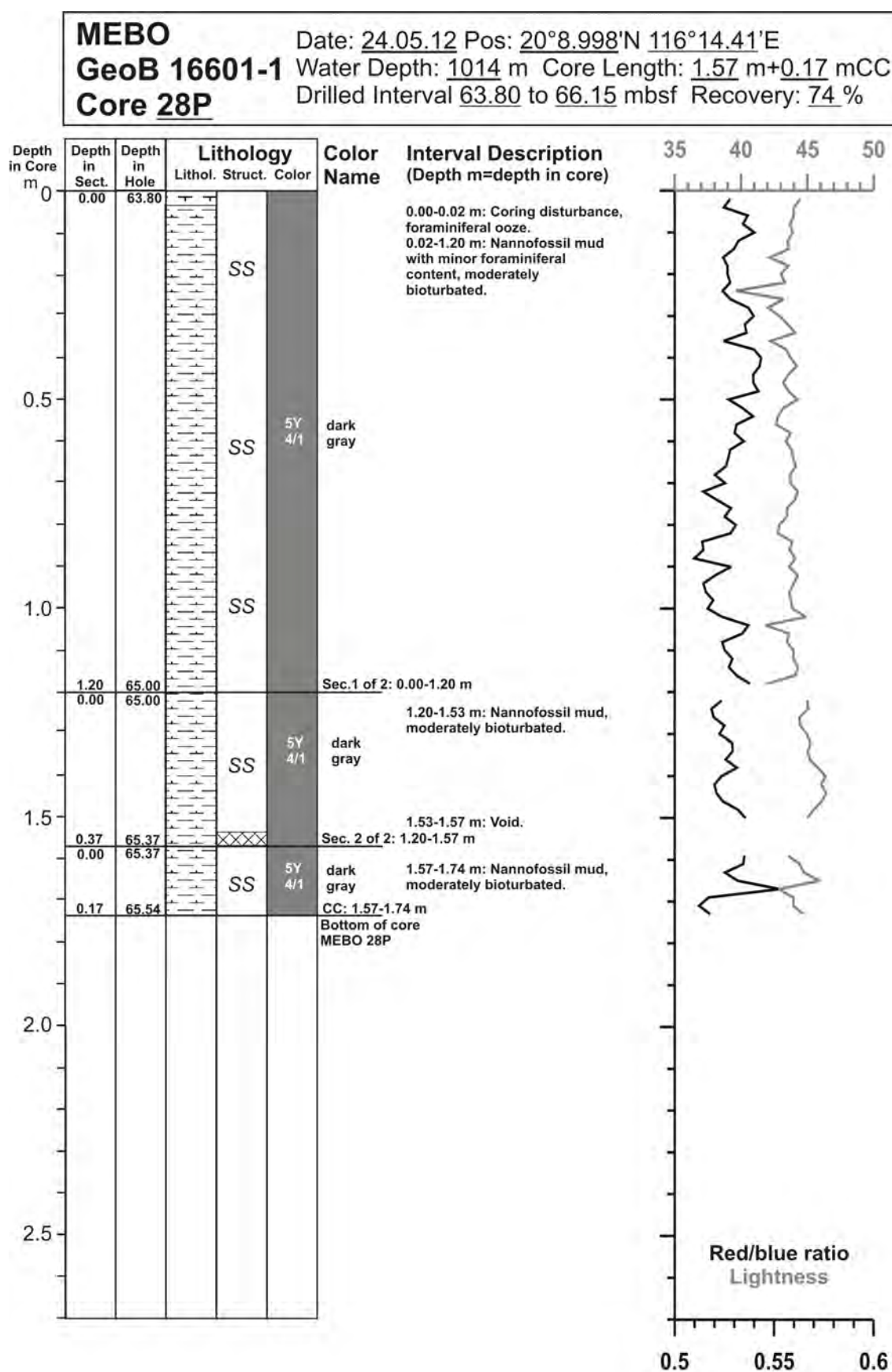


Fig. 10.32: Core description of MeBo core GeoB 16601-1 (28/28).

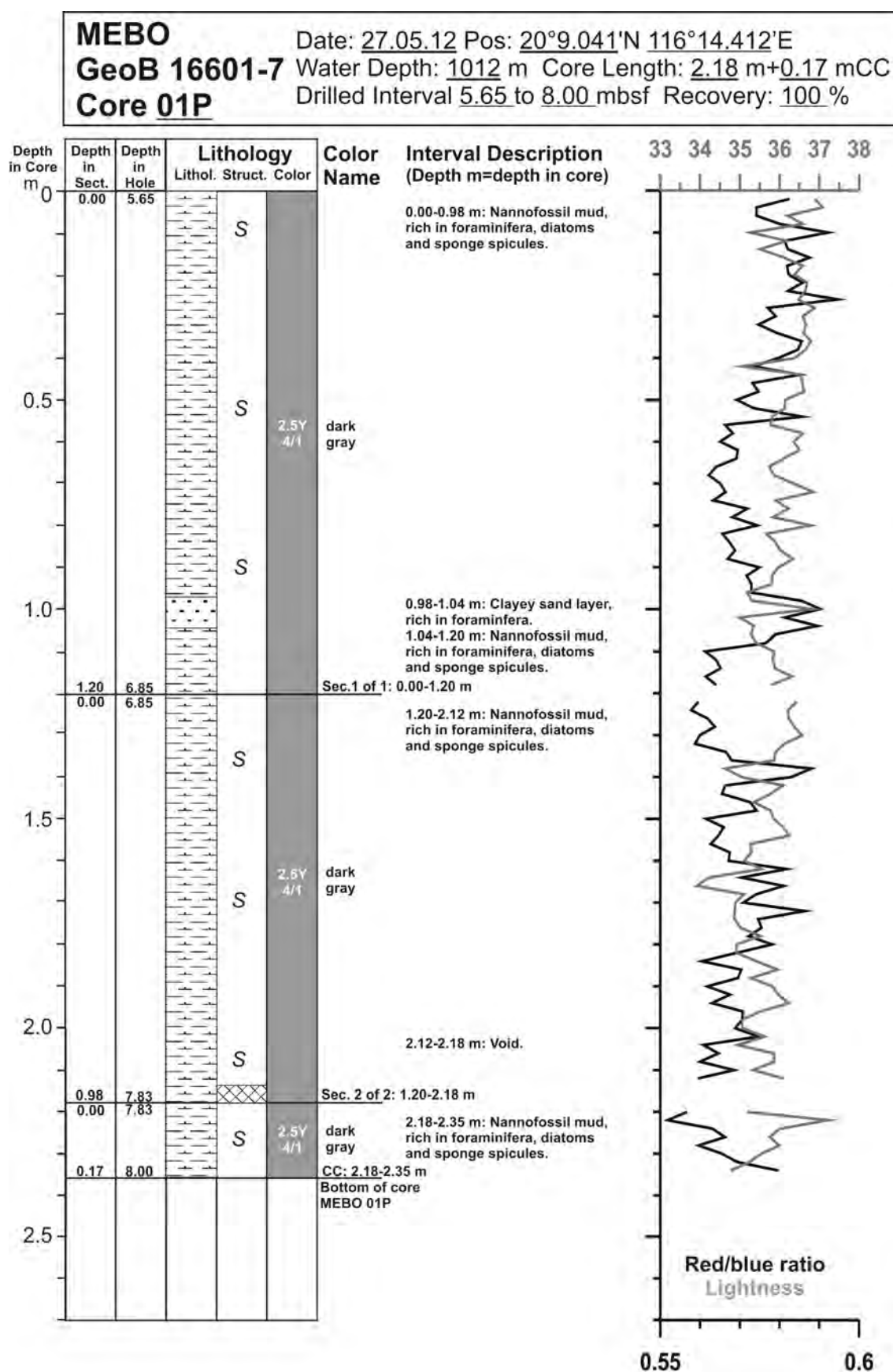


Fig. 10.33: Core description of MeBo core GeoB 16601-7 (1/29).

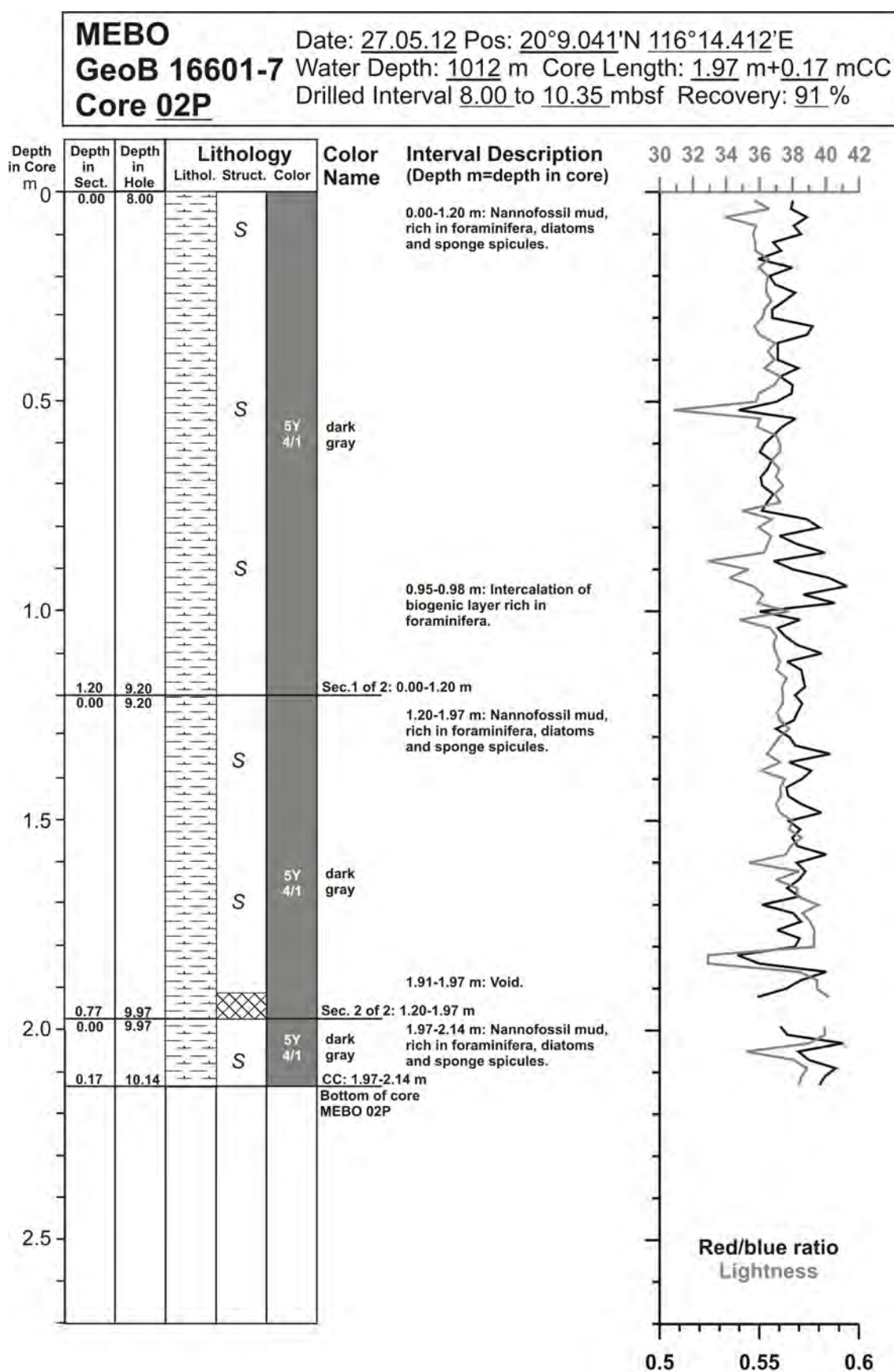


Fig. 10.34: Core description of MeBo core GeoB 16601-7 (2/29).

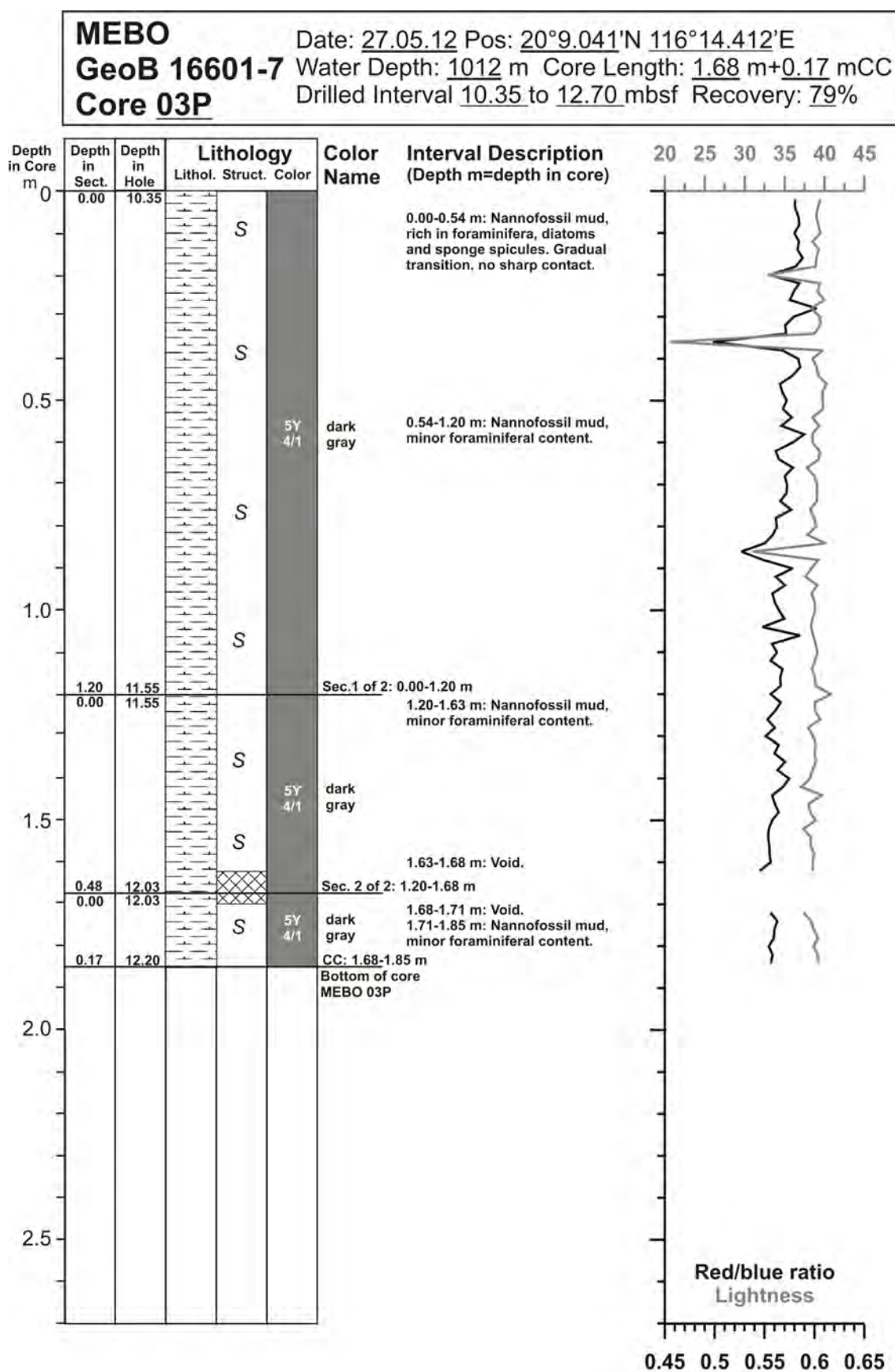


Fig. 10.35: Core description of MeBo core GeoB 16601-7 (3/29).

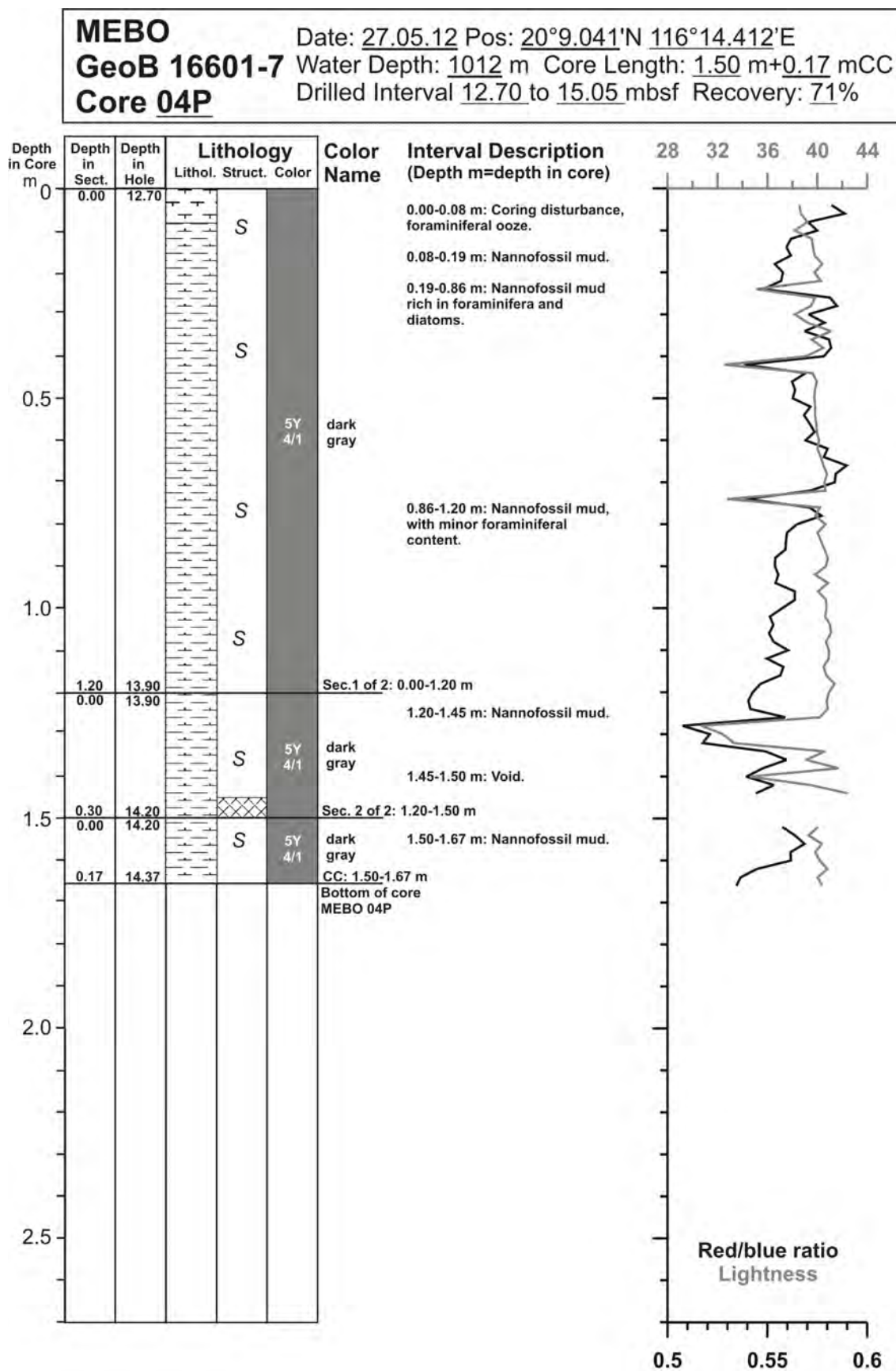


Fig. 10.36: Core description of MeBo core GeoB 16601-7 (4/29).

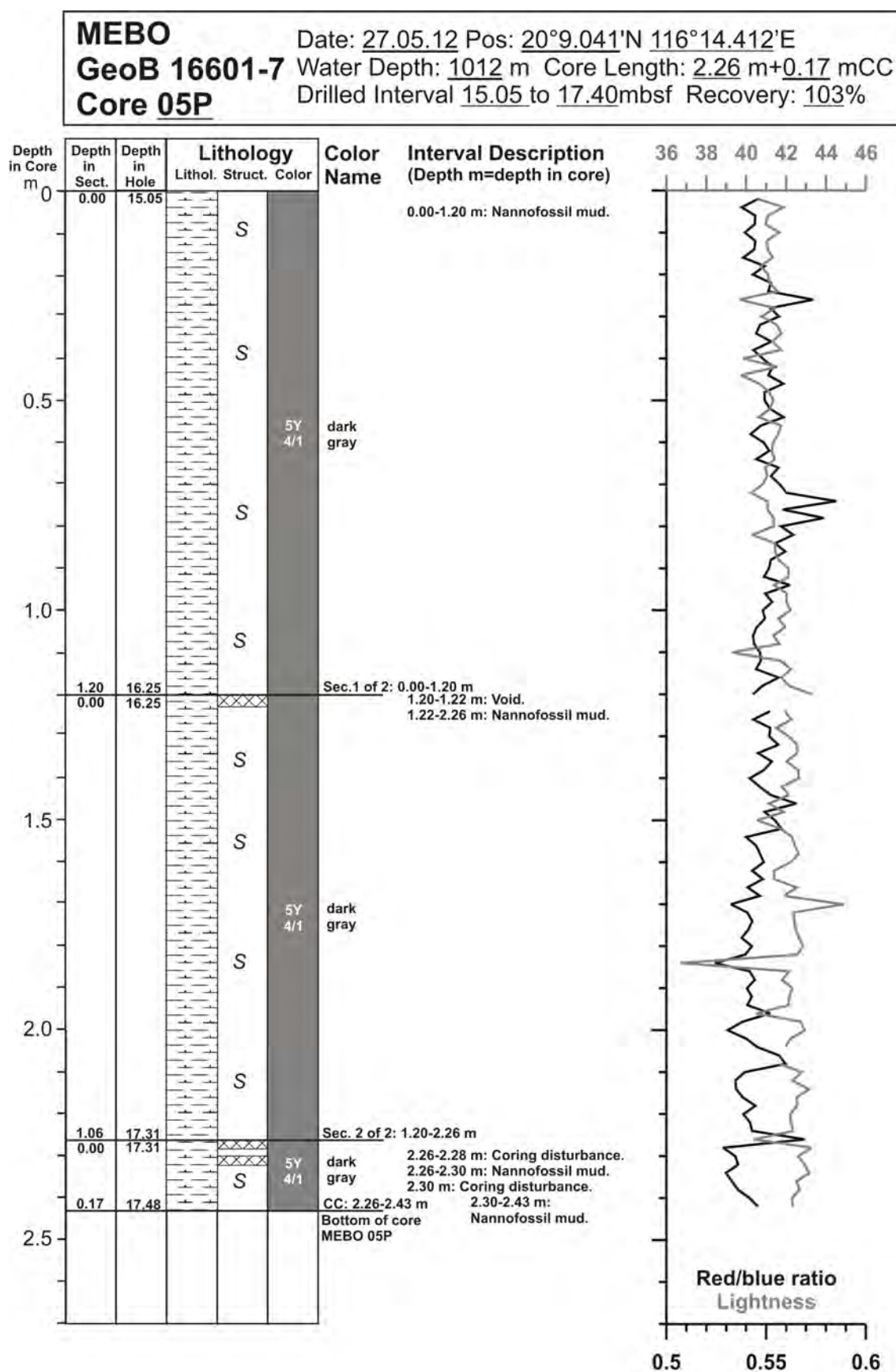


Fig. 10.37: Core description of MeBo core GeoB 16601-7 (5/29).

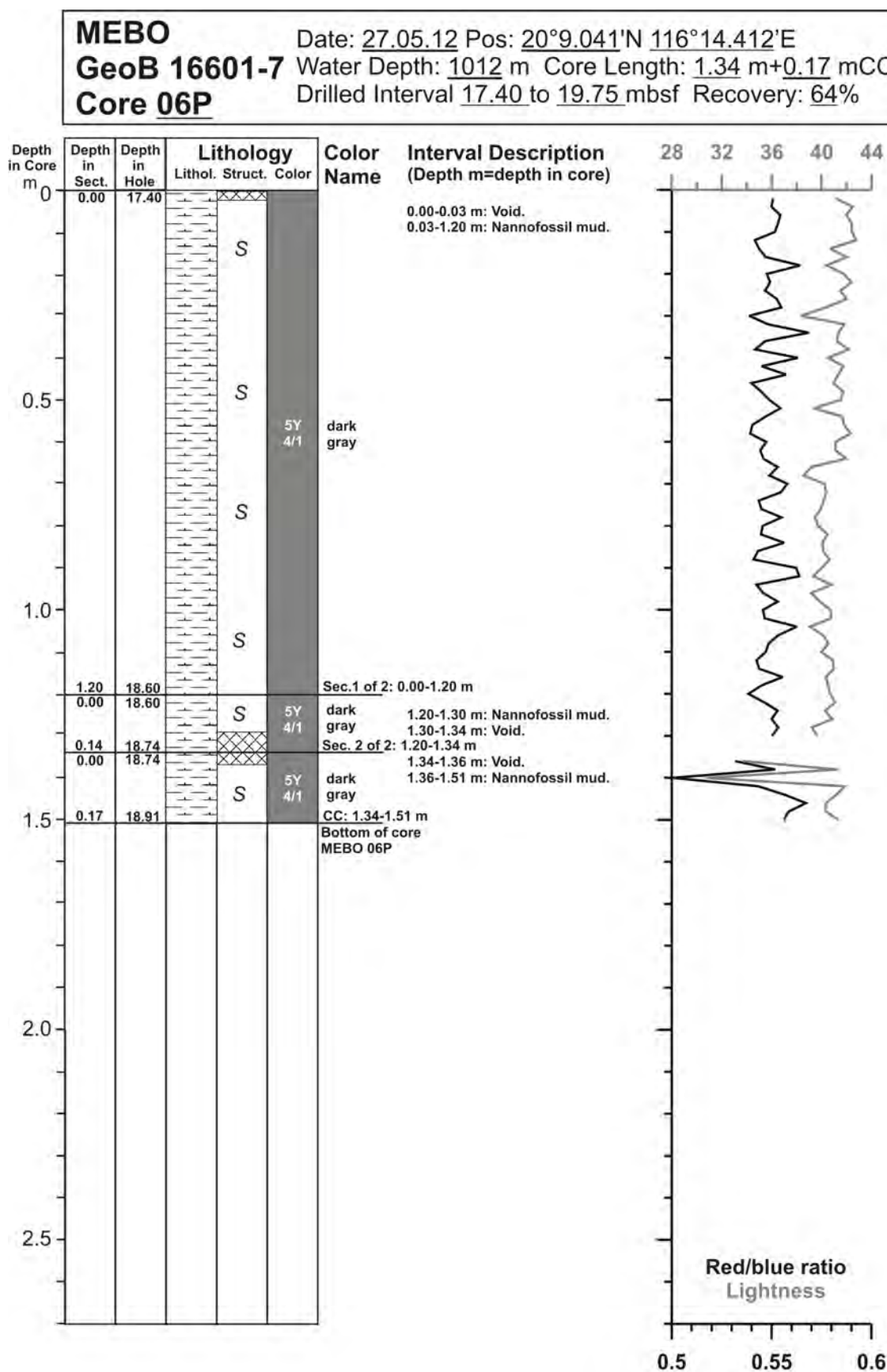


Fig. 10.38: Core description of MeBo core GeoB 16601-7 (6/29).

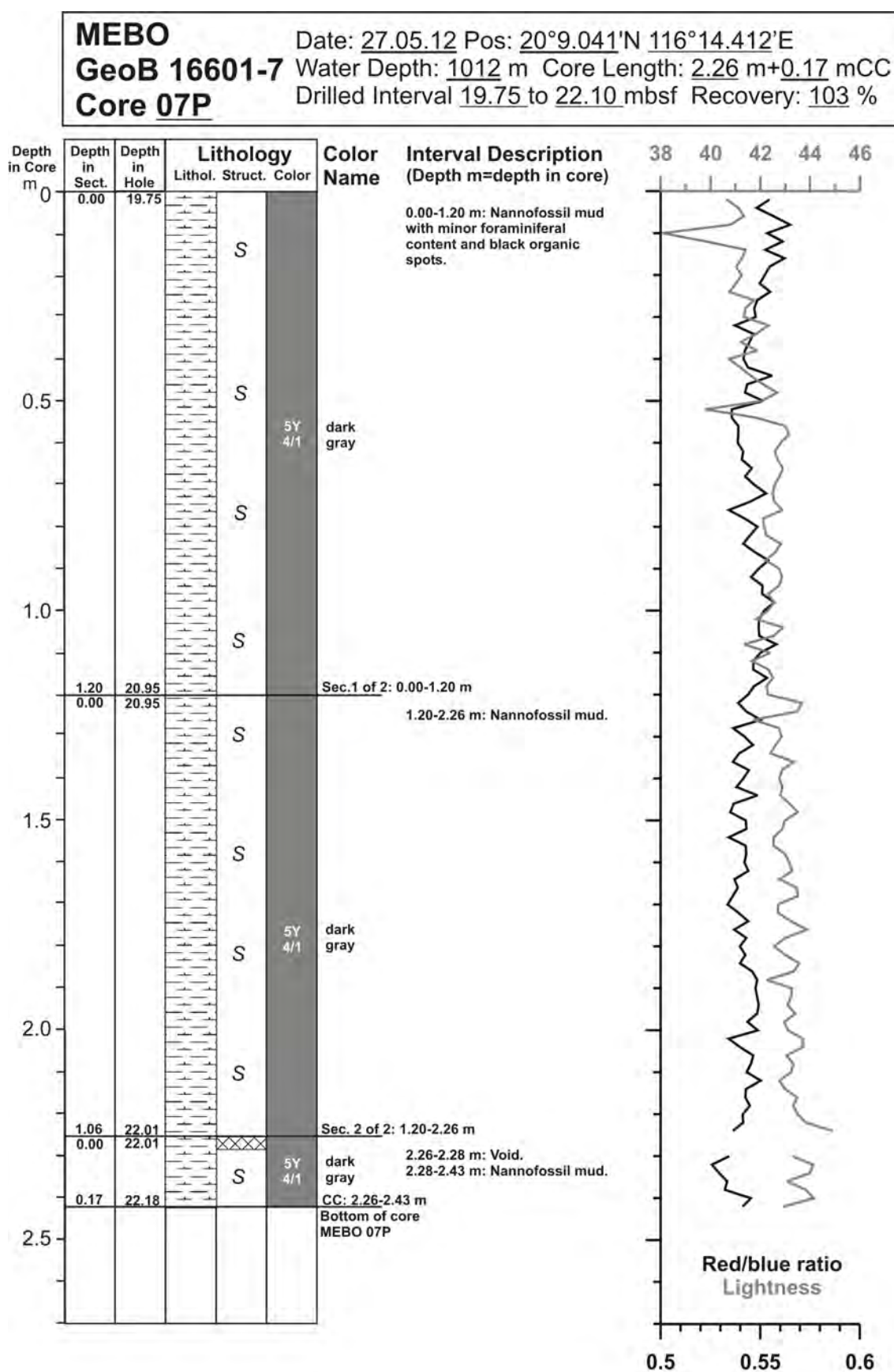


Fig. 10.39: Core description of MeBo core GeoB 16601-7 (7/29).

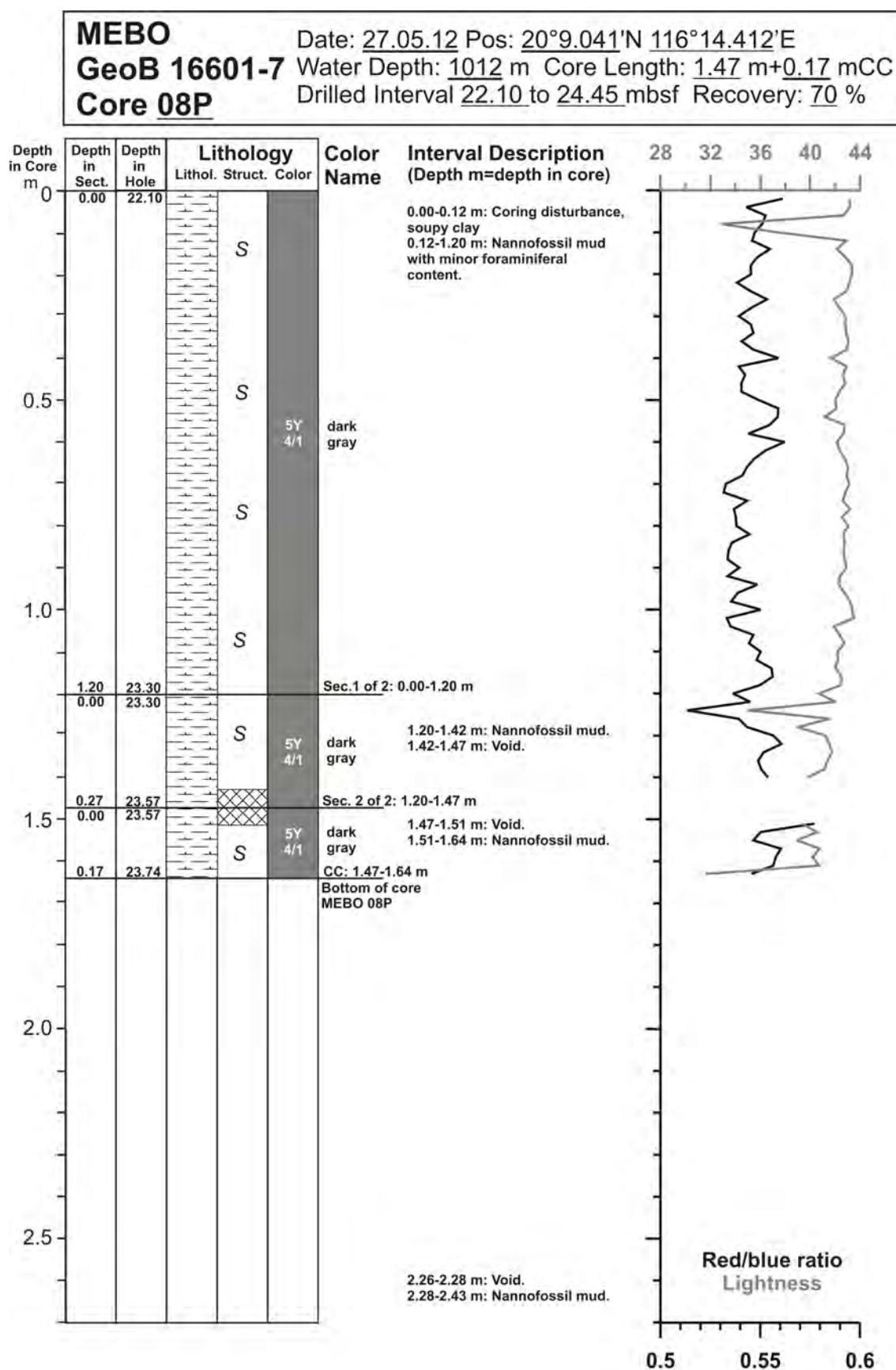


Fig. 10.40: Core description of MeBo core GeoB 16601-7 (8/29).

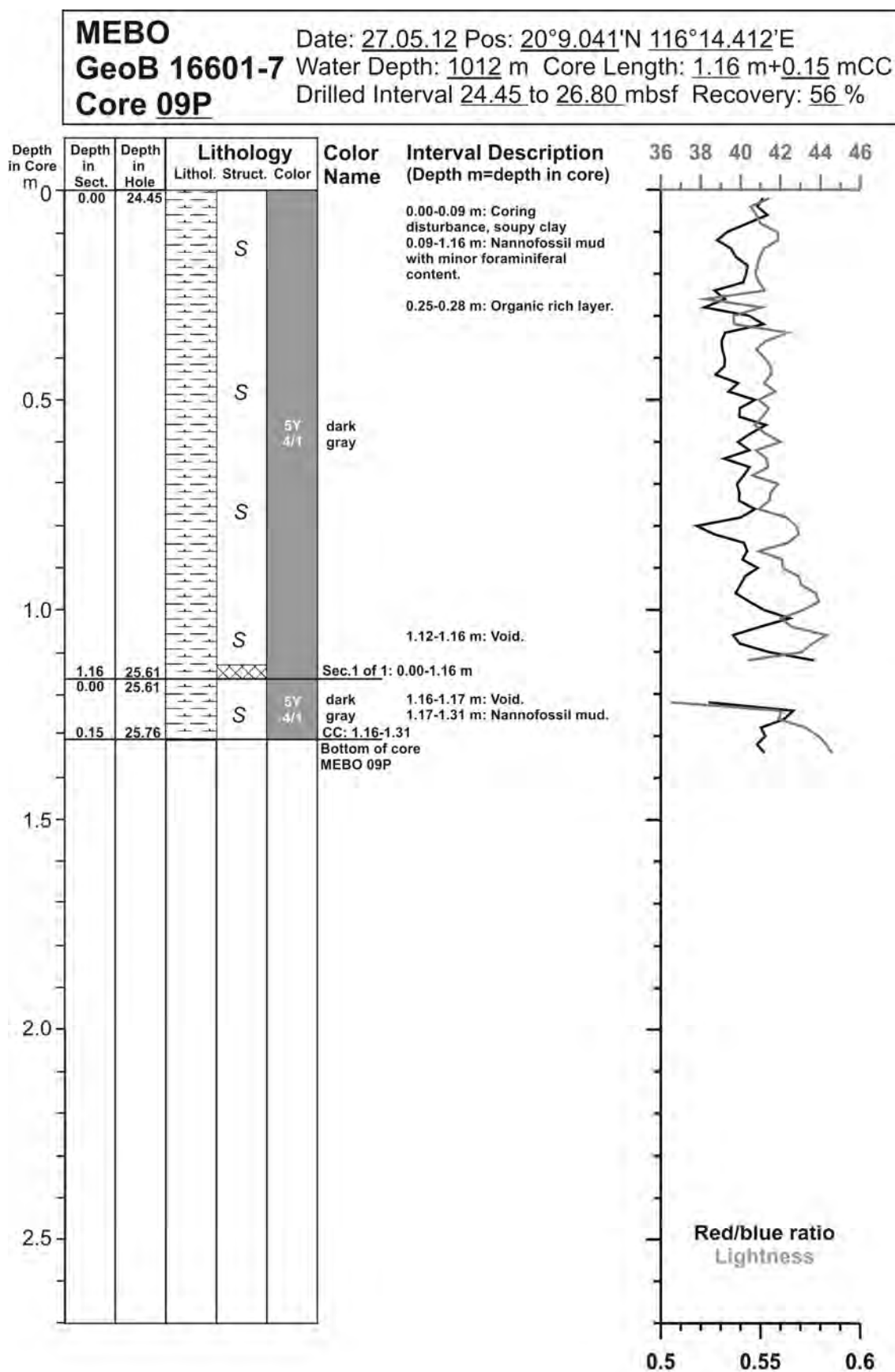


Fig. 10.41: Core description of MeBo core GeoB 16601-7 (9/29).

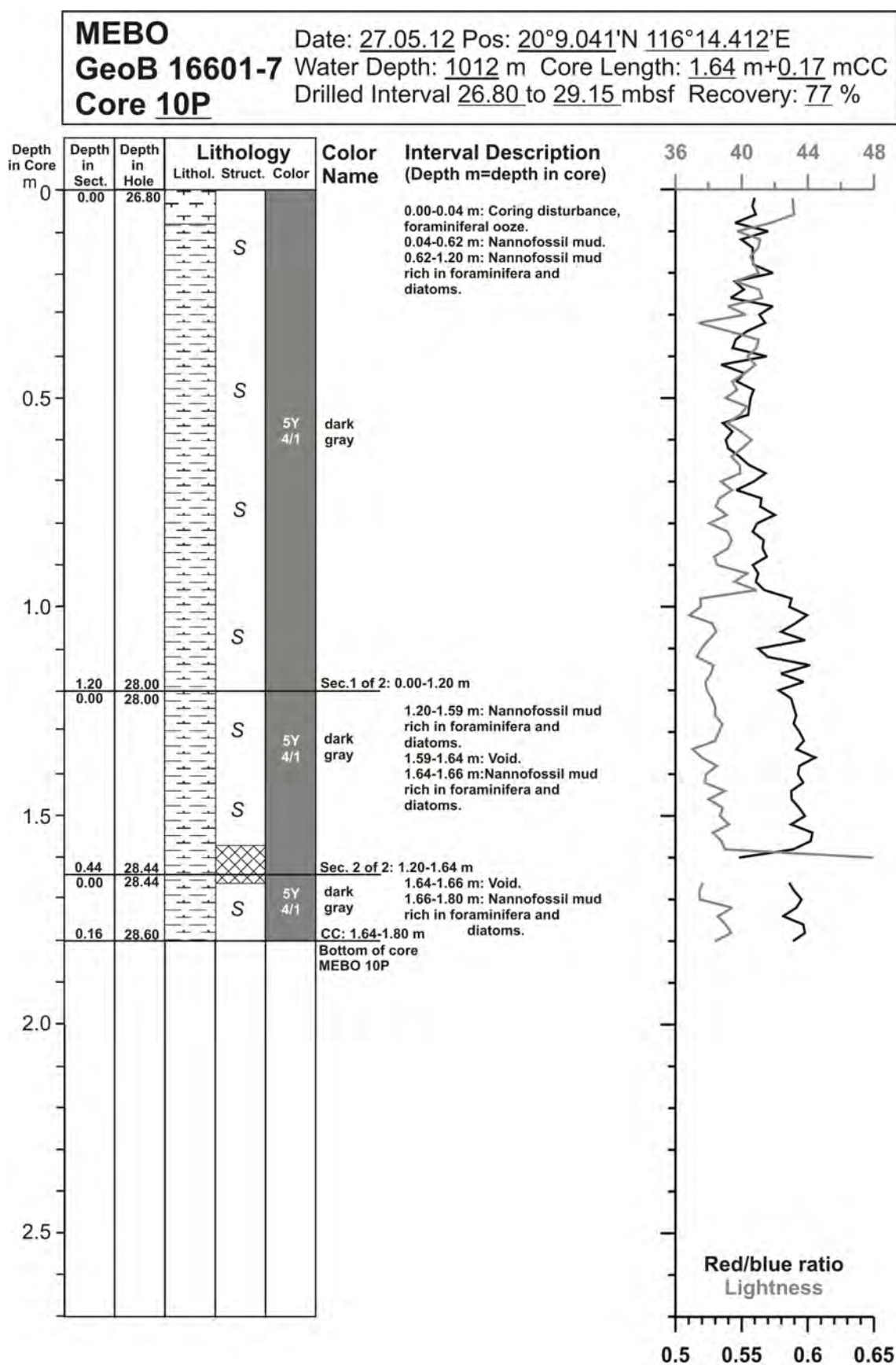


Fig. 10.42: Core description of MeBo core GeoB 16601-7 (10/29).

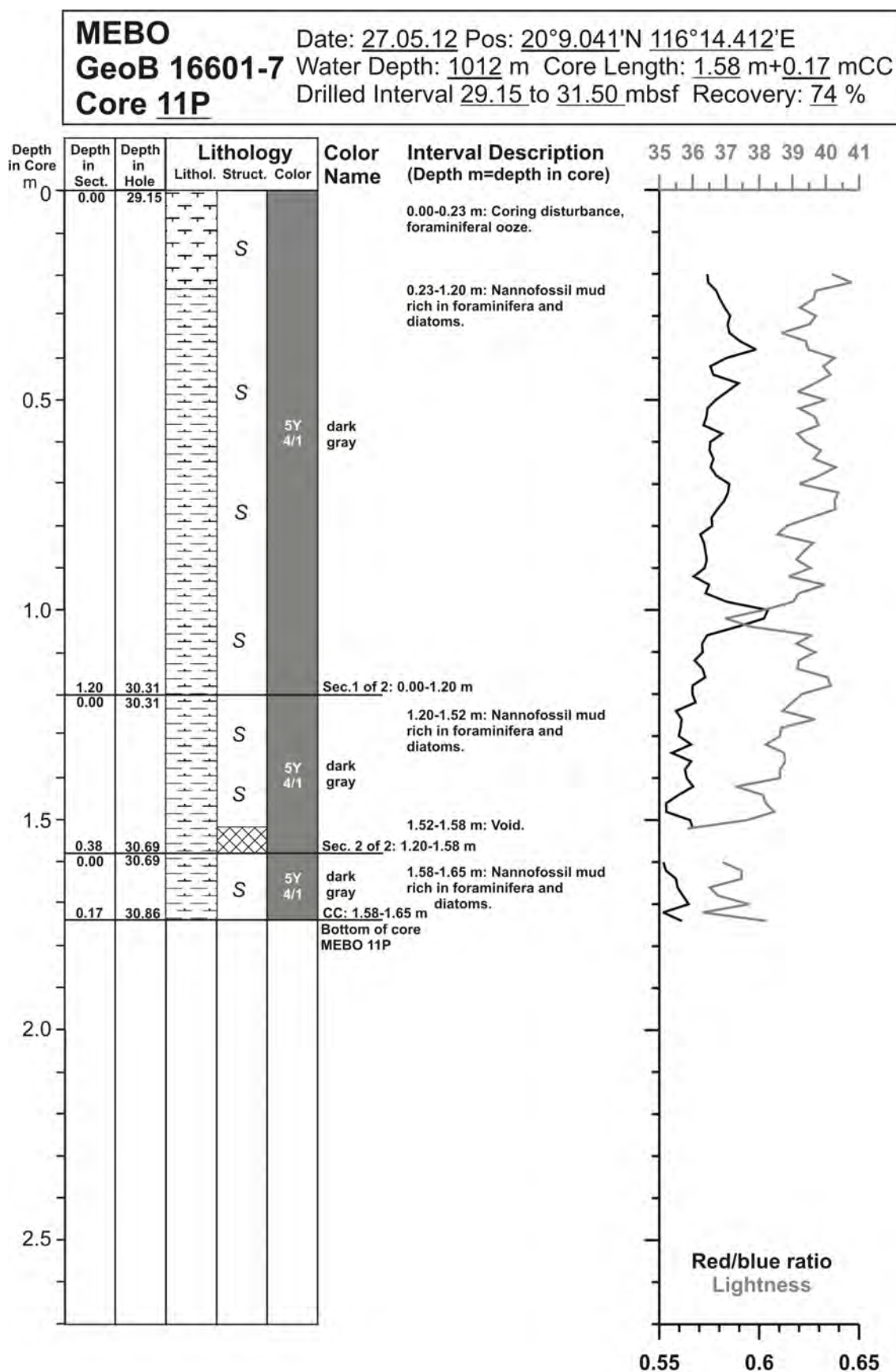


Fig. 10.43: Core description of MeBo core GeoB 16601-7 (11/29).

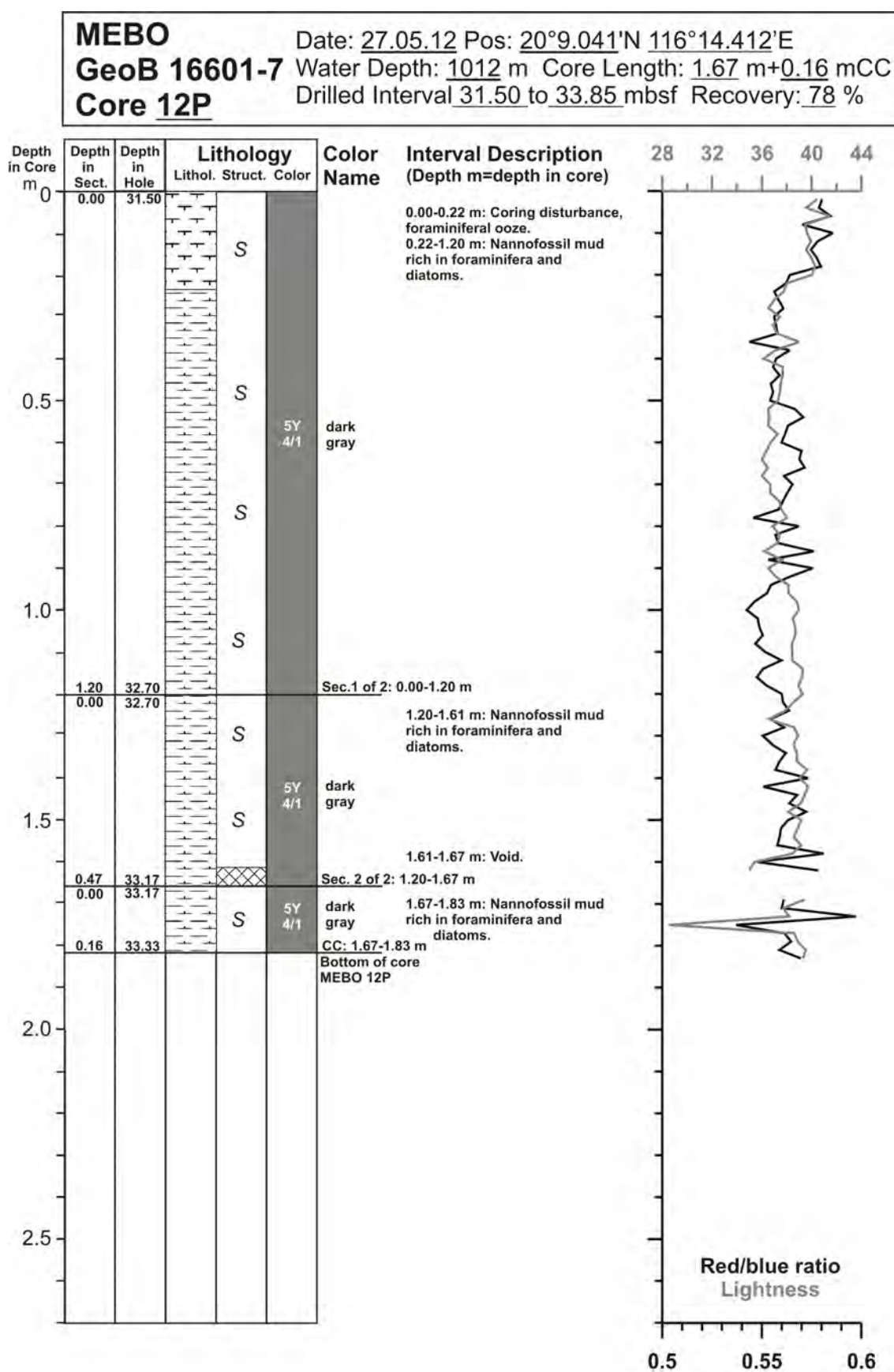


Fig. 10.44: Core description of MeBo core GeoB 16601-7 (12/29).

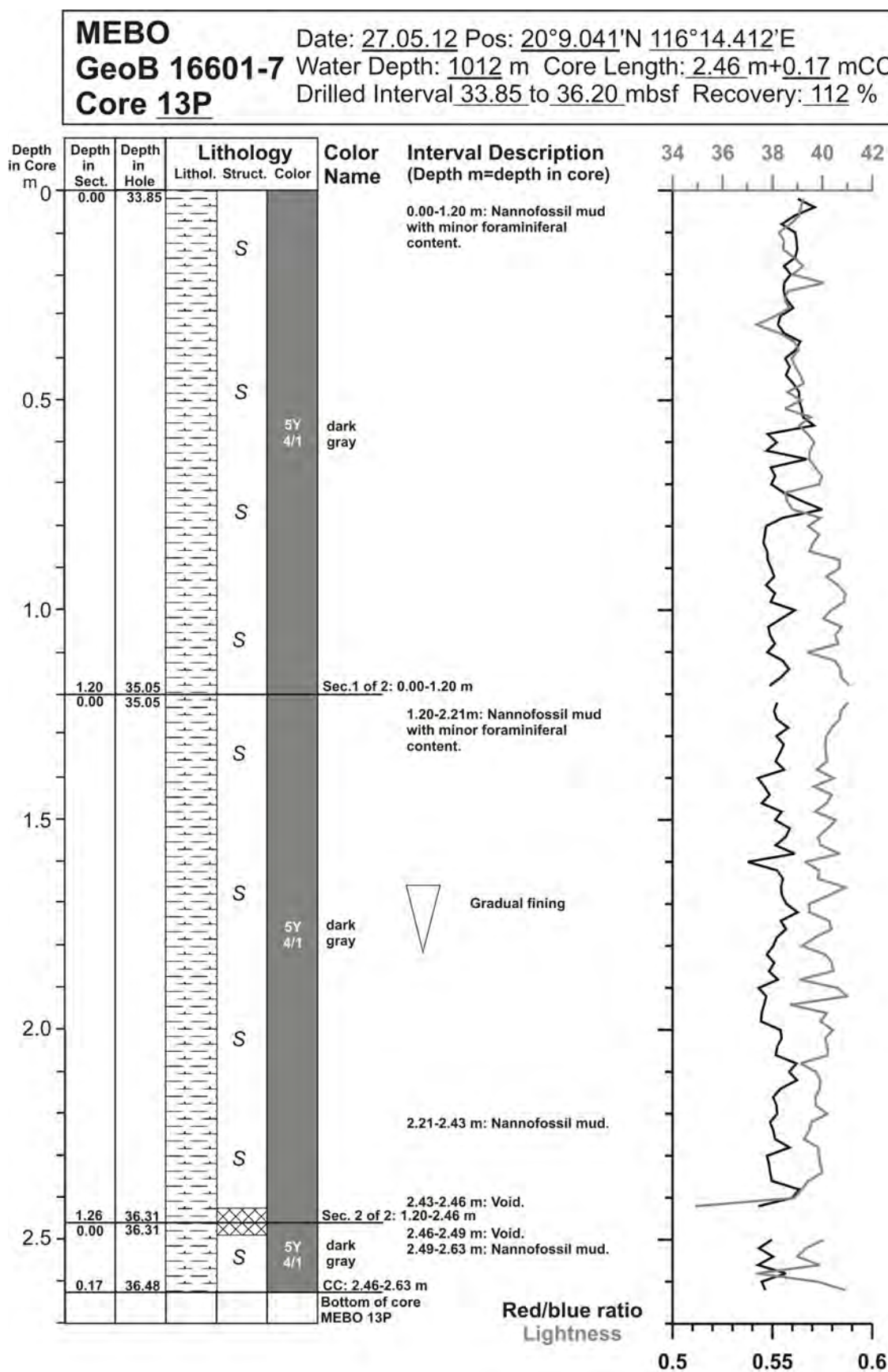


Fig. 10.45: Core description of MeBo core GeoB 16601-7 (13/29).

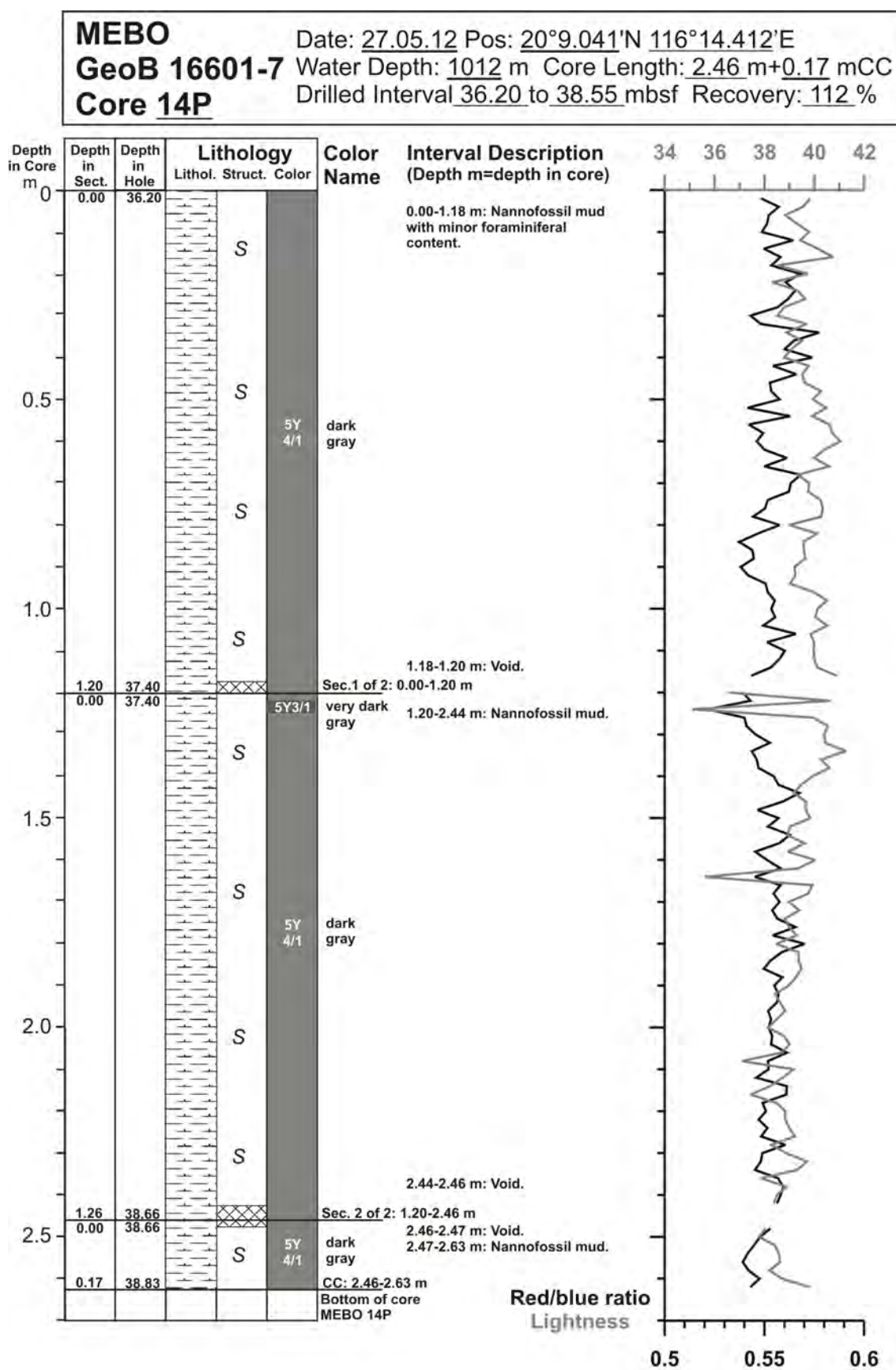


Fig. 10.46: Core description of MeBo core GeoB 16601-7 (14/29).

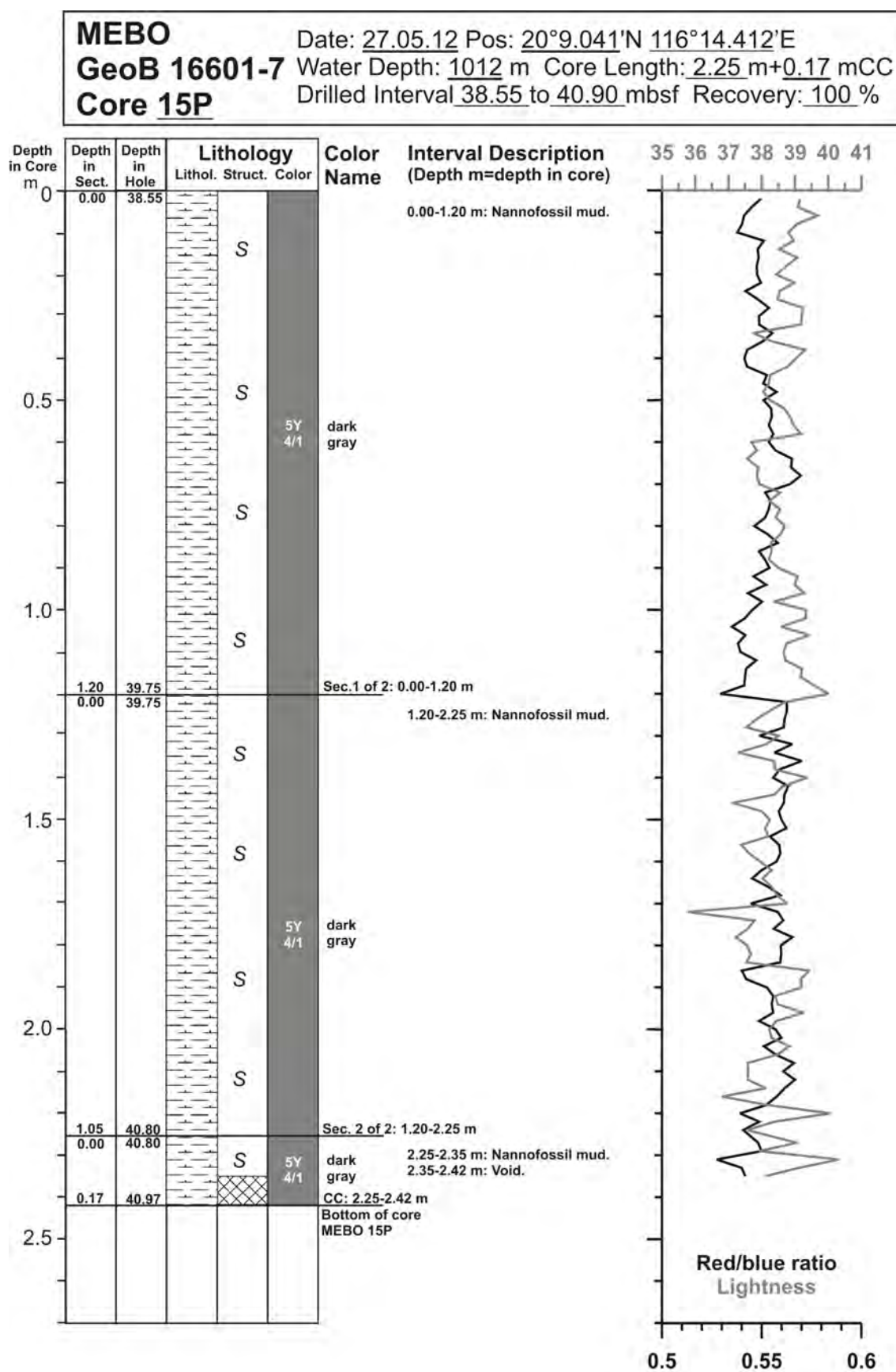


Fig. 10.47: Core description of MeBo core GeoB 16601-7 (15/29).

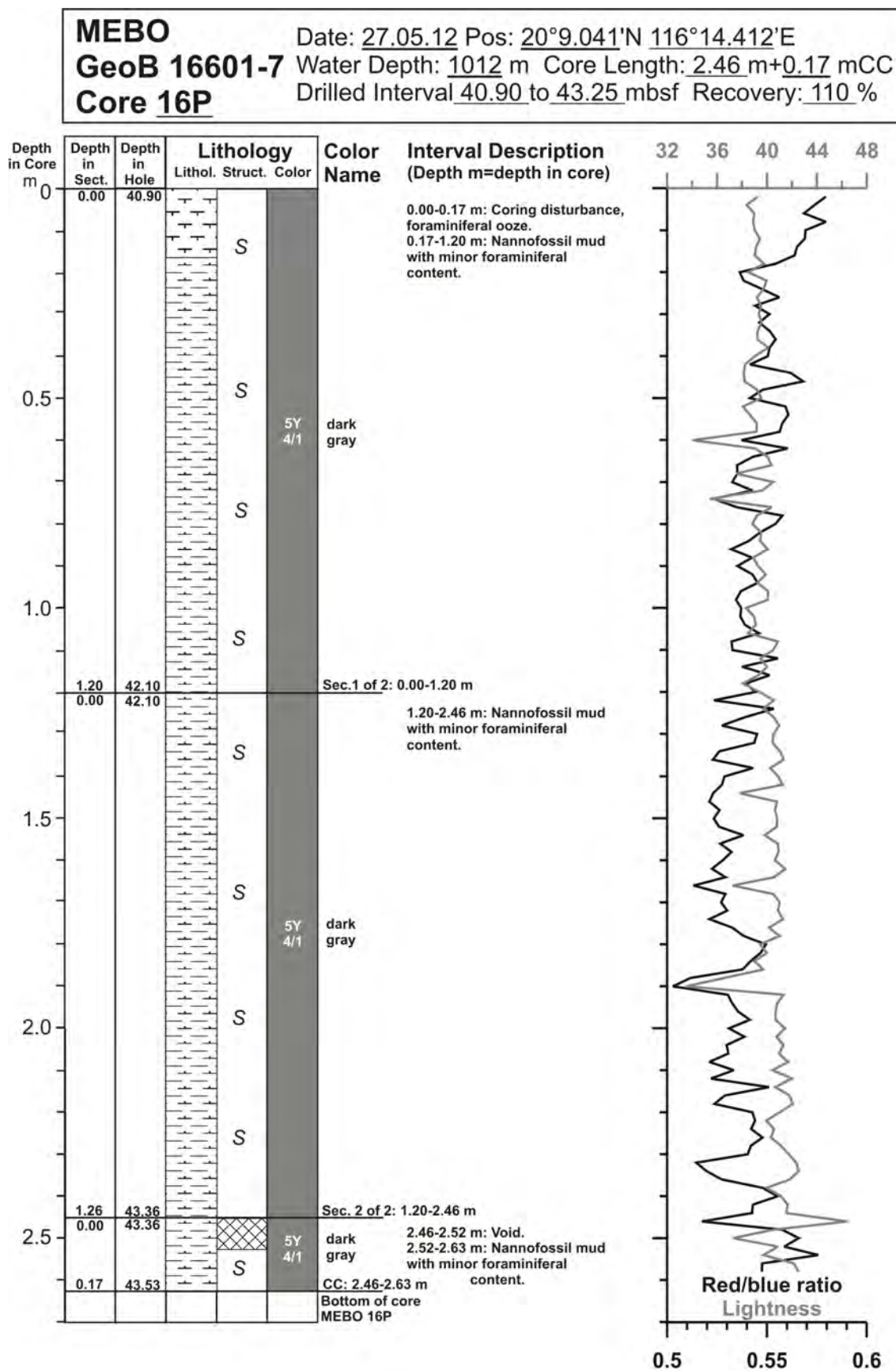


Fig. 10.48: Core description of MeBo core GeoB 16601-7 (16/29).

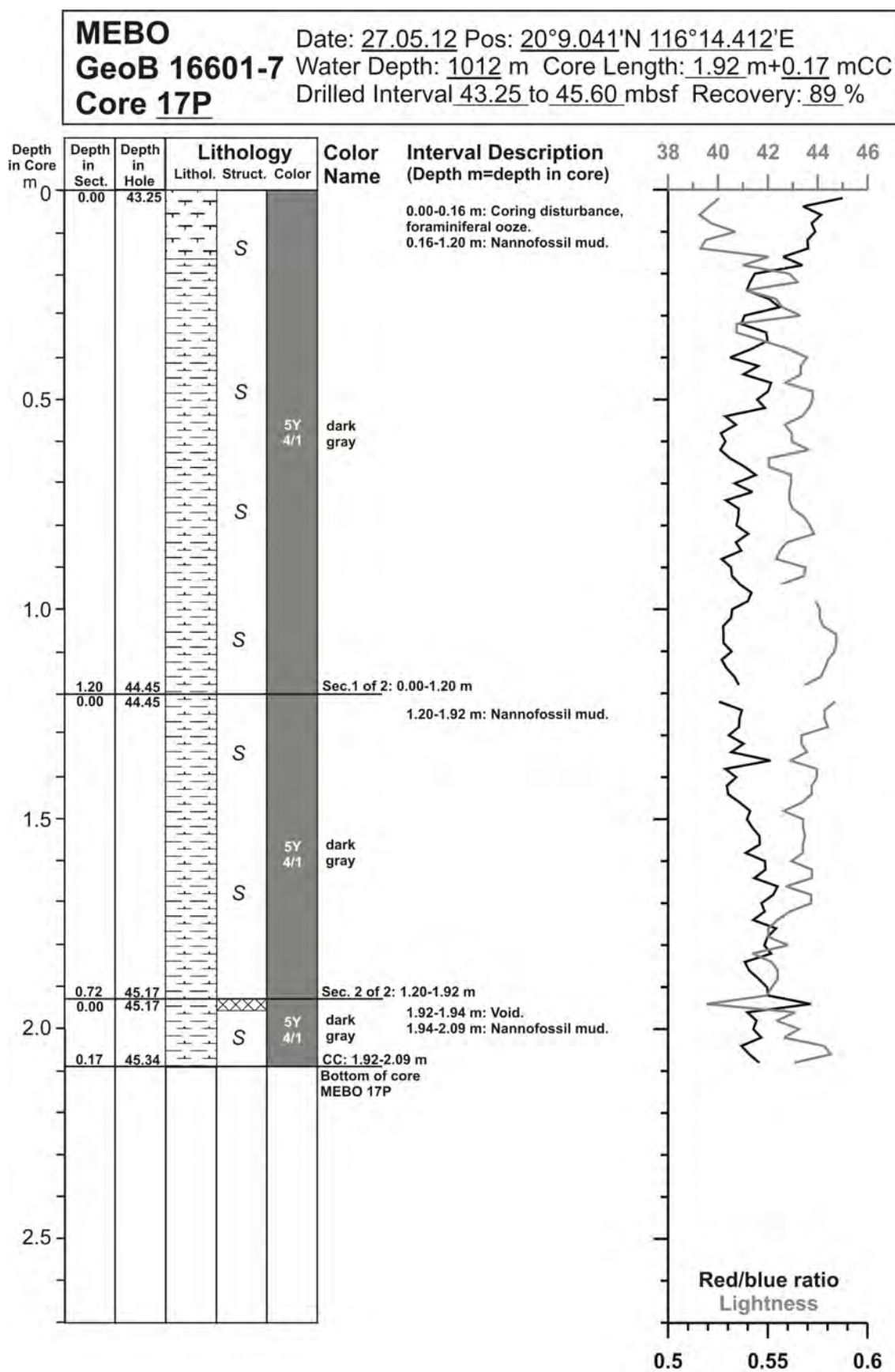


Fig. 10.49: Core description of MeBo core GeoB 16601-7 (17/29).

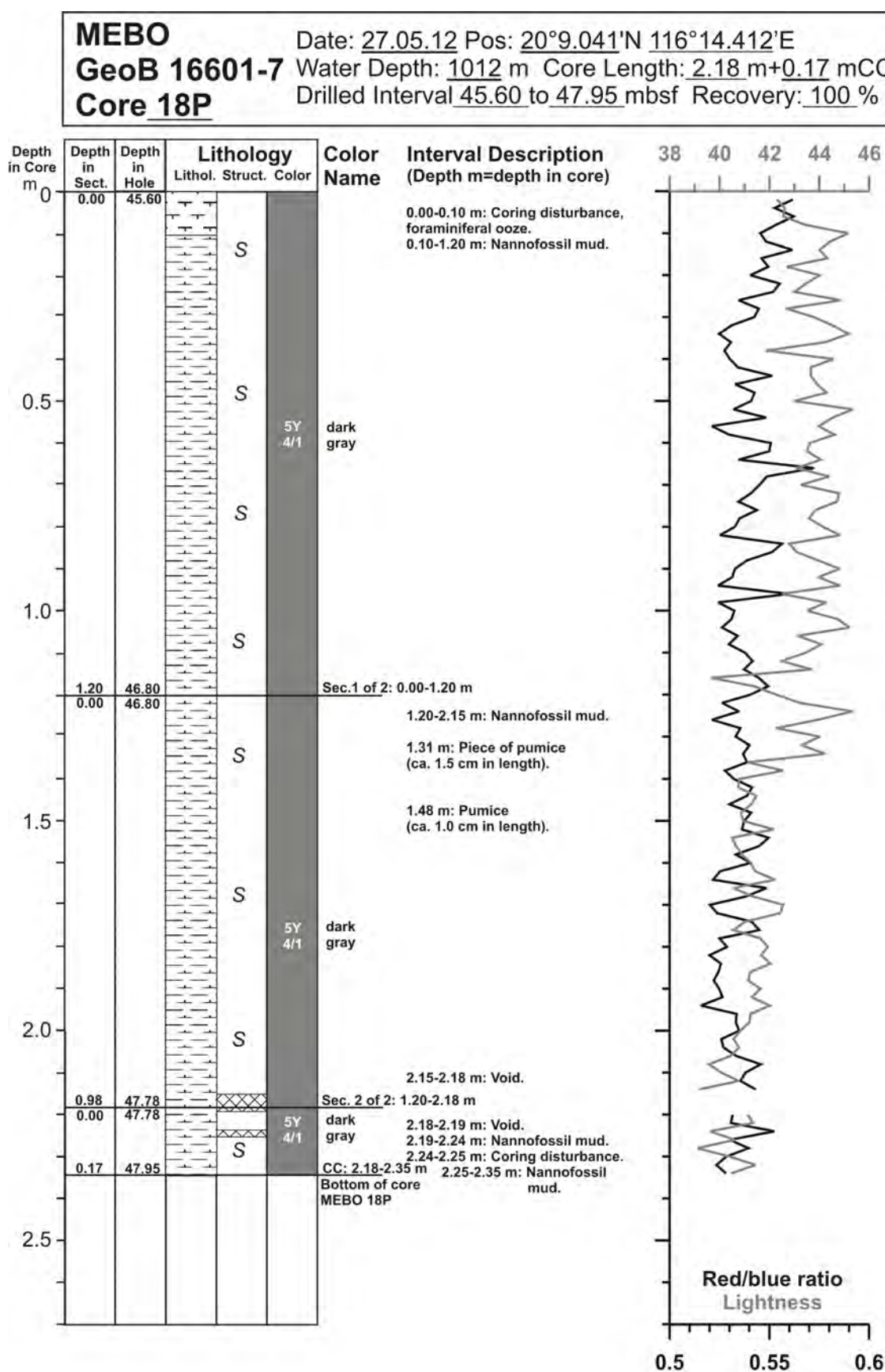


Fig. 10.50: Core description of MeBo core GeoB 16601-7 (18/29).

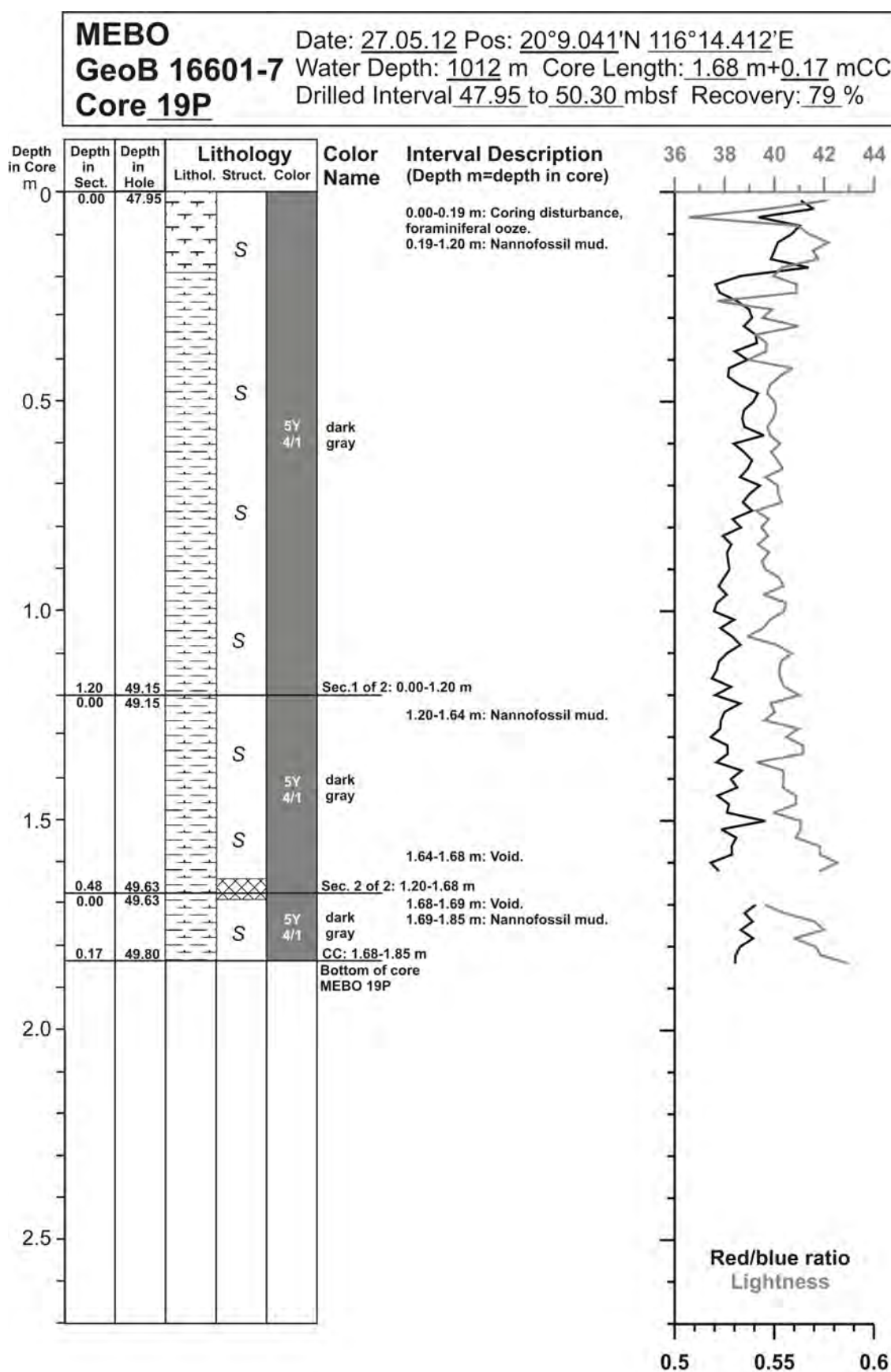


Fig. 10.51: Core description of MeBo core GeoB 16601-7 (19/29).

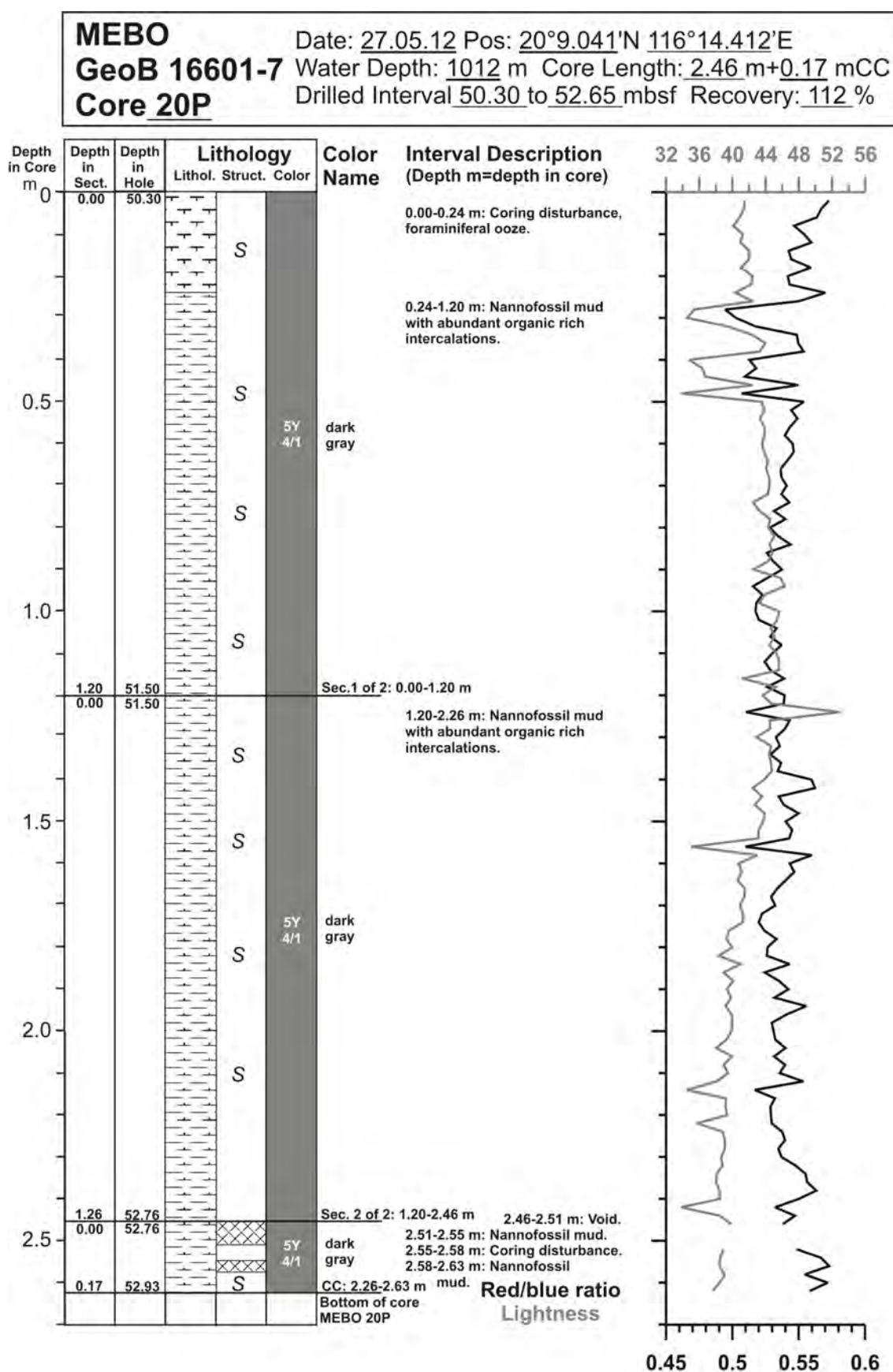


Fig. 10.52: Core description of MeBo core GeoB 16601-7 (20/29).

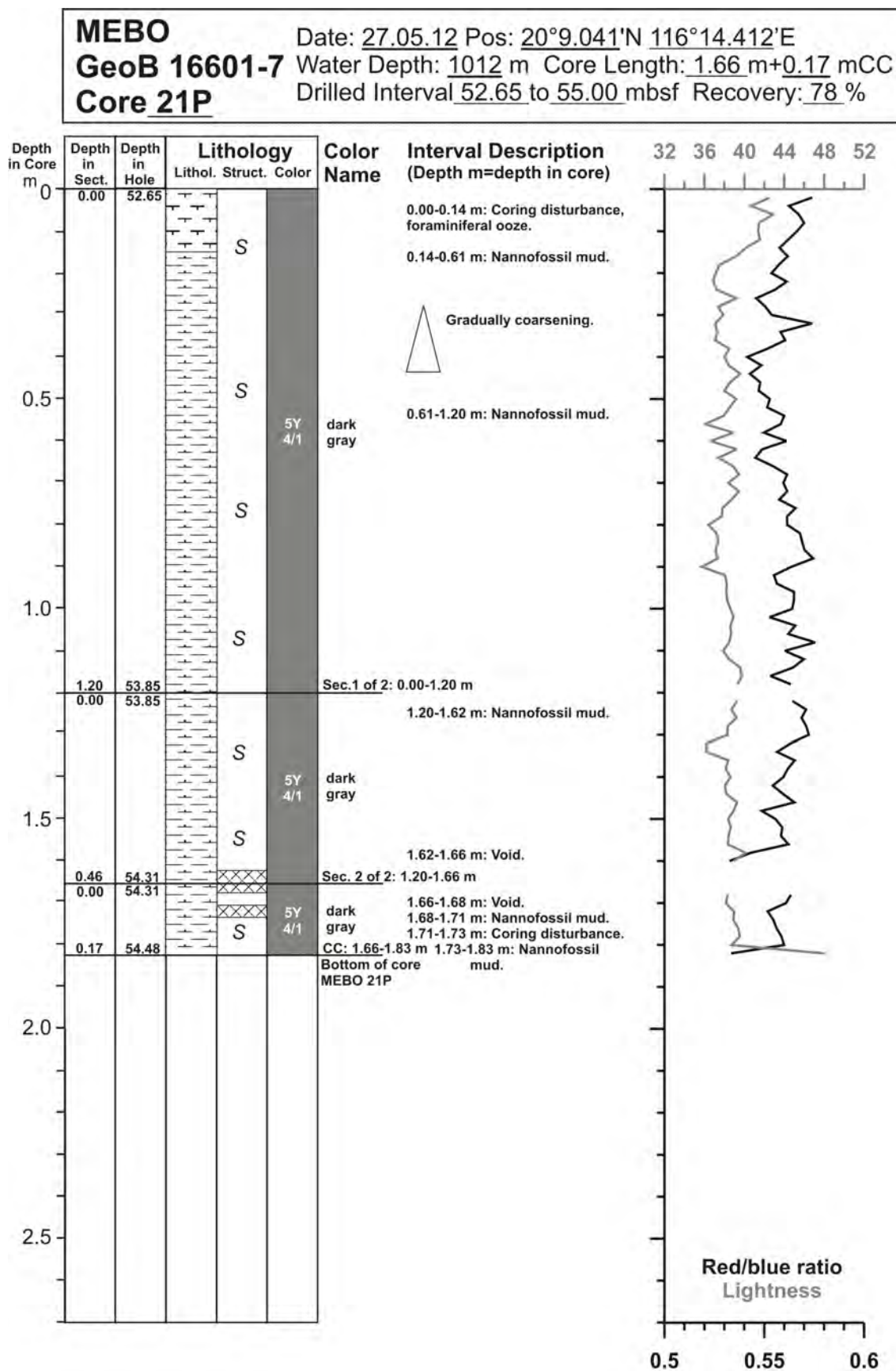


Fig. 10.53: Core description of MeBo core GeoB 16601-7 (21/29).

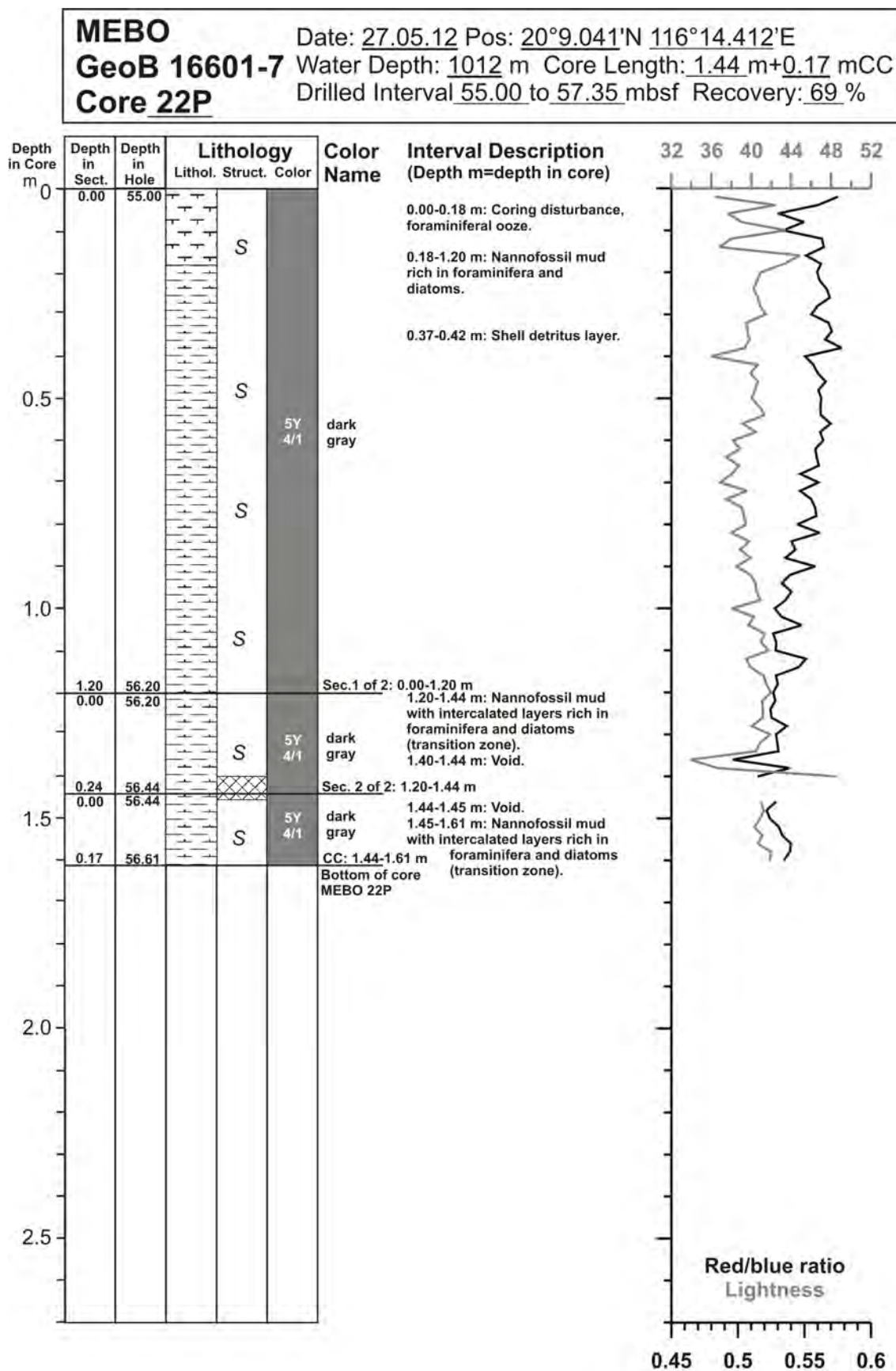


Fig. 10.54: Core description of MeBo core GeoB 16601-7 (22/29).

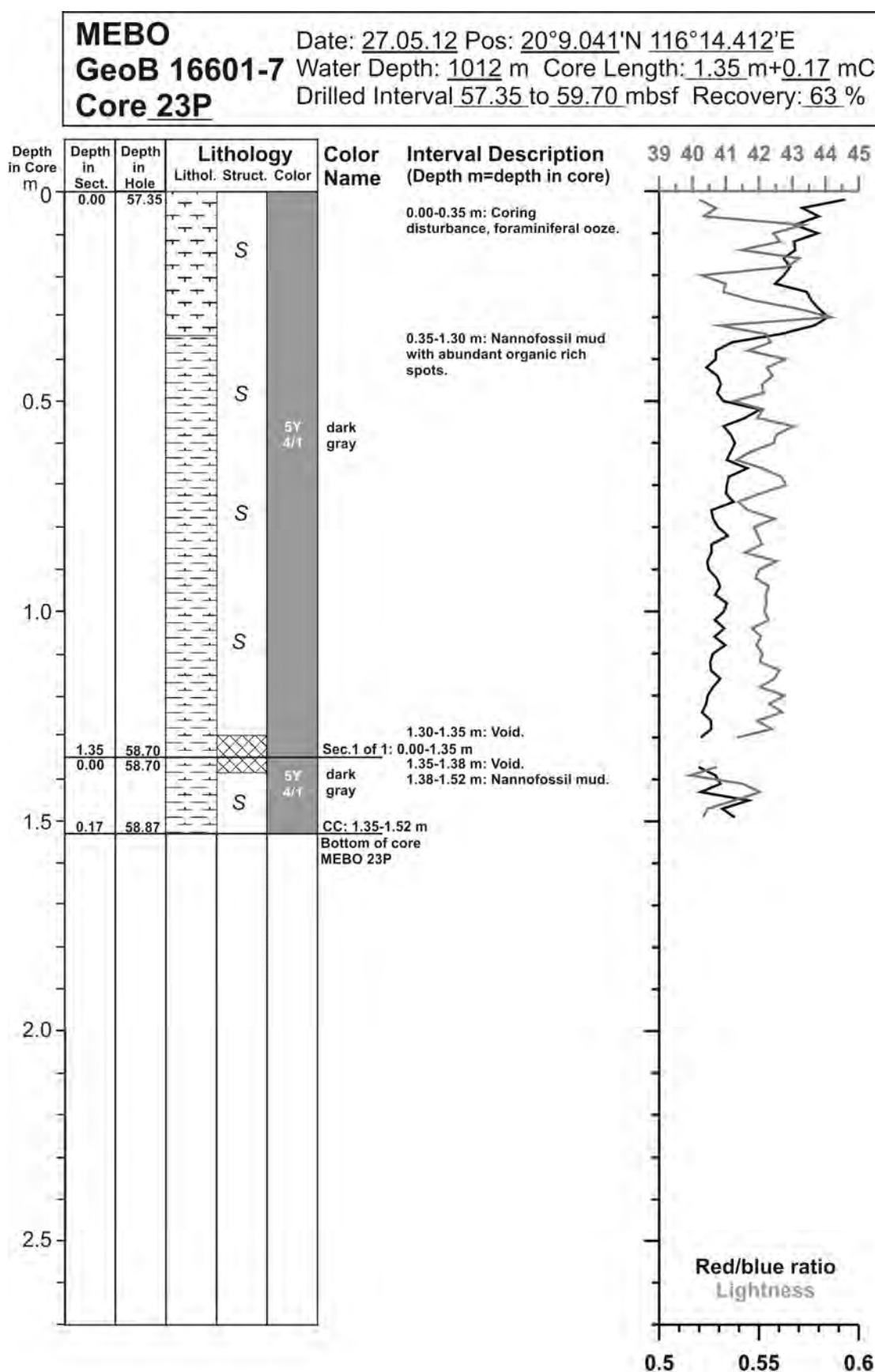


Fig. 10.55: Core description of MeBo core GeoB 16601-7 (23/29).

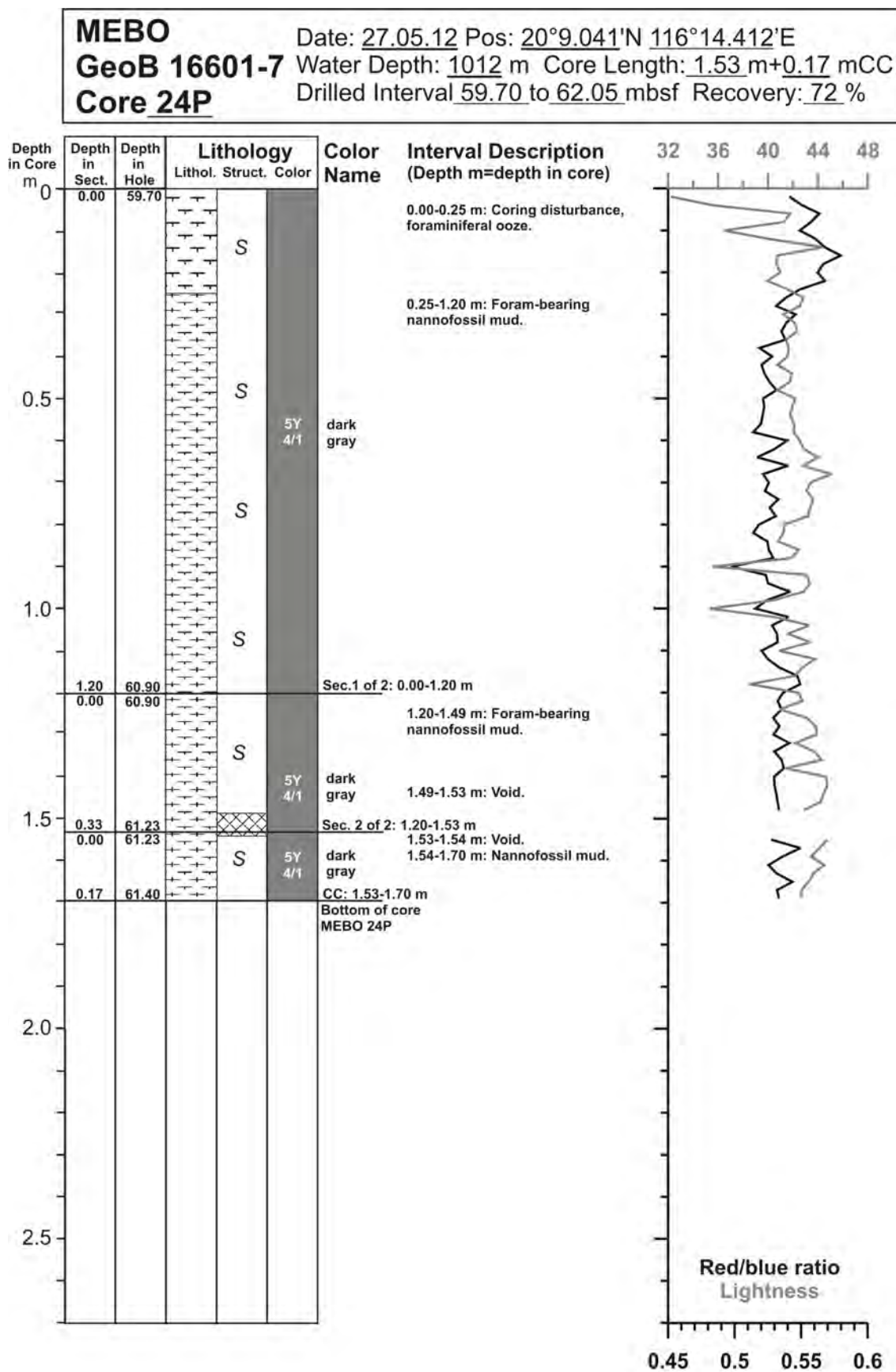


Fig. 10.56: Core description of MeBo core GeoB 16601-7 (24/29).

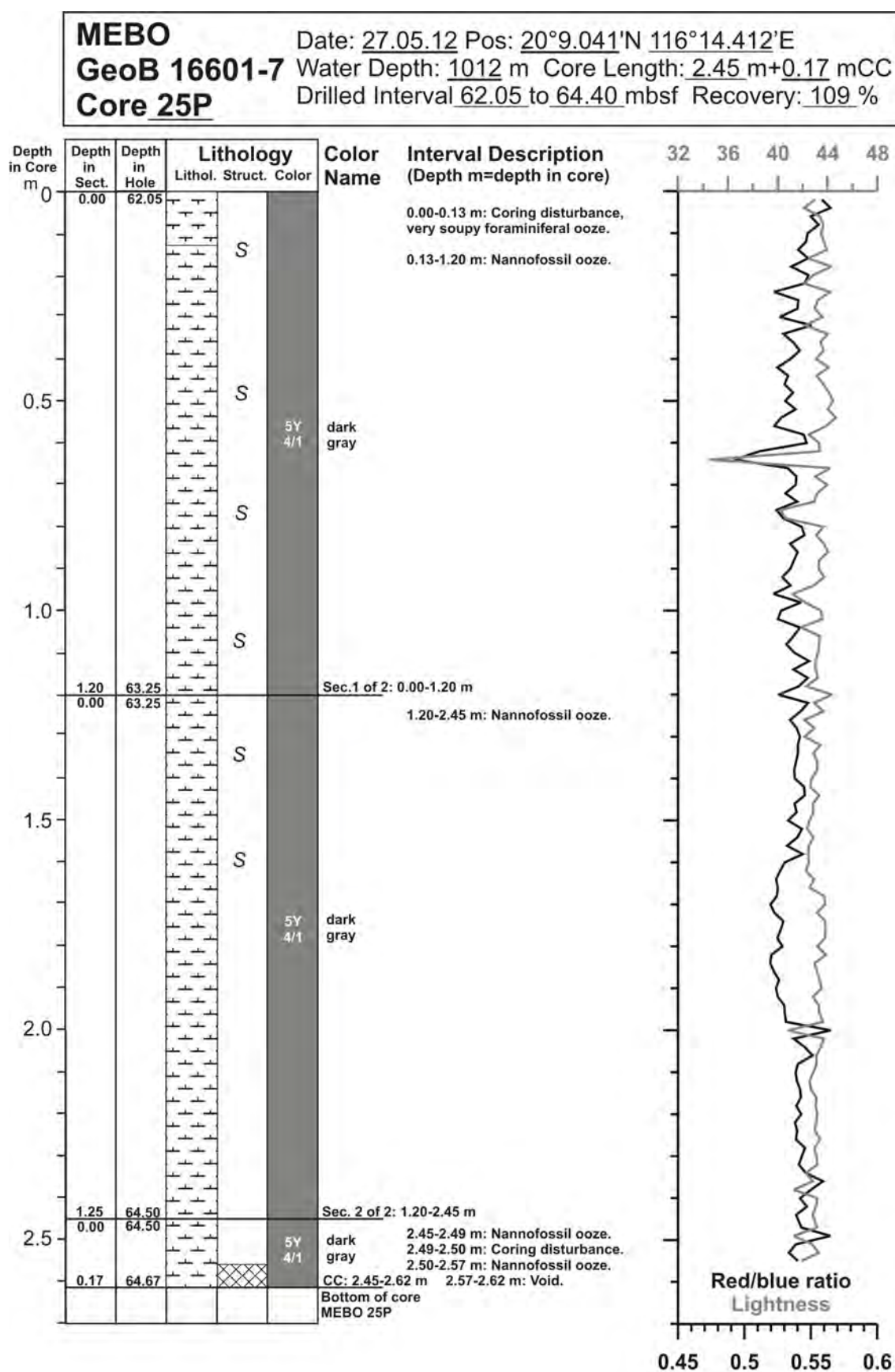


Fig. 10.57: Core description of MeBo core GeoB 16601-7 (25/29).

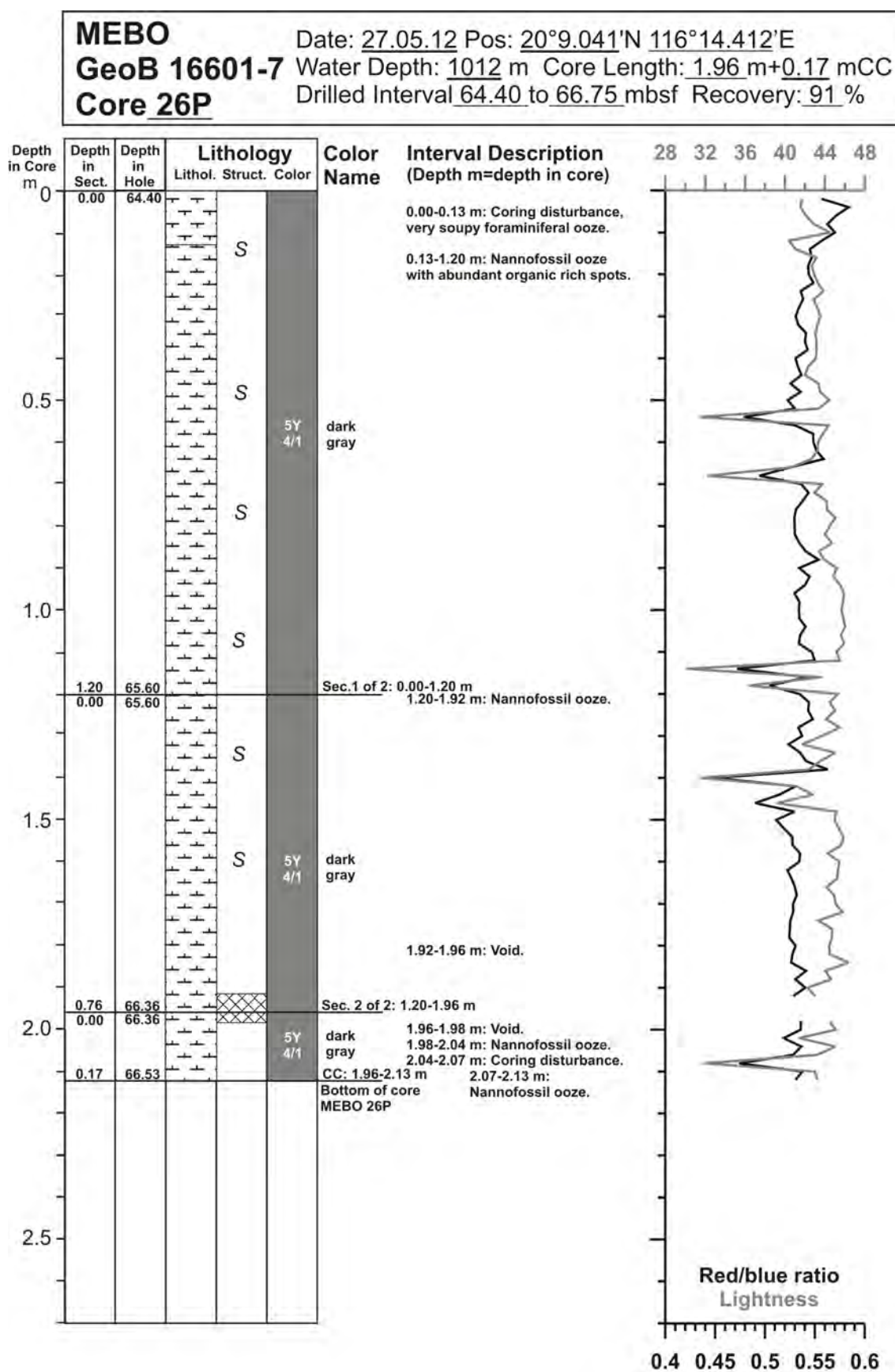


Fig. 10.58: Core description of MeBo core GeoB 16601-7 (26/29).

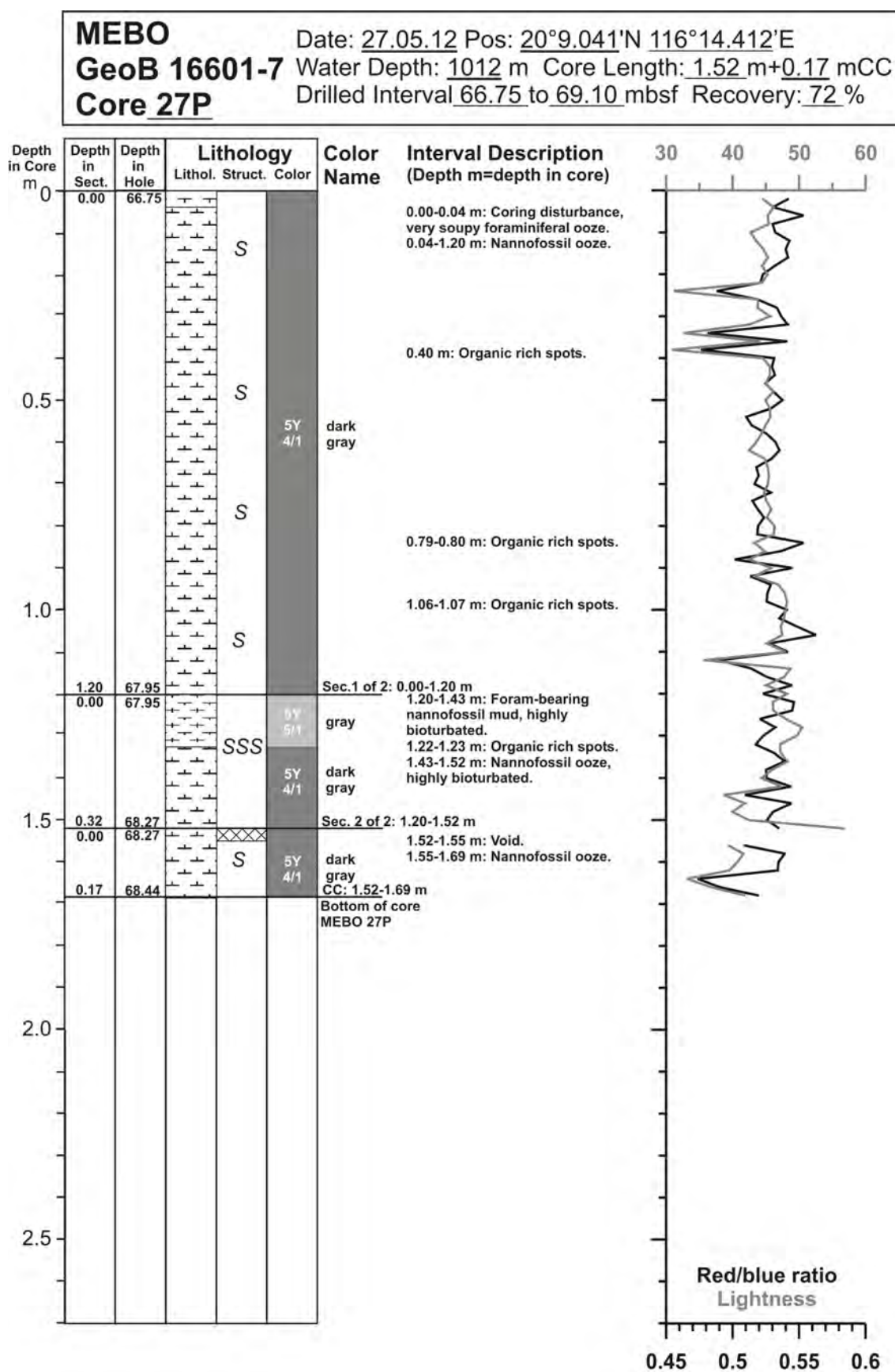


Fig. 10.59: Core description of MeBo core GeoB 16601-7 (27/29).

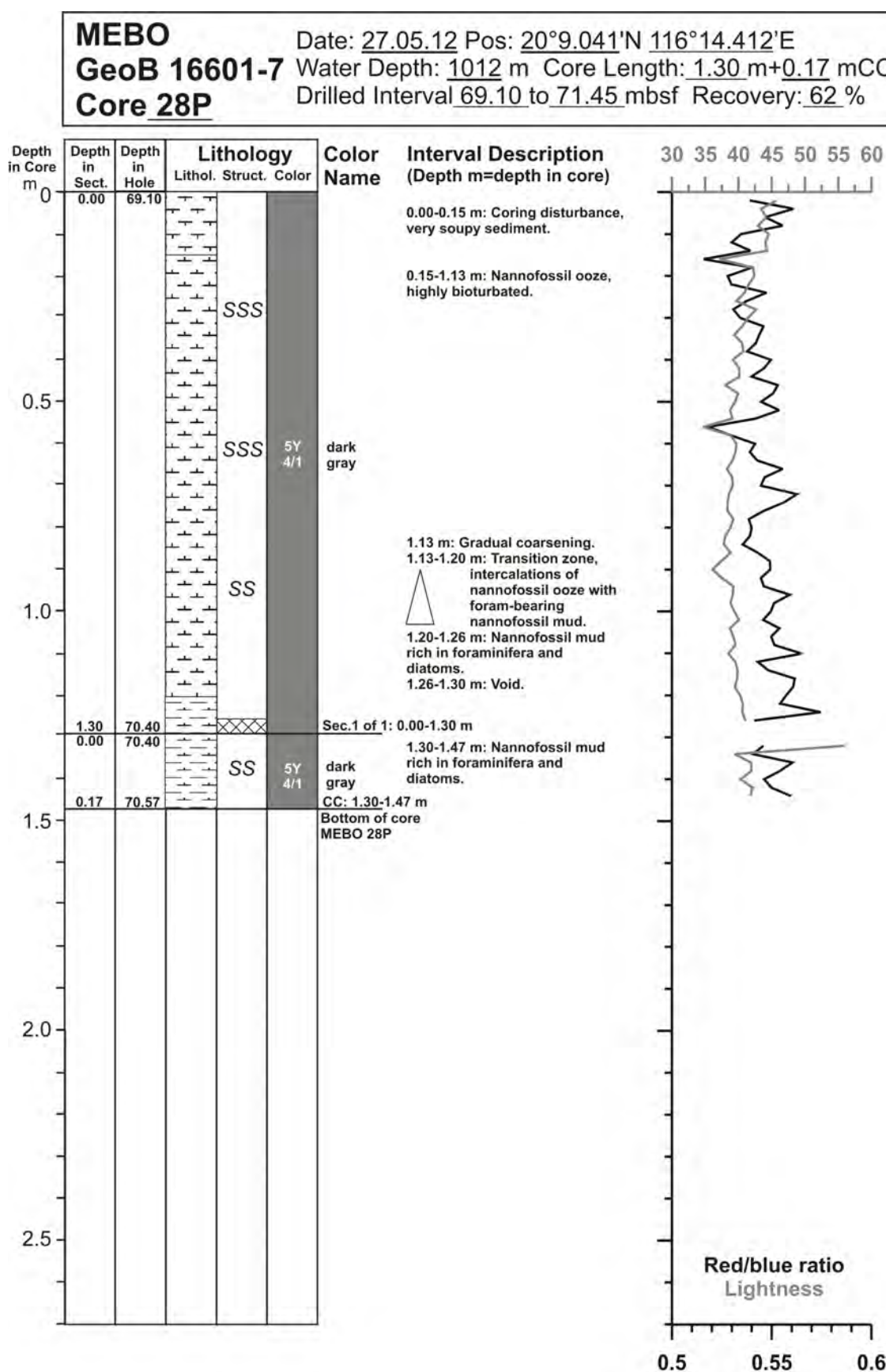


Fig. 10.60: Core description of MeBo core GeoB 16601-7 (28/29).

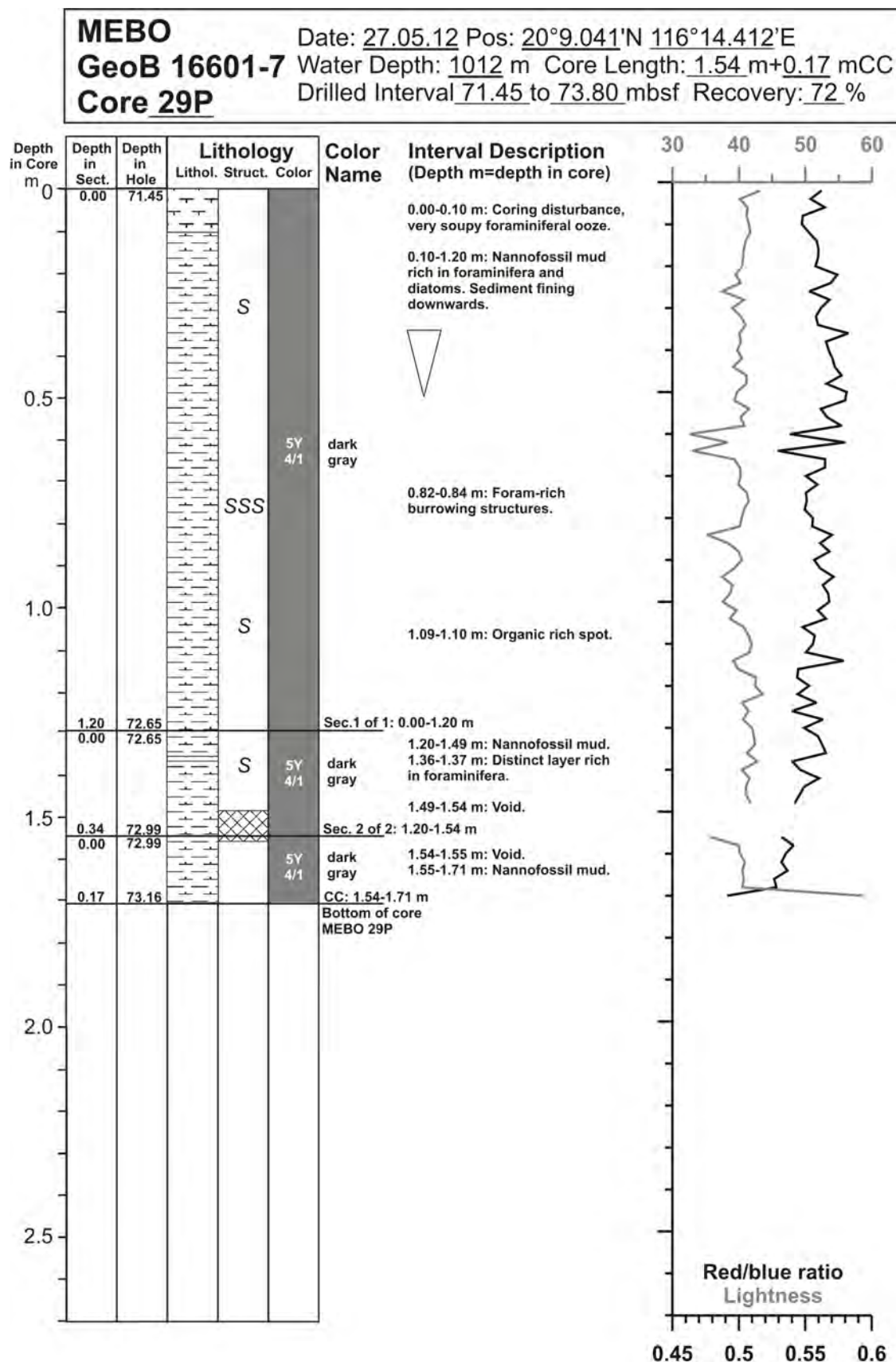


Fig. 10.61: Core description of MeBo core GeoB 16601-7 (29/29).

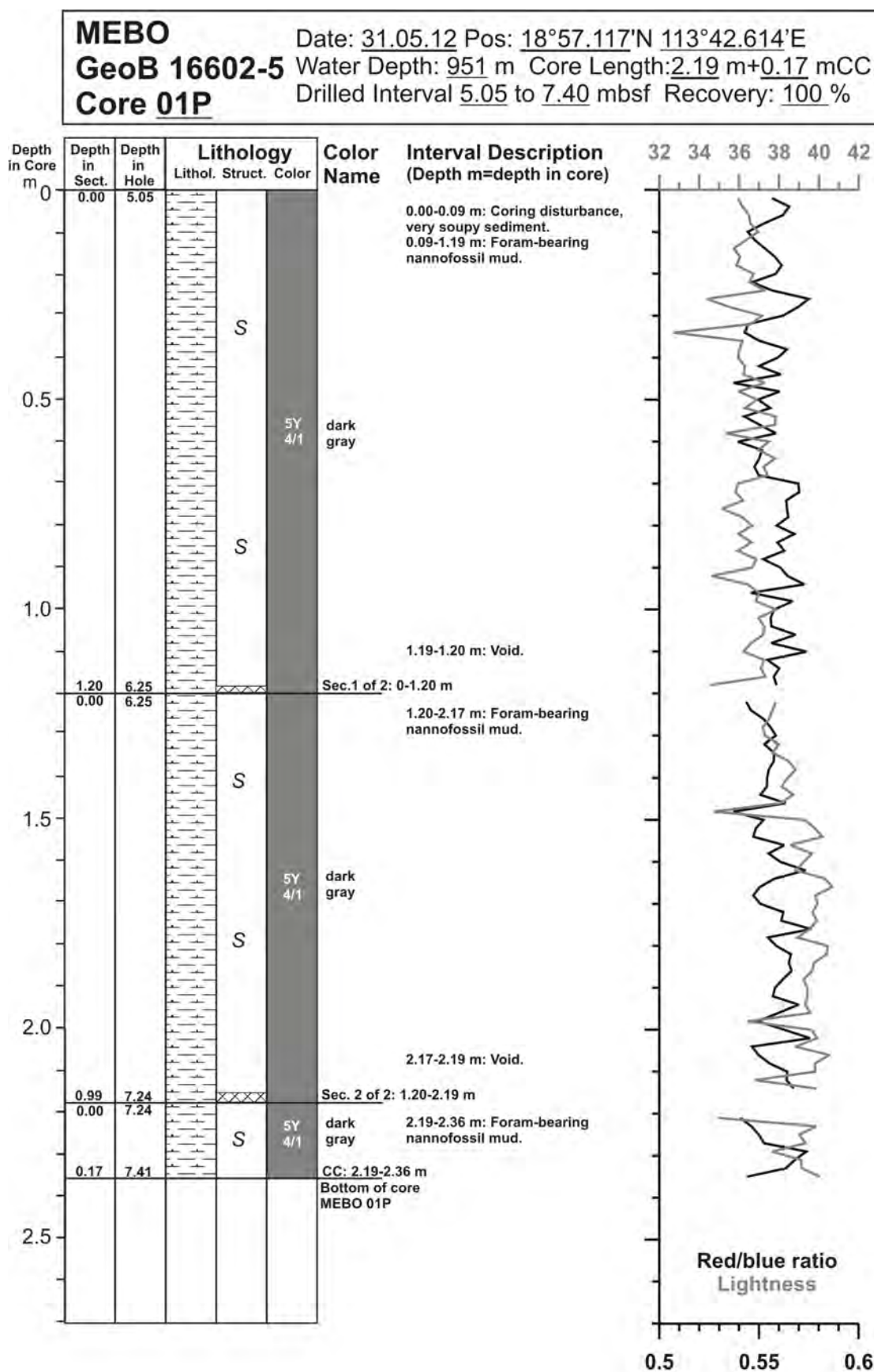


Fig. 10.62: Core description of MeBo core GeoB 16602-5 (1/29).

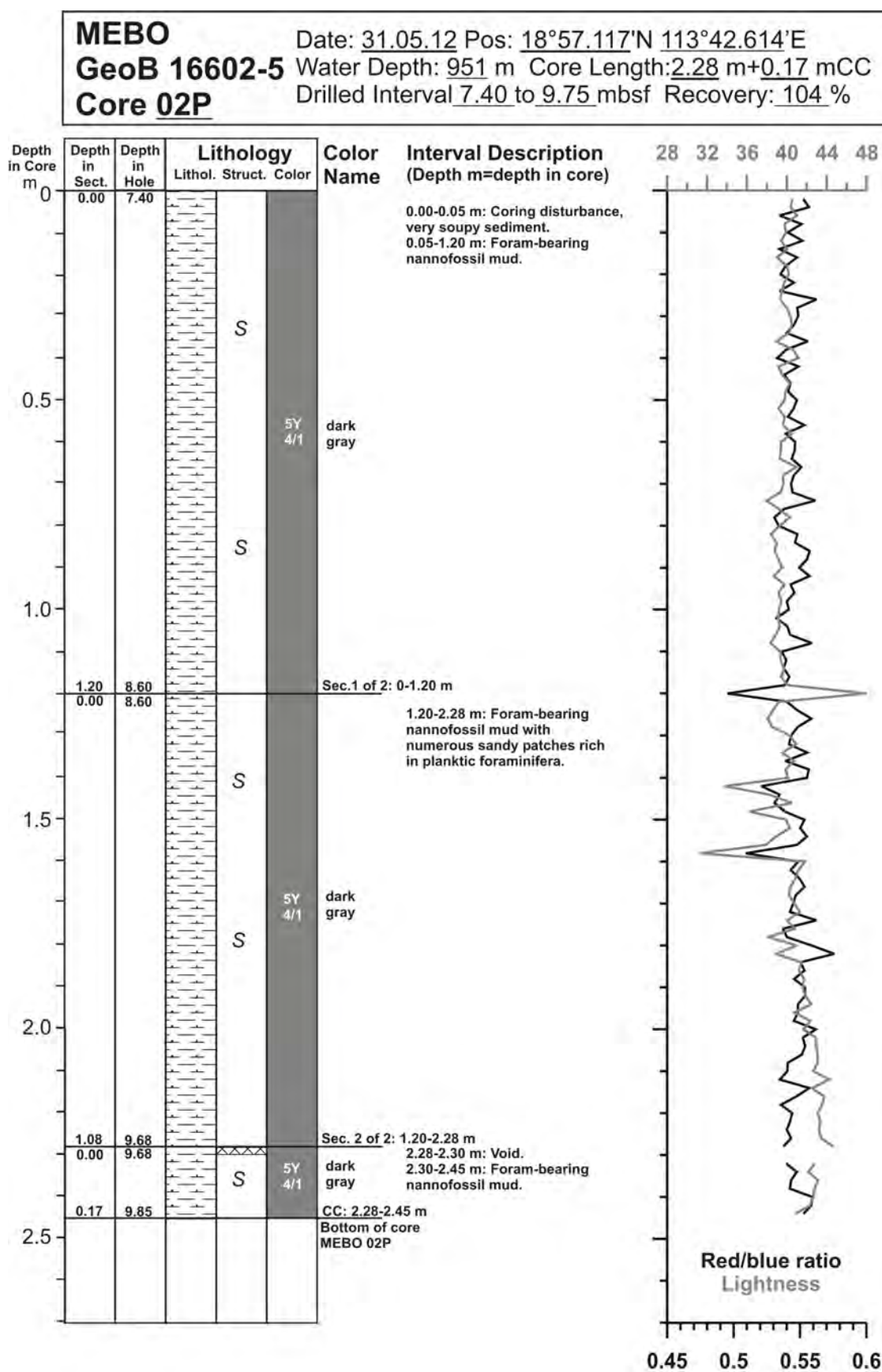


Fig. 10.63: Core description of MeBo core GeoB 16602-5 (2/29).

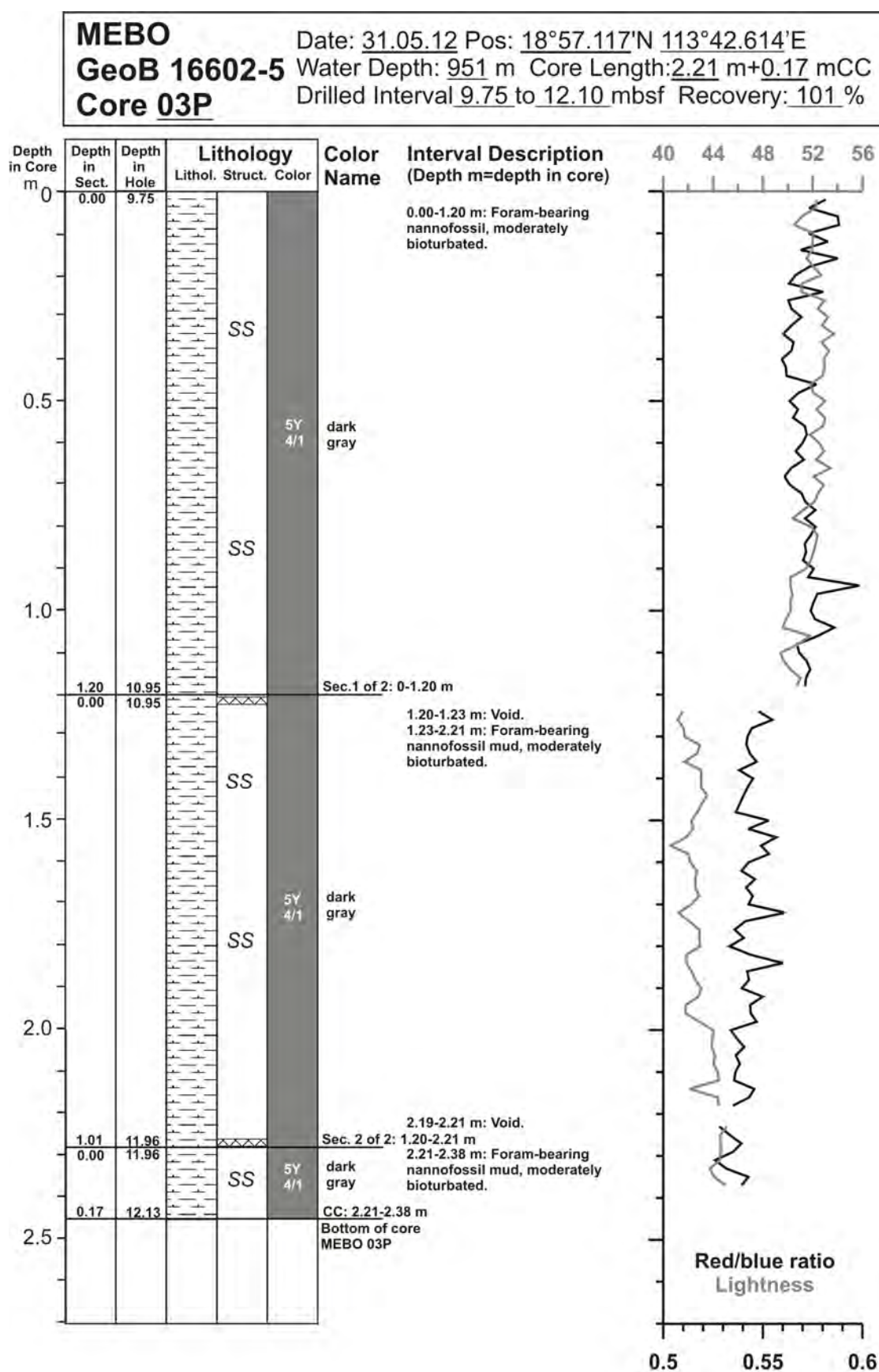


Fig. 10.64: Core description of MeBo core GeoB 16602-5 (3/29).

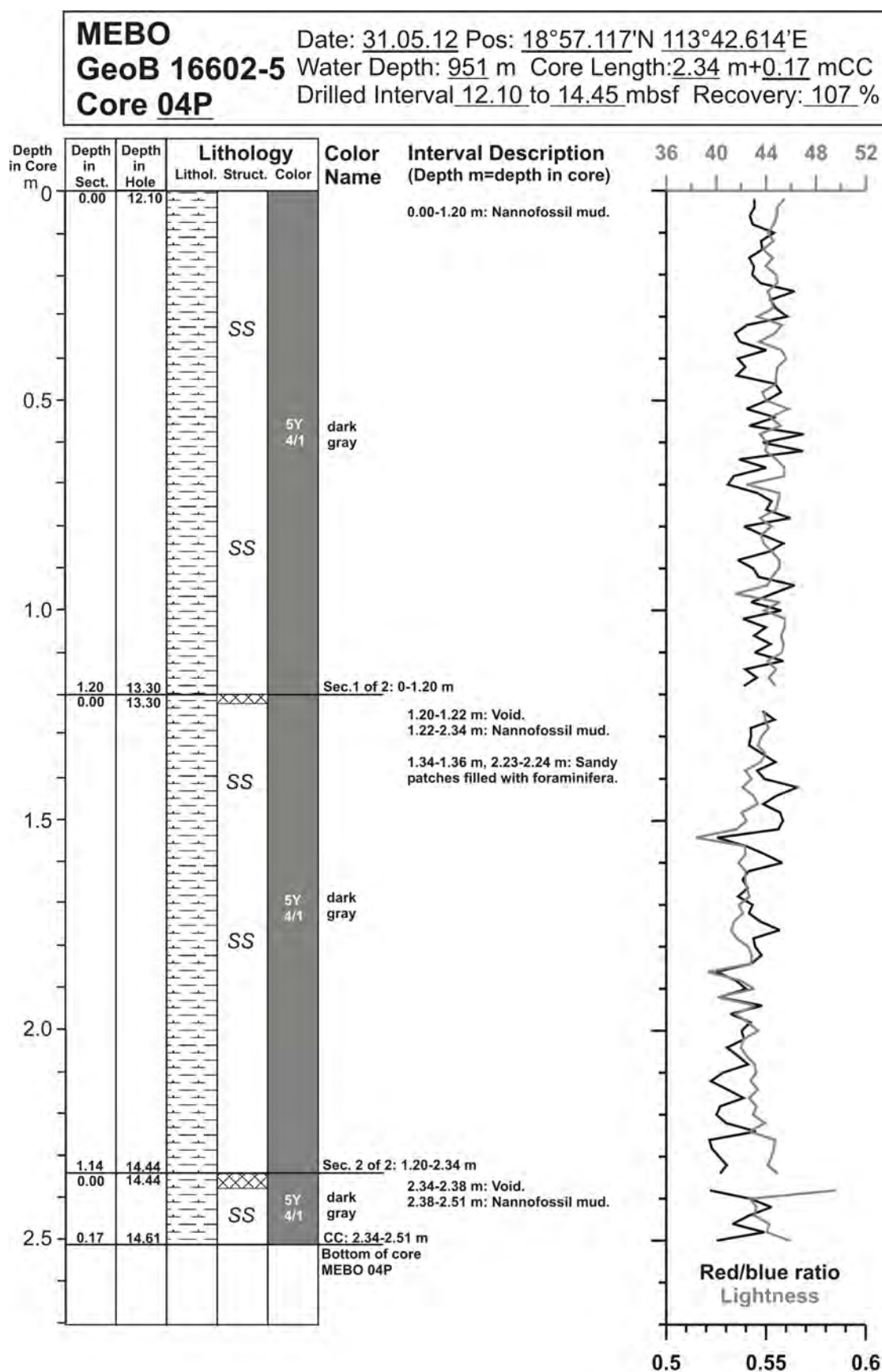


Fig. 10.65: Core description of MeBo core GeoB 16602-5 (4/29).

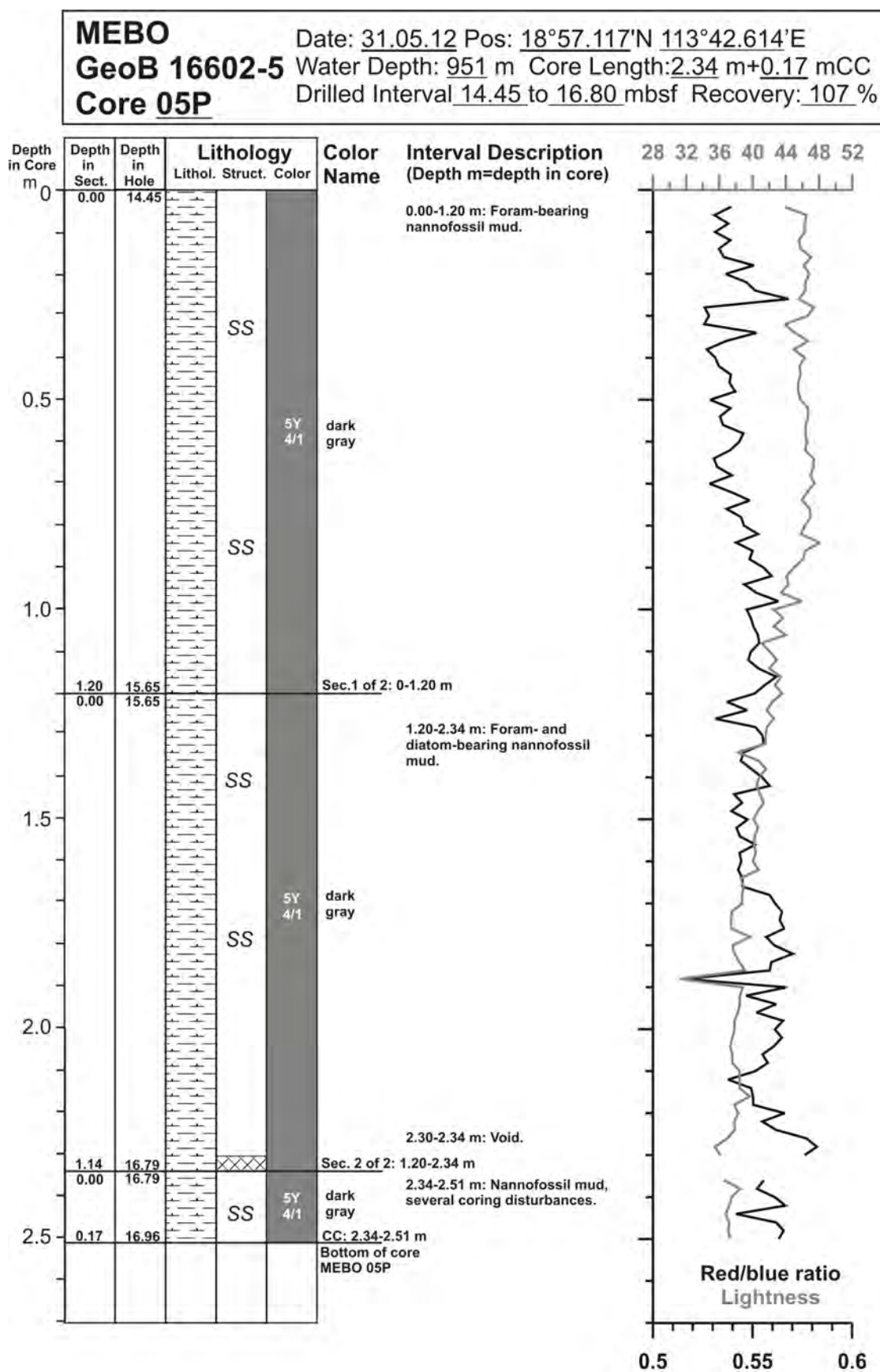


Fig. 10.66: Core description of MeBo core GeoB 16602-5 (5/29).

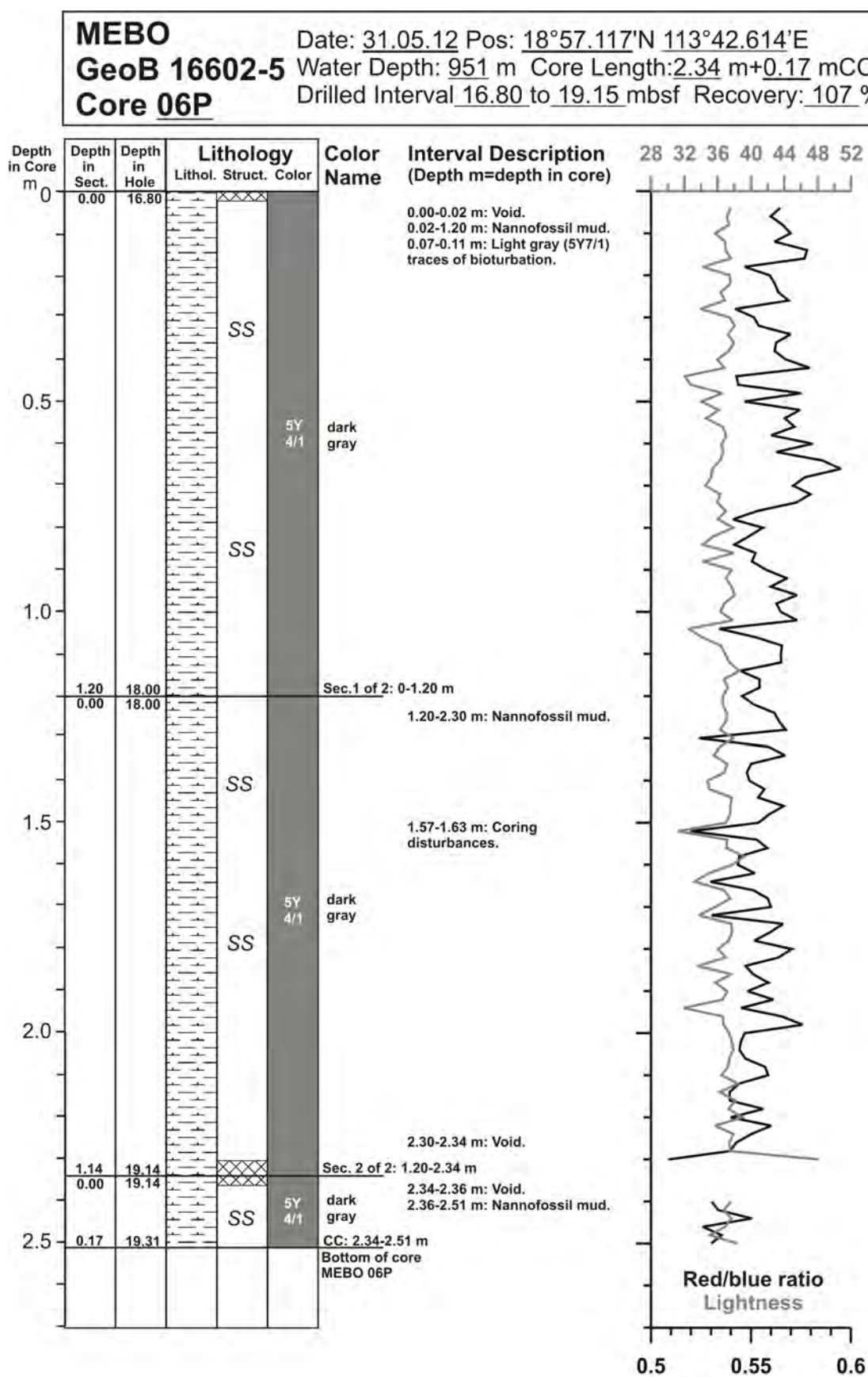


Fig. 10.67: Core description of MeBo core GeoB 16602-5 (6/29).

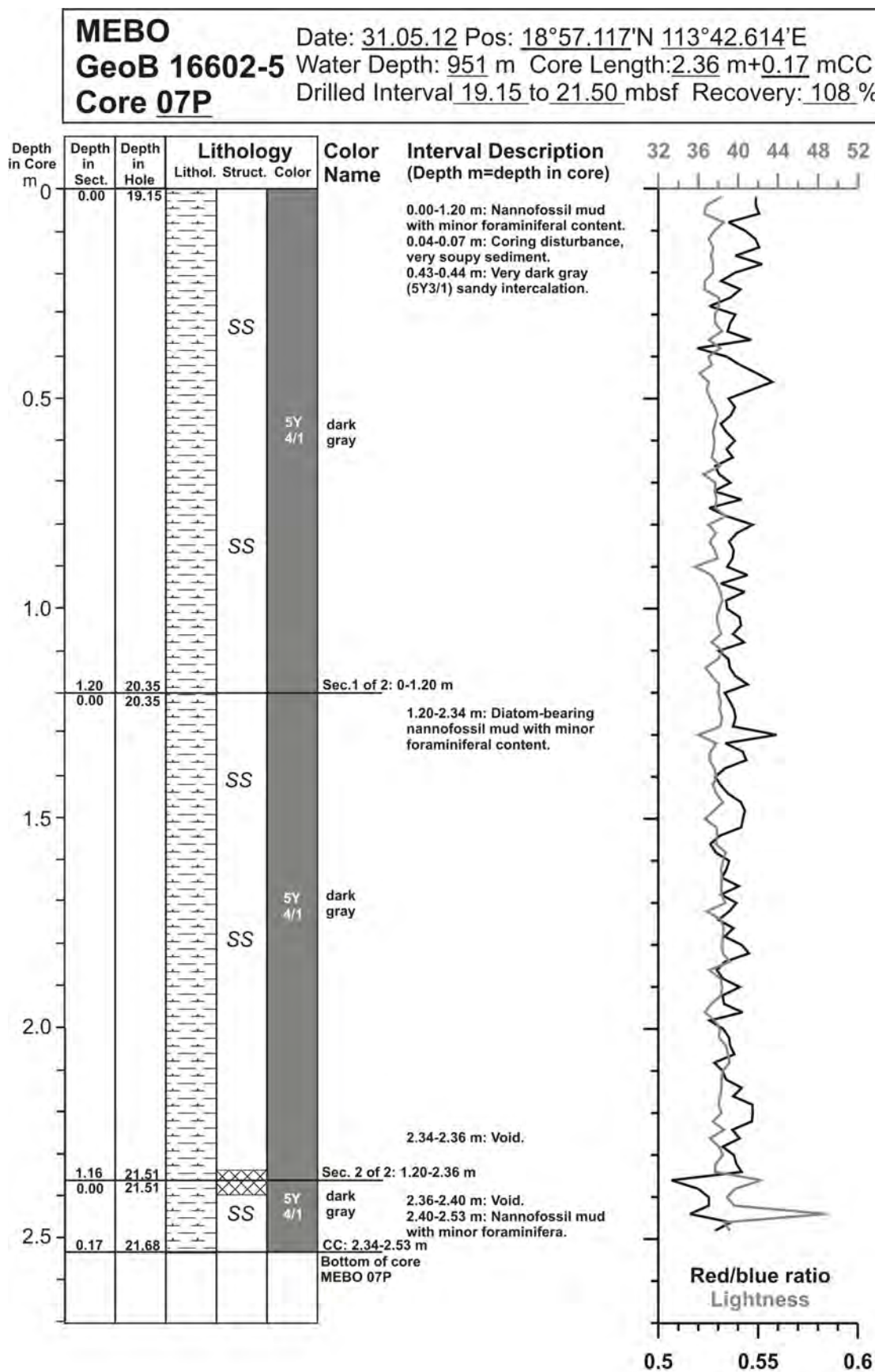


Fig. 10.68: Core description of MeBo core GeoB 16602-5 (7/29).

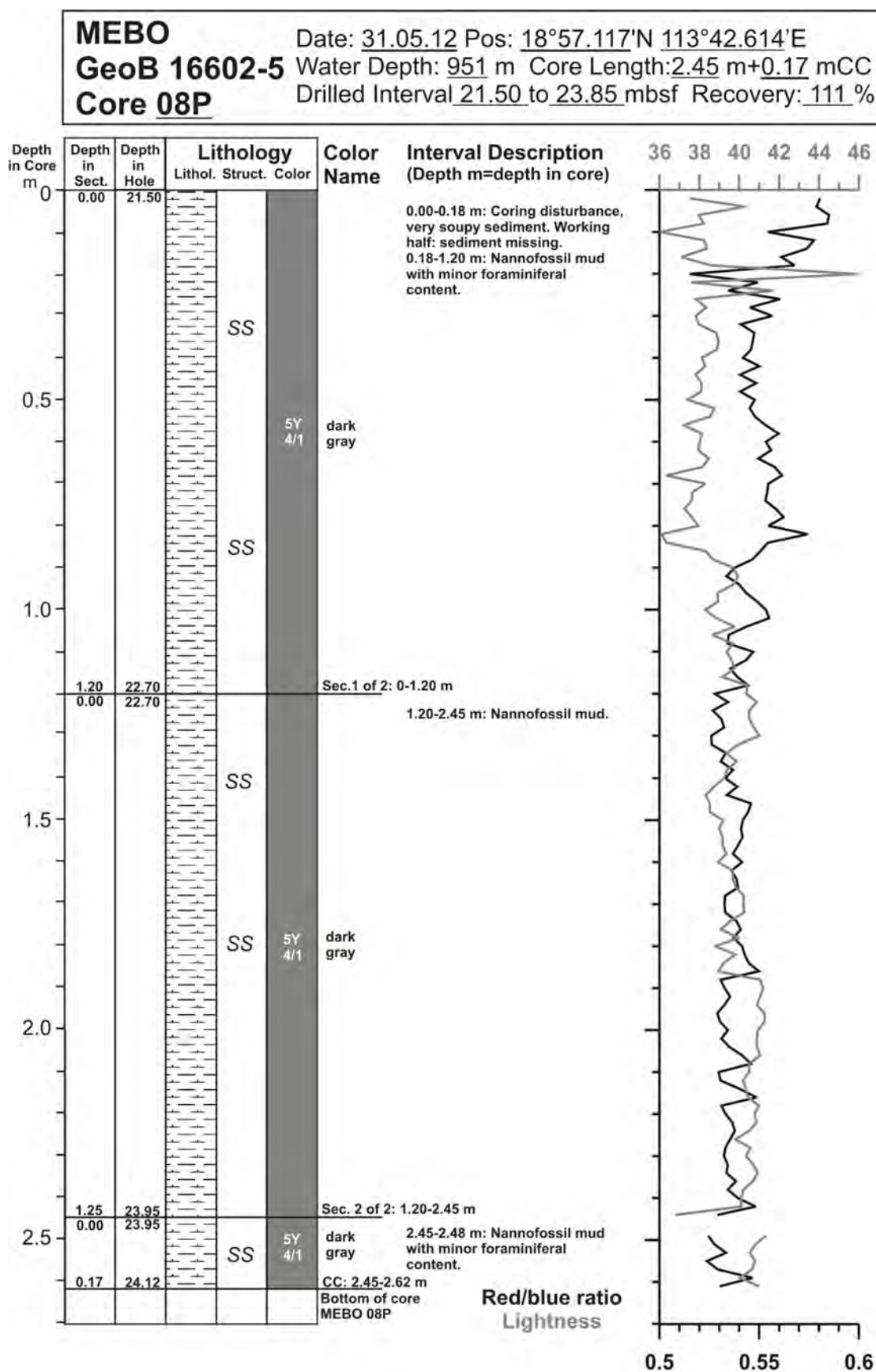


Fig. 10.69: Core description of MeBo core GeoB 16602-5 (8/29).

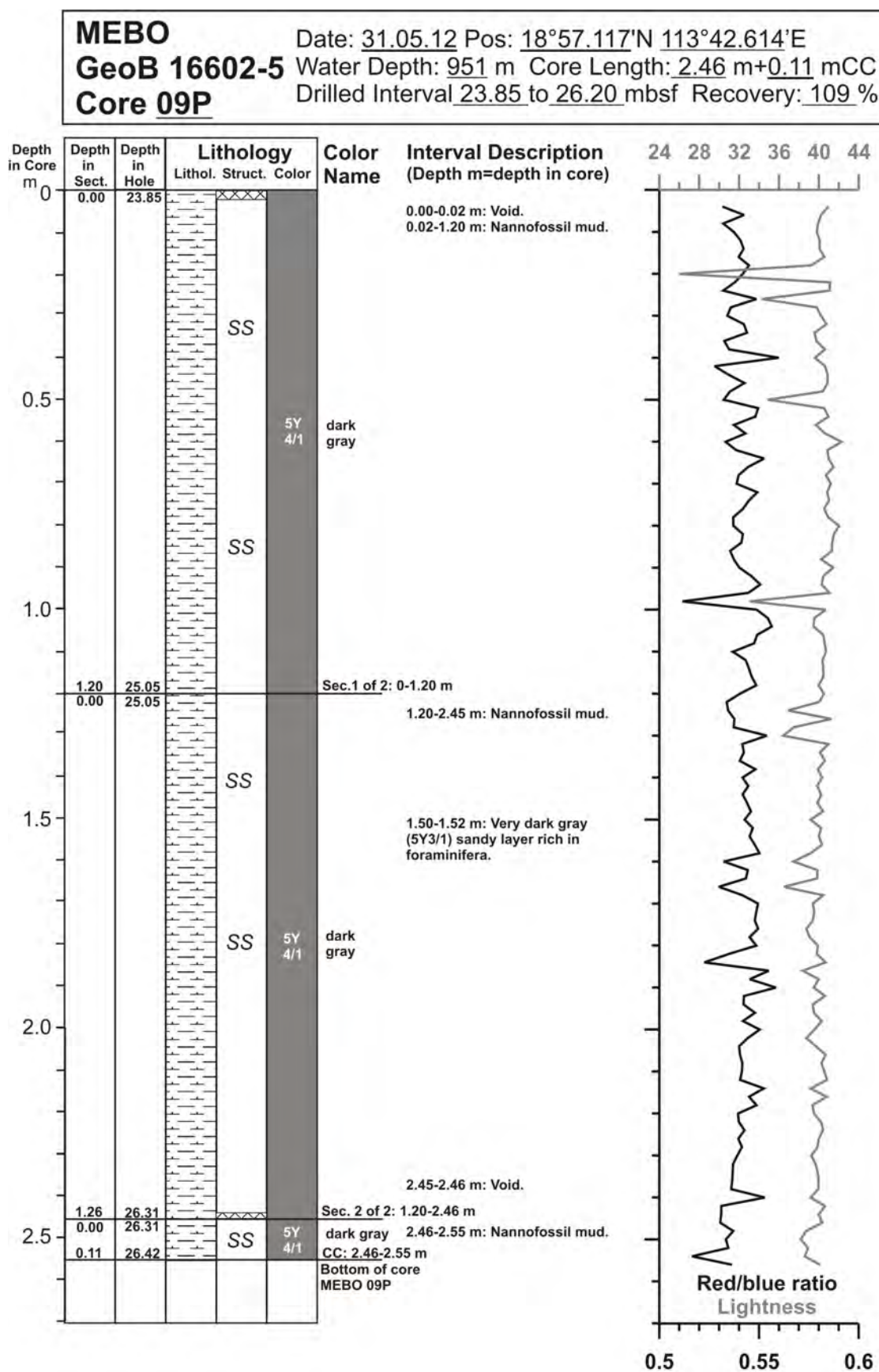


Fig. 10.70: Core description of MeBo core GeoB 16602-5 (9/29).

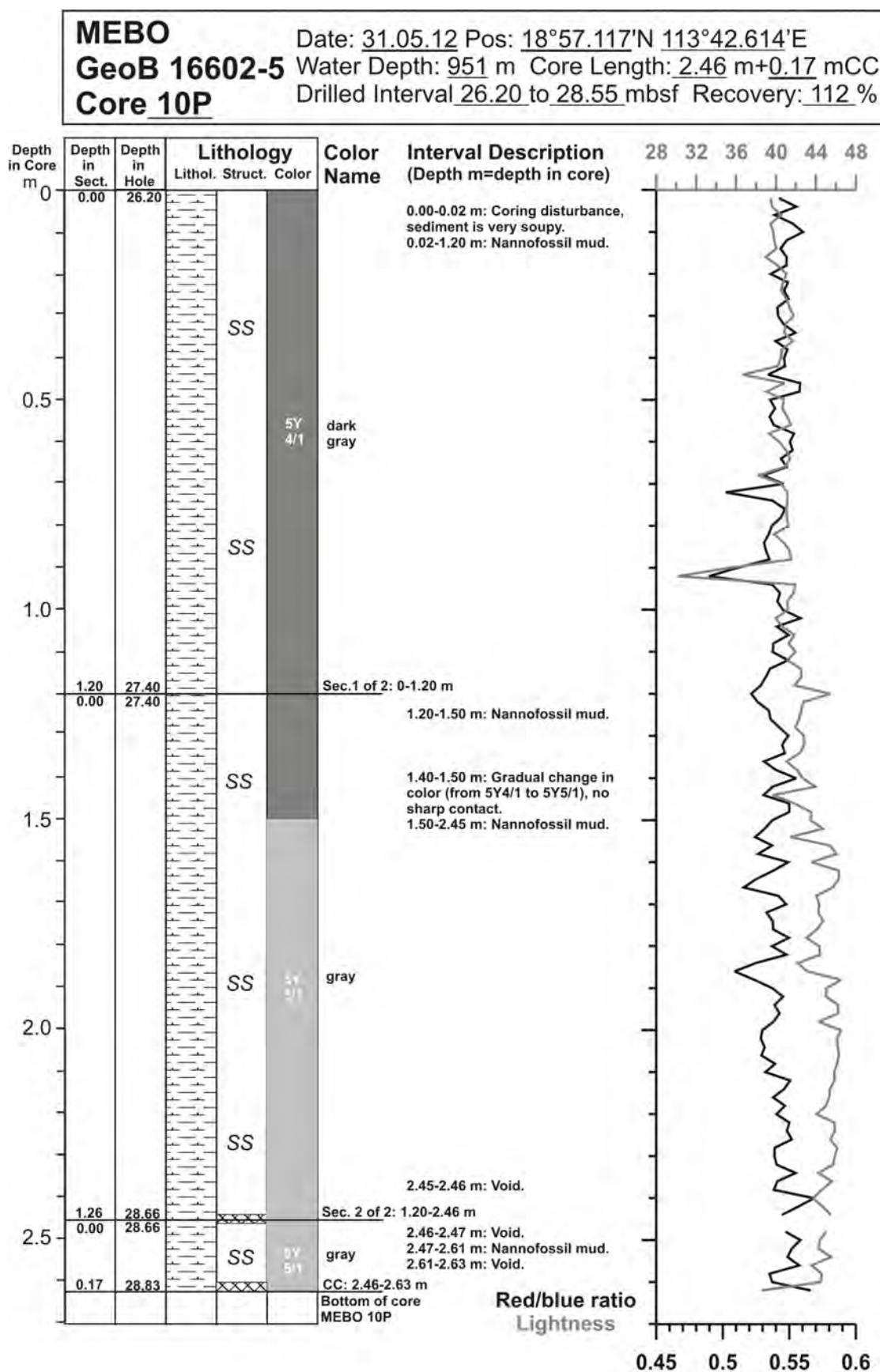


Fig. 10.71: Core description of MeBo core GeoB 16602-5 (10/29).

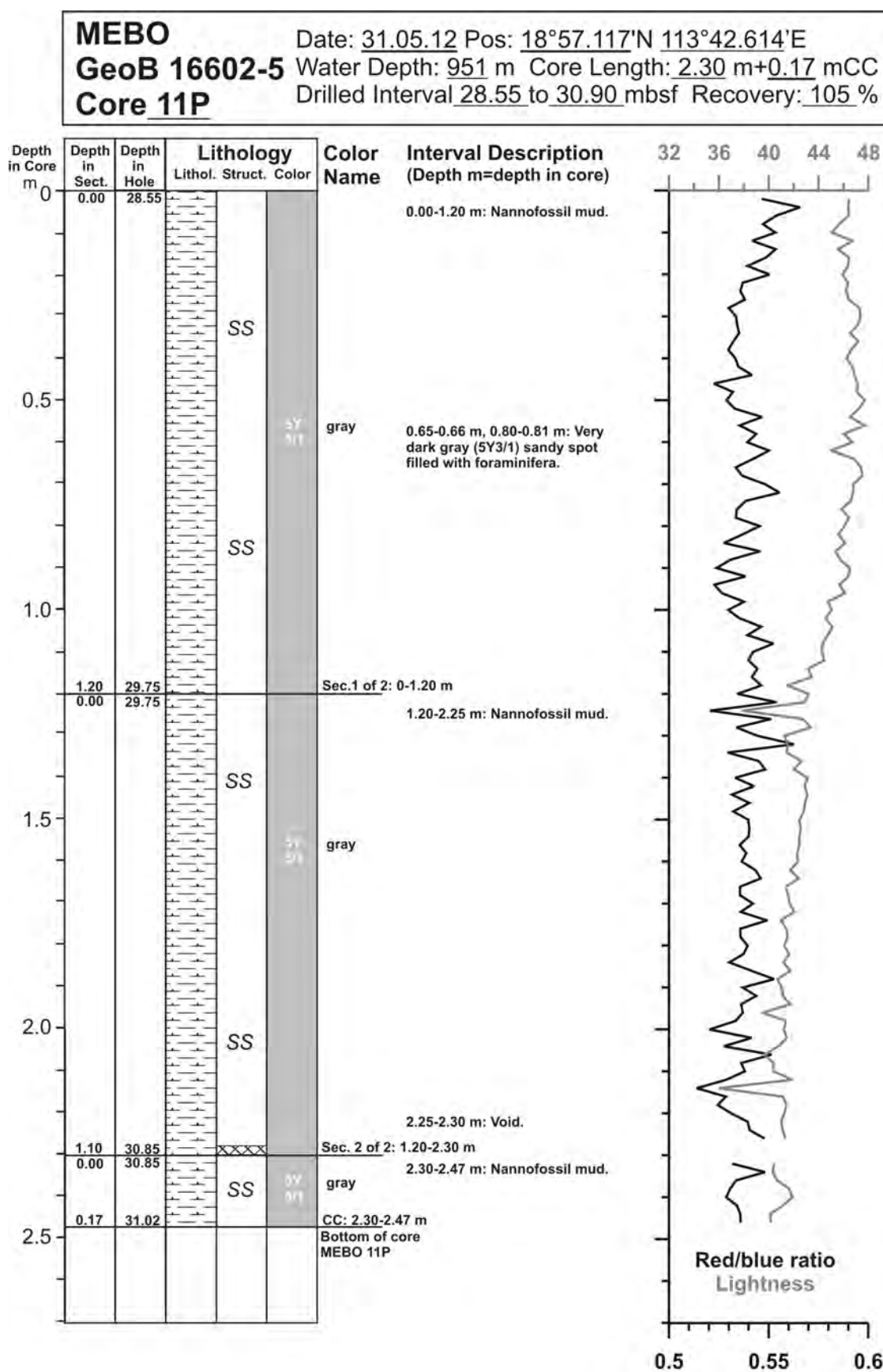


Fig. 10.72: Core description of MeBo core GeoB 16602-5 (11/29).

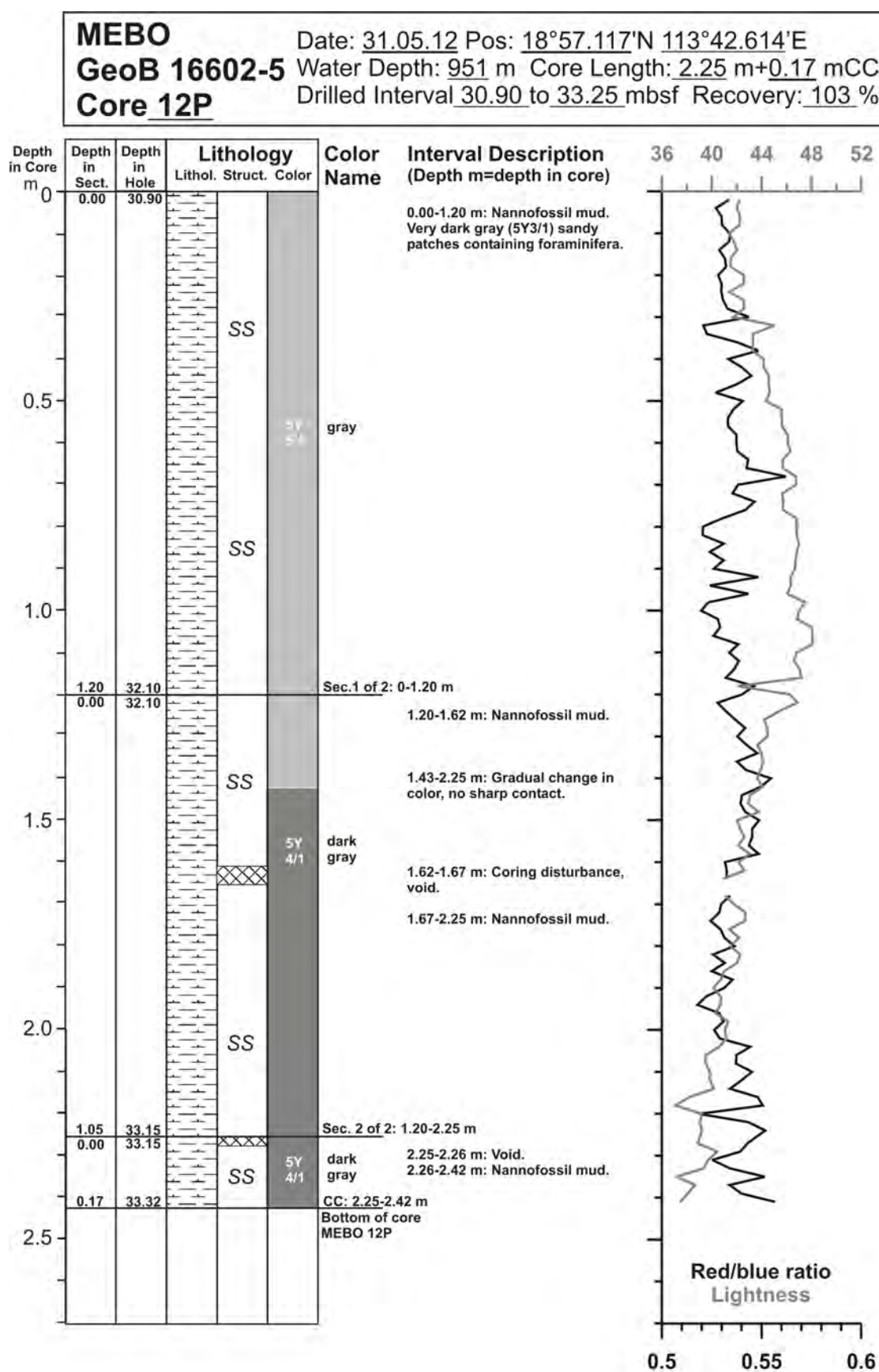


Fig. 10.73: Core description of MeBo core GeoB 16602-5 (12/29).

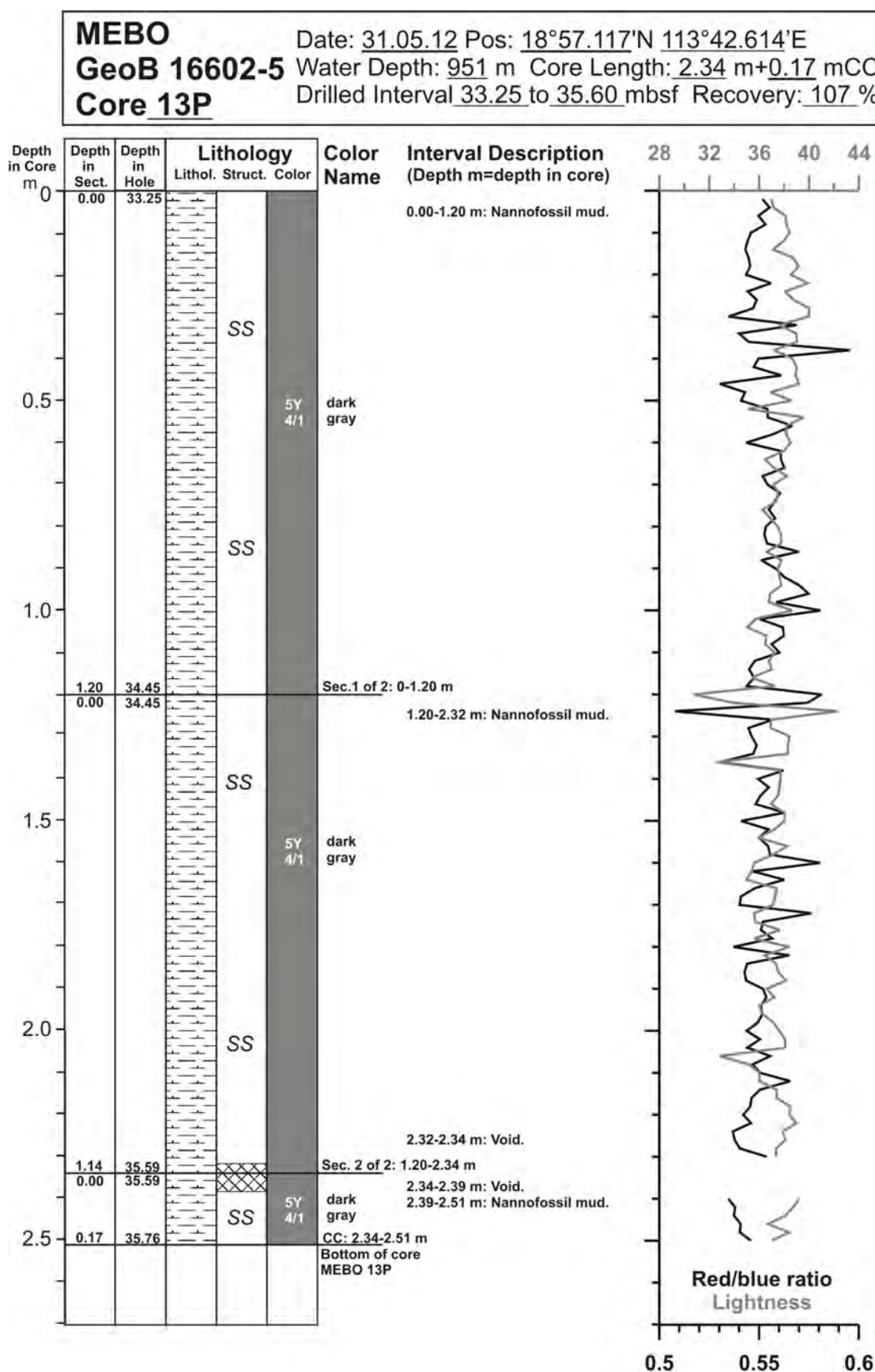


Fig. 10.74: Core description of MeBo core GeoB 16602-5 (13/29).

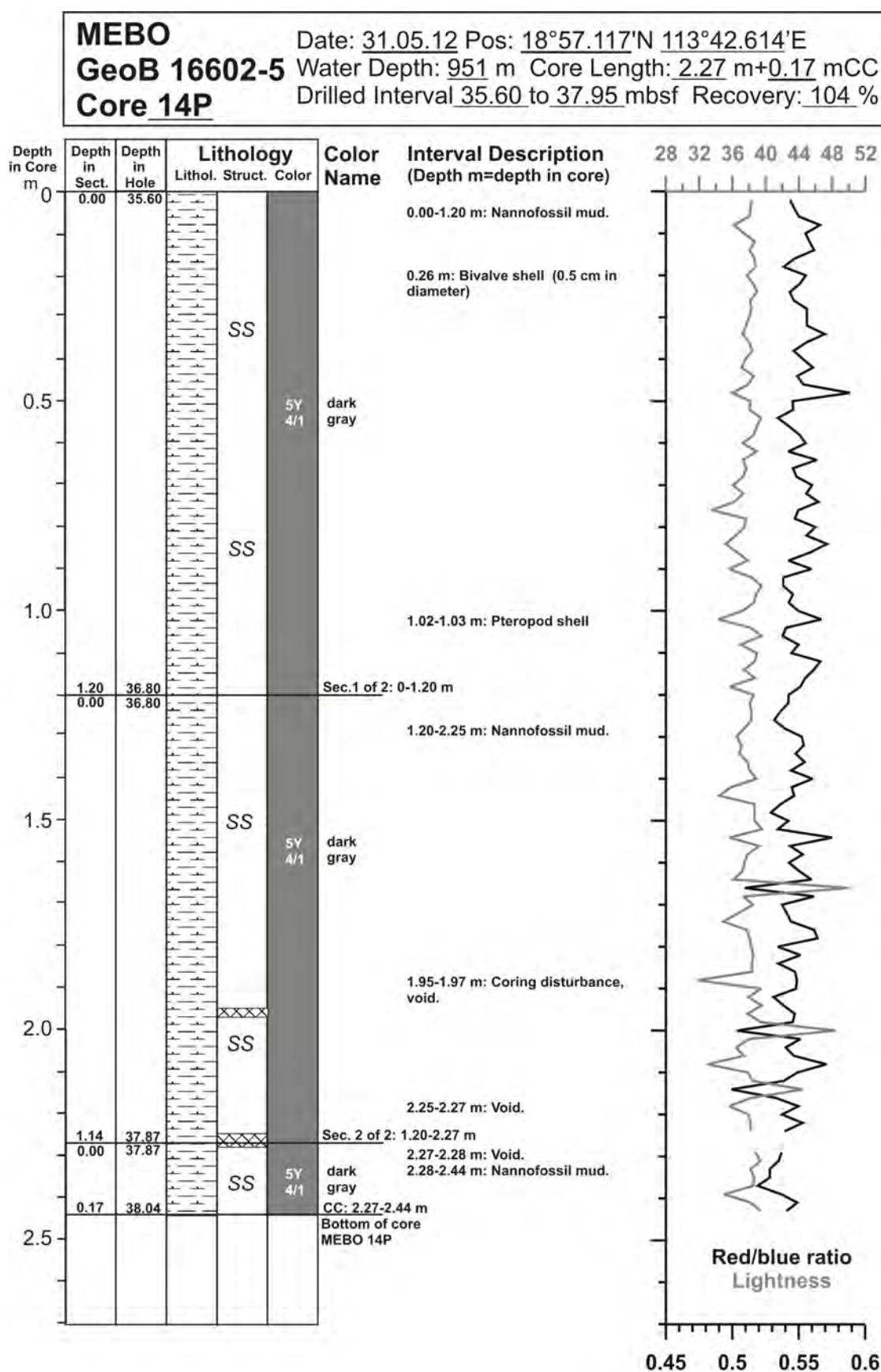


Fig. 10.75: Core description of MeBo core GeoB 16602-5 (14/29).

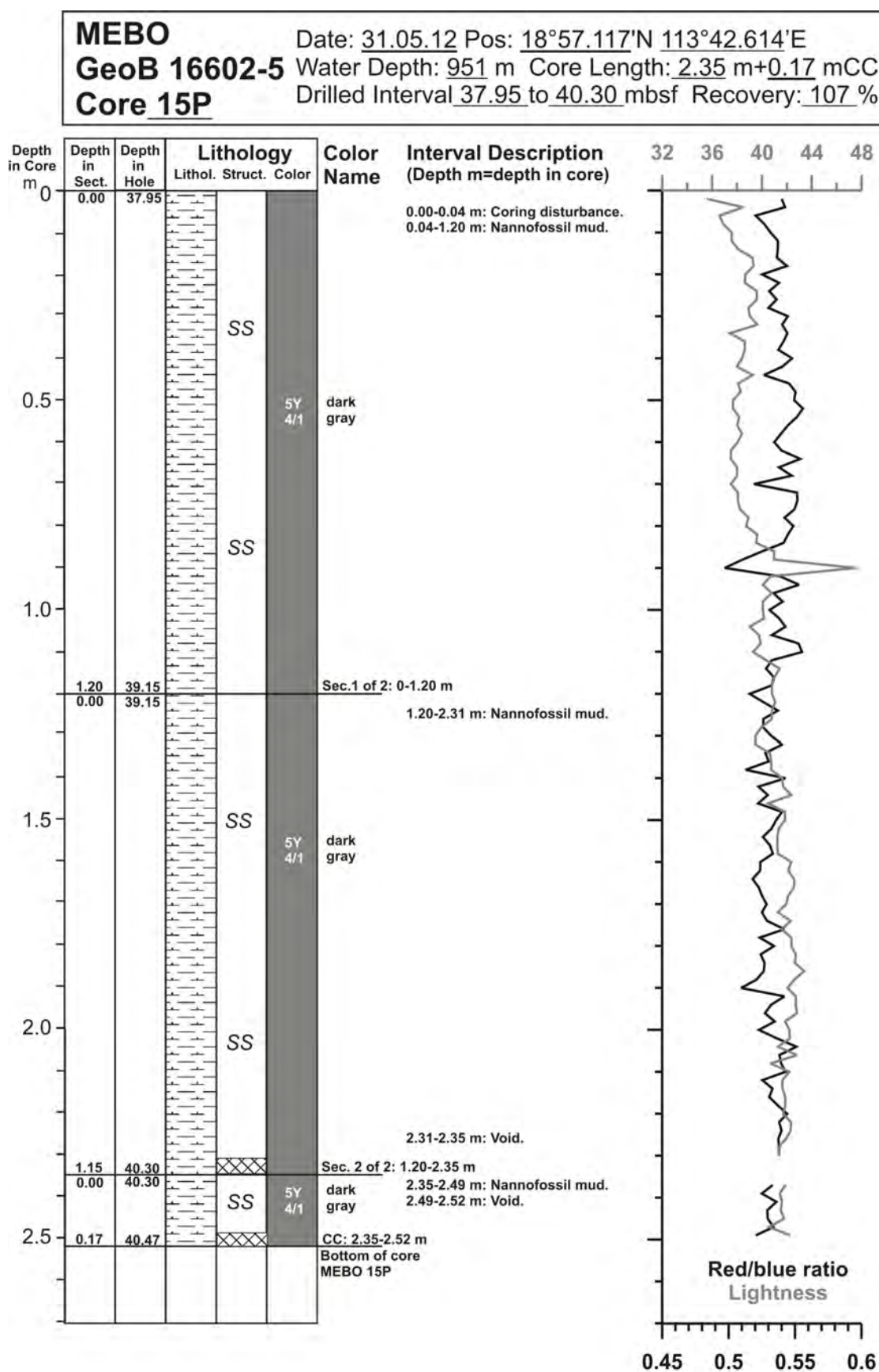


Fig. 10.76: Core description of MeBo core GeoB 16602-5 (15/29).

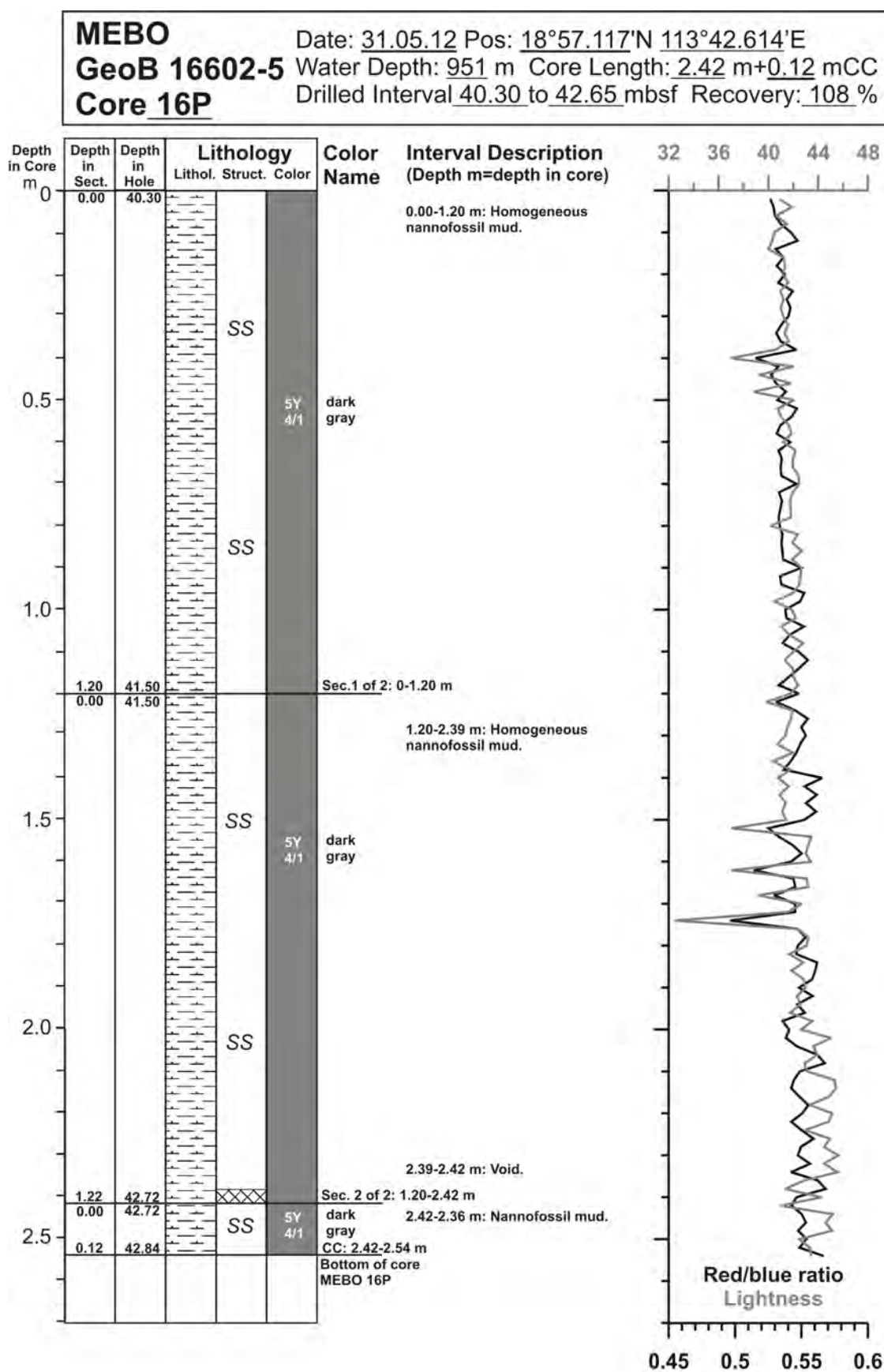


Fig. 10.77: Core description of MeBo core GeoB 16602-5 (16/29).

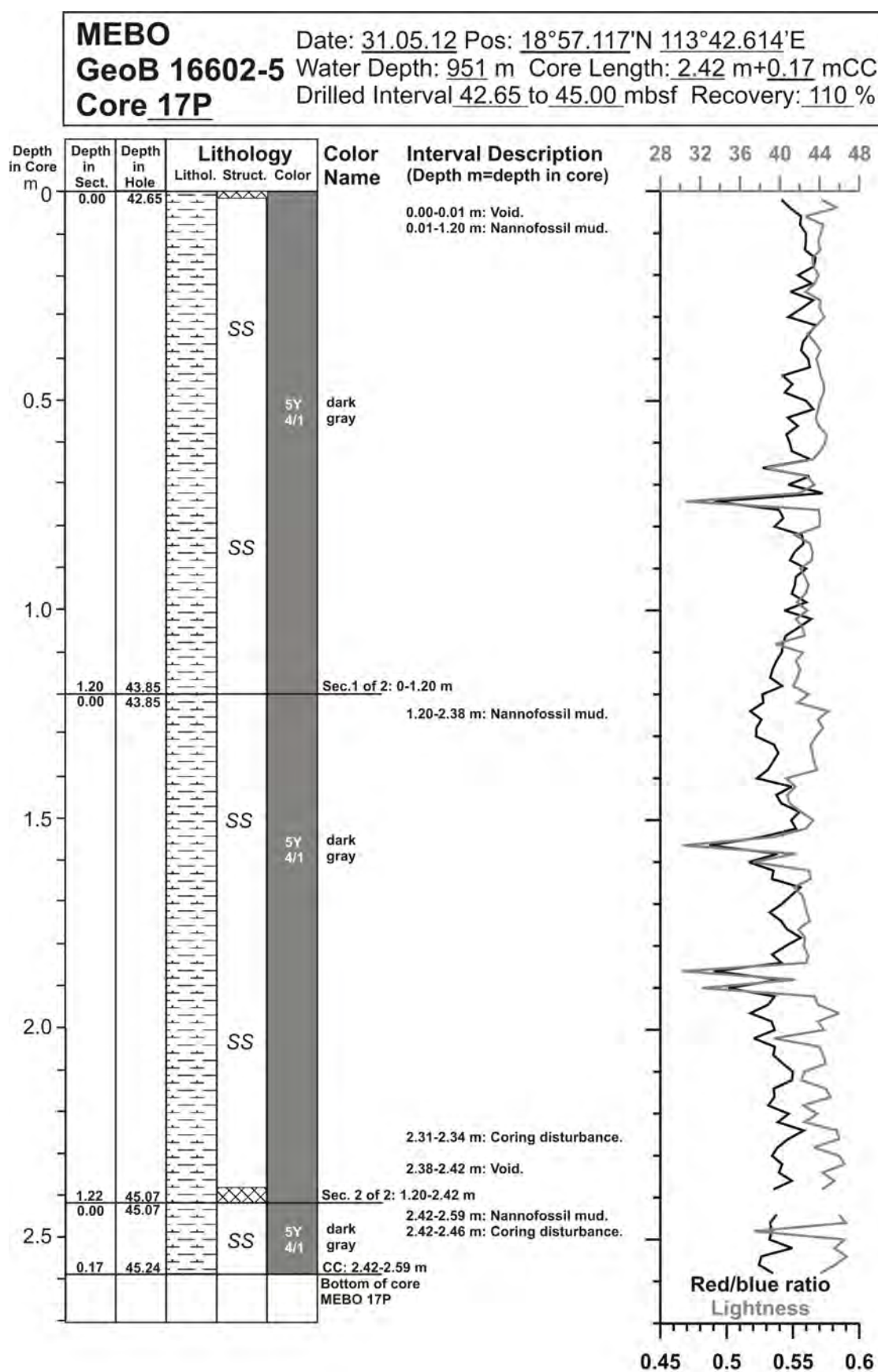


Fig. 10.78: Core description of MeBo core GeoB 16602-5 (17/29).

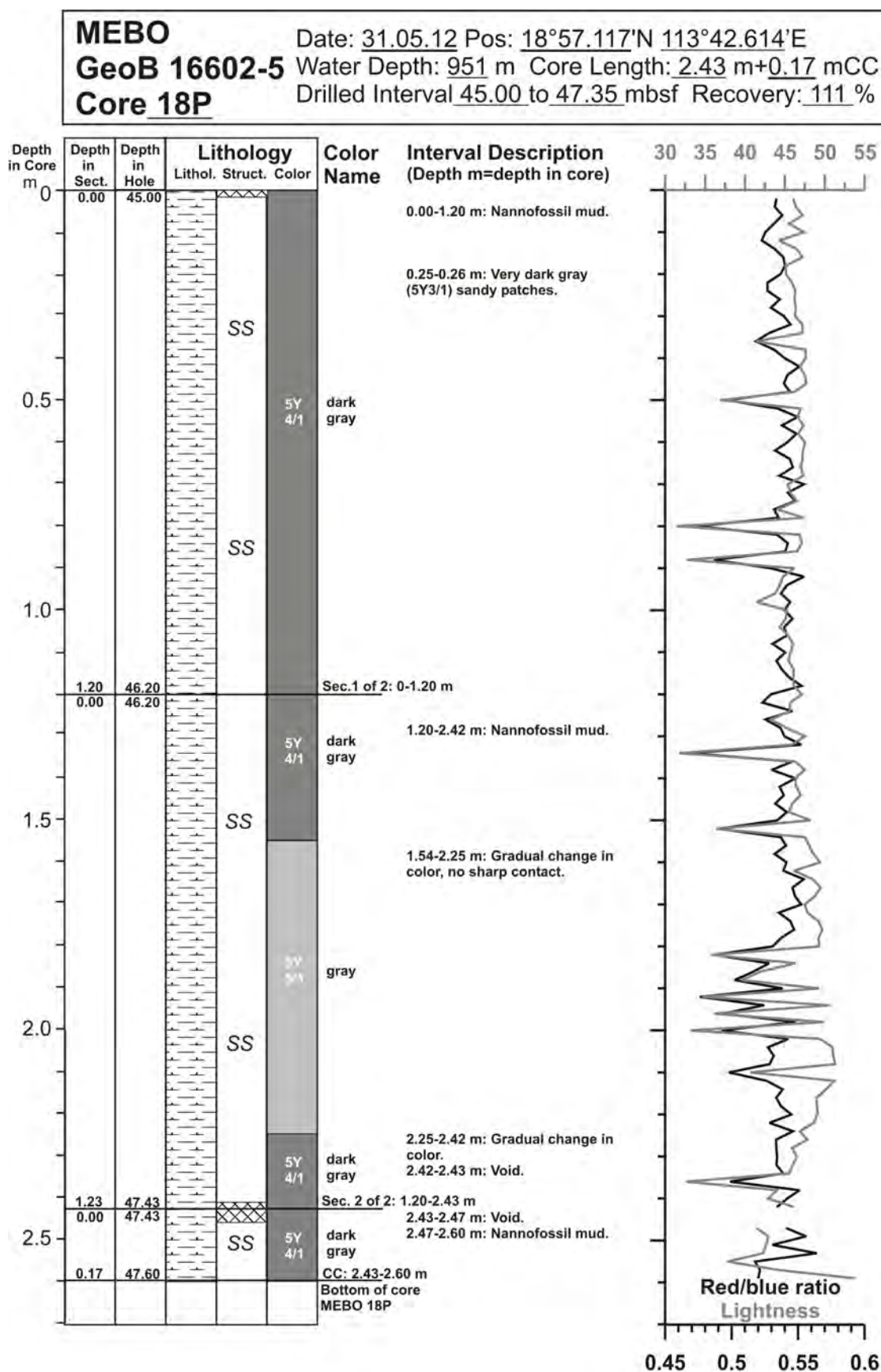


Fig. 10.79: Core description of MeBo core GeoB 16602-5 (18/29).

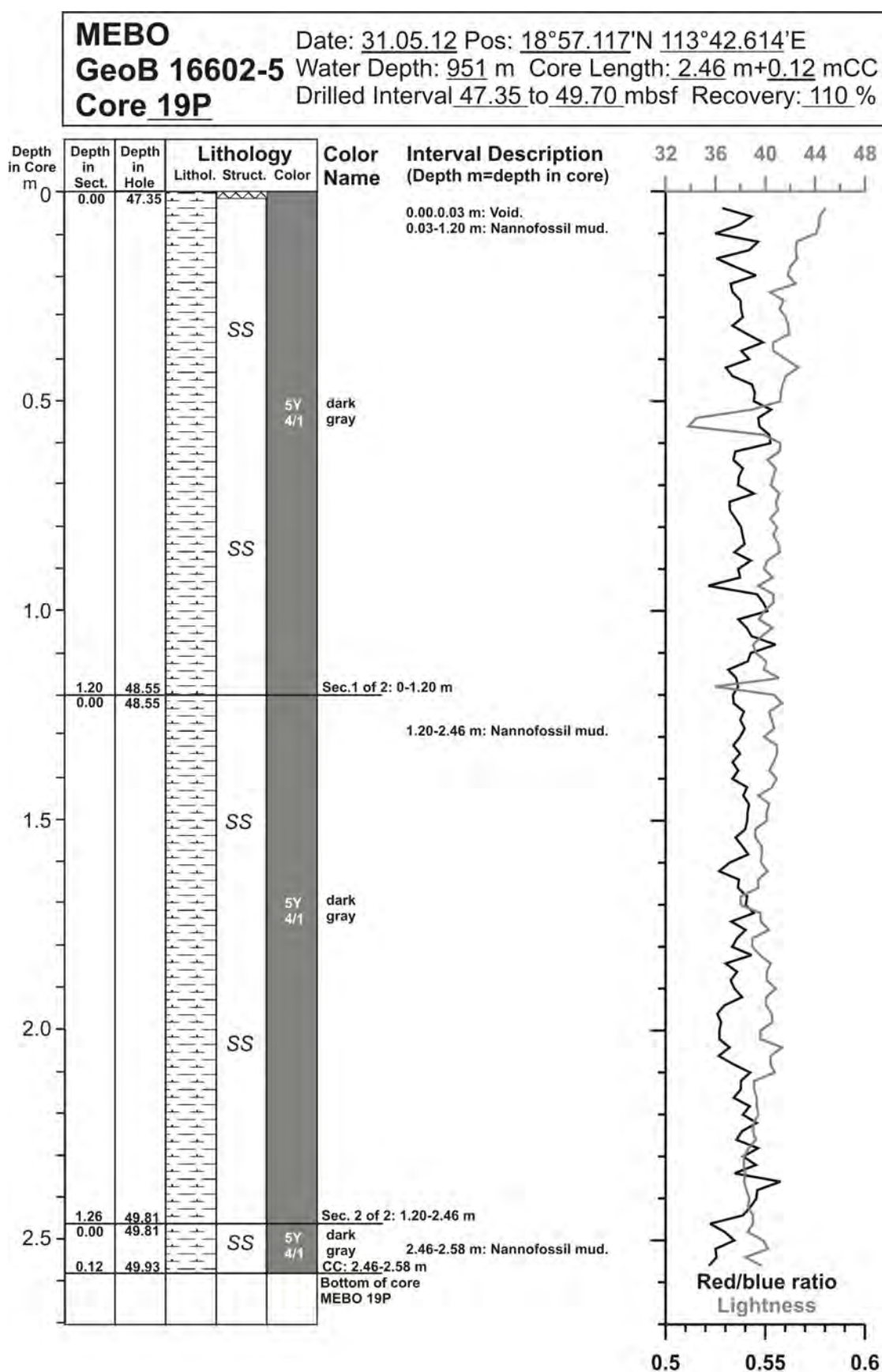


Fig. 10.80: Core description of MeBo core GeoB 16602-5 (19/29).

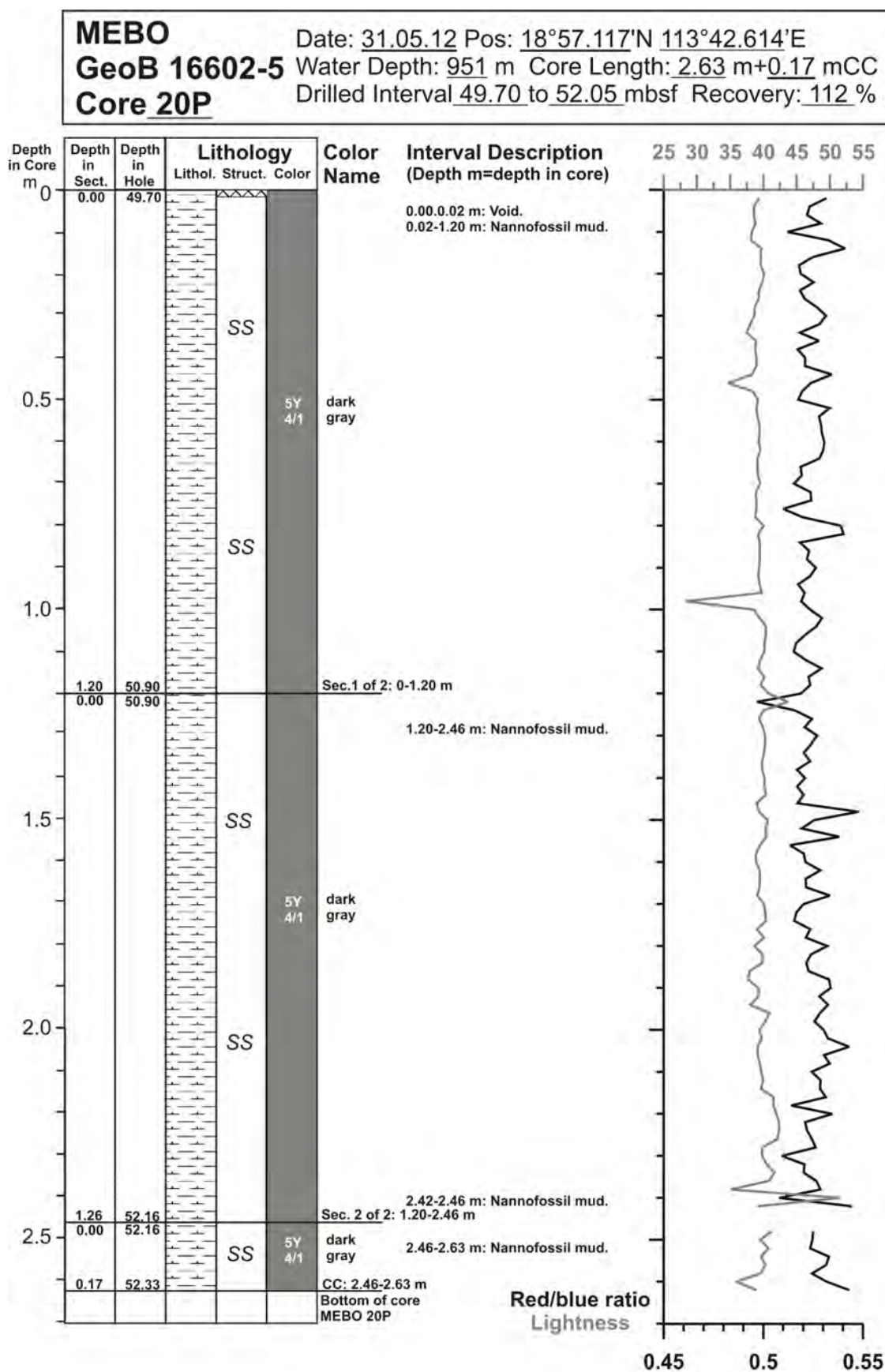


Fig. 10.81: Core description of MeBo core GeoB 16602-5 (20/29).

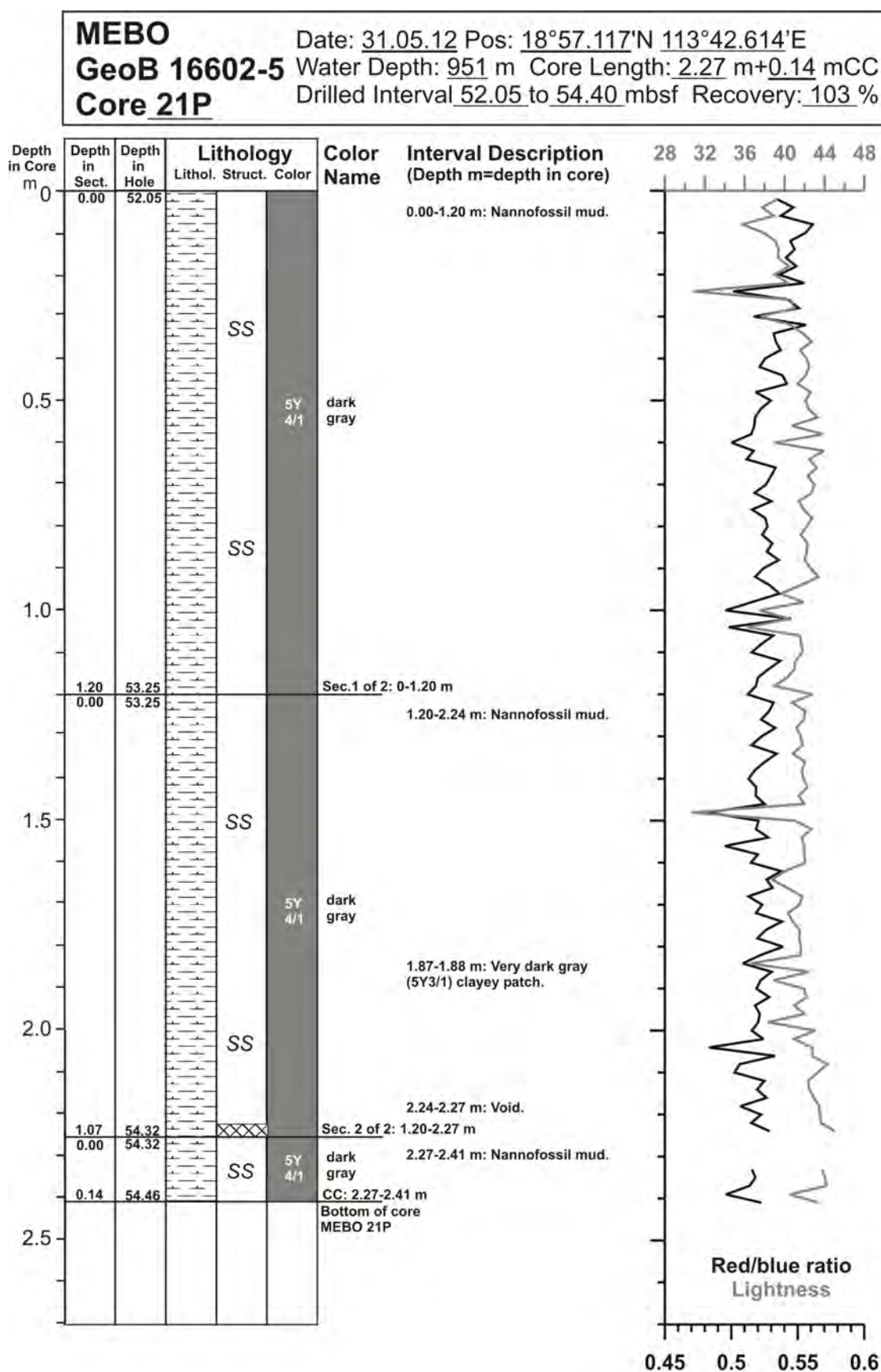


Fig. 10.82: Core description of MeBo core GeoB 16602-5 (21/29).

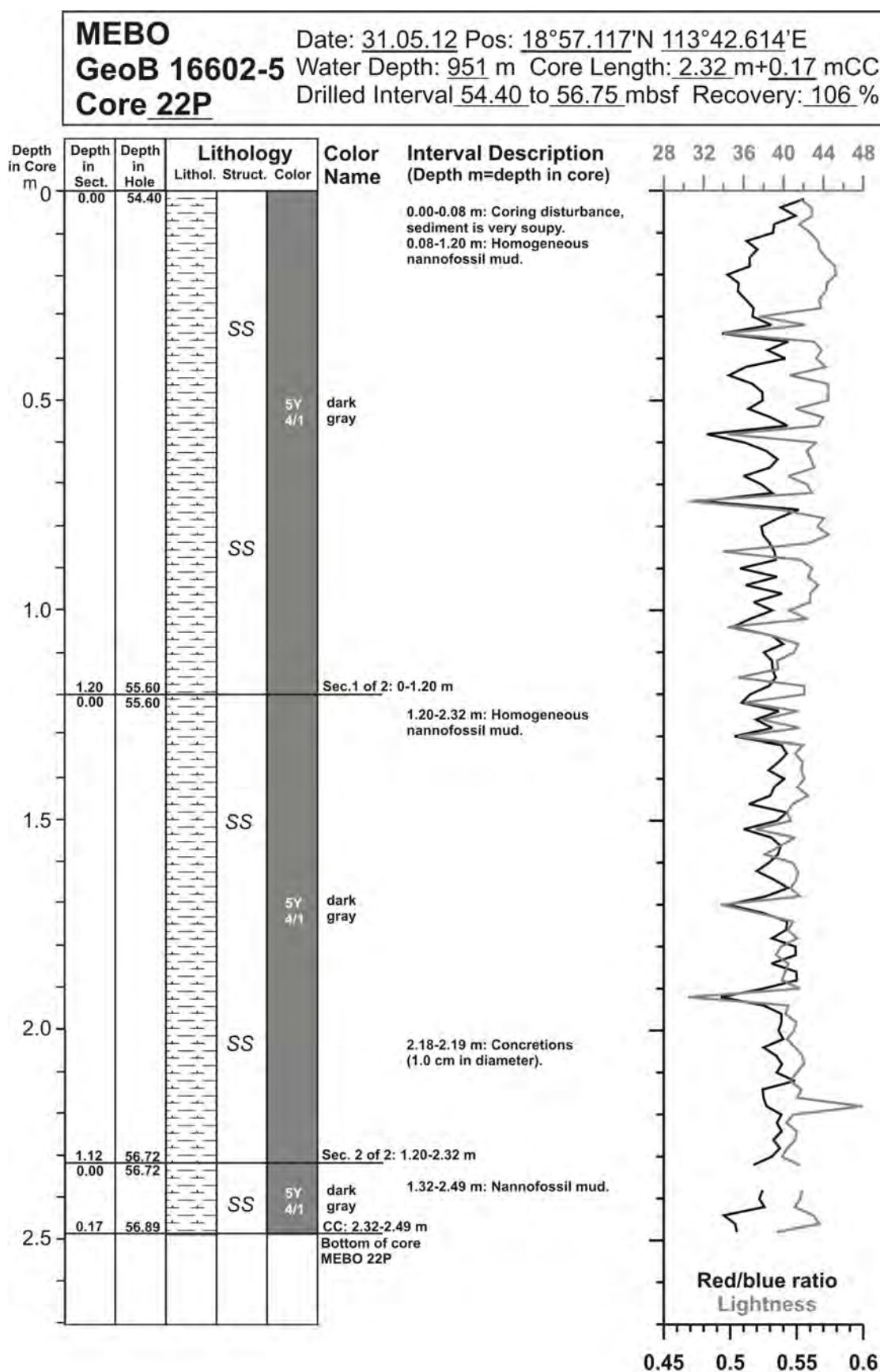


Fig. 10.83: Core description of MeBo core GeoB 16602-5 (22/29).

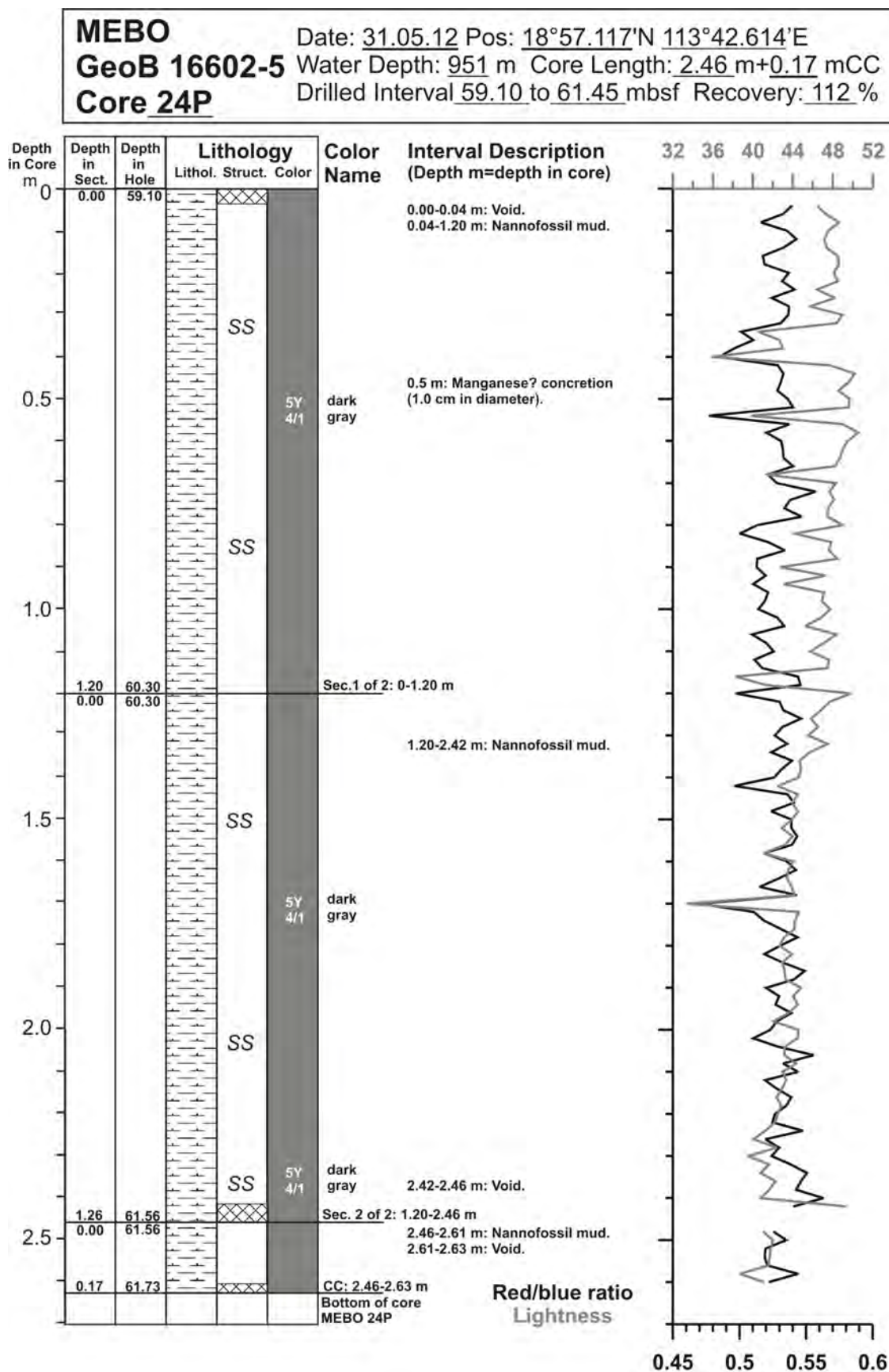


Fig. 10.85: Core description of MeBo core GeoB 16602-5 (24/29).

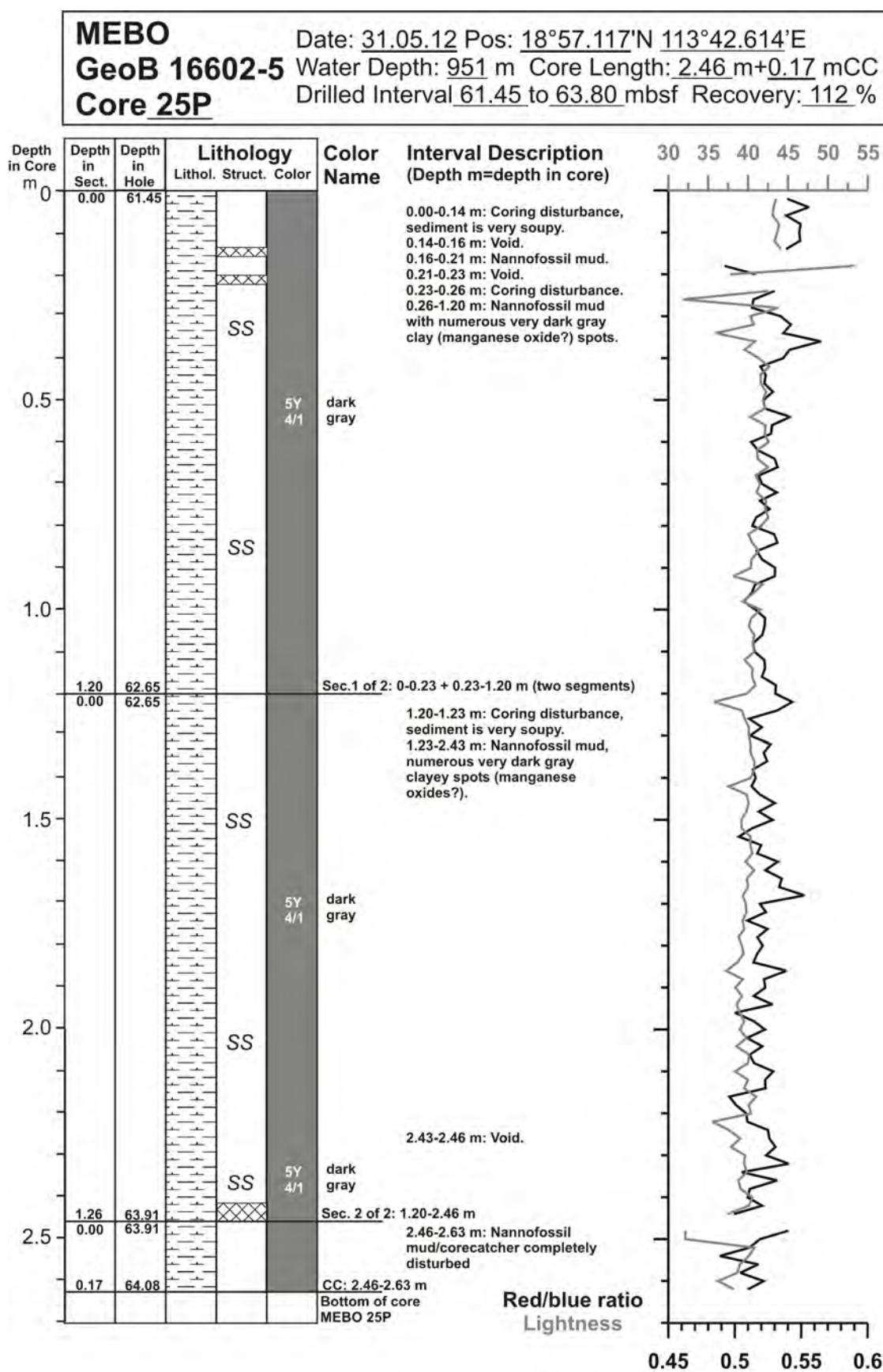


Fig. 10.86: Core description of MeBo core GeoB 16602-5 (25/29).

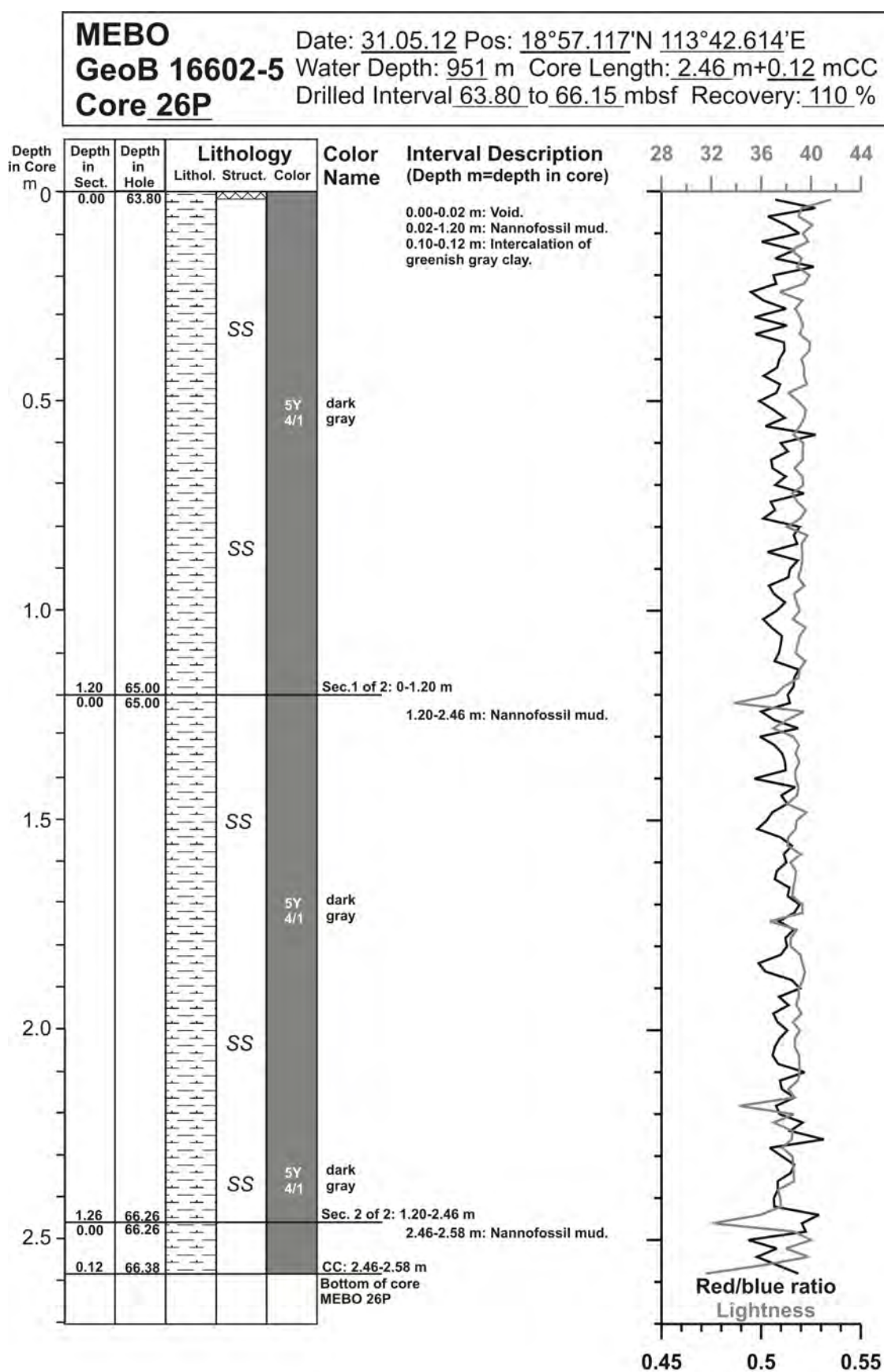


Fig. 10.87: Core description of MeBo core GeoB 16602-5 (26/29).

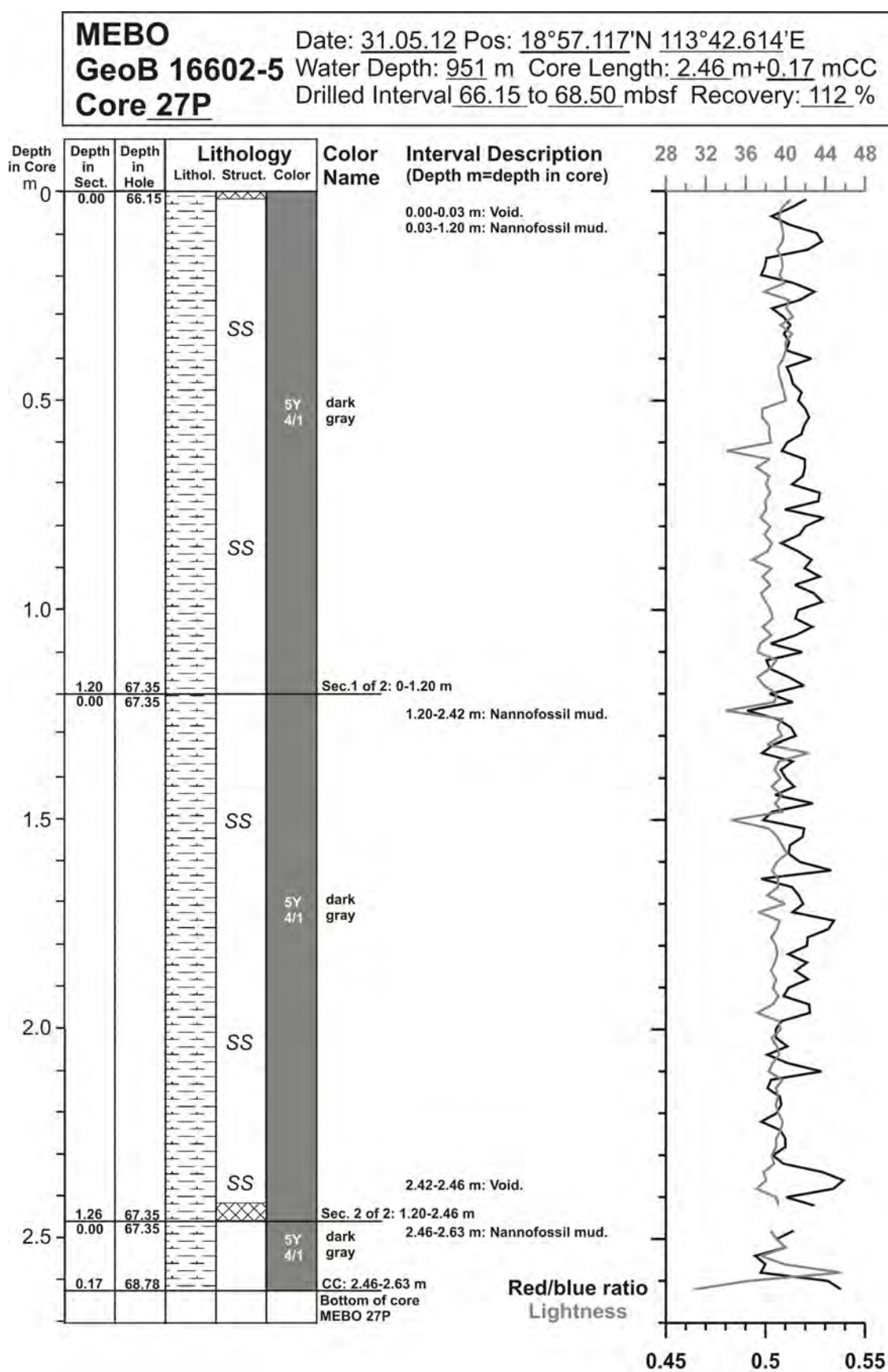


Fig. 10.88: Core description of MeBo core GeoB 16602-5 (27/29).

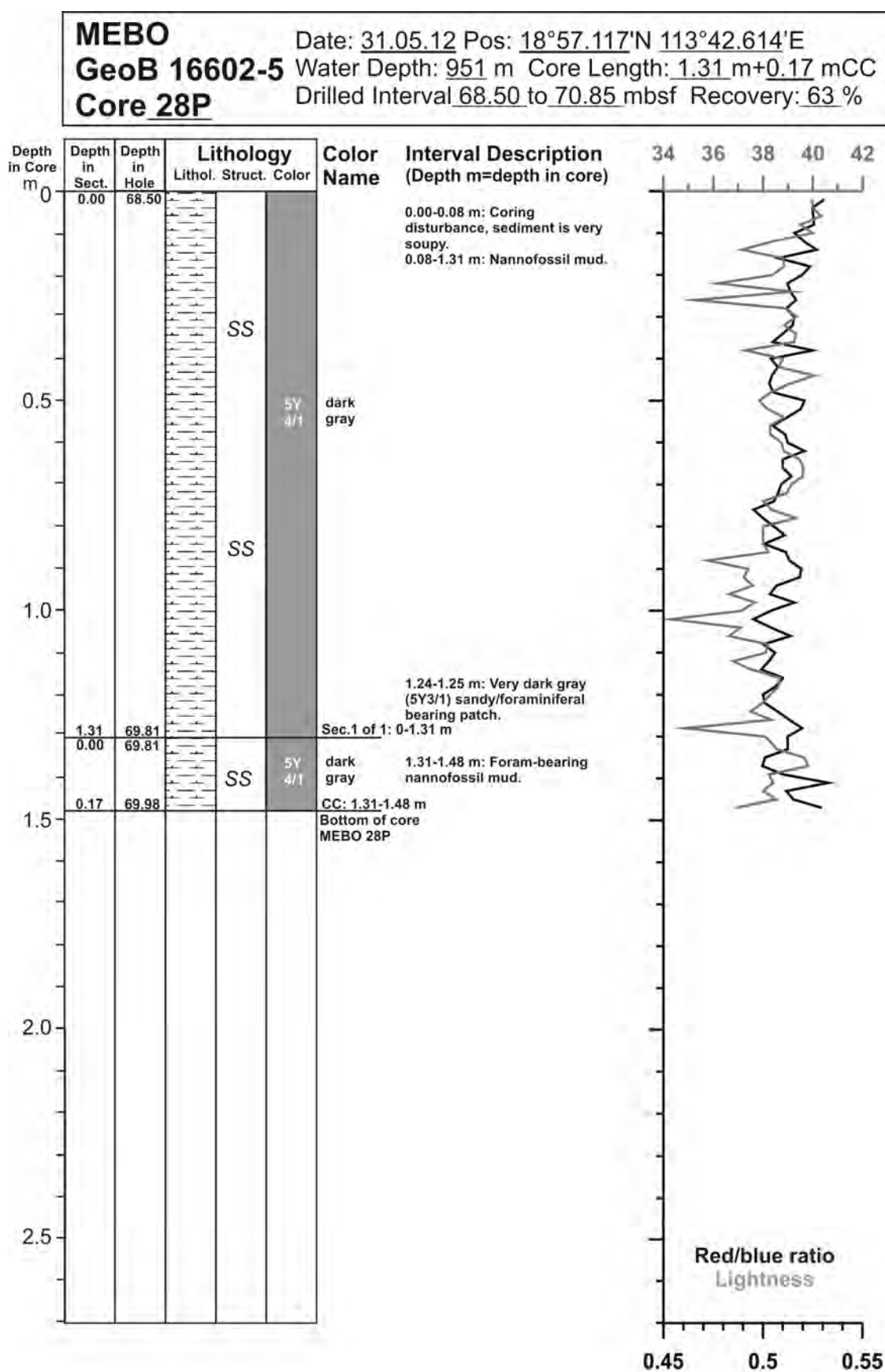


Fig. 10.89: Core description of MeBo core GeoB 16602-5 (28/29).

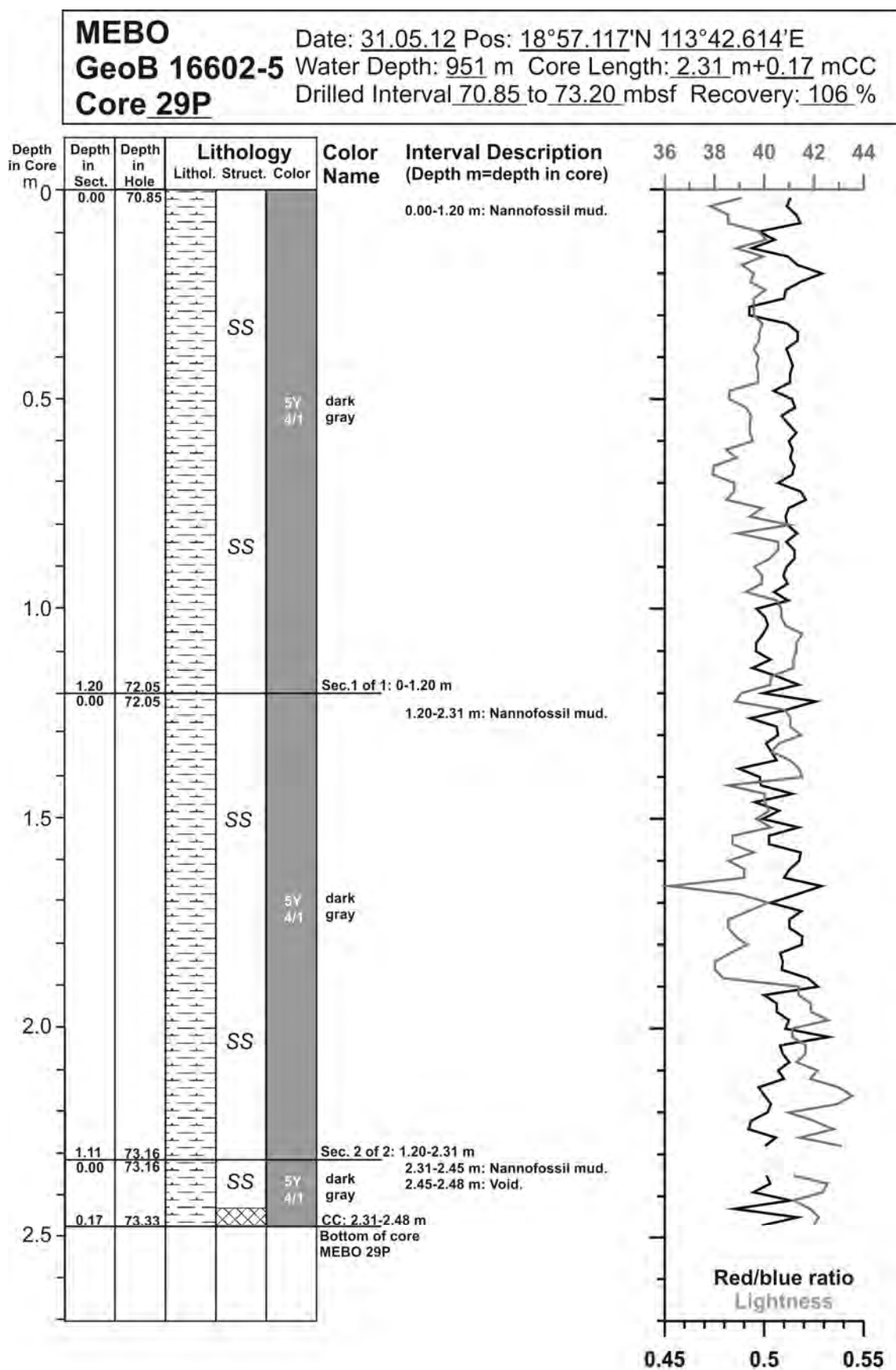


Fig. 10.90: Core description of MeBo core GeoB 16602-5 (29/29).

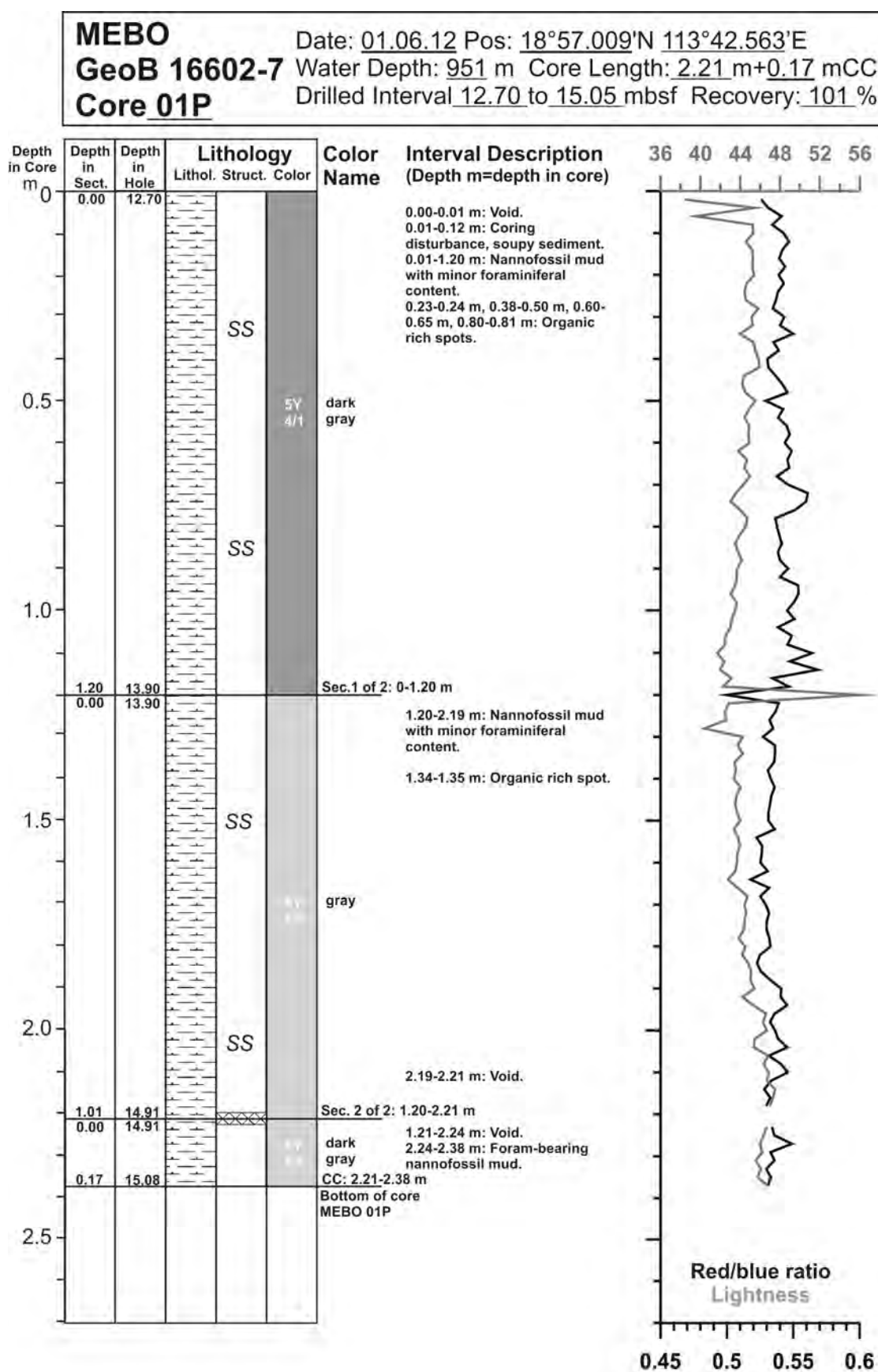


Fig. 10.91: Core description of MeBo core GeoB 16602-7 (1/29).

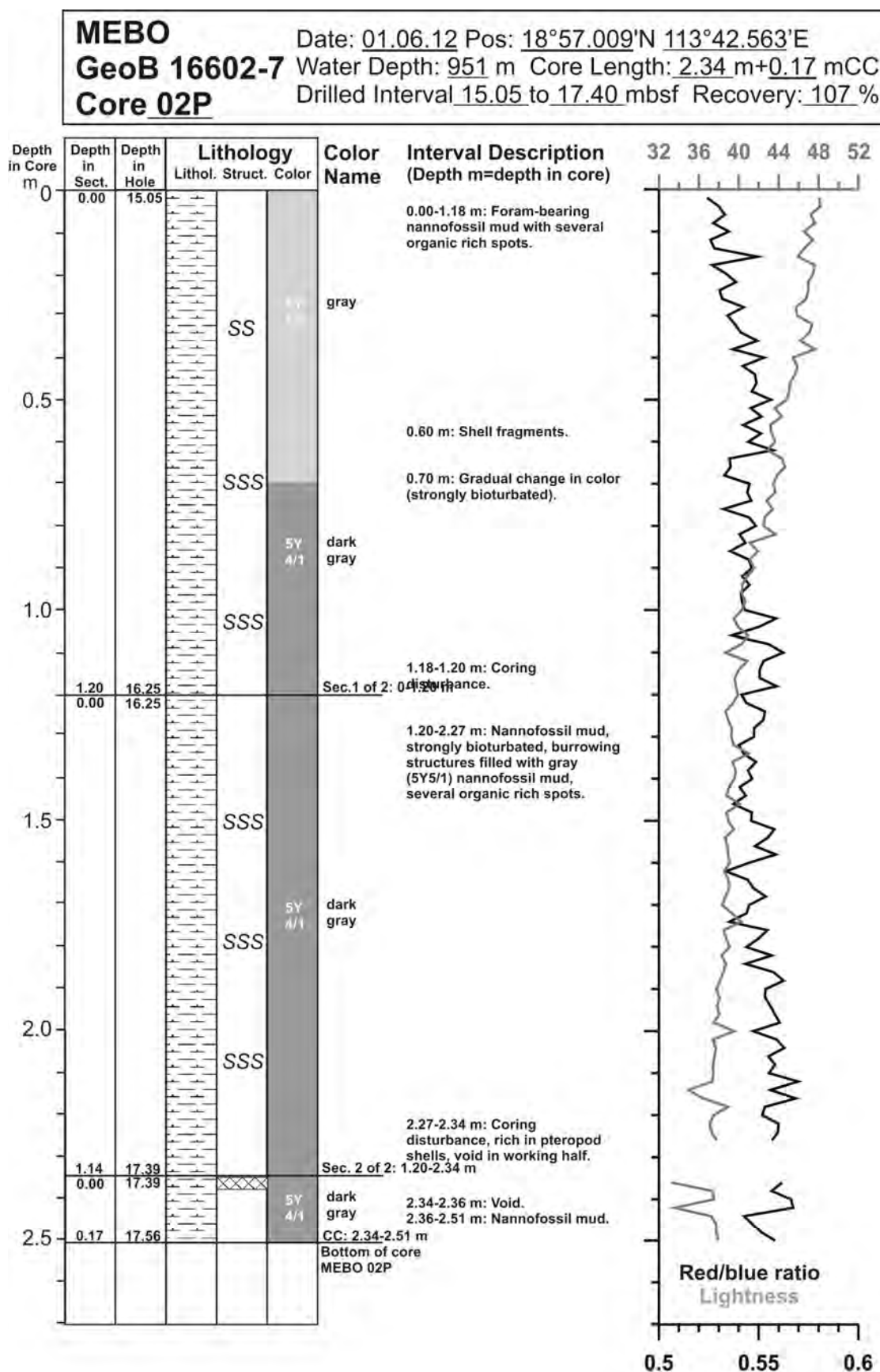


Fig. 10.92: Core description of MeBo core GeoB 16602-7 (2/29).

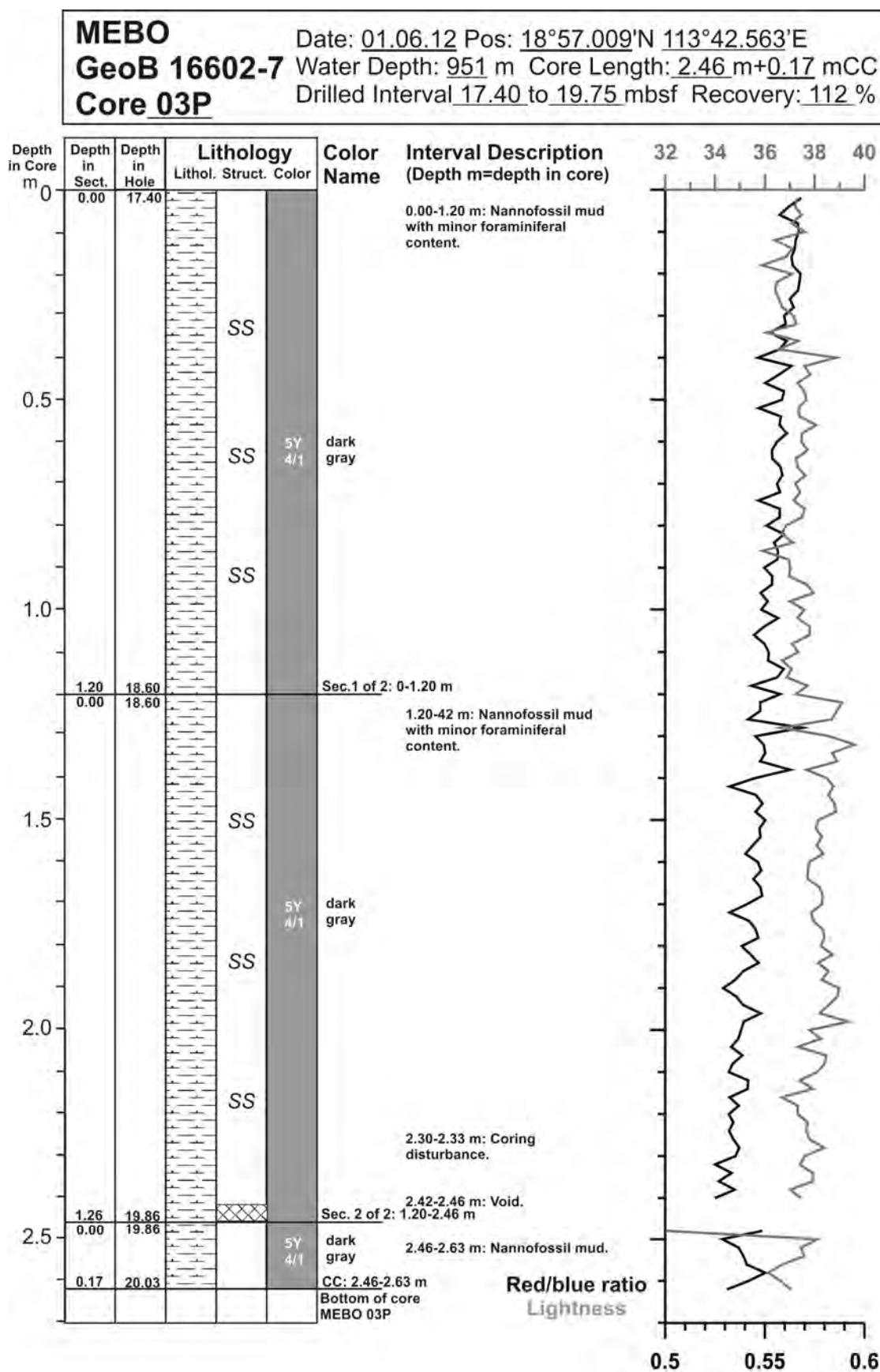


Fig. 10.93: Core description of MeBo core GeoB 16602-7 (3/29).

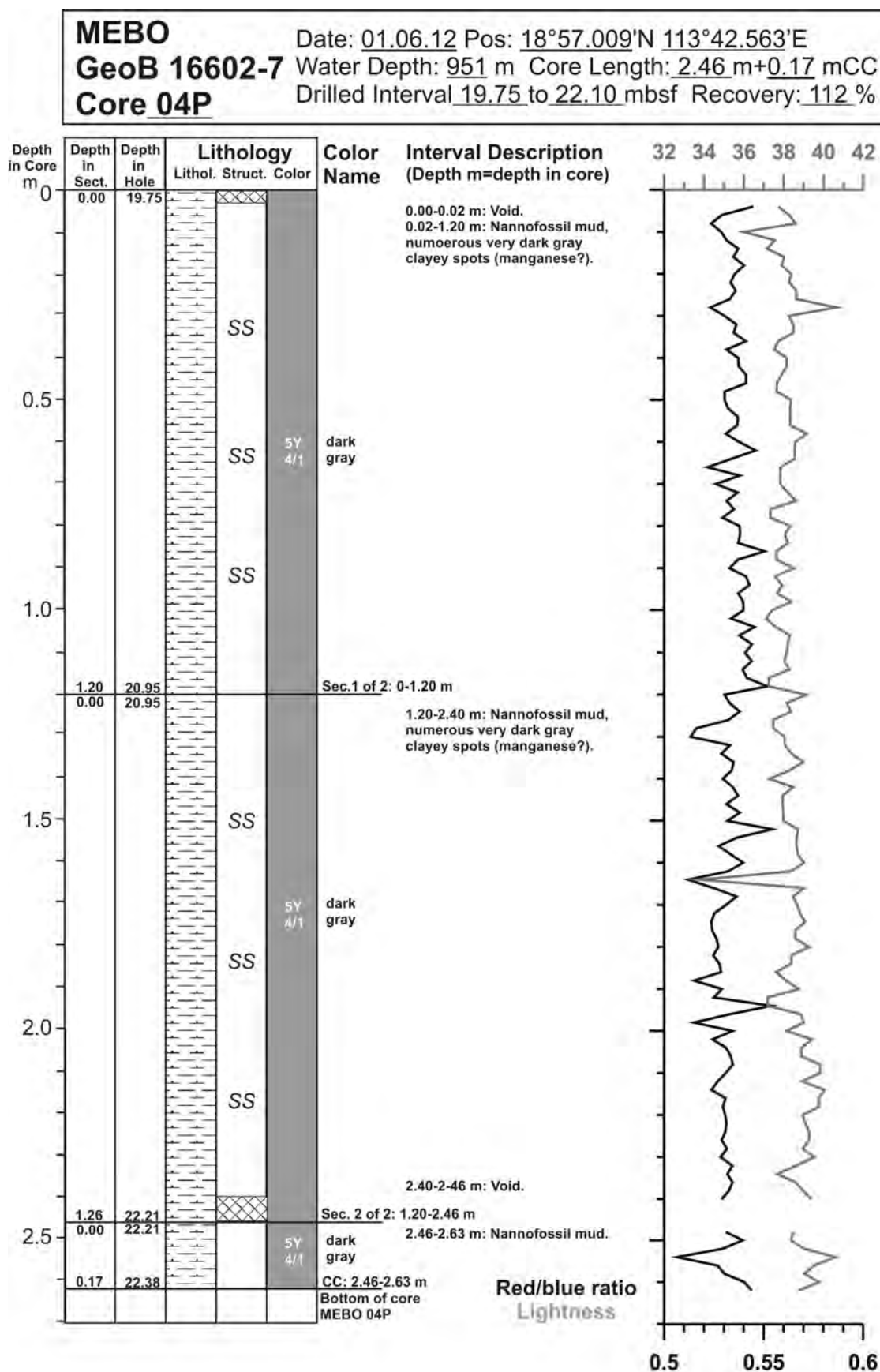


Fig. 10.94: Core description of MeBo core GeoB 16602-7 (4/29).

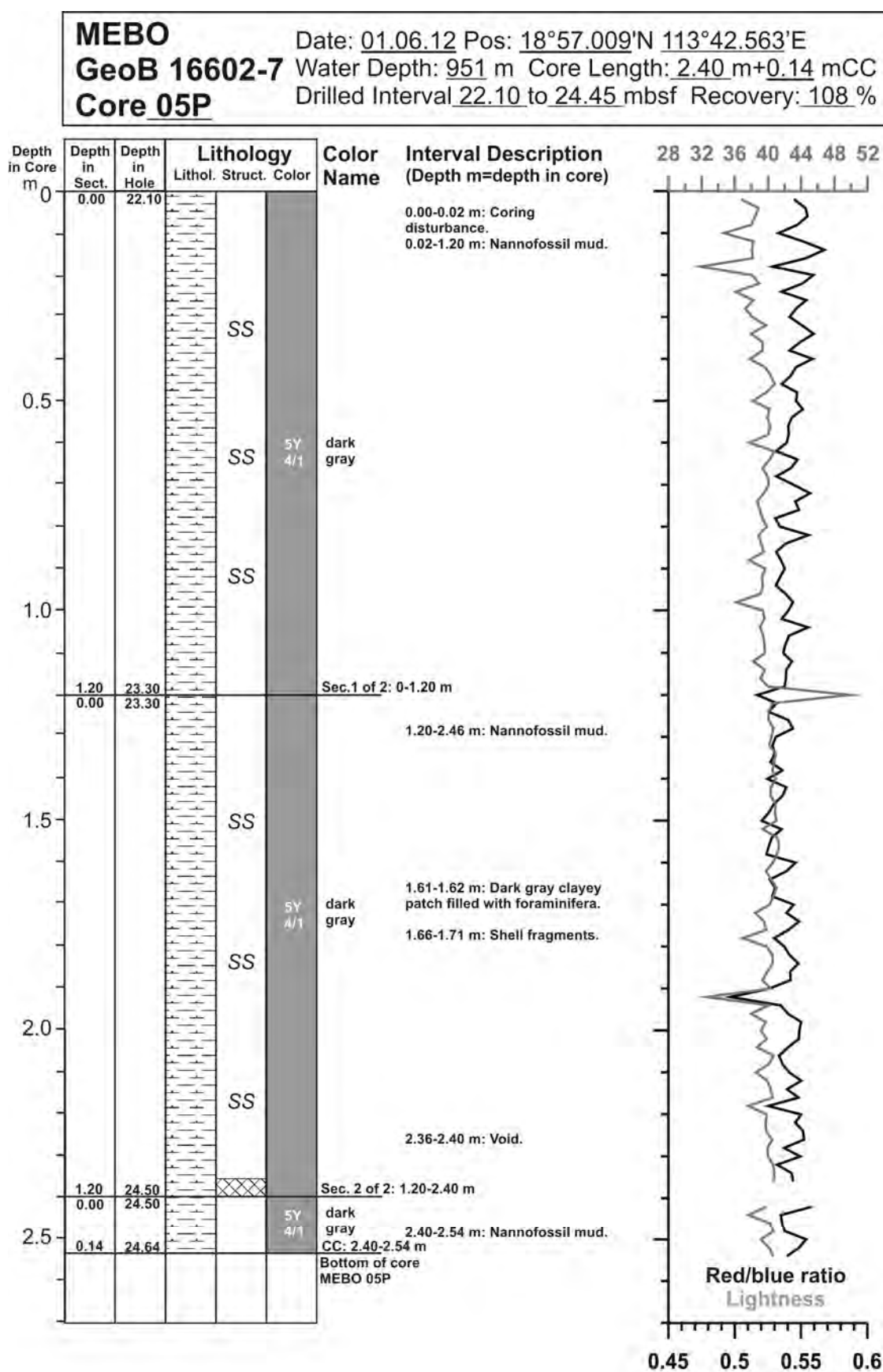


Fig. 10.95: Core description of MeBo core GeoB 16602-7 (5/29).

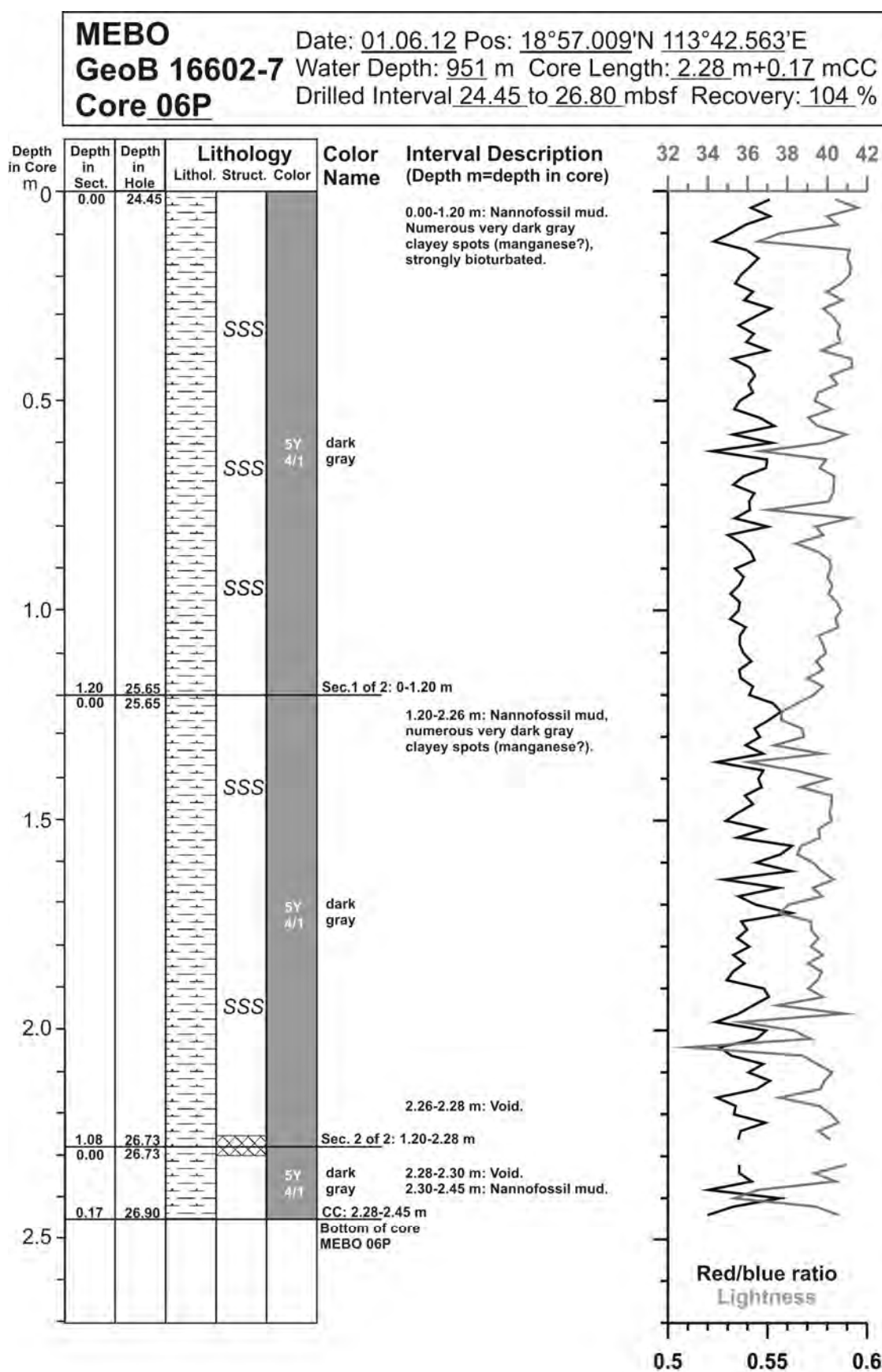


Fig. 10.96: Core description of MeBo core GeoB 16602-7 (6/29).

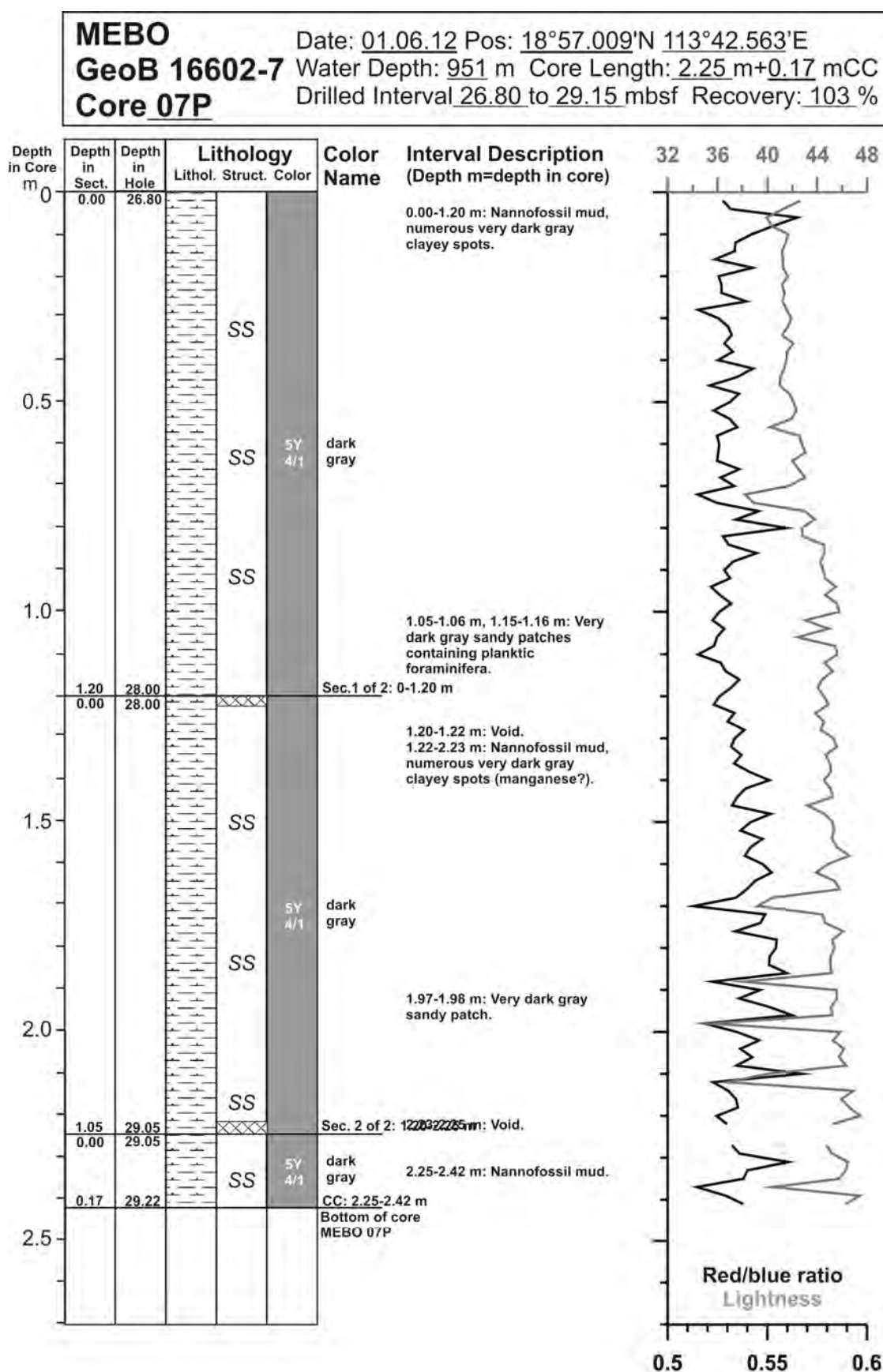


Fig. 10.97: Core description of MeBo core GeoB 16602-7 (7/29).

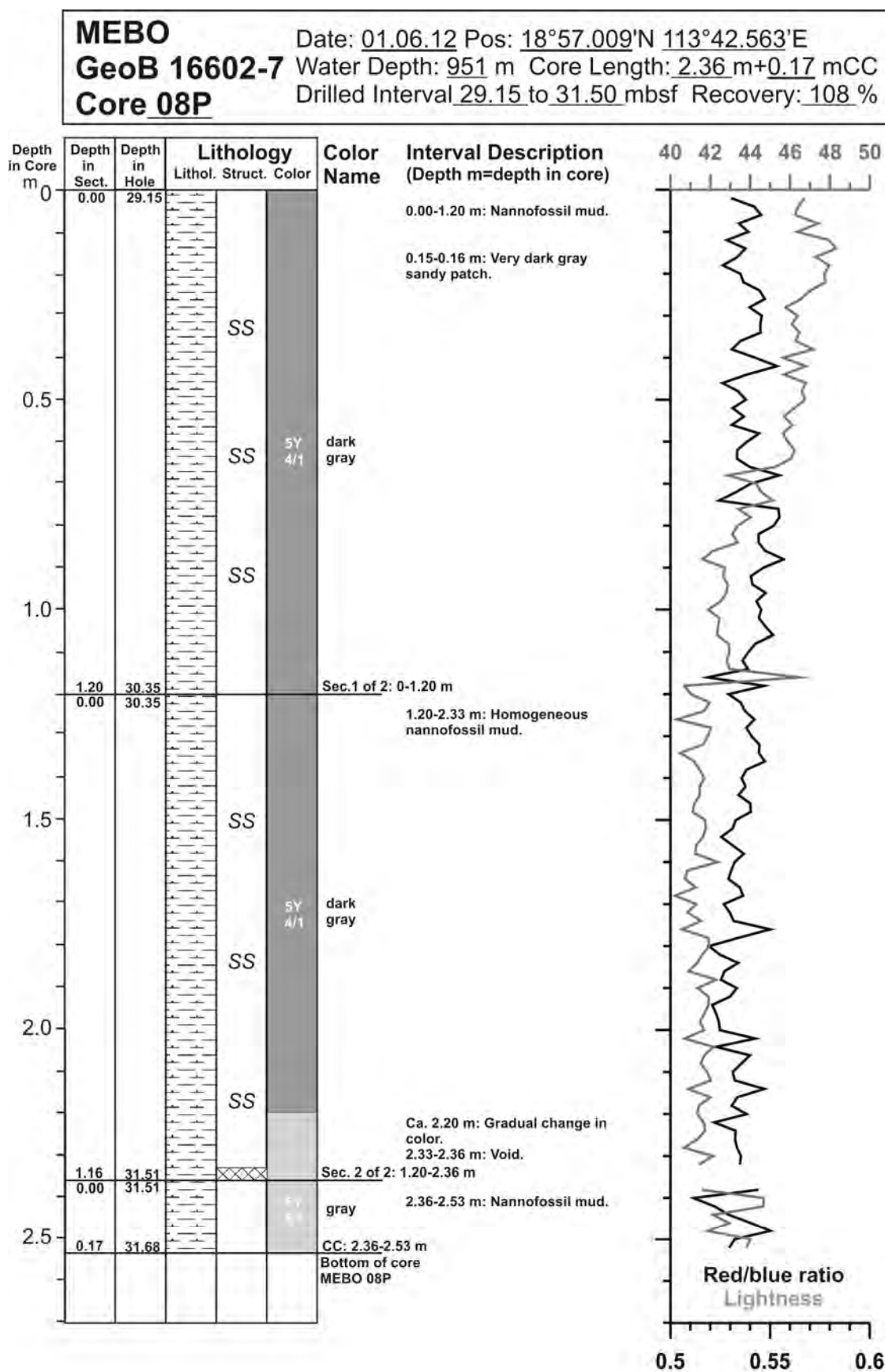


Fig. 10.98: Core description of MeBo core GeoB 16602-7 (8/29).

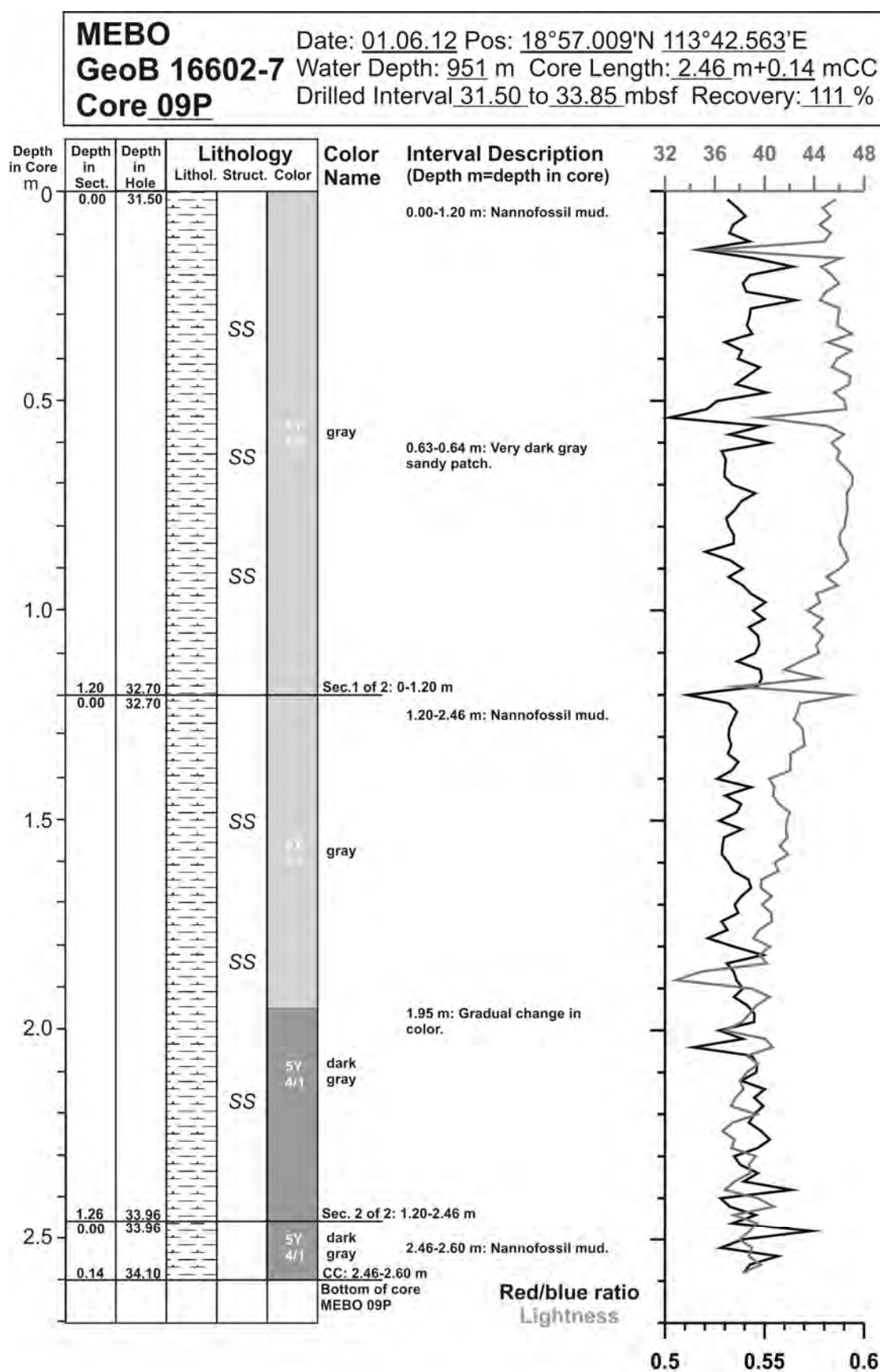


Fig. 10.99: Core description of MeBo core GeoB 16602-7 (9/29).

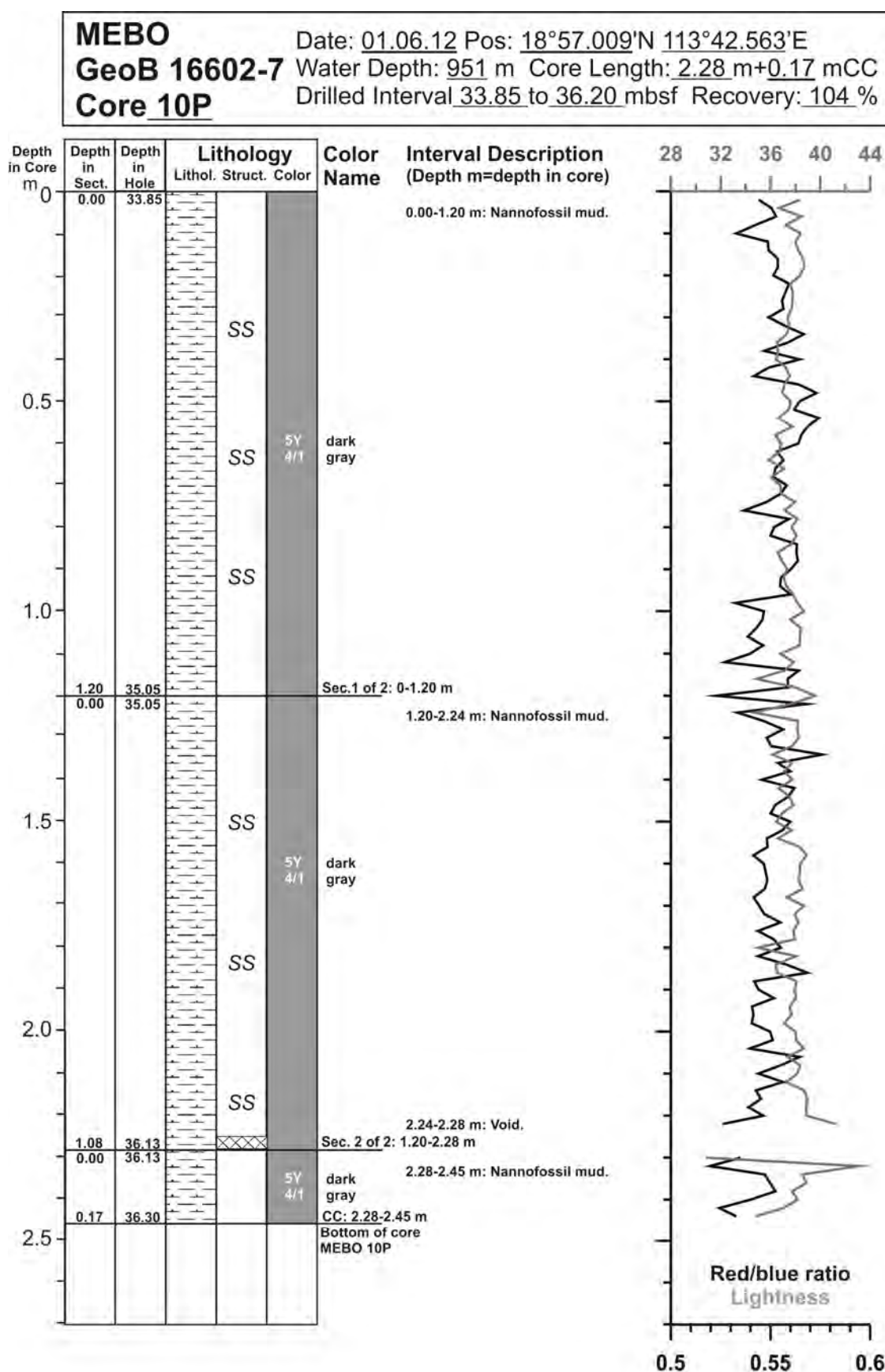


Fig. 10.100: Core description of MeBo core GeoB 16602-7 (10/29).

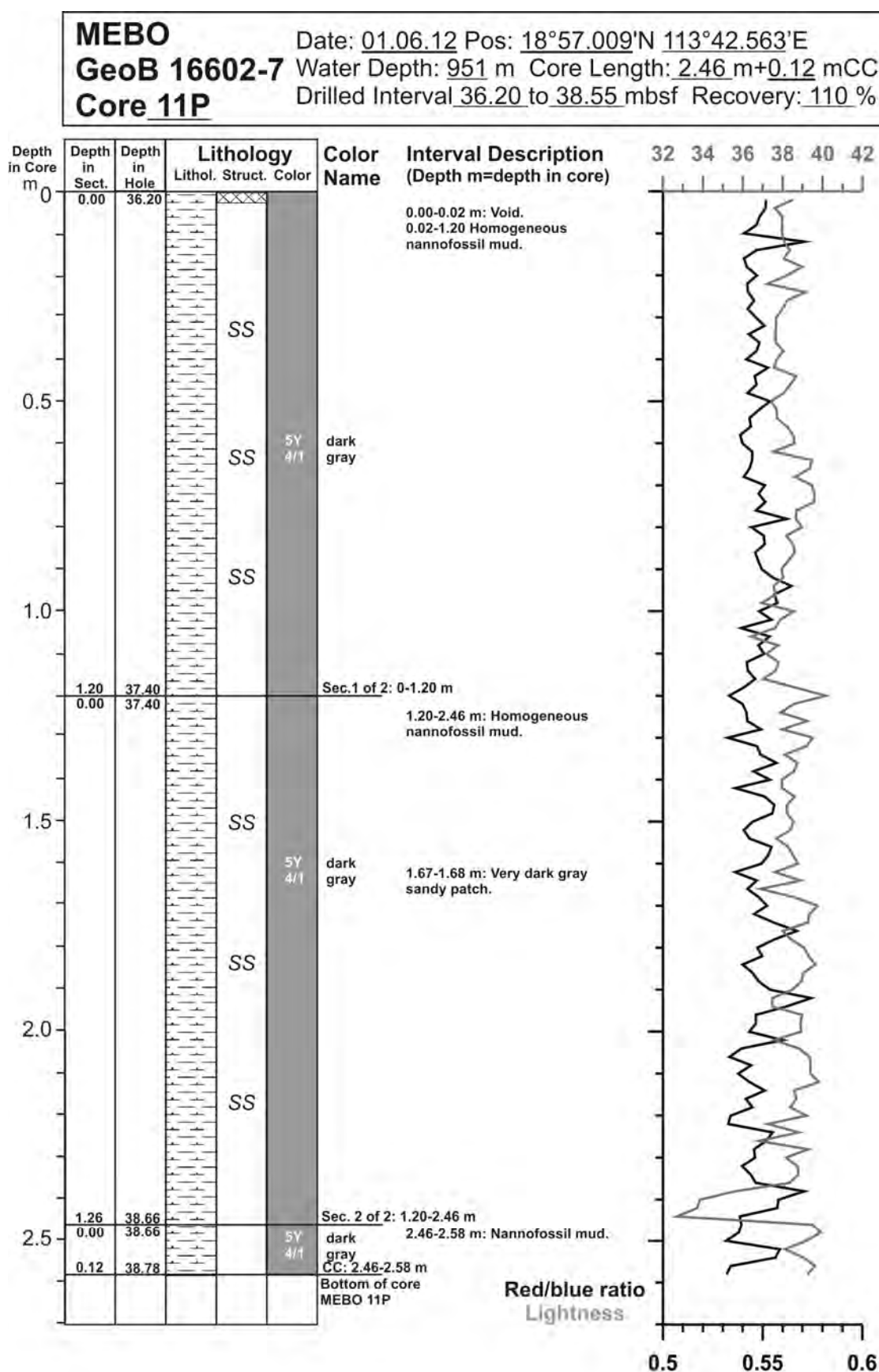


Fig. 10.101: Core description of MeBo core GeoB 16602-7 (11/29).

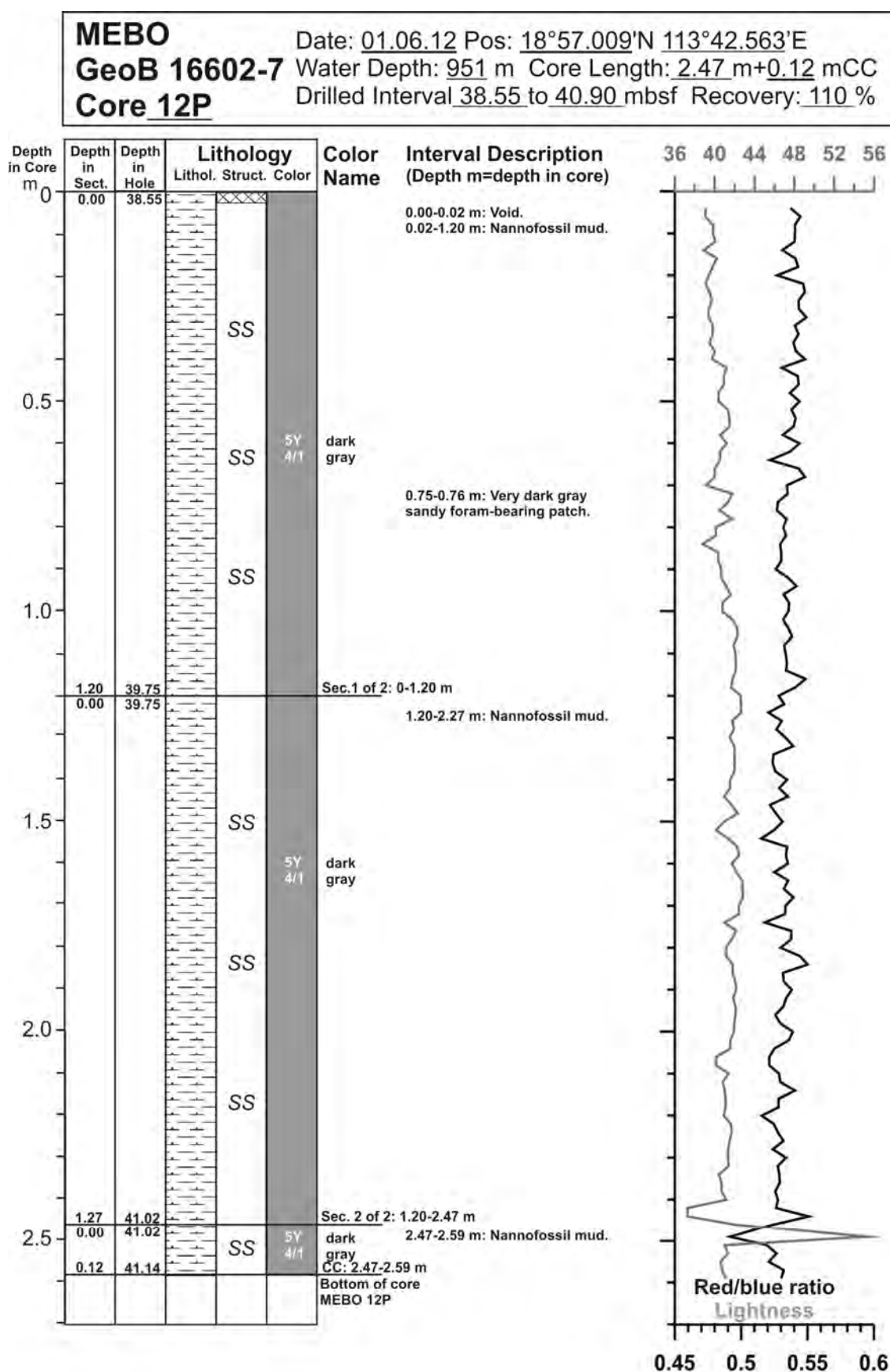


Fig. 10.102: Core description of MeBo core GeoB 16602-7 (12/29).

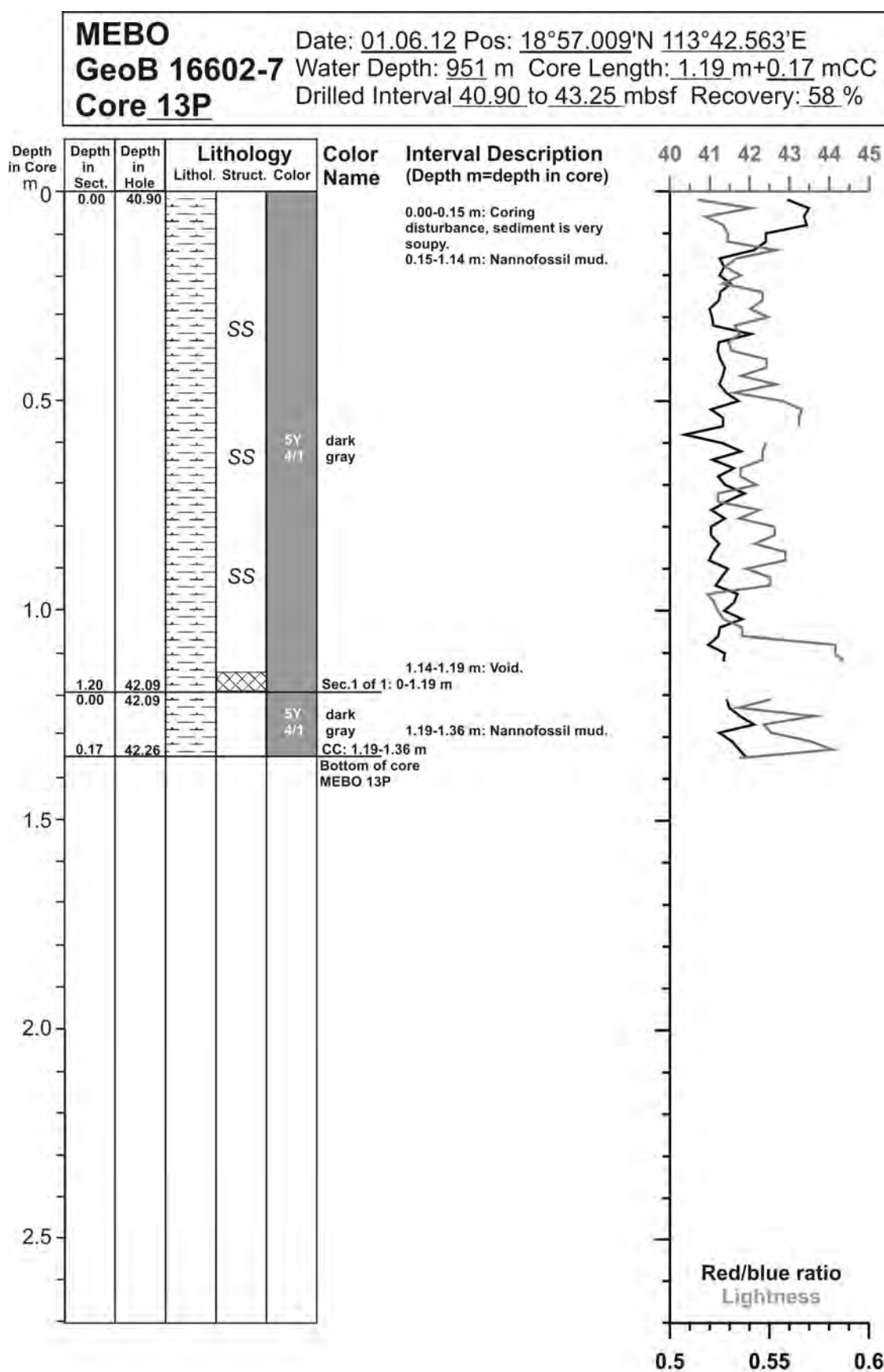


Fig. 10.103: Core description of MeBo core GeoB 16602-7 (13/29).

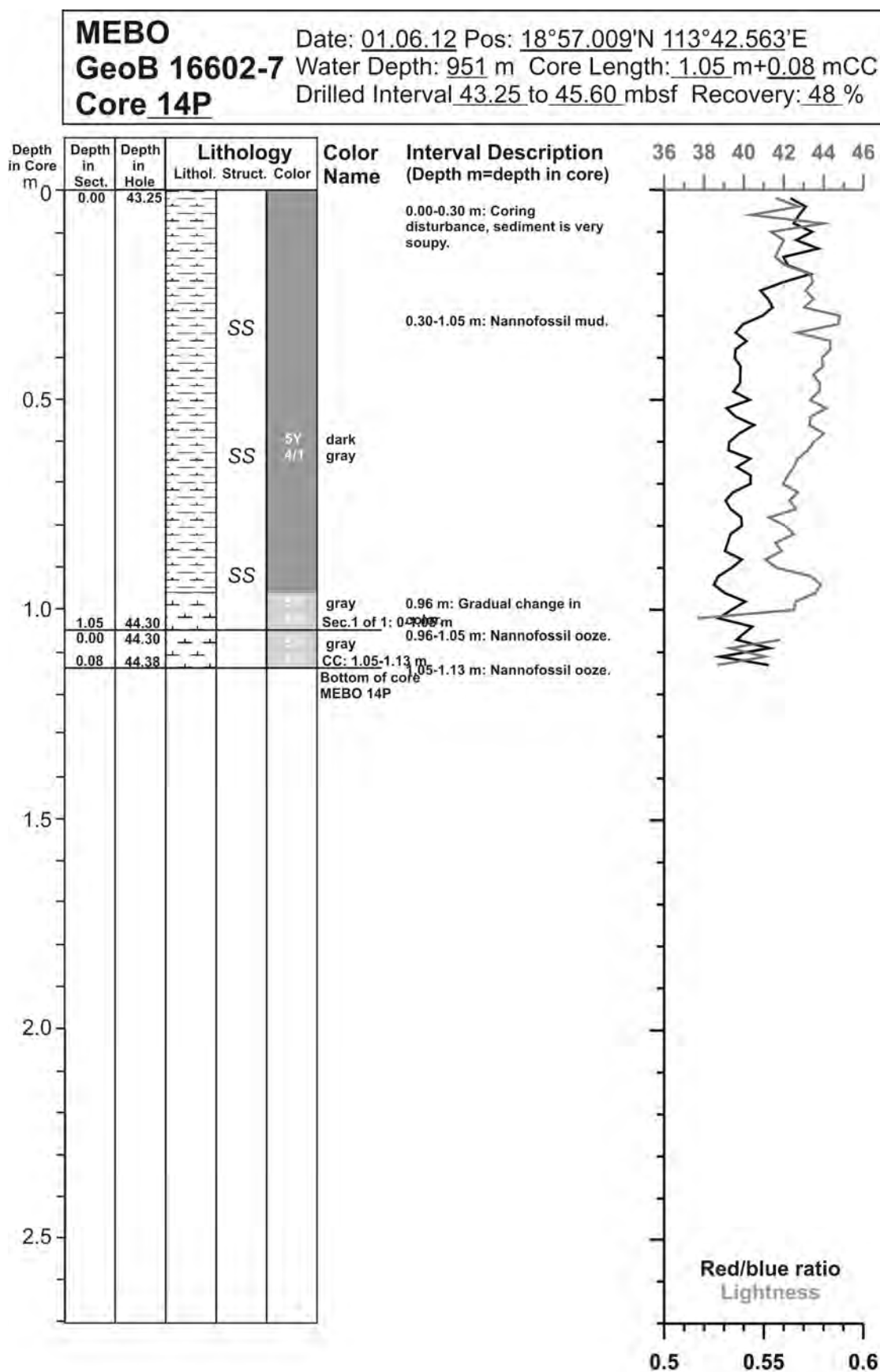


Fig. 10.104: Core description of MeBo core GeoB 16602-7 (14/29).

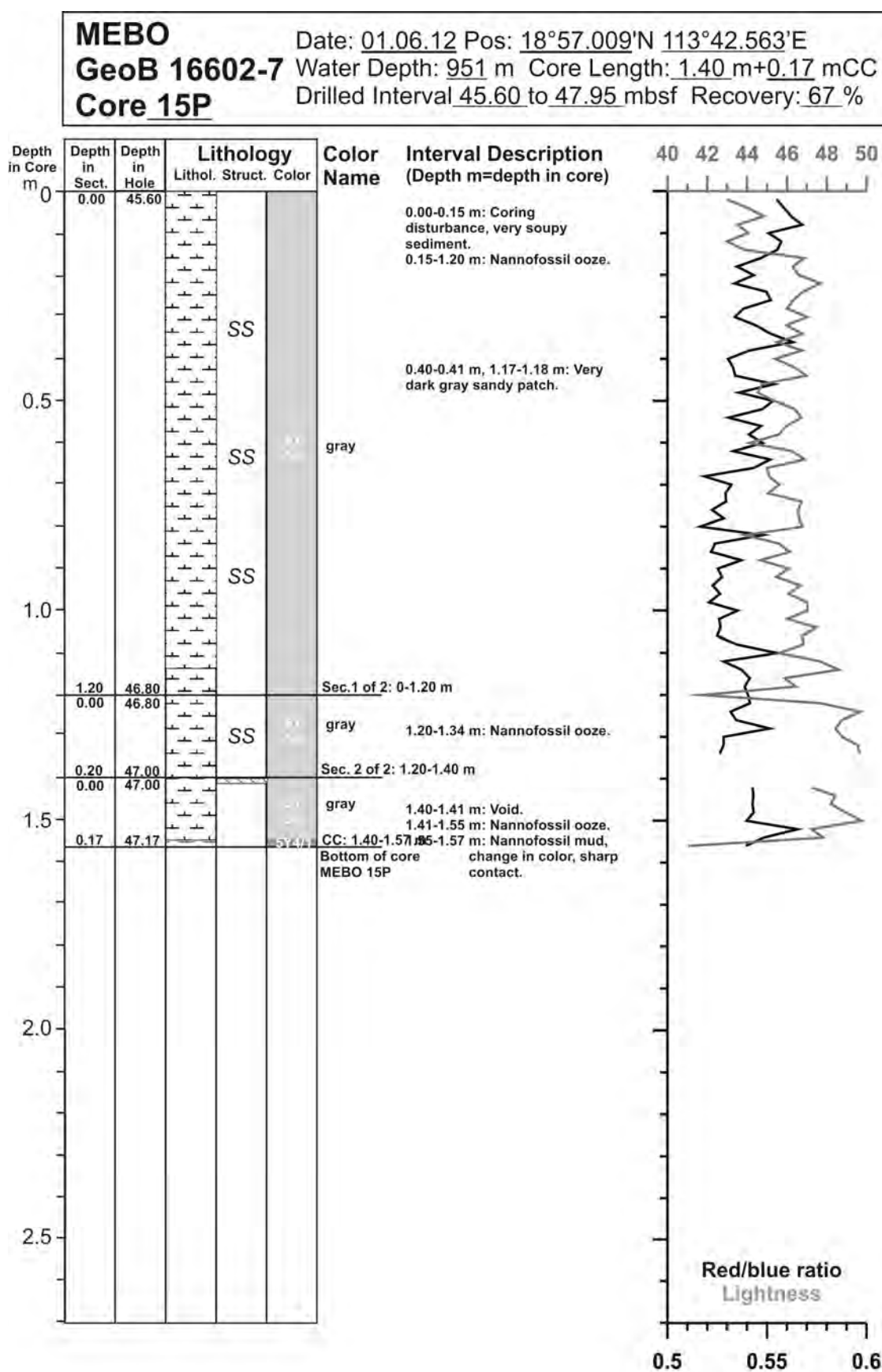


Fig. 10.105: Core description of MeBo core GeoB 16602-7 (15/29).

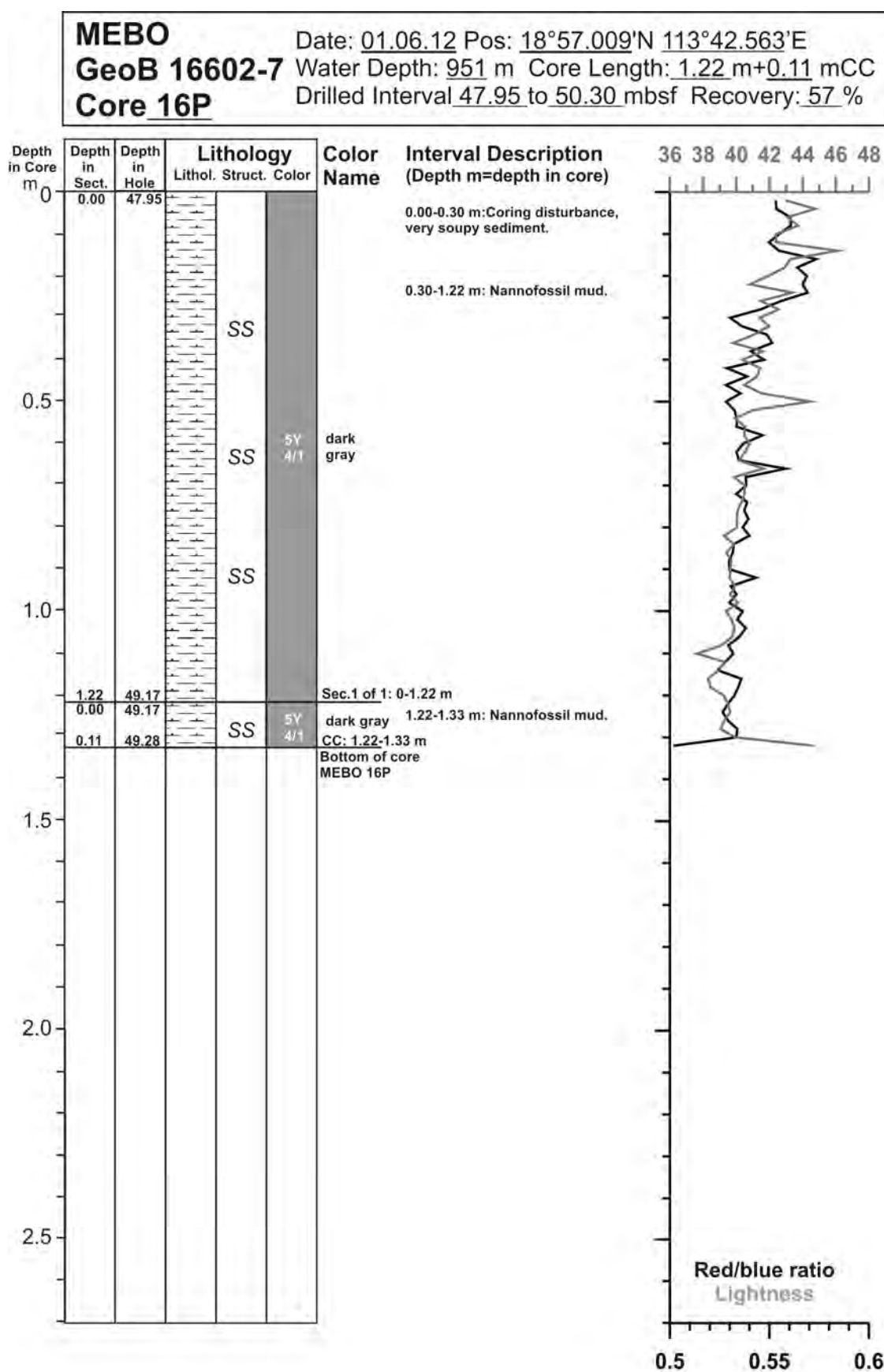


Fig. 10.106: Core description of MeBo core GeoB 16602-7 (16/29).

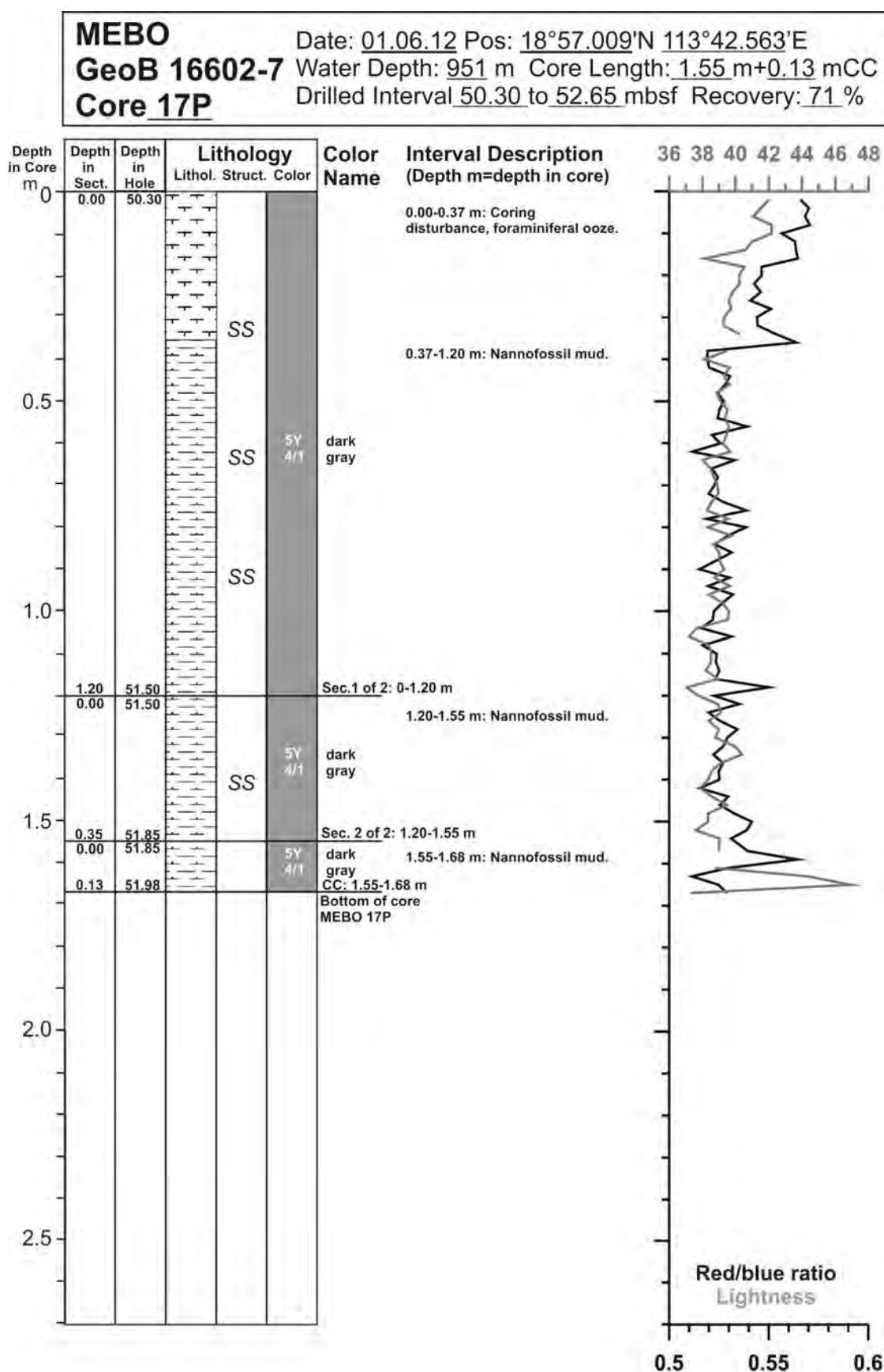


Fig. 10.107: Core description of MeBo core GeoB 16602-7 (17/29).

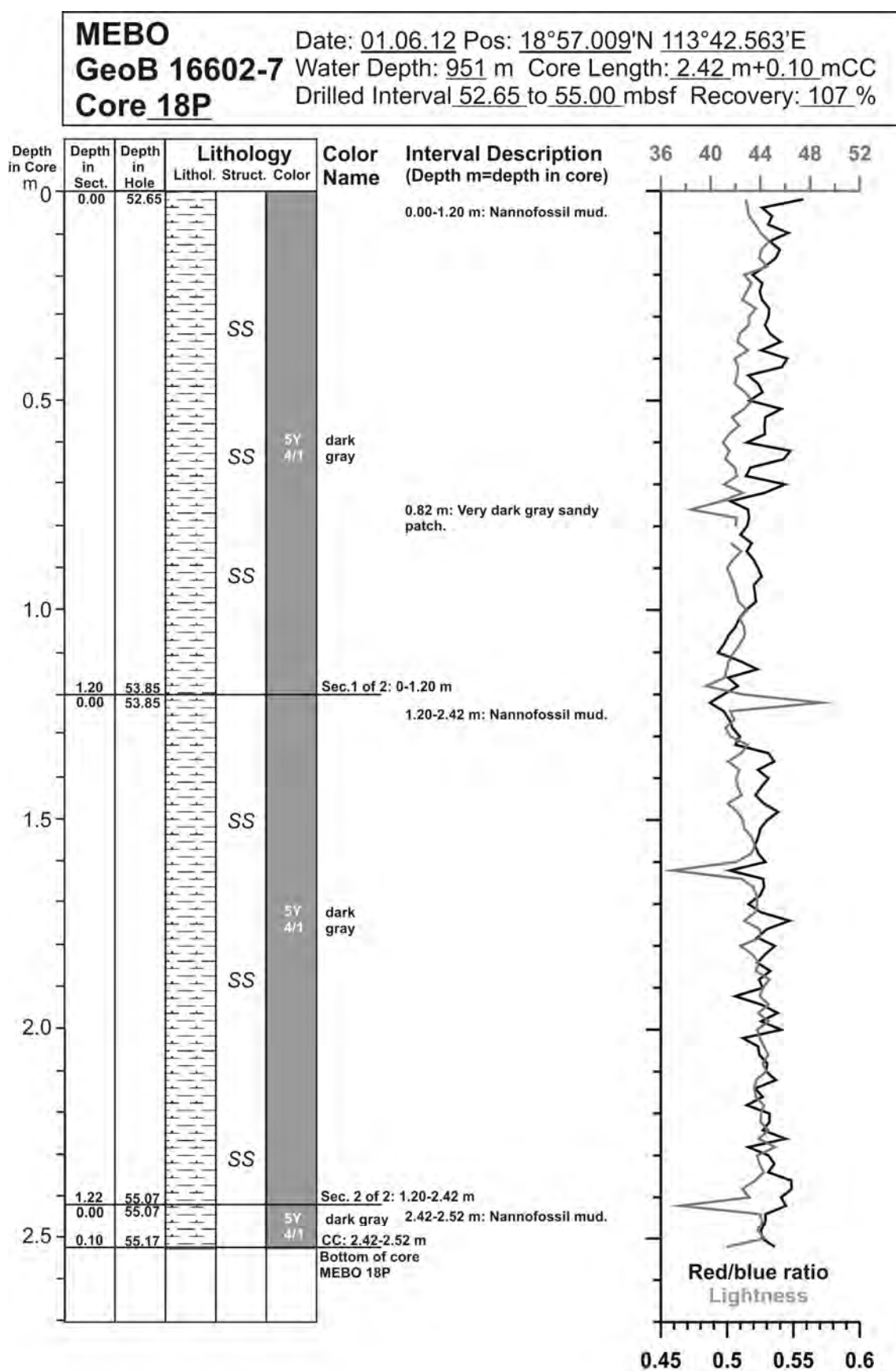


Fig. 10.108: Core description of MeBo core GeoB 16602-7 (18/29).

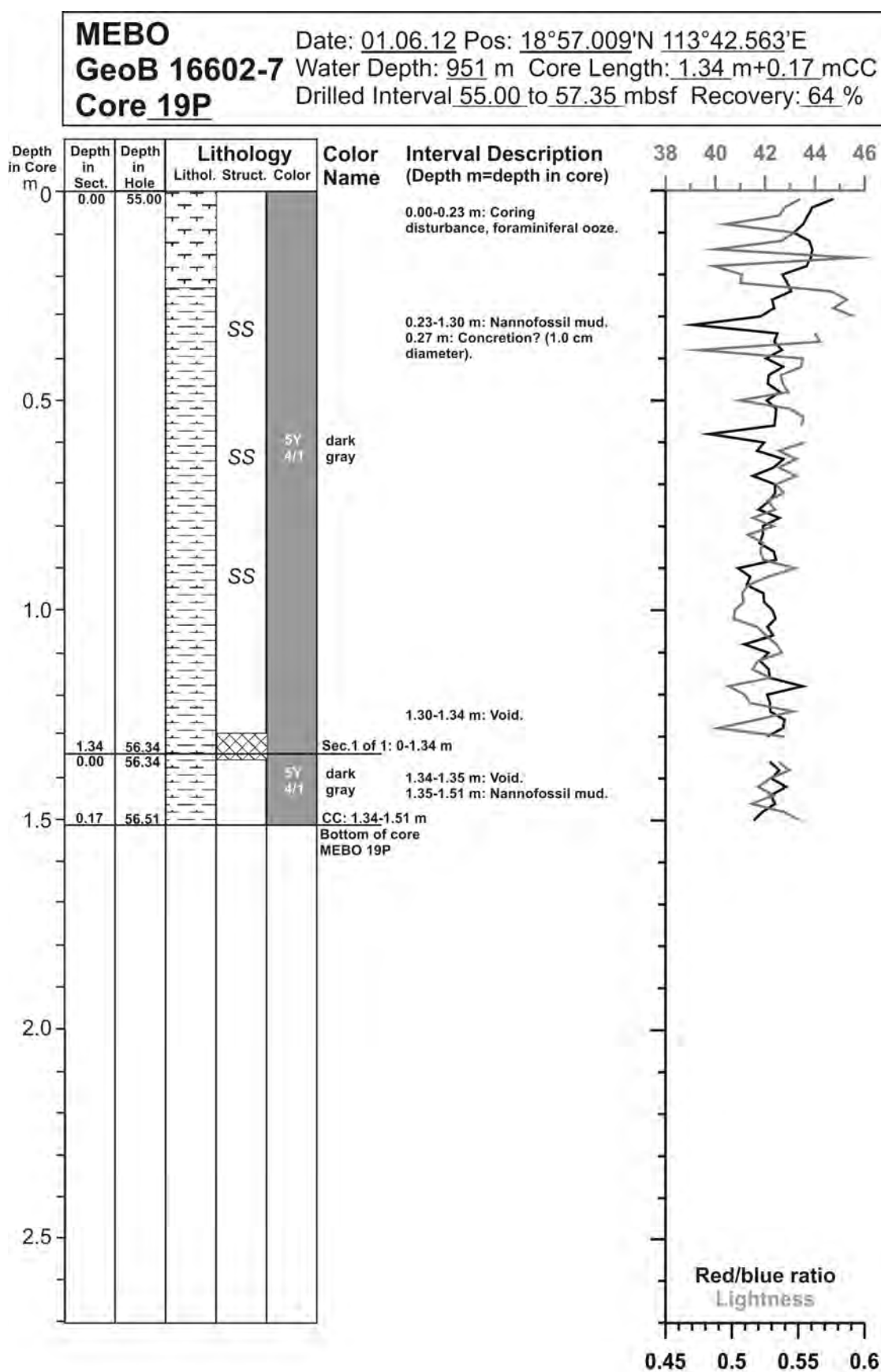


Fig. 10.109: Core description of MeBo core GeoB 16602-7 (19/29).

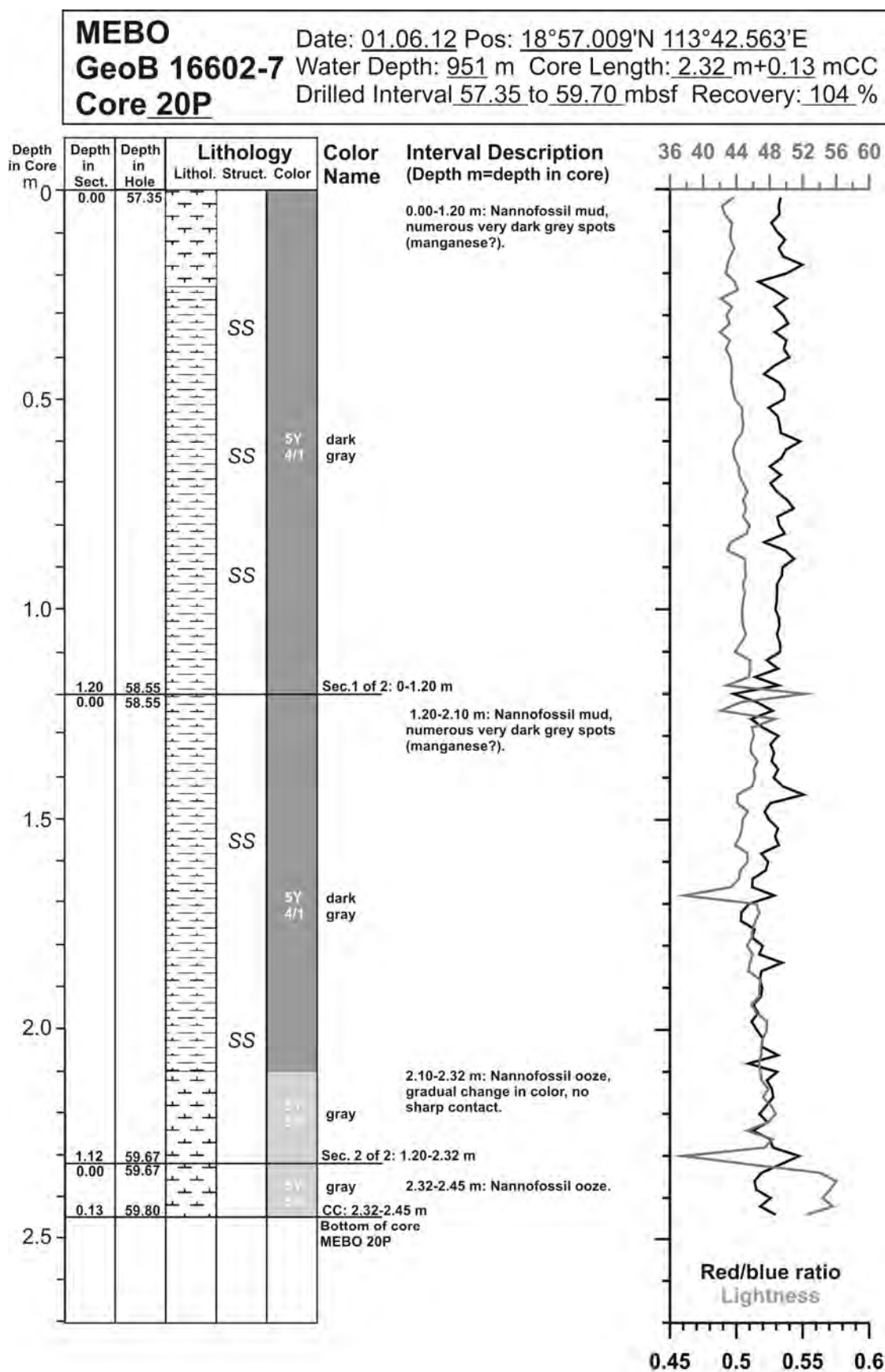


Fig. 10.110: Core description of MeBo core GeoB 16602-7 (20/29).

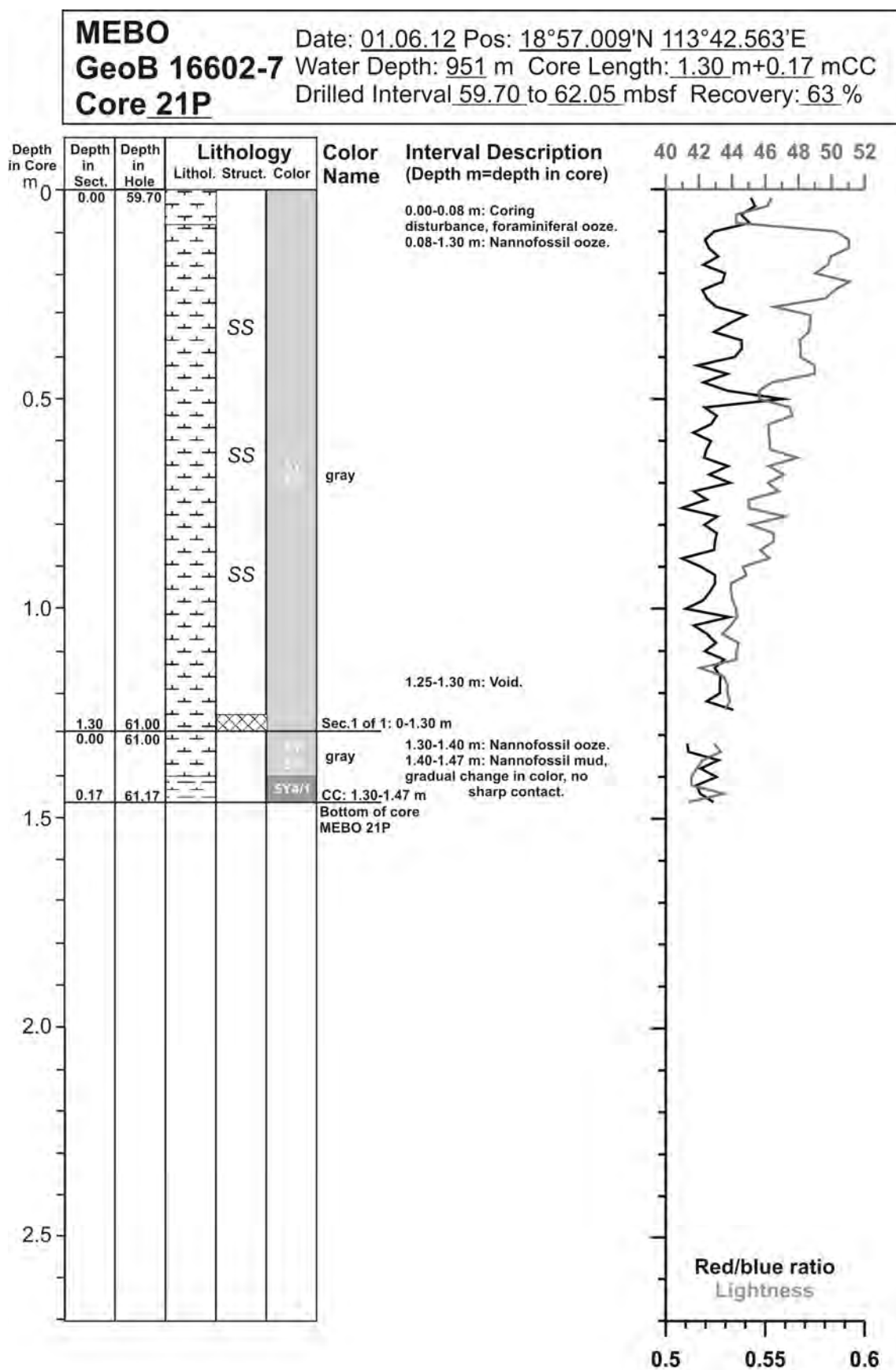


Fig. 10.111: Core description of MeBo core GeoB 16602-7 (21/29).

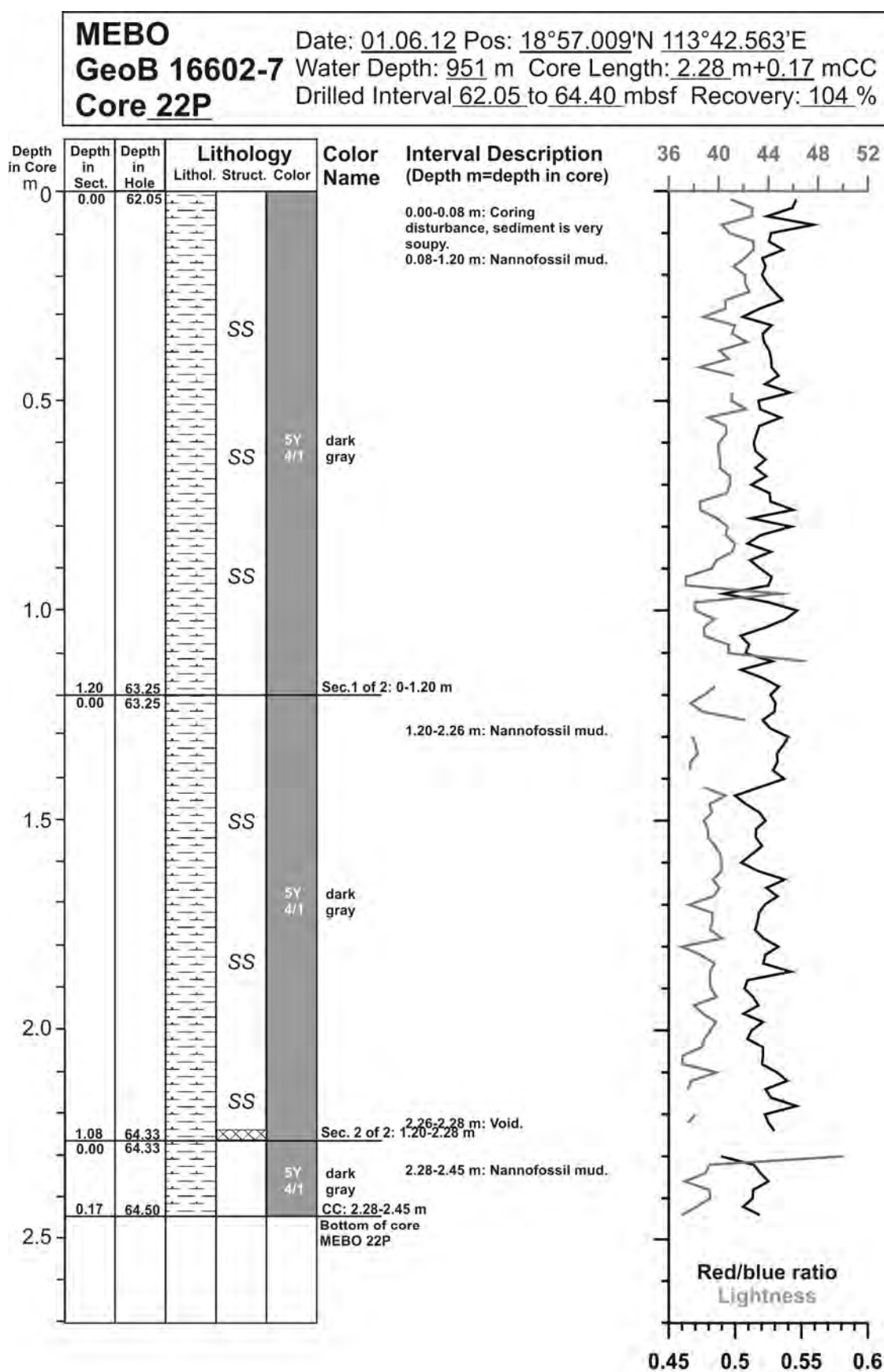


Fig. 10.112: Core description of MeBo core GeoB 16602-7 (22/29).

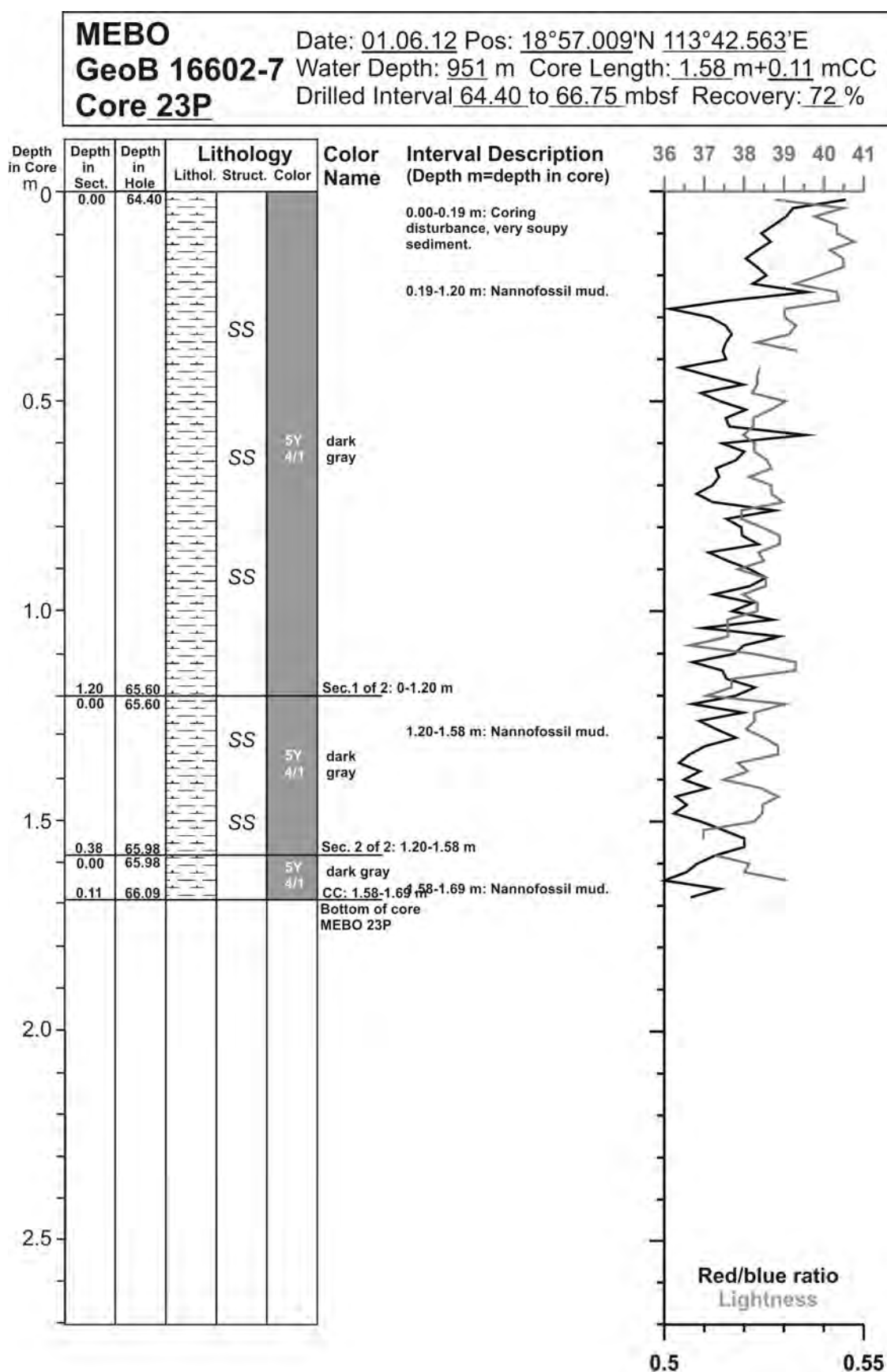


Fig. 10.113: Core description of MeBo core GeoB 16602-7 (23/29).

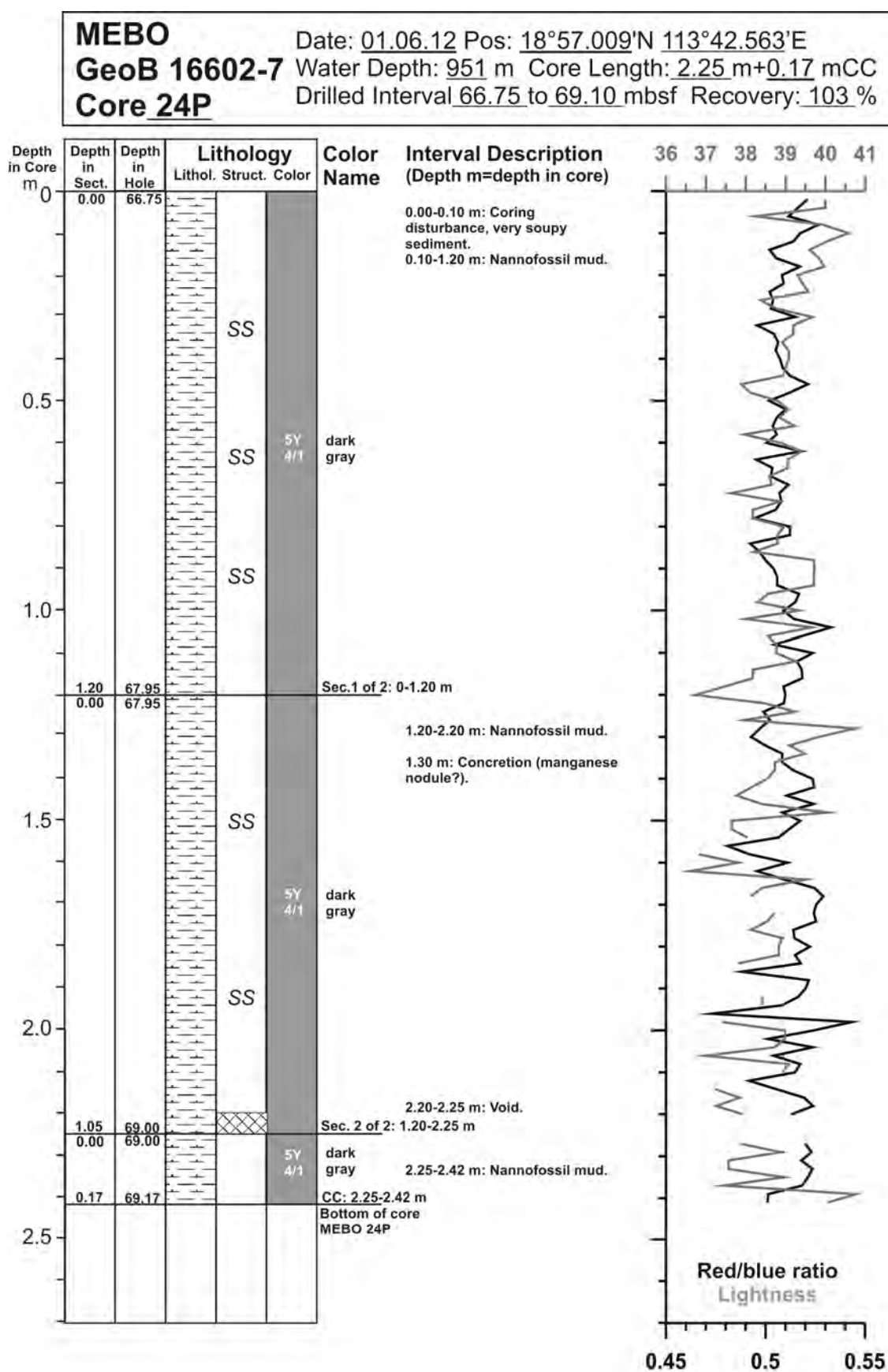


Fig. 10.114: Core description of MeBo core GeoB 16602-7 (24/29).

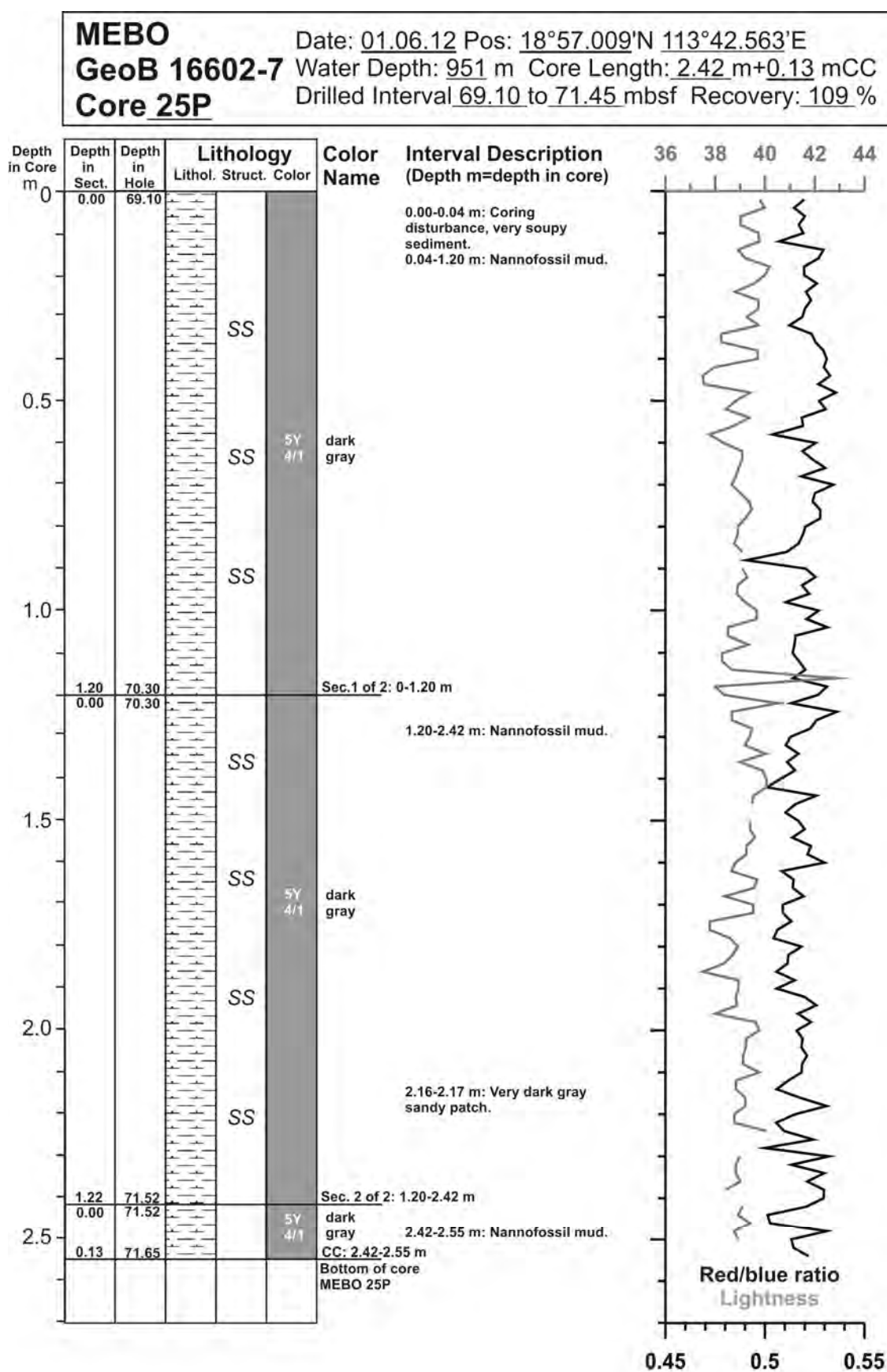


Fig. 10.115: Core description of MeBo core GeoB 16602-7 (25/29).

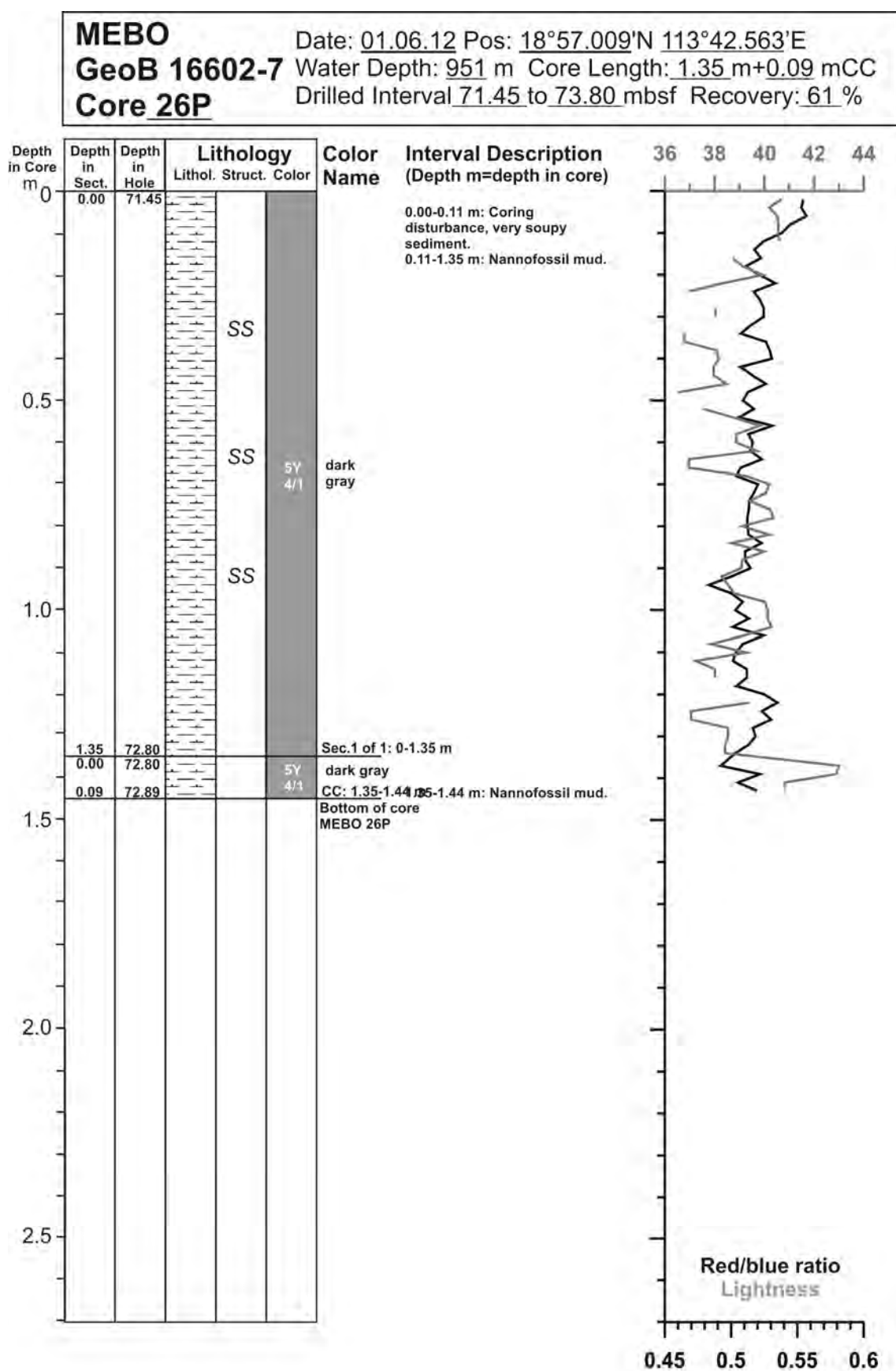


Fig. 10.116: Core description of MeBo core GeoB 16602-7 (26/29).

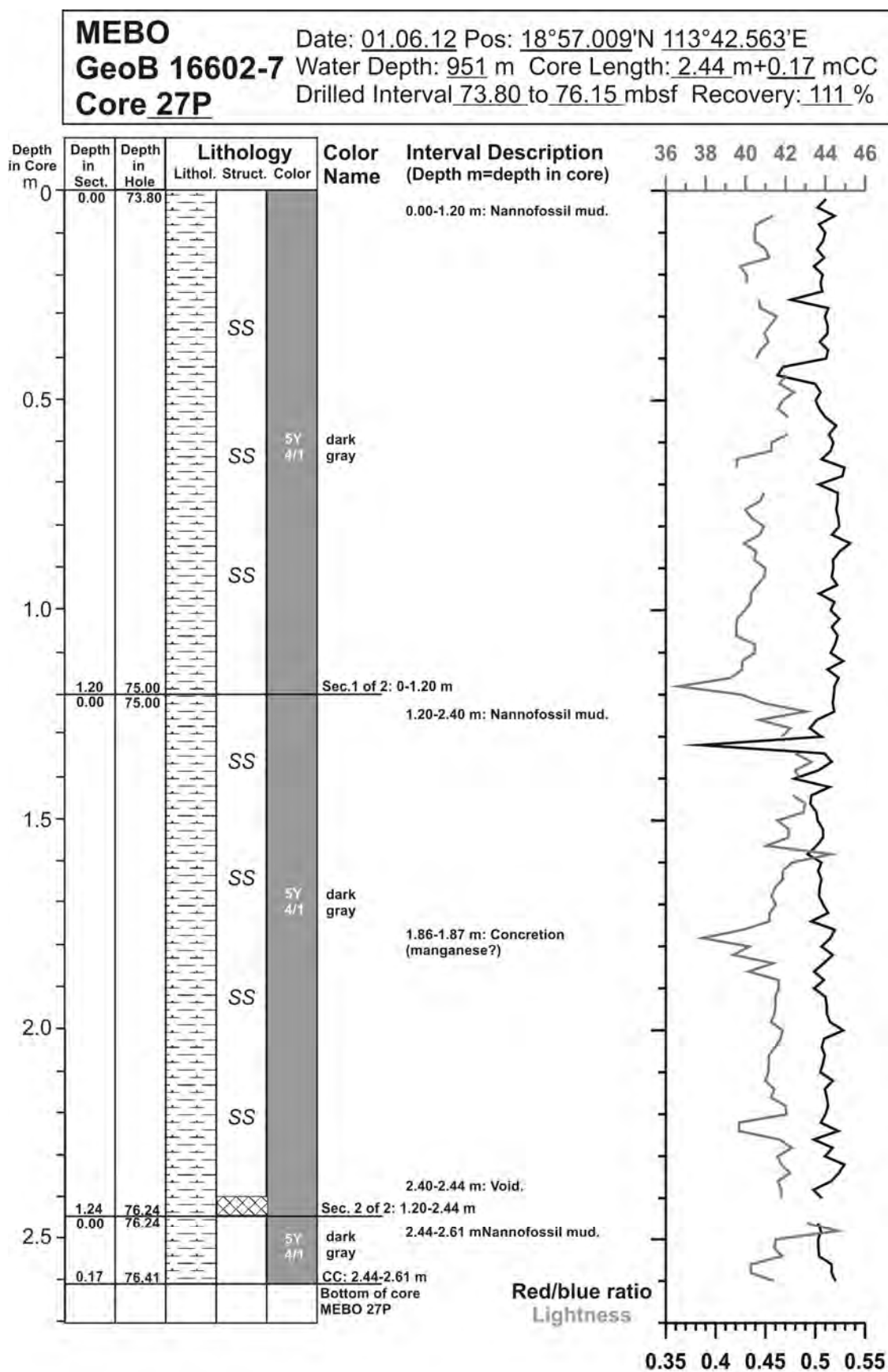


Fig. 10.117: Core description of MeBo core GeoB 16602-7 (27/29).

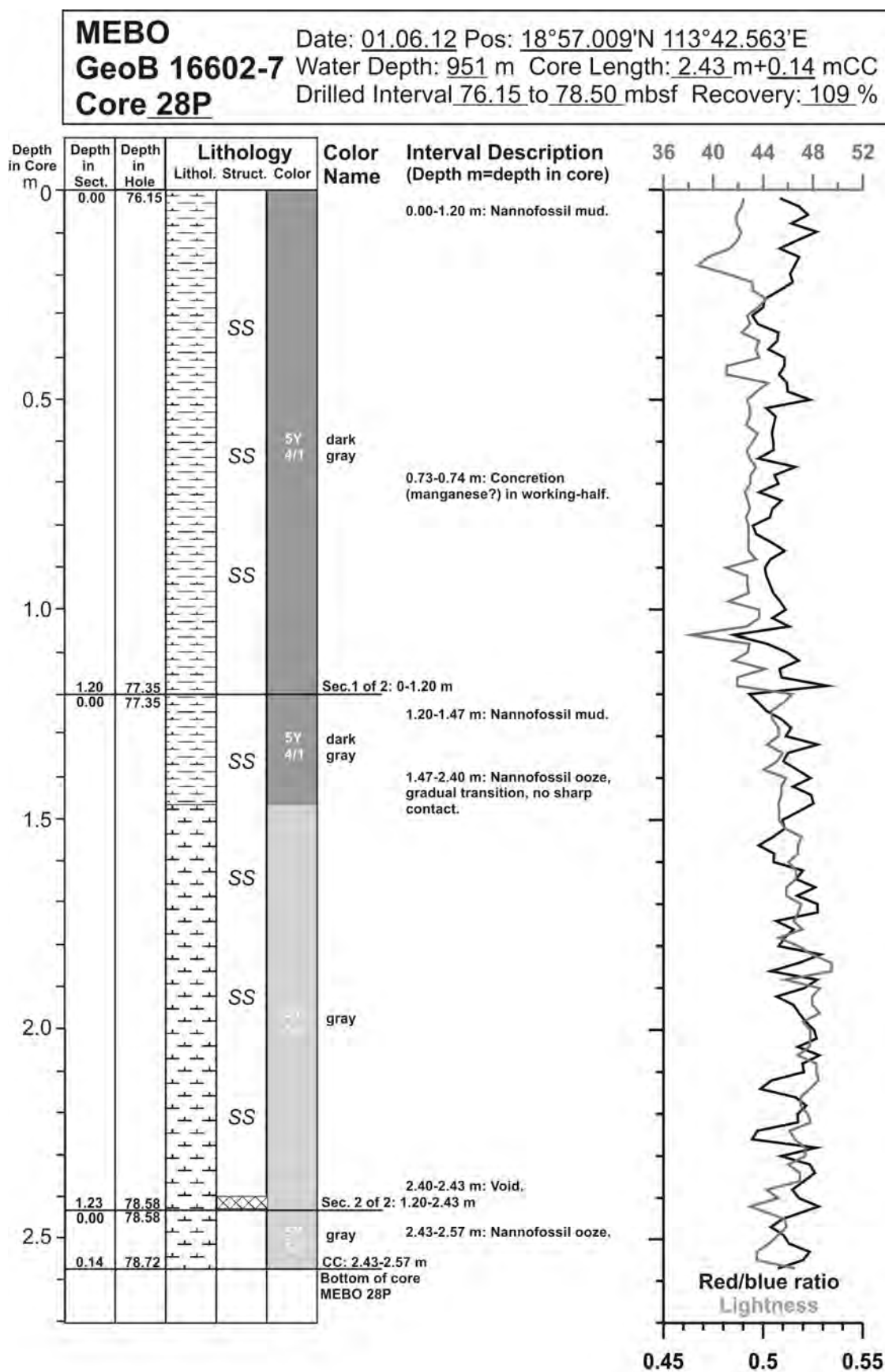


Fig. 10.118: Core description of MeBo core GeoB 16602-7 (28/29).

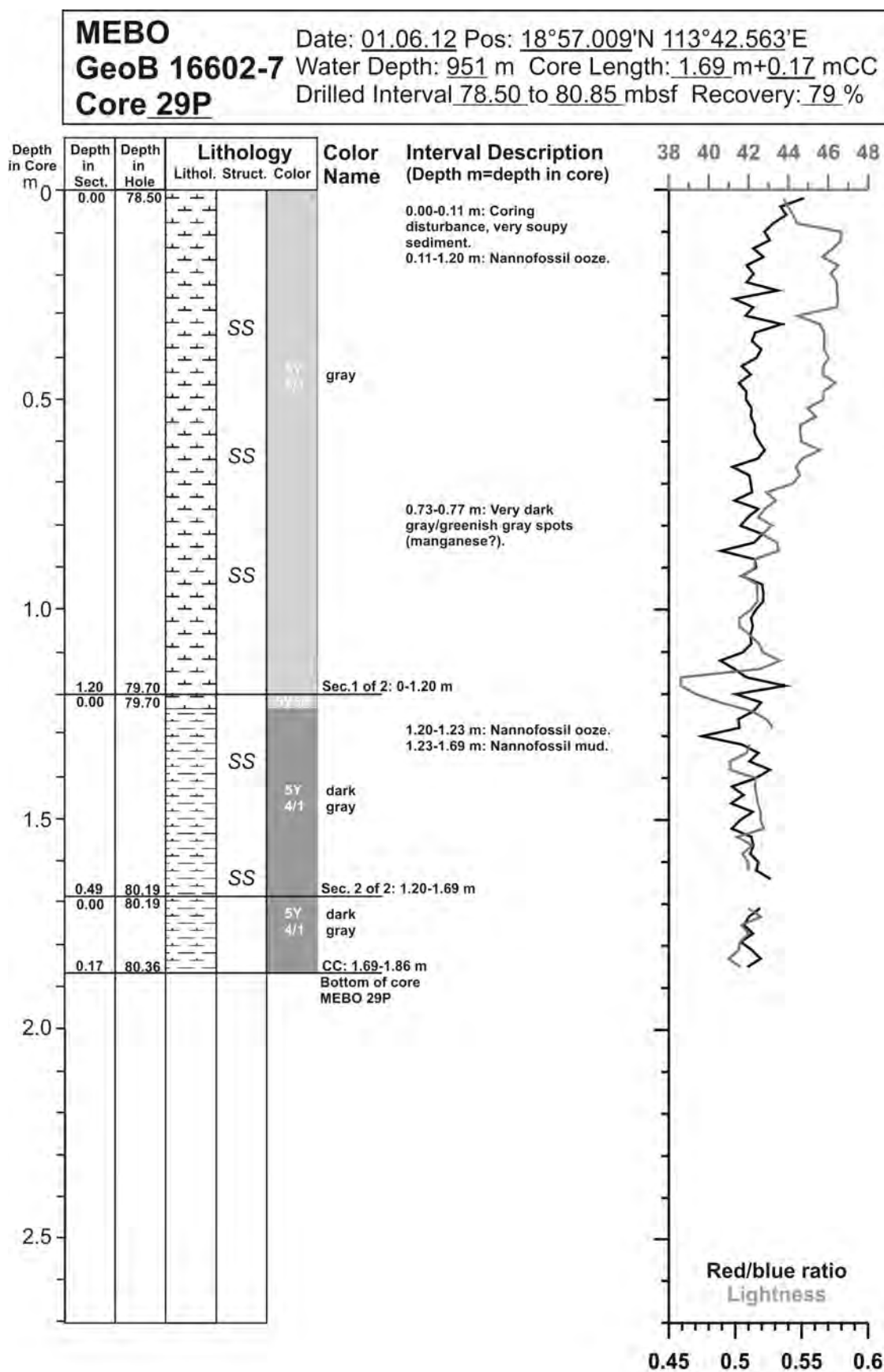


Fig. 10.119: Core description of MeBo core GeoB 16602-7 (29/29).

11 Station list SO-221

MeBo	Deep-Sea Drill Rig	MN	Multi-net	GC corer	Gravity
CTD	CTD and rosette water sampler	MUC	Multi-corer		

Station (GeoB)	Gear	Date	UTC	Latitude (°N)	Longitude (°E)	Water depth (m)	Instrument depth (m)	Remarks
16601-1	MeBo	23.05.2012	02:40	20°09,03′	116°14,38′	1014	Beg. launch	
		24.05.2012	16:44	20°08,82′	116°14,01′	1024	End recovery	
16601-2	CTD	25.05.2012	01:00	20°09,04′	116°14,39′	1024	800	
16601-3	MN	25.05.2012	02:21	20°09,05′	116°14,35′	1016	700	
16601-4	MUC	25.05.2012	04:11	20°09,05′	116°14,38′	1016	bottom	not released
16601-5	MUC	25.05.2012	05:25	20°09,05′	116°14,41′	1016	bottom	10/10
16601-6	GC 12m	25.05.2012	06:50	20°09,07′	116°14,41′	1015	bottom	10,3m
16601-7	MeBo	25.05.2012	10:06	20°09,06′	116°14,41′	1012	Beg. launch	
		27.05.2012	00:33	20°09,02′	116°14,38′	1016	End recovery	
16601-8	MN	27.05.2012	00:34	20°09,02′	116°14,38′	1017	100	
16602-1	CTD	29.05.2012	02:00	18°57,10′	113°42,62′	954	800	
16602-2	MN	29.05.2012	03:31	18°57,11′	113°42,63′	955	700	
16602-3	MUC	29.05.2012	05:18	18°57,11′	113°42,64′	955	bottom	10/10
16602-4	GC 12m	29.05.2012	06:26	18°57,10′	113°42,64′	955	bottom	9,7m
16602-5	MeBo	30.05.2012	00:00	18°57,11′	113°42,63′	951	Beg. launch	
		31.05.2012	08:22	18°57,18′	113°42,64′	952	End recovery	
16602-6	MN	31.05.2012	08:23	18°57,18′	113°42,63′	959	100	
16602-7	MeBo	01.06.2012	00:54	18°57,11′	113°42,55′	954	Beg. launch	
		02.06.2012	10:59	18°57,16′	113°42,57′	952	End recovery	
16602-8	MeBo	03.06.2012	02:00	18°57,09′	113°42,56′	954	Beg. launch	
		04.06.2012	11:21	18°57,20′	113°52,65′	952	End recovery	
16603-1	GC 12m	29.05.2012	08:23	18°55,55′	113°43,33′	980	bottom	9,3m
16603-2	MUC	29.05.2012	08:41	18°55,54′	113°43,29′	979	bottom	not released
16604-1	GC 6m	31.05.2012	12:00	18°39,44′	113°30,66′	912	bottom	tube empty

Publications of this series:

- No. 1** **Wefer, G., E. Suess and cruise participants**
Bericht über die POLARSTERN-Fahrt ANT IV/2, Rio de Janeiro - Punta Arenas, 6.11. - 1.12.1985.
60 pages, Bremen, 1986.
- No. 2** **Hoffmann, G.**
Holozänstratigraphie und Küstenlinienverlagerung an der andalusischen Mittelmeerküste.
173 pages, Bremen, 1988. (out of print)
- No. 3** **Wefer, G. and cruise participants**
Bericht über die METEOR-Fahrt M 6/6, Libreville - Las Palmas, 18.2. - 23.3.1988.
97 pages, Bremen, 1988.
- No. 4** **Wefer, G., G.F. Lutze, T.J. Müller, O. Pfannkuche, W. Schenke, G. Siedler, W. Zenk**
Kurzbericht über die METEOR-Expedition No. 6, Hamburg - Hamburg, 28.10.1987 - 19.5.1988.
29 pages, Bremen, 1988. (out of print)
- No. 5** **Fischer, G.**
Stabile Kohlenstoff-Isotope in partikulärer organischer Substanz aus dem Südpolarmeer
(Atlantischer Sektor). 161 pages, Bremen, 1989.
- No. 6** **Berger, W.H. and G. Wefer**
Partikelfluß und Kohlenstoffkreislauf im Ozean.
Bericht und Kurzfassungen über den Workshop vom 3.-4. Juli 1989 in Bremen.
57 pages, Bremen, 1989.
- No. 7** **Wefer, G. and cruise participants**
Bericht über die METEOR - Fahrt M 9/4, Dakar - Santa Cruz, 19.2. - 16.3.1989.
103 pages, Bremen, 1989.
- No. 8** **Kölling, M.**
Modellierung geochemischer Prozesse im Sickerwasser und Grundwasser.
135 pages, Bremen, 1990.
- No. 9** **Heinze, P.-M.**
Das Auftriebsgeschehen vor Peru im Spätquartär. 204 pages, Bremen, 1990. (out of print)
- No. 10** **Willems, H., G. Wefer, M. Rinski, B. Donner, H.-J. Bellmann, L. Eißmann, A. Müller,
B.W. Flemming, H.-C. Höfle, J. Merkt, H. Streif, G. Hertweck, H. Kuntze, J. Schwaar,
W. Schäfer, M.-G. Schulz, F. Grube, B. Menke**
Beiträge zur Geologie und Paläontologie Norddeutschlands: Exkursionsführer.
202 pages, Bremen, 1990.
- No. 11** **Wefer, G. and cruise participants**
Bericht über die METEOR-Fahrt M 12/1, Kapstadt - Funchal, 13.3.1990 - 14.4.1990.
66 pages, Bremen, 1990.
- No. 12** **Dahmke, A., H.D. Schulz, A. Kölling, F. Kracht, A. Lücke**
Schwermetallspuren und geochemische Gleichgewichte zwischen Porenlösung und Sediment
im Wesermündungsgebiet. BMFT-Projekt MFU 0562, Abschlußbericht. 121 pages, Bremen, 1991.
- No. 13** **Rostek, F.**
Physikalische Strukturen von Tiefseesedimenten des Südatlantiks und ihre Erfassung in
Echolotregistrierungen. 209 pages, Bremen, 1991.
- No. 14** **Baumann, M.**
Die Ablagerung von Tschernobyl-Radiocäsium in der Norwegischen See und in der Nordsee.
133 pages, Bremen, 1991. (out of print)
- No. 15** **Kölling, A.**
Frühdiaagenetische Prozesse und Stoff-Flüsse in marinen und ästuarinen Sedimenten.
140 pages, Bremen, 1991.
- No. 16** **SFB 261 (ed.)**
1. Kolloquium des Sonderforschungsbereichs 261 der Universität Bremen (14.Juni 1991):
Der Südatlantik im Spätquartär: Rekonstruktion von Stoffhaushalt und Stromsystemen.
Kurzfassungen der Vorträge und Poster. 66 pages, Bremen, 1991.
- No. 17** **Pätzold, J. and cruise participants**
Bericht und erste Ergebnisse über die METEOR-Fahrt M 15/2, Rio de Janeiro - Vitoria,
18.1. - 7.2.1991. 46 pages, Bremen, 1993.
- No. 18** **Wefer, G. and cruise participants**
Bericht und erste Ergebnisse über die METEOR-Fahrt M 16/1, Pointe Noire - Recife,
27.3. - 25.4.1991. 120 pages, Bremen, 1991.
- No. 19** **Schulz, H.D. and cruise participants**
Bericht und erste Ergebnisse über die METEOR-Fahrt M 16/2, Recife - Belem, 28.4. - 20.5.1991.
149 pages, Bremen, 1991.

- No. 20 Berner, H.**
Mechanismen der Sedimentbildung in der Fram-Straße, im Arktischen Ozean und in der Norwegischen See. 167 pages, Bremen, 1991.
- No. 21 Schneider, R.**
Spätquartäre Produktivitätsänderungen im östlichen Angola-Becken: Reaktion auf Variationen im Passat-Monsun-Windsystem und in der Advektion des Benguela-Küstenstroms. 198 pages, Bremen, 1991. (out of print)
- No. 22 Hebbeln, D.**
Spätquartäre Stratigraphie und Paläozoo- und Paläobotanographie in der Fram-Straße. 174 pages, Bremen, 1991.
- No. 23 Lücke, A.**
Umsetzungsprozesse organischer Substanz während der Frühdiagenese in ästuarinen Sedimenten. 137 pages, Bremen, 1991.
- No. 24 Wefer, G. and cruise participants**
Bericht und erste Ergebnisse der METEOR-Fahrt M 20/1, Bremen - Abidjan, 18.11.- 22.12.1991. 74 pages, Bremen, 1992.
- No. 25 Schulz, H.D. and cruise participants**
Bericht und erste Ergebnisse der METEOR-Fahrt M 20/2, Abidjan - Dakar, 27.12.1991 - 3.2.1992. 173 pages, Bremen, 1992.
- No. 26 Gingeles, F.**
Zur klimaabhängigen Bildung biogener und terrigener Sedimente und ihrer Veränderung durch die Frühdiagenese im zentralen und östlichen Südatlantik. 202 pages, Bremen, 1992.
- No. 27 Bickert, T.**
Rekonstruktion der spätquartären Bodenwasserzirkulation im östlichen Südatlantik über stabile Isotope benthischer Foraminiferen. 205 pages, Bremen, 1992. (out of print)
- No. 28 Schmidt, H.**
Der Benguela-Strom im Bereich des Walfisch-Rückens im Spätquartär. 172 pages, Bremen, 1992.
- No. 29 Meinecke, G.**
Spätquartäre Oberflächenwassertemperaturen im östlichen äquatorialen Atlantik. 181 pages, Bremen, 1992.
- No. 30 Bathmann, U., U. Bleil, A. Dahmke, P. Müller, A. Nehrkorn, E.-M. Nöthig, M. Olesch, J. Pätzold, H.D. Schulz, V. Smetacek, V. Spieß, G. Wefer, H. Willems**
Bericht des Graduierten Kollegs. Stoff-Flüsse in marinen Geosystemen. Berichtszeitraum Oktober 1990 - Dezember 1992. 396 pages, Bremen, 1992.
- No. 31 Damm, E.**
Frühdiagenetische Verteilung von Schwermetallen in Schlicksedimenten der westlichen Ostsee. 115 pages, Bremen, 1992.
- No. 32 Antia, E.E.**
Sedimentology, Morphodynamics and Facies Association of a mesotidal Barrier Island Shoreface (Spiekeroog, Southern North Sea). 370 pages, Bremen, 1993.
- No. 33 Duinker, J. and G. Wefer (ed.)**
Bericht über den 1. JGOFS-Workshop. 1./2. Dezember 1992 in Bremen. 83 pages, Bremen, 1993.
- No. 34 Kasten, S.**
Die Verteilung von Schwermetallen in den Sedimenten eines stadtbremischen Hafenbeckens. 103 pages, Bremen, 1993.
- No. 35 Spieß, V.**
Digitale Sedimentographie. Neue Wege zu einer hochauflösenden Akustostratigraphie. 199 pages, Bremen, 1993.
- No. 36 Schinzel, U.**
Laborversuche zu frühdiagenetischen Reaktionen von Eisen (III) - Oxidhydraten in marinen Sedimenten. 189 pages, Bremen, 1993.
- No. 37 Sieger, R.**
CoTAM - ein Modell zur Modellierung des Schwermetalltransports in Grundwasserleitern. 56 pages, Bremen, 1993. (out of print)
- No. 38 Willems, H. (ed.)**
Geoscientific Investigations in the Tethyan Himalayas. 183 pages, Bremen, 1993.
- No. 39 Hamer, K.**
Entwicklung von Laborversuchen als Grundlage für die Modellierung des Transportverhaltens von Arsenat, Blei, Cadmium und Kupfer in wassergesättigten Säulen. 147 pages, Bremen, 1993.
- No. 40 Sieger, R.**
Modellierung des Stofftransports in porösen Medien unter Ankopplung kinetisch gesteuerter Sorptions- und Redoxprozesse sowie thermischer Gleichgewichte. 158 pages, Bremen, 1993.

- No. 41 Thießen, W.**
Magnetische Eigenschaften von Sedimenten des östlichen Südatlantiks und ihre paläozoo- und paläogeographische Relevanz. 170 pages, Bremen, 1993.
- No. 42 Spieß, V. and cruise participants**
Report and preliminary results of METEOR-Cruise M 23/1, Kapstadt - Rio de Janeiro, 4.-25.2.1993. 139 pages, Bremen, 1994.
- No. 43 Bleil, U. and cruise participants**
Report and preliminary results of METEOR-Cruise M 23/2, Rio de Janeiro - Recife, 27.2.-19.3.1993. 133 pages, Bremen, 1994.
- No. 44 Wefer, G. and cruise participants**
Report and preliminary results of METEOR-Cruise M 23/3, Recife - Las Palmas, 21.3. - 12.4.1993. 71 pages, Bremen, 1994.
- No. 45 Giese, M. and G. Wefer (ed.)**
Bericht über den 2. JGOFS-Workshop. 18./19. November 1993 in Bremen. 93 pages, Bremen, 1994.
- No. 46 Balzer, W. and cruise participants**
Report and preliminary results of METEOR-Cruise M 22/1, Hamburg - Recife, 22.9. - 21.10.1992. 24 pages, Bremen, 1994.
- No. 47 Stax, R.**
Zyklische Sedimentation von organischem Kohlenstoff in der Japan See: Anzeiger für Änderungen von Paläozoo- und paläogeographie und Paläoklima im Spätkänozoikum. 150 pages, Bremen, 1994.
- No. 48 Skowronek, F.**
Frühdiagenetische Stoff-Flüsse gelöster Schwermetalle an der Oberfläche von Sedimenten des Weser Ästuars. 107 pages, Bremen, 1994.
- No. 49 Dersch-Hansmann, M.**
Zur Klimaentwicklung in Ostasien während der letzten 5 Millionen Jahre: Terrigener Sedimenteintrag in die Japan See (ODP Ausfahrt 128). 149 pages, Bremen, 1994.
- No. 50 Zabel, M.**
Frühdiagenetische Stoff-Flüsse in Oberflächen-Sedimenten des äquatorialen und östlichen Südatlantik. 129 pages, Bremen, 1994.
- No. 51 Bleil, U. and cruise participants**
Report and preliminary results of SONNE-Cruise SO 86, Buenos Aires - Capetown, 22.4. - 31.5.93. 116 pages, Bremen, 1994.
- No. 52 Symposium: The South Atlantic: Present and Past Circulation.**
Bremen, Germany, 15 - 19 August 1994. Abstracts. 167 pages, Bremen, 1994.
- No. 53 Kretzmann, U.B.**
57Fe-Mössbauer-Spektroskopie an Sedimenten - Möglichkeiten und Grenzen. 183 pages, Bremen, 1994.
- No. 54 Bachmann, M.**
Die Karbonatrampe von Organyà im oberen Oberapt und unteren Unterapt (NE-Spanien, Prov. Lerida): Fazies, Zyklus- und Sequenzstratigraphie. 147 pages, Bremen, 1994. (out of print)
- No. 55 Kemle-von Mücke, S.**
Oberflächenwasserstruktur und -zirkulation des Südostatlantiks im Spätquartär. 151 pages, Bremen, 1994.
- No. 56 Petermann, H.**
Magnetotaktische Bakterien und ihre Magnetosome in Oberflächensedimenten des Südatlantiks. 134 pages, Bremen, 1994.
- No. 57 Mulitza, S.**
Spätquartäre Variationen der oberflächennahen Hydrographie im westlichen äquatorialen Atlantik. 97 pages, Bremen, 1994.
- No. 58 Segl, M. and cruise participants**
Report and preliminary results of METEOR-Cruise M 29/1, Buenos-Aires - Montevideo, 17.6. - 13.7.1994. 94 pages, Bremen, 1994.
- No. 59 Bleil, U. and cruise participants**
Report and preliminary results of METEOR-Cruise M 29/2, Montevideo - Rio de Janeiro. 15.7. - 8.8.1994. 153 pages, Bremen, 1994.
- No. 60 Henrich, R. and cruise participants**
Report and preliminary results of METEOR-Cruise M 29/3, Rio de Janeiro - Las Palmas. 11.8. - 5.9.1994. Bremen, 1994. (out of print)

- No. 61 Sagemann, J.**
Saisonale Variationen von Porenwasserprofilen, Nährstoff-Flüssen und Reaktionen in intertidalen Sedimenten des Weser-Ästuars. 110 pages, Bremen, 1994. (out of print)
- No. 62 Giese, M. and G. Wefer**
Bericht über den 3. JGOFS-Workshop. 5./6. Dezember 1994 in Bremen. 84 pages, Bremen, 1995.
- No. 63 Mann, U.**
Genese kretazischer Schwarzschiefer in Kolumbien: Globale vs. regionale/lokale Prozesse. 153 pages, Bremen, 1995. (out of print)
- No. 64 Willems, H., Wan X., Yin J., Dongdui L., Liu G., S. Dürr, K.-U. Gräfe**
The Mesozoic development of the N-Indian passive margin and of the Xigaze Forearc Basin in southern Tibet, China. – Excursion Guide to IGCP 362 Working-Group Meeting "Integrated Stratigraphy". 113 pages, Bremen, 1995. (out of print)
- No. 65 Hünken, U.**
Liefergebiets - Charakterisierung proterozoischer Goldseifen in Ghana anhand von Fluideinschluß - Untersuchungen. 270 pages, Bremen, 1995.
- No. 66 Nyandwi, N.**
The Nature of the Sediment Distribution Patterns in ther Spiekeroog Backbarrier Area, the East Frisian Islands. 162 pages, Bremen, 1995.
- No. 67 Isenbeck-Schröter, M.**
Transportverhalten von Schwermetallkationen und Oxoanionen in wassergesättigten Sanden. - Laborversuche in Säulen und ihre Modellierung -. 182 pages, Bremen, 1995.
- No. 68 Hebbeln, D. and cruise participants**
Report and preliminary results of SONNE-Cruise SO 102, Valparaiso - Valparaiso, 95. 134 pages, Bremen, 1995.
- No. 69 Willems, H. (Sprecher), U.Bathmann, U. Bleil, T. v. Dobeneck, K. Herterich, B.B. Jorgensen, E.-M. Nöthig, M. Olesch, J. Pätzold, H.D. Schulz, V. Smetacek, V. Speiß. G. Wefer**
Bericht des Graduierten-Kollegs Stoff-Flüsse in marine Geosystemen. Berichtszeitraum Januar 1993 - Dezember 1995. 45 & 468 pages, Bremen, 1995.
- No. 70 Giese, M. and G. Wefer**
Bericht über den 4. JGOFS-Workshop. 20./21. November 1995 in Bremen. 60 pages, Bremen, 1996. (out of print)
- No. 71 Meggers, H.**
Pliozän-quartäre Karbonatsedimentation und Paläozeanographie des Nordatlantiks und des Europäischen Nordmeeres - Hinweise aus planktischen Foraminiferengemeinschaften. 143 pages, Bremen, 1996. (out of print)
- No. 72 Teske, A.**
Phylogenetische und ökologische Untersuchungen an Bakterien des oxidativen und reduktiven marinen Schwefelkreislaufs mittels ribosomaler RNA. 220 pages, Bremen, 1996. (out of print)
- No. 73 Andersen, N.**
Biogeochemische Charakterisierung von Sinkstoffen und Sedimenten aus ostatlantischen Produktions-Systemen mit Hilfe von Biomarkern. 215 pages, Bremen, 1996.
- No. 74 Treppke, U.**
Saisonalität im Diatomeen- und Silikoflagellatenfluß im östlichen tropischen und subtropischen Atlantik. 200 pages, Bremen, 1996.
- No. 75 Schüring, J.**
Die Verwendung von Steinkohlebergematerialien im Deponiebau im Hinblick auf die Pyritverwitterung und die Eignung als geochemische Barriere. 110 pages, Bremen, 1996.
- No. 76 Pätzold, J. and cruise participants**
Report and preliminary results of VICTOR HENSEN cruise JOPS II, Leg 6, Fortaleza - Recife, 10.3. - 26.3. 1995 and Leg 8, Vitória - Vitória, 10.4. - 23.4.1995. 87 pages, Bremen, 1996.
- No. 77 Bleil, U. and cruise participants**
Report and preliminary results of METEOR-Cruise M 34/1, Cape Town - Walvis Bay, 3.-26.1.1996. 129 pages, Bremen, 1996.
- No. 78 Schulz, H.D. and cruise participants**
Report and preliminary results of METEOR-Cruise M 34/2, Walvis Bay - Walvis Bay, 29.1.-18.2.96 133 pages, Bremen, 1996.
- No. 79 Wefer, G. and cruise participants**
Report and preliminary results of METEOR-Cruise M 34/3, Walvis Bay - Recife, 21.2.-17.3.1996. 168 pages, Bremen, 1996.

- No. 80** **Fischer, G. and cruise participants**
Report and preliminary results of METEOR-Cruise M 34/4, Recife - Bridgetown, 19.3.-15.4.1996.
105 pages, Bremen, 1996.
- No. 81** **Kulbrok, F.**
Biostratigraphie, Fazies und Sequenzstratigraphie einer Karbonatrampe in den Schichten der Oberkreide und des Alttertiärs Nordost-Ägyptens (Eastern Desert, N'Golf von Suez, Sinai).
153 pages, Bremen, 1996.
- No. 82** **Kasten, S.**
Early Diagenetic Metal Enrichments in Marine Sediments as Documents of Nonsteady-State Depositional Conditions. Bremen, 1996.
- No. 83** **Holmes, M.E.**
Reconstruction of Surface Ocean Nitrate Utilization in the Southeast Atlantic Ocean Based on Stable Nitrogen Isotopes. 113 pages, Bremen, 1996.
- No. 84** **Rühlemann, C.**
Akkumulation von Carbonat und organischem Kohlenstoff im tropischen Atlantik: Spätquartäre Produktivitäts-Variationen und ihre Steuerungsmechanismen. 139 pages, Bremen, 1996.
- No. 85** **Ratmeyer, V.**
Untersuchungen zum Eintrag und Transport lithogener und organischer partikulärer Substanz im östlichen subtropischen Nordatlantik. 154 pages, Bremen, 1996.
- No. 86** **Cepek, M.**
Zeitliche und räumliche Variationen von Coccolithophoriden-Gemeinschaften im subtropischen Ost-Atlantik: Untersuchungen an Plankton, Sinkstoffen und Sedimenten. 156 pages, Bremen, 1996.
- No. 87** **Otto, S.**
Die Bedeutung von gelöstem organischen Kohlenstoff (DOC) für den Kohlenstofffluß im Ozean. 150 pages, Bremen, 1996.
- No. 88** **Hensen, C.**
Frühdiagenetische Prozesse und Quantifizierung benthischer Stoff-Flüsse in Oberflächensedimenten des Südatlantiks. 132 pages, Bremen, 1996.
- No. 89** **Giese, M. and G. Wefer**
Bericht über den 5. JGOFS-Workshop. 27./28. November 1996 in Bremen. 73 pages, Bremen, 1997.
- No. 90** **Wefer, G. and cruise participants**
Report and preliminary results of METEOR-Cruise M 37/1, Lisbon - Las Palmas, 4.-23.12.1996. 79 pages, Bremen, 1997.
- No. 91** **Isenbeck-Schröter, M., E. Bedbur, M. Kofod, B. König, T. Schramm & G. Mattheß**
Occurrence of Pesticide Residues in Water - Assessment of the Current Situation in Selected EU Countries. 65 pages, Bremen 1997.
- No. 92** **Kühn, M.**
Geochemische Folgereaktionen bei der hydrogeothermalen Energiegewinnung. 129 pages, Bremen 1997.
- No. 93** **Determann, S. & K. Herterich**
JGOFS-A6 "Daten und Modelle": Sammlung JGOFS-relevanter Modelle in Deutschland. 26 pages, Bremen, 1997.
- No. 94** **Fischer, G. and cruise participants**
Report and preliminary results of METEOR-Cruise M 38/1, Las Palmas - Recife, 25.1.-1.3.1997, with Appendix: Core Descriptions from METEOR Cruise M 37/1. Bremen, 1997.
- No. 95** **Bleil, U. and cruise participants**
Report and preliminary results of METEOR-Cruise M 38/2, Recife - Las Palmas, 4.3.-14.4.1997. 126 pages, Bremen, 1997.
- No. 96** **Neuer, S. and cruise participants**
Report and preliminary results of VICTOR HENSEN-Cruise 96/1. Bremen, 1997.
- No. 97** **Villinger, H. and cruise participants**
Fahrtbericht SO 111, 20.8. - 16.9.1996. 115 pages, Bremen, 1997.
- No. 98** **Lüning, S.**
Late Cretaceous - Early Tertiary sequence stratigraphy, paleoecology and geodynamics of Eastern Sinai, Egypt. 218 pages, Bremen, 1997.
- No. 99** **Haese, R.R.**
Beschreibung und Quantifizierung frühdiagenetischer Reaktionen des Eisens in Sedimenten des Südatlantiks. 118 pages, Bremen, 1997.

- No. 100 Lührte, R. von**
Verwertung von Bremer Baggergut als Material zur Oberflächenabdichtung von Deponien - Geochemisches Langzeitverhalten und Schwermetall-Mobilität (Cd, Cu, Ni, Pb, Zn). Bremen, 1997.
- No. 101 Ebert, M.**
Der Einfluß des Redoxmilieus auf die Mobilität von Chrom im durchströmten Aquifer. 135 pages, Bremen, 1997.
- No. 102 Krögel, F.**
Einfluß von Viskosität und Dichte des Seewassers auf Transport und Ablagerung von Wattsedimenten (Langeooger Rückseitenwatt, südliche Nordsee). 168 pages, Bremen, 1997.
- No. 103 Kerntopf, B.**
Dinoflagellate Distribution Patterns and Preservation in the Equatorial Atlantic and Offshore North-West Africa. 137 pages, Bremen, 1997.
- No. 104 Breitzke, M.**
Elastische Wellenausbreitung in marinen Sedimenten - Neue Entwicklungen der Ultraschall Sedimentphysik und Sedimentechographie. 298 pages, Bremen, 1997.
- No. 105 Marchant, M.**
Rezente und spätquartäre Sedimentation planktischer Foraminiferen im Peru-Chile Strom. 115 pages, Bremen, 1997.
- No. 106 Habicht, K.S.**
Sulfur isotope fractionation in marine sediments and bacterial cultures. 125 pages, Bremen, 1997.
- No. 107 Hamer, K., R.v. Lührte, G. Becker, T. Felis, S. Keffel, B. Strotmann, C. Waschowitz, M. Kölling, M. Isenbeck-Schröter, H.D. Schulz**
Endbericht zum Forschungsvorhaben 060 des Landes Bremen: Baggergut der Hafengruppe Bremen-Stadt: Modelluntersuchungen zur Schwermetallmobilität und Möglichkeiten der Verwertung von Hafenschlick aus Bremischen Häfen. 98 pages, Bremen, 1997.
- No. 108 Greeff, O.W.**
Entwicklung und Erprobung eines benthischen Landersystemes zur in situ-Bestimmung von Sulfatreduktionsraten mariner Sedimente. 121 pages, Bremen, 1997.
- No. 109 Pätzold, M. und G. Wefer**
Bericht über den 6. JGOFS-Workshop am 4./5.12.1997 in Bremen. Im Anhang: Publikationen zum deutschen Beitrag zur Joint Global Ocean Flux Study (JGOFS), Stand 1/1998. 122 pages, Bremen, 1998.
- No. 110 Landenberger, H.**
CoTReM, ein Multi-Komponenten Transport- und Reaktions-Modell. 142 pages, Bremen, 1998.
- No. 111 Villinger, H. und Fahrtteilnehmer**
Fahrtbericht SO 124, 4.10. - 16.10.199. 90 pages, Bremen, 1997.
- No. 112 Gietl, R.**
Biostratigraphie und Sedimentationsmuster einer nordostägyptischen Karbonatrampe unter Berücksichtigung der Alveolinen-Faunen. 142 pages, Bremen, 1998.
- No. 113 Ziebis, W.**
The Impact of the Thalassinidean Shrimp *Callinassa truncata* on the Geochemistry of permeable, coastal Sediments. 158 pages, Bremen 1998.
- No. 114 Schulz, H.D. and cruise participants**
Report and preliminary results of METEOR-Cruise M 41/1, Málaga - Libreville, 13.2.-15.3.1998. Bremen, 1998.
- No. 115 Völker, D.J.**
Untersuchungen an strömungsbeeinflussten Sedimentationsmustern im Südozean. Interpretation sedimentechographischer Daten und numerische Modellierung. 152 pages, Bremen, 1998.
- No. 116 Schlünz, B.**
Riverine Organic Carbon Input into the Ocean in Relation to Late Quaternary Climate Change. 136 pages, Bremen, 1998.
- No. 117 Kuhnert, H.**
Aufzeichnung des Klimas vor Westaustralien in stabilen Isotopen in Korallenskeletten. 109 pages, Bremen, 1998.
- No. 118 Kirst, G.**
Rekonstruktion von Oberflächenwassertemperaturen im östlichen Südatlantik anhand von Alkenonen. 130 pages, Bremen, 1998.
- No. 119 Dürkoop, A.**
Der Brasil-Strom im Spätquartär: Rekonstruktion der oberflächennahen Hydrographie während der letzten 400 000 Jahre. 121 pages, Bremen, 1998.

- No. 120 Lamy, F.**
Spätquartäre Variationen des terrigenen Sedimenteintrags entlang des chilenischen Kontinentalhangs als Abbild von Klimavariabilität im Milanković- und Sub-Milanković-Zeitbereich. 141 pages, Bremen, 1998.
- No. 121 Neuer, S. and cruise participants**
Report and preliminary results of POSEIDON-Cruise Pos 237/2, Vigo – Las Palmas, 18.3.-31.3.1998. 39 pages, Bremen, 1998
- No. 122 Romero, O.E.**
Marine planktonic diatoms from the tropical and equatorial Atlantic: temporal flux patterns and the sediment record. 205 pages, Bremen, 1998.
- No. 123 Spiess, V. und Fahrtteilnehmer**
Report and preliminary results of RV SONNE Cruise 125, Cochín – Chittagong, 17.10.-17.11.1997. 128 pages, Bremen, 1998.
- No. 124 Arz, H.W.**
Dokumentation von kurzfristigen Klimaschwankungen des Spätquartärs in Sedimenten des westlichen äquatorialen Atlantiks. 96 pages, Bremen, 1998.
- No. 125 Wolff, T.**
Mixed layer characteristics in the equatorial Atlantic during the late Quaternary as deduced from planktonic foraminifera. 132 pages, Bremen, 1998.
- No. 126 Dittert, N.**
Late Quaternary Planktic Foraminifera Assemblages in the South Atlantic Ocean: Quantitative Determination and Preservational Aspects. 165 pages, Bremen, 1998.
- No. 127 Höll, C.**
Kalkige und organisch-wandige Dinoflagellaten-Zysten in Spätquartären Sedimenten des tropischen Atlantiks und ihre palökologische Auswertbarkeit. 121 pages, Bremen, 1998.
- No. 128 Hencke, J.**
Redoxreaktionen im Grundwasser: Etablierung und Verlagerung von Reaktionsfronten und ihre Bedeutung für die Spurenelement-Mobilität. 122 pages, Bremen 1998.
- No. 129 Pätzold, J. and cruise participants**
Report and preliminary results of METEOR-Cruise M 41/3, Vitória, Brasil – Salvador de Bahia, Brasil, 18.4. - 15.5.1998. Bremen, 1999.
- No. 130 Fischer, G. and cruise participants**
Report and preliminary results of METEOR-Cruise M 41/4, Salvador de Bahia, Brasil – Las Palmas, Spain, 18.5. – 13.6.1998. Bremen, 1999.
- No. 131 Schlünz, B. and G. Wefer**
Bericht über den 7. JGOFS-Workshop am 3. und 4.12.1998 in Bremen. Im Anhang: Publikationen zum deutschen Beitrag zur Joint Global Ocean Flux Study (JGOFS), Stand 1/ 1999. 100 pages, Bremen, 1999.
- No. 132 Wefer, G. and cruise participants**
Report and preliminary results of METEOR-Cruise M 42/4, Las Palmas - Las Palmas - Viana do Castelo; 26.09.1998 - 26.10.1998. 104 pages, Bremen, 1999.
- No. 133 Felis, T.**
Climate and ocean variability reconstructed from stable isotope records of modern subtropical corals (Northern Red Sea). 111 pages, Bremen, 1999.
- No. 134 Draschba, S.**
North Atlantic climate variability recorded in reef corals from Bermuda. 108 pages, Bremen, 1999.
- No. 135 Schmieder, F.**
Magnetic Cyclostratigraphy of South Atlantic Sediments. 82 pages, Bremen, 1999.
- No. 136 Rieß, W.**
In situ measurements of respiration and mineralisation processes – Interaction between fauna and geochemical fluxes at active interfaces. 68 pages, Bremen, 1999.
- No. 137 Devey, C.W. and cruise participants**
Report and shipboard results from METEOR-cruise M 41/2, Libreville – Vitoria, 18.3. – 15.4.98. 59 pages, Bremen, 1999.
- No. 138 Wenzhöfer, F.**
Biogeochemical processes at the sediment water interface and quantification of metabolically driven calcite dissolution in deep sea sediments. 103 pages, Bremen, 1999.
- No. 139 Klump, J.**
Biogenic barite as a proxy of paleoproductivity variations in the Southern Peru-Chile Current. 107 pages, Bremen, 1999.

- No. 140** **Huber, R.**
Carbonate sedimentation in the northern Northatlantic since the late pliocene. 103 pages, Bremen, 1999.
- No. 141** **Schulz, H.**
Nitrate-storing sulfur bacteria in sediments of coastal upwelling. 94 pages, Bremen, 1999.
- No. 142** **Mai, S.**
Die Sedimentverteilung im Wattenmeer: ein Simulationsmodell. 114 pages, Bremen, 1999.
- No. 143** **Neuer, S. and cruise participants**
Report and preliminary results of Poseidon Cruise 248, Las Palmas - Las Palmas, 15.2.-26.2.1999. 45 pages, Bremen, 1999.
- No. 144** **Weber, A.**
Schwefelkreislauf in marinen Sedimenten und Messung von in situ Sulfatreduktionsraten. 122 pages, Bremen, 1999.
- No. 145** **Hadeler, A.**
Sorptionenreaktionen im Grundwasser: Unterschiedliche Aspekte bei der Modellierung des Transportverhaltens von Zink. 122 pages, 1999.
- No. 146** **Dierßen, H.**
Zum Kreislauf ausgewählter Spurenmetalle im Südatlantik: Vertikaltransport und Wechselwirkung zwischen Partikeln und Lösung. 167 pages, Bremen, 1999.
- No. 147** **Zühlsdorff, L.**
High resolution multi-frequency seismic surveys at the Eastern Juan de Fuca Ridge Flank and the Cascadia Margin – Evidence for thermally and tectonically driven fluid upflow in marine sediments. 118 pages, Bremen 1999.
- No. 148** **Kinkel, H.**
Living and late Quaternary Coccolithophores in the equatorial Atlantic Ocean: response of distribution and productivity patterns to changing surface water circulation. 183 pages, Bremen, 2000.
- No. 149** **Pätzold, J. and cruise participants**
Report and preliminary results of METEOR Cruise M 44/3, Aqaba (Jordan) - Safaga (Egypt) – Dubá (Saudi Arabia) – Suez (Egypt) - Haifa (Israel), 12.3.-26.3.-2.4.-4.4.1999. 135 pages, Bremen, 2000.
- No. 150** **Schlünz, B. and G. Wefer**
Bericht über den 8. JGOFS-Workshop am 2. und 3.12.1999 in Bremen. Im Anhang: Publikationen zum deutschen Beitrag zur Joint Global Ocean Flux Study (JGOFS), Stand 1/ 2000. 95 pages, Bremen, 2000.
- No. 151** **Schnack, K.**
Biostratigraphie und fazielle Entwicklung in der Oberkreide und im Alttertiär im Bereich der Kharga Schwelle, Westliche Wüste, SW-Ägypten. 142 pages, Bremen, 2000.
- No. 152** **Karwath, B.**
Ecological studies on living and fossil calcareous dinoflagellates of the equatorial and tropical Atlantic Ocean. 175 pages, Bremen, 2000.
- No. 153** **Moustafa, Y.**
Paleoclimatic reconstructions of the Northern Red Sea during the Holocene inferred from stable isotope records of modern and fossil corals and molluscs. 102 pages, Bremen, 2000.
- No. 154** **Villinger, H. and cruise participants**
Report and preliminary results of SONNE-cruise 145-1 Balboa – Talcahuana, 21.12.1999 – 28.01.2000. 147 pages, Bremen, 2000.
- No. 155** **Rusch, A.**
Dynamik der Feinfraktion im Oberflächenhorizont permeabler Schelfsedimente. 102 pages, Bremen, 2000.
- No. 156** **Moos, C.**
Reconstruction of upwelling intensity and paleo-nutrient gradients in the northwest Arabian Sea derived from stable carbon and oxygen isotopes of planktic foraminifera. 103 pages, Bremen, 2000.
- No. 157** **Xu, W.**
Mass physical sediment properties and trends in a Wadden Sea tidal basin. 127 pages, Bremen, 2000.
- No. 158** **Meinecke, G. and cruise participants**
Report and preliminary results of METEOR Cruise M 45/1, Malaga (Spain) - Lissabon (Portugal), 19.05. - 08.06.1999. 39 pages, Bremen, 2000.
- No. 159** **Vink, A.**
Reconstruction of recent and late Quaternary surface water masses of the western subtropical Atlantic Ocean based on calcareous and organic-walled dinoflagellate cysts. 160 pages, Bremen, 2000.
- No. 160** **Willems, H. (Sprecher), U. Bleil, R. Henrich, K. Herterich, B.B. Jørgensen, H.-J. Kuß, M. Olesch, H.D. Schulz, V. Spieß, G. Wefer**
Abschlußbericht des Graduierten-Kollegs Stoff-Flüsse in marine Geosystemen. Zusammenfassung und Berichtszeitraum Januar 1996 - Dezember 2000. 340 pages, Bremen, 2000.

- No. 161 Sprengel, C.**
Untersuchungen zur Sedimentation und Ökologie von Coccolithophoriden im Bereich der Kanarischen Inseln: Saisonale Flussmuster und Karbonatexport. 165 pages, Bremen, 2000.
- No. 162 Donner, B. and G. Wefer**
Bericht über den JGOFS-Workshop am 18.-21.9.2000 in Bremen: Biogeochemical Cycles: German Contributions to the International Joint Global Ocean Flux Study. 87 pages, Bremen, 2000.
- No. 163 Neuer, S. and cruise participants**
Report and preliminary results of Meteor Cruise M 45/5, Bremen – Las Palmas, October 1 – November 3, 1999. 93 pages, Bremen, 2000.
- No. 164 Devey, C. and cruise participants**
Report and preliminary results of Sonne Cruise SO 145/2, Talcahuano (Chile) - Arica (Chile), February 4 – February 29, 2000. 63 pages, Bremen, 2000.
- No. 165 Freudenthal, T.**
Reconstruction of productivity gradients in the Canary Islands region off Morocco by means of sinking particles and sediments. 147 pages, Bremen, 2000.
- No. 166 Adler, M.**
Modeling of one-dimensional transport in porous media with respect to simultaneous geochemical reactions in CoTReM. 147 pages, Bremen, 2000.
- No. 167 Santamarina Cuneo, P.**
Fluxes of suspended particulate matter through a tidal inlet of the East Frisian Wadden Sea (southern North Sea). 91 pages, Bremen, 2000.
- No. 168 Benthien, A.**
Effects of CO₂ and nutrient concentration on the stable carbon isotope composition of C_{37:2} alkenones in sediments of the South Atlantic Ocean. 104 pages, Bremen, 2001.
- No. 169 Lavik, G.**
Nitrogen isotopes of sinking matter and sediments in the South Atlantic. 140 pages, Bremen, 2001.
- No. 170 Budziak, D.**
Late Quaternary monsoonal climate and related variations in paleoproductivity and alkenone-derived sea-surface temperatures in the western Arabian Sea. 114 pages, Bremen, 2001.
- No. 171 Gerhardt, S.**
Late Quaternary water mass variability derived from the pteropod preservation state in sediments of the western South Atlantic Ocean and the Caribbean Sea. 109 pages, Bremen, 2001.
- No. 172 Bleil, U. and cruise participants**
Report and preliminary results of Meteor Cruise M 46/3, Montevideo (Uruguay) – Mar del Plata (Argentina), January 4 – February 7, 2000. Bremen, 2001.
- No. 173 Wefer, G. and cruise participants**
Report and preliminary results of Meteor Cruise M 46/4, Mar del Plata (Argentina) – Salvador da Bahia (Brazil), February 10 – March 13, 2000. With partial results of METEOR cruise M 46/2. 136 pages, Bremen, 2001.
- No. 174 Schulz, H.D. and cruise participants**
Report and preliminary results of Meteor Cruise M 46/2, Recife (Brazil) – Montevideo (Uruguay), December 2 – December 29, 1999. 107 pages, Bremen, 2001.
- No. 175 Schmidt, A.**
Magnetic mineral fluxes in the Quaternary South Atlantic: Implications for the paleoenvironment. 97 pages, Bremen, 2001.
- No. 176 Bruhns, P.**
Crystal chemical characterization of heavy metal incorporation in brick burning processes. 93 pages, Bremen, 2001.
- No. 177 Karius, V.**
Baggergut der Hafengruppe Bremen-Stadt in der Ziegelherstellung. 131 pages, Bremen, 2001.
- No. 178 Adegbie, A. T.**
Reconstruction of paleoenvironmental conditions in Equatorial Atlantic and the Gulf of Guinea Basins for the last 245,000 years. 113 pages, Bremen, 2001.
- No. 179 Spieß, V. and cruise participants**
Report and preliminary results of R/V Sonne Cruise SO 149, Victoria - Victoria, 16.8. - 16.9.2000. 100 pages, Bremen, 2001.
- No. 180 Kim, J.-H.**
Reconstruction of past sea-surface temperatures in the eastern South Atlantic and the eastern South Pacific across Termination I based on the Alkenone Method. 114 pages, Bremen, 2001.

- No. 181** **von Lom-Keil, H.**
Sedimentary waves on the Namibian continental margin and in the Argentine Basin – Bottom flow reconstructions based on high resolution echosounder data. 126 pages, Bremen, 2001.
- No. 182** **Hebbeln, D. and cruise participants**
PUCK: Report and preliminary results of R/V Sonne Cruise SO 156, Valparaiso (Chile) - Talcahuano (Chile), March 29 - May 14, 2001. 195 pages, Bremen, 2001.
- No. 183** **Wendler, J.**
Reconstruction of astronomically-forced cyclic and abrupt paleoecological changes in the Upper Cretaceous Boreal Realm based on calcareous dinoflagellate cysts. 149 pages, Bremen, 2001.
- No. 184** **Volbers, A.**
Planktic foraminifera as paleoceanographic indicators: production, preservation, and reconstruction of upwelling intensity. Implications from late Quaternary South Atlantic sediments. 122 pages, Bremen, 2001.
- No. 185** **Bleil, U. and cruise participants**
Report and preliminary results of R/V METEOR Cruise M 49/3, Montevideo (Uruguay) - Salvador (Brasil), March 9 - April 1, 2001. 99 pages, Bremen, 2001.
- No. 186** **Scheibner, C.**
Architecture of a carbonate platform-to-basin transition on a structural high (Campanian-early Eocene, Eastern Desert, Egypt) – classical and modelling approaches combined. 173 pages, Bremen, 2001.
- No. 187** **Schneider, S.**
Quartäre Schwankungen in Strömungsintensität und Produktivität als Abbild der Wassermassen-Variabilität im äquatorialen Atlantik (ODP Sites 959 und 663): Ergebnisse aus Siltkorn-Analysen. 134 pages, Bremen, 2001.
- No. 188** **Uliana, E.**
Late Quaternary biogenic opal sedimentation in diatom assemblages in Kongo Fan sediments. 96 pages, Bremen, 2002.
- No. 189** **Esper, O.**
Reconstruction of Recent and Late Quaternary oceanographic conditions in the eastern South Atlantic Ocean based on calcareous- and organic-walled dinoflagellate cysts. 130 pages, Bremen, 2001.
- No. 190** **Wendler, I.**
Production and preservation of calcareous dinoflagellate cysts in the modern Arabian Sea. 117 pages, Bremen, 2002.
- No. 191** **Bauer, J.**
Late Cenomanian – Santonian carbonate platform evolution of Sinai (Egypt): stratigraphy, facies, and sequence architecture. 178 pages, Bremen, 2002.
- No. 192** **Hildebrand-Habel, T.**
Die Entwicklung kalkiger Dinoflagellaten im Südatlantik seit der höheren Oberkreide. 152 pages, Bremen, 2002.
- No. 193** **Hecht, H.**
Sauerstoff-Optopoden zur Quantifizierung von Pyritverwitterungsprozessen im Labor- und Langzeit-in-situ-Einsatz. Entwicklung - Anwendung – Modellierung. 130 pages, Bremen, 2002.
- No. 194** **Fischer, G. and cruise participants**
Report and Preliminary Results of RV METEOR-Cruise M49/4, Salvador da Bahia – Halifax, 4.4.-5.5.2001. 84 pages, Bremen, 2002.
- No. 195** **Gröger, M.**
Deep-water circulation in the western equatorial Atlantic: inferences from carbonate preservation studies and silt grain-size analysis. 95 pages, Bremen, 2002.
- No. 196** **Meinecke, G. and cruise participants**
Report of RV POSEIDON Cruise POS 271, Las Palmas - Las Palmas, 19.3.-29.3.2001. 19 pages, Bremen, 2002.
- No. 197** **Meggers, H. and cruise participants**
Report of RV POSEIDON Cruise POS 272, Las Palmas - Las Palmas, 1.4.-14.4.2001. 19 pages, Bremen, 2002. (out of print)
- No. 198** **Gräfe, K.-U.**
Stratigraphische Korrelation und Steuerungsfaktoren Sedimentärer Zyklen in ausgewählten Borealen und Tethyalen Becken des Cenoman/Turon (Oberkreide) Europas und Nordwestafrikas. 197 pages, Bremen, 2002.
- No. 199** **Jahn, B.**
Mid to Late Pleistocene Variations of Marine Productivity in and Terrigenous Input to the Southeast Atlantic. 97 pages, Bremen, 2002.
- No. 200** **Al-Rousan, S.**
Ocean and climate history recorded in stable isotopes of coral and foraminifers from the northern Gulf of Aqaba. 116 pages, Bremen, 2002.

- No. 201** **Azouzi, B.**
Regionalisierung hydraulischer und hydrogeochemischer Daten mit geostatistischen Methoden. 108 pages, Bremen, 2002.
- No. 202** **Spieß, V. and cruise participants**
Report and preliminary results of METEOR Cruise M 47/3, Libreville (Gabun) - Walvis Bay (Namibia), 01.06 - 03.07.2000. 70 pages, Bremen 2002.
- No. 203** **Spieß, V. and cruise participants**
Report and preliminary results of METEOR Cruise M 49/2, Montevideo (Uruguay) - Montevideo, 13.02 - 07.03.2001. 84 pages, Bremen 2002.
- No. 204** **Mollenhauer, G.**
Organic carbon accumulation in the South Atlantic Ocean: Sedimentary processes and glacial/interglacial Budgets. 139 pages, Bremen 2002.
- No. 205** **Spieß, V. and cruise participants**
Report and preliminary results of METEOR Cruise M49/1, Cape Town (South Africa) - Montevideo (Uruguay), 04.01.2001 - 10.02.2001. 57 pages, Bremen, 2003.
- No. 206** **Meier, K.J.S.**
Calcareous dinoflagellates from the Mediterranean Sea: taxonomy, ecology and palaeoenvironmental application. 126 pages, Bremen, 2003.
- No. 207** **Rakic, S.**
Untersuchungen zur Polymorphie und Kristallchemie von Silikaten der Zusammensetzung $\text{Me}_2\text{Si}_2\text{O}_5$ (Me:Na, K). 139 pages, Bremen, 2003.
- No. 208** **Pfeifer, K.**
Auswirkungen frühdiagenetischer Prozesse auf Calcit- und Barytgehalte in marinen Oberflächen-sedimenten. 110 pages, Bremen, 2003.
- No. 209** **Heuer, V.**
Spurenelemente in Sedimenten des Südatlantik. Primärer Eintrag und frühdiagenetische Überprägung. 136 pages, Bremen, 2003.
- No. 210** **Streng, M.**
Phylogenetic Aspects and Taxonomy of Calcareous Dinoflagellates. 157 pages, Bremen 2003.
- No. 211** **Boeckel, B.**
Present and past coccolith assemblages in the South Atlantic: implications for species ecology, carbonate contribution and palaeoceanographic applicability. 157 pages, Bremen, 2003.
- No. 212** **Precht, E.**
Advective interfacial exchange in permeable sediments driven by surface gravity waves and its ecological consequences. 131 pages, Bremen, 2003.
- No. 213** **Frenz, M.**
Grain-size composition of Quaternary South Atlantic sediments and its paleoceanographic significance. 123 pages, Bremen, 2003.
- No. 214** **Meggers, H. and cruise participants**
Report and preliminary results of METEOR Cruise M 53/1, Limassol - Las Palmas - Mindelo, 30.03.2002 - 03.05.2002. 81 pages, Bremen, 2003.
- No. 215** **Schulz, H.D. and cruise participants**
Report and preliminary results of METEOR Cruise M 58/1, Dakar - Las Palmas, 15.04..2003 - 12.05.2003. Bremen, 2003.
- No. 216** **Schneider, R. and cruise participants**
Report and preliminary results of METEOR Cruise M 57/1, Cape Town - Walvis Bay, 20.01. - 08.02.2003. 123 pages, Bremen, 2003.
- No. 217** **Kallmeyer, J.**
Sulfate reduction in the deep Biosphere. 157 pages, Bremen, 2003.
- No. 218** **Røy, H.**
Dynamic Structure and Function of the Diffusive Boundary Layer at the Seafloor. 149 pages, Bremen, 2003.
- No. 219** **Pätzold, J., C. Hübscher and cruise participants**
Report and preliminary results of METEOR Cruise M 52/2&3, Istanbul - Limassol - Limassol, 04.02. - 27.03.2002. Bremen, 2003.
- No. 220** **Zabel, M. and cruise participants**
Report and preliminary results of METEOR Cruise M 57/2, Walvis Bay - Walvis Bay, 11.02. - 12.03.2003. 136 pages, Bremen 2003.
- No. 221** **Salem, M.**
Geophysical investigations of submarine prolongations of alluvial fans on the western side of the Gulf of Aqaba-Red Sea. 100 pages, Bremen, 2003.

- No. 222** **Tilch, E.**
Oszillation von Wattflächen und deren fossiles Erhaltungspotential (Spiekerooger Rückseitenwatt, südliche Nordsee). 137 pages, Bremen, 2003.
- No. 223** **Frisch, U. and F. Kockel**
Der Bremen-Knoten im Strukturnetz Nordwest-Deutschlands. Stratigraphie, Paläogeographie, Strukturgeologie. 379 pages, Bremen, 2004.
- No. 224** **Kolonic, S.**
Mechanisms and biogeochemical implications of Cenomanian/Turonian black shale formation in North Africa: An integrated geochemical, millennial-scale study from the Tarfaya-LaAyoune Basin in SW Morocco. 174 pages, Bremen, 2004. Report online available only.
- No. 225** **Panteleit, B.**
Geochemische Prozesse in der Salz- Süßwasser Übergangszone. 106 pages, Bremen, 2004.
- No. 226** **Seiter, K.**
Regionalisierung und Quantifizierung benthischer Mineralisationsprozesse. 135 pages, Bremen, 2004.
- No. 227** **Bleil, U. and cruise participants**
Report and preliminary results of METEOR Cruise M 58/2, Las Palmas – Las Palmas (Canary Islands, Spain), 15.05. – 08.06.2003. 123 pages, Bremen, 2004.
- No. 228** **Kopf, A. and cruise participants**
Report and preliminary results of SONNE Cruise SO175, Miami - Bremerhaven, 12.11 - 30.12.2003. 218 pages, Bremen, 2004.
- No. 229** **Fabian, M.**
Near Surface Tilt and Pore Pressure Changes Induced by Pumping in Multi-Layered Poroelastic Half-Spaces. 121 pages, Bremen, 2004.
- No. 230** **Segl, M. , and cruise participants**
Report and preliminary results of POSEIDON cruise 304 Galway – Lisbon, 5. – 22. Oct. 2004. 27 pages, Bremen 2004
- No. 231** **Meinecke, G. and cruise participants**
Report and preliminary results of POSEIDON Cruise 296, Las Palmas – Las Palmas, 04.04 – 14.04.2003. 42 pages, Bremen 2005.
- No. 232** **Meinecke, G. and cruise participants**
Report and preliminary results of POSEIDON Cruise 310, Las Palmas – Las Palmas, 12.04 – 26.04.2004. 49 pages, Bremen 2005.
- No. 233** **Meinecke, G. and cruise participants**
Report and preliminary results of METEOR Cruise 58/3, Las Palmas - Ponta Delgada, 11.06 - 24.06.2003. 50 pages, Bremen 2005.
- No. 234** **Feseker, T.**
Numerical Studies on Groundwater Flow in Coastal Aquifers. 219 pages. Bremen 2004.
- No. 235** **Sahling, H. and cruise participants**
Report and preliminary results of R/V POSEIDON Cruise P317/4, Istanbul-Istanbul , 16 October - 4 November 2004. 92 pages, Bremen 2004.
- No. 236** **Meinecke, G. und Fahrtteilnehmer**
Report and preliminary results of POSEIDON Cruise 305, Las Palmas (Spain) - Lisbon (Portugal), October 28th – November 6th, 2004. 43 pages, Bremen 2005.
- No. 237** **Ruhland, G. and cruise participants**
Report and preliminary results of POSEIDON Cruise 319, Las Palmas (Spain) - Las Palmas (Spain), December 6th – December 17th, 2004. 50 pages, Bremen 2005.
- No. 238** **Chang, T.S.**
Dynamics of fine-grained sediments and stratigraphic evolution of a back-barrier tidal basin of the German Wadden Sea (southern North Sea). 102 pages, Bremen 2005.
- No. 239** **Lager, T.**
Predicting the source strength of recycling materials within the scope of a seepage water prognosis by means of standardized laboratory methods. 141 pages, Bremen 2005.
- No. 240** **Meinecke, G.**
DOLAN - Operationelle Datenübertragung im Ozean und Laterales Akustisches Netzwerk in der Tiefsee. Abschlußbericht. 42 pages, Bremen 2005.
- No. 241** **Guasti, E.**
Early Paleogene environmental turnover in the southern Tethys as recorded by foraminiferal and organic-walled dinoflagellate cysts assemblages. 203 pages, Bremen 2005.
- No. 242** **Riedinger, N.**
Preservation and diagenetic overprint of geochemical and geophysical signals in ocean margin sediments related to depositional dynamics. 91 pages, Bremen 2005.

- No. 243 Ruhland, G. and cruise participants**
Report and preliminary results of POSEIDON cruise 320, Las Palmas (Spain) - Las Palmas (Spain), March 08th - March 18th, 2005. 57 pages, Bremen 2005.
- No. 244 Inthorn, M.**
Lateral particle transport in nepheloid layers – a key factor for organic matter distribution and quality in the Benguela high-productivity area. 127 pages, Bremen, 2006.
- No. 245 Aspetsberger, F.**
Benthic carbon turnover in continental slope and deep sea sediments: importance of organic matter quality at different time scales. 136 pages, Bremen, 2006.
- No. 246 Hebbeln, D. and cruise participants**
Report and preliminary results of RV SONNE Cruise SO-184, PABESIA, Durban (South Africa) – Cilacap (Indonesia) – Darwin (Australia), July 08th - September 13th, 2005. 142 pages, Bremen 2006.
- No. 247 Ratmeyer, V. and cruise participants**
Report and preliminary results of RV METEOR Cruise M61/3. Development of Carbonate Mounds on the Celtic Continental Margin, Northeast Atlantic. Cork (Ireland) – Ponta Delgada (Portugal), 04.06. – 21.06.2004. 64 pages, Bremen 2006.
- No. 248 Wien, K.**
Element Stratigraphy and Age Models for Pelagites and Gravity Mass Flow Deposits based on Shipboard XRF Analysis. 100 pages, Bremen 2006.
- No. 249 Krastel, S. and cruise participants**
Report and preliminary results of RV METEOR Cruise M65/2, Dakar - Las Palmas, 04.07. – 26.07.2005. 185 pages, Bremen 2006.
- No. 250 Heil, G.M.N.**
Abrupt Climate Shifts in the Western Tropical to Subtropical Atlantic Region during the Last Glacial. 121 pages, Bremen 2006.
- No. 251 Ruhland, G. and cruise participants**
Report and preliminary results of POSEIDON Cruise 330, Las Palmas – Las Palmas, November 21th – December 03rd, 2005. 48 pages, Bremen 2006.
- No. 252 Mulitza, S. and cruise participants**
Report and preliminary results of METEOR Cruise M65/1, Dakar – Dakar, 11.06.- 1.07.2005. 149 pages, Bremen 2006.
- No. 253 Kopf, A. and cruise participants**
Report and preliminary results of POSEIDON Cruise P336, Heraklion - Heraklion, 28.04. – 17.05.2006. 127 pages, Bremen, 2006.
- No. 254 Wefer, G. and cruise participants**
Report and preliminary results of R/V METEOR Cruise M65/3, Las Palmas - Las Palmas (Spain), July 31st - August 10th, 2005. 24 pages, Bremen 2006.
- No. 255 Hanebuth, T.J.J. and cruise participants**
Report and first results of the POSEIDON Cruise P342 GALIOMAR, Vigo – Lisboa (Portugal), August 19th – September 06th, 2006. Distribution Pattern, Residence Times and Export of Sediments on the Pleistocene/Holocene Galician Shelf (NW Iberian Peninsula). 203 pages, Bremen, 2007.
- No. 256 Ahke, A.**
Composition of molecular organic matter pools, pigments and proteins, in Benguela upwelling and Arctic Sediments. 192 pages, Bremen 2007.
- No. 257 Becker, V.**
Seeper - Ein Modell für die Praxis der Sickerwasserprognose. 170 pages, Bremen 2007.
- No. 258 Ruhland, G. and cruise participants**
Report and preliminary results of Poseidon cruise 333, Las Palmas (Spain) – Las Palmas (Spain), March 1st – March 10th, 2006. 32 pages, Bremen 2007.
- No. 259 Fischer, G., G. Ruhland and cruise participants**
Report and preliminary results of Poseidon cruise 344, leg 1 and leg 2, Las Palmas (Spain) – Las Palmas (Spain), Oct. 20th – Nov 2nd & Nov. 4th – Nov 13th, 2006. 46 pages, Bremen 2007.
- No. 260 Westphal, H. and cruise participants**
Report and preliminary results of Poseidon cruise 346, MACUMA. Las Palmas (Spain) – Las Palmas (Spain), 28.12.2006 – 15.1.2007. 49 pages, Bremen 2007.
- No. 261 Bohrmann, G., T. Pape, and cruise participants**
Report and preliminary results of R/V METEOR Cruise M72/3, Istanbul – Trabzon – Istanbul, March 17th – April 23rd, 2007. Marine gas hydrates of the Eastern Black Sea. 130 pages, Bremen 2007.
- No. 262 Bohrmann, G., and cruise participants**
Report and preliminary results of R/V METEOR Cruise M70/3, Iraklion – Iraklion, 21 November – 8 December 2006. Cold Seeps of the Anaximander Mountains / Eastern Mediterranean. 75 pages, Bremen 2008.

- No. 263 Bohrmann, G., Spiess, V., and cruise participants**
Report and preliminary results of R/V Meteor Cruise M67/2a and 2b, Balboa -- Tampico -- Bridgetown, 15 March -- 24 April, 2006. Fluid seepage in the Gulf of Mexico. Bremen 2008.
- No. 264 Kopf, A., and cruise participants**
Report and preliminary results of Meteor Cruise M73/1: LIMA-LAMO (Ligurian Margin Landslide Measurements & Observatory), Cadiz, 22.07.2007 – Genoa, 11.08.2007. 170 pages, Bremen 2008.
- No. 265 Hebbeln, D., and cruise participants**
Report and preliminary results of RV Pelagia Cruise 64PE284. Cold-water Corals in the Gulf of Cádiz and on Coral Patch Seamount (NE Atlantic). Portimão - Portimão, 18.02. - 09.03.2008. 90 pages, Bremen 2008.
- No. 266 Bohrmann, G. and cruise participants**
Report and preliminary results of R/V Meteor Cruise M74/3, Fujairah – Male, 30 October - 28 November, 2007. Cold Seeps of the Makran subduction zone (Continental margin of Pakistan). 161 pages, Bremen 2008.
- No. 267 Sachs, O.**
Benthic organic carbon fluxes in the Southern Ocean: Regional differences and links to surface primary production and carbon export. 143 pages, Bremen, 2008.
- No. 268 Zonneveld, K. and cruise participants**
Report and preliminary results of R/V POSEIDON Cruise P339, Piräus - Messina, 16 June - 2 July 2006. CAPPUCCINO - Calabrian and Adriatic palaeoproductivity and climatic variability in the last two millenia. 61 pages, Bremen, 2008.
- No. 269 Ruhland, G. and cruise participants**
Report and preliminary results of R/V POSEIDON Cruise P360, Las Palmas (Spain) - Las Palmas (Spain), Oct. 29th - Nov. 6th, 2007. 27 pages, Bremen, 2008.
- No. 270 Ruhland, G., G. Fischer and cruise participants**
Report and preliminary results of R/V POSEIDON Cruise 365 (Leg 1+2). Leg 1: Las Palmas - Las Palmas, 13.4. - 16.4.2008. Leg 2: Las Palmas - Las Palmas, 18.4. - 29.4.2008. 40 pages, Bremen, 2009.
- No. 271 Kopf, A. and cruise participants**
Report and preliminary results of R/V POSEIDON Cruise P386: NAIL (Nice Airport Landslide), La Seyne sur Mer, 20.06.2009 – La Seyne sur Mer, 06.07.2009. 161 pages, Bremen, 2009.
- No. 272 Freudenthal, T., G. Fischer and cruise participants**
Report and preliminary results of Maria S. Merian Cruise MSM04/4 a & b, Las Palmas (Spain) – Las Palmas (Spain), Feb 27th – Mar 16th & Mar 19th – Apr 1st, 2007. 117 pages, Bremen 2009.
- No. 273 Hebbeln, D., C. Wienberg, L. Beuck, A. Freiwald, P. Wintersteller and cruise participants**
Report and preliminary results of R/V POSEIDON Cruise POS 385 "Cold-Water Corals of the Alboran Sea (western Mediterranean Sea)", Faro - Toulon, May 29 - June 16, 2009. 79 pages, Bremen 2009.
- No. 274 Zonneveld, K. and cruise participants**
Report and preliminary results of R/V Poseidon Cruises P 366-1 and P 366-2, Las Palmas - Las Palmas - Vigo, 03 -19 May 2008 and 22 -30 May 2008. PERGAMOM Proxy Education and Research cruise off Galicai, Morocco and Mauretania. 47 pages, Bremen 2010.
- No. 275 Wienberg, C. and cruise participants**
Report and preliminary results of RV POSEIDON cruise POS400 "CORICON - Cold-water corals along the Irish continental margin", Vigo - Cork, June 29 - July 15 2010. 46 pages, Bremen 2010.
- No. 276 Villinger, H. and cruise participants**
Report and preliminary results of R/V Sonne Cruise SO 207, Caldera-Caldera, 21 June -13 July, 2010. SeamountFlux: Efficient cooling in young oceanic crust caused by circulation of seawater through seamounts (Guatemala Basin, East Pacific Ocean). 161 pages, Bremen 2010.
- No. 277 Fischer, G. and cruise participants**
Report and preliminary results of RV POSEIDON Cruise POS 396, Las Palmas - Las Palmas (Spain), 24 February - 8 March 2010. 22 pages, Bremen 2011.
- No. 278 Bohrmann, G. and cruise participants**
Report and preliminary results of RV MARIA S. MERIAN Cruise MSM 15/2, Istanbul (Turkey) – Piraeus (Greece), 10 May - 2 June 2010. Origin and structure of methane, gas hydrates and fluid flows in the Black Sea. 130 pages, Bremen 2011.
- No. 279 Hebbeln, D. and cruise participants**
Report and preliminary results of RV SONNE Cruise SO-211, Valparaíso - Valparaíso, 2 November – 29 November 2010. ChiMeBo. Bremen 2011.
- No. 280 Bach, W. and cruise participants**
Report and preliminary results of RV SONNE Cruise SO 216, Townsville (Australia) - Makassar (Indonesia), June 14 – July 23, 2011. BAMBUS, Back-Arc Manus Basin Underwater Solfataras. 87 pages, Bremen 2011.

- No. 281 Bohrmann, G. and cruise participants**
Report and preliminary results of RV METEOR Cruise M84/2, Istanbul – Istanbul, 26 February – 02 April, 2011. Origin and Distribution of Methane and Methane Hydrates in the Black Sea. 164 pages, Bremen 2011.
- No. 282 Zonneveld, K. and cruise participants**
Report and preliminary results of R/V POSEIDON Cruise P398, Las Palmas – Lissabon, 1 – 16 April 2010. PAPOCA, Production and preservation of organic carbon in relationship to dust input and nepheloid layers in the upwelling area off NW Africa. 33 pages, Bremen 2011.
- No. 283 Hanebuth, T. J. J. and cruise participants**
Report and preliminary results of RV METEOR Cruise M84/4, GALIOMAR III, Vigo – Vigo, 1st – 28th May, 2011. 139 pages, Bremen 2012.
- No. 284 Kopf, A. and cruise participants**
Report and preliminary results of RV POSEIDON Cruise P410: MUDFLOW (Mud volcanism, Faulting and Fluid Flow on the Mediterranean Ridge Accretionary Complex), Heraklion / Greece, 12.03.2011 – Taranto / Italy, 01.04.2011. 128 pages, Bremen 2012.
- No. 285 Krastel, S., G. Wefer and cruise participants**
Report and preliminary results of RV METEOR Cruise M78/3. Sediment transport off Uruguay and Argentina: From the shelf to the deep sea. 19.05.2009 – 06.07.2009, Montevideo (Uruguay) – Montevideo (Uruguay). 79 pages, Bremen 2012.
- No. 286 Kopf, A. and cruise participants**
Report and preliminary results of RV POSEIDON Cruise P429. MEDFLUIDS: Slope Stability, Mud volcanism, Faulting and Fluid Flow in the Eastern Mediterranean Sea (Cretan Sea, Mediterranean Ridge) and Ligurian Margin (Nice slope), Heraklion / Greece, 22.03.2012 – La Seyne sur Mer / France, 06.04.2012. 80 pages, Bremen 2012.
- No. 287 Fischer, G. and cruise participants**
Report and preliminary results of RV POSEIDON Cruise P425. Las Palmas – Las Palmas, 16.01.2012 – 30.01.2012. 32 pages, Bremen 2012.
- No. 288 Mohtadi, M. and cruise participants**
Report and preliminary results of RV SONNE Cruise SO 221. INVERS. Hong Kong – Hong Kong, 17.05.2012 – 07.06.2012. 168 pages, Bremen 2012.